POLITECNICO
MILANO 1863

DIPARTIMENTO DI ELETTRONICA
INFORMAZIONE E BIOINGEGNERIA

Neuromodulation approaches for the rehabilitation of neurological diseases: Noninvasive Electrical Stimulation and robotics

Doctoral Programme in
Biomedical Engineering

Author: **Francesca Dell'Eva**

Advisors: Prof.Alessandra Pedrocchi, Prof.Emilia Ambrosini
Tutor: Prof. Giuseppe Pozzi
Coordinator: Prof. Gabriele Angelo Dubini

XXXVI Cycle of the Doctoral Programme in Bioengineering

Abstract

Neurological disorders, including Spinal Cord Injury (SCI) and stroke, affect over one billion people worldwide, severely impacting their sensorimotor functions and quality of life. The growing incidence of neurological disorders, coupled with the aging population, is causing an increase in the number of subjects who need rehabilitation therapies to restore physiological and motor functions that strongly impact the independence and community participation of affected individuals. Therefore, the optimization of such therapies is fundamental to maximize their efficacy.

In this work, we will mainly focus on motor rehabilitation, specifically the one of the lower limbs, intended for gait training. Motor rehabilitation takes advantage of neuroplasticity through intense, task-oriented and repetitive exercises. This approach is widely recognized as the key mechanism driving functional improvements, especially during the initial phases following injury.

Besides the Conventional Therapy approach, the integration of technologies within rehabilitation has gained increasing interest over time. On one hand, Rehabilitation Robotics has been introduced into clinical practice with the use of mechatronic devices for supporting or actuating limbs during therapy. These systems enable tailored, repetitive and challenging exercises, but are strongly limited by a heavy and bulky structure which decreases their usability and acceptability from end-users. On the other hand, Electrical Stimulation (ES) has received particular attention over the past years, offering promising neuromodulation benefits for sensorimotor recovery in neurological disorders. It involves the delivery of low-energy electrical pulses to nerves located either peripherally or centrally. In the former case, it is termed Neuro-Muscular Electrical Stimulation (NMES), further categorized into Functional Electrical Stimulation (FES) and Sensory Afferent Electrical Stimulation (SAES). FES triggers muscle contractions to produce functional movements, thus it is administered at an intensity surpassing the motor threshold. SAES, instead, mainly focuses on sensory fibers for eliciting changes in sensorimotor functions. The latter alternative, instead, refers to Spinal Cord Stimulation (SCS), primarily employed to modulate muscle activity and alleviate spasticity. These ES-based strategies are associated with several peripheral and central advantages, depending on their spe-

cific nature. Nevertheless, they also face some limitations such as the high variability of stimulation-induced responses, both between subjects and within the same one, and the early appearance of muscle fatigue, particularly relevant when ES is delivered above the motor threshold. Some of these limitations can be overcome by combining ES-based neuromodulation techniques with robotics.

This thesis aims to explore these different neuromodulation approaches, focusing on their working principle and induced neurological effects to discuss their potential application in rehabilitation settings. First, it wonders whether by exploiting FES-induced movement, it could be possible to reduce motors' power in hybrid devices and, consequently, realize lighter devices. In the direction of improving the device usability, the possibility of using textile electrodes in place of hydrogel ones was also investigated, given their potential integration into clothes. Moreover, it inspects the neuromodulatory effects of SCS and the potential benefits of its combination with residual voluntary signals. Finally, the topic of afferent stimulation is expanded by comparing the reflex waves generated by SCS and SAES, inferring that they could elicit similar neuromodulatory effects.

The first research question is addressed by integrating FES within a robotic device, realizing what is usually referred to as *hybrid* system. As encouraged by literature studies, this combination would enhance the advantages of the two technologies and mitigate their disadvantages. The addition of FES would directly engage the subject's muscles in movement execution and reduce the motors' contribution; simultaneously, the robotic support would be beneficial in delaying the onset of stimulation-induced muscle fatigue, a primary constraint in prolonged stimulation training. To this aim, the *TwinFES* prototype was realized by combining two commercial electrical stimulators into a motorized lower-limb exoskeleton (*Twin*, Italian Institute of Technology). The primary study focus has been the development of a cooperative control strategy that, integrating the two technologies, enables FES assistance to adapt and compensate for reductions in motor torque. An extensive validation of this hybrid control system was carried out on healthy subjects and individuals affected by either complete/incomplete SCI or stroke, recruited at the Villa Beretta rehabilitation center. Results of both studies confirmed the possibility of reducing motors' power enabled by the inclusion of FES and proved that engaging subjects' muscles in the movement execution increases the device's usability. Nevertheless, the complexity of the overall system emerged as a primary limitation of the device.

Current research is trying to tackle these shortcomings, such as the challenging fit and the need for precise electrode placement by therapists, aiming to present such systems as everyday assistive devices and increase users' acceptance. In this direction, the possibility of using textile electrodes to improve the wearability of FES-based systems was explored. A novel set of textile electrodes was developed by integrating commercial screen-printed

electrodes into textile strips and validated with respect to traditional hydrogel ones, in terms of electrical properties, overall stimulation comfort and performance on 14 healthy subjects. Collected results reported no significant differences among the two electrode types, confirming the possibility of substituting hydrogel samples with textile ones that, given their possible integration into clothes, would ease hybrid devices' donning and doffing processes. Furthermore, the textile alternative would facilitate the transition from clinical-based therapies to home-based solutions.

Then, the focus is shifted to sensory stimulation strategies, namely SCS and SAES, which act on afferent fibers to modulate the excitability of the central nervous system. Rather than inducing a movement, such stimulations aim to facilitate the possibility of residual weak signals to produce movements. To this aim, a protocol combining SCS with cycling was tested on four complete SCI individuals while recording the EMG signals of their lower-limbs muscles. Despite the limited number of performed sessions, preliminary but encouraging observations were retrieved from this study. These included a reduction of spasticity and some benefits on bladder and bowel function, which persisted for days after the stimulation. Direct motor facilitation was not reported, probably due to the limited number of performed sessions, but rather a promising SCS-dependent modulation of the EMG signal was observed.

Finally, the investigation of afferent stimulation advances by comparing SCS and SAES, considering that both are based on a reflex-mediated activity. The study was motivated by the attempt to find an alternative solution to SCS, given its limitations: the impossibility of applying it in the presence of spinal metal implants, the difficulty of an autonomous placement of electrodes and the high intensity of required stimulation currents. Tests involved twelve healthy participants and compared the reflex waves induced by the two types of sensory ES in terms of shape, amplitude and latency. The study confirmed that the two types of stimulation techniques trigger the same spinal circuits but at different locations over the reflex arc. These preliminary results paved the way for future studies analyzing whether similar therapeutic benefits are prompted by the two strategies, in view of promoting their interchangeable use depending on the specific case.

This work proposes the use of electrical stimulation therapies, and their possible integration with robotics, as a valid option for the rehabilitation of neurological diseases. It highlights the importance of defining the therapy's intent to determine the appropriate stimulation strategy to be applied, with FES mainly employed for the induction of functional movements and sensory stimulation (SCS and SAES) mainly intended for neuromodulation. By sending afferent signals to the brain, both alternatives were also demonstrated to promote plasticity processes and motor learning, particularly when combining the proprioceptive feedback from stimulation with volitional efforts. On one hand,

this study proves the efficacy of cooperative FES-motor control strategies, particularly in reducing motor torque demands and prolonging benefits of FES, reducing muscle fatigue. Improvements in system usability were also observed, which could be further enhanced by replacing hydrogel electrodes with textile ones, given their demonstrated equivalent properties. On the other hand, it explores the therapeutic benefits of SCS and offers a preliminary investigation of SAES, emphasizing the need for further inspection of its therapeutic impact. Challenges and limitations of these techniques are also discussed, prompting further research to develop more advanced and flexible systems aimed at improving rehabilitation outcomes.

Keywords: Neurorehabilitation, Rehabilitation robotics, Neuromodulation, Functional Electrical Stimulation, Hybrid exoskeleton, Cooperative control, Spinal Cord Stimulation

Contents

Abstract **i**

Contents **v**

1 Introduction **1**
1.1 Context . . . 2
1.1.1 Neurological disorders: Spinal Cord Injury and stroke . . . 2
1.1.2 The relevance of rehabilitation and motor learning . . . 4
1.2 Rehabilitation robotics . . . 6
1.2.1 Lower-Limb powered exoskeleton: State of the Art . . . 9
1.3 Electrical Stimulation as a tool for neuromodulation . . . 12
1.3.1 Working Principle . . . 14
1.3.2 Stimulation Parameters . . . 15
1.3.3 Fibers Recruitment . . . 16
1.3.4 Electrodes . . . 17
1.4 Use of ES in Rehabilitation . . . 18
1.4.1 Functional Electrical Stimulation (FES) . . . 24
1.4.2 Sensory Afferent Electrical Stimulation (SAES) . . . 29
1.4.3 Spinal Cord Stimulation (SCS) . . . 31
1.5 Hybrid systems . . . 36
1.5.1 Definition, advantages and disadvantages . . . 36
1.5.2 Control strategies for hybrid systems . . . 38
1.5.3 Hybrid systems in literature: context and limitations . . . 40
1.6 Thesis goal and road map . . . 43

2 Development and validation of a Hybrid system for walking **47**
2.1 State of the Art . . . 48
2.2 Objective of the study . . . 58
2.3 Materials and Methods . . . 59
2.3.1 Experimental Setup . . . 59

2.3.2 Calibration . . . 62
2.3.3 TwinFES control . . . 62
2.4 Testing on non-disabled subjects . . . 66
2.4.1 Experimental Protocol . . . 66
2.4.2 Data Analysis and Statistics . . . 67
2.4.3 Results . . . 67
2.5 Testing on target users . . . 74
2.5.1 Experimental Protocol . . . 74
2.5.2 Data Analysis and Statistics . . . 75
2.5.3 Results . . . 75
2.6 Discussion . . . 85
2.7 Conclusions . . . 87

3 Investigation of textile electrodes for delivering transcutaneous electrical stimulation 89
3.1 State of the Art . . . 90
3.1.1 Electrodes characteristics . . . 91
3.1.2 Production Methods . . . 92
3.1.3 Evaluation Methods . . . 92
3.1.4 Examples . . . 94
3.2 Objective of the study . . . 95
3.3 Materials and Methods . . . 96
3.3.1 Ink-based printed textile electrodes . . . 96
3.3.2 Self-adhesive hydrogel electrodes . . . 97
3.3.3 Skin-electrode impedance . . . 97
3.3.4 Tests on non-disabled subjects . . . 98
3.4 Results and Discussion . . . 106
3.4.1 Skin-electrode impedance . . . 106
3.4.2 Tests on non-disabled subjects . . . 107
3.4.3 Limitations . . . 111
3.5 Conclusions . . . 111

4 Neurorehabilitation effects of transcutaneous Spinal Cord Stimulation 113
4.1 State of the Art . . . 114
4.1.1 tSCS parameters and setting . . . 115
4.1.2 tSCS applications for spinal injury recovery . . . 119
4.2 Objective of the study . . . 120
4.3 Materials and Methods . . . 121

4.3.1 Experimental Setup . . . 121
4.4 Testing on non-disabled subjects . . . 123
4.4.1 Experimental Protocol . . . 123
4.4.2 Data Analysis . . . 124
4.4.3 Results and Discussion . . . 124
4.5 Testing on subjects with SCI . . . 126
4.5.1 Experimental Protocol . . . 126
4.5.2 Data Analysis . . . 128
4.5.3 Results and Discussion . . . 129
4.6 Conclusions . . . 134

5 Comparison of the neuromodulatory effects of peripheral and central electrical stimulation 137
5.1 State of the Art . . . 138
5.2 Objective of the study . . . 139
5.3 Materials and Methods . . . 140
5.3.1 Experimental Setup . . . 140
5.3.2 Experimental Protocol . . . 141
5.3.3 Data Analysis . . . 143
5.4 Results . . . 144
5.4.1 Representative Subject . . . 144
5.4.2 All Subjects . . . 147
5.5 Discussion . . . 150
5.6 Conclusion . . . 152

6 Conclusion and future perspectives 153
6.1 Key take-home messages of the thesis, limitations and future perspectives . 153

Bibliography 159

A List of relevant scientific publications 185
A.1 International peer-reviewed journals . . . 185
A.2 Contributions at international conferences . . . 185

List of Figures 187

List of Tables 193

1 | Introduction

Chapter Contents

1.1 Context . . . 2
1.1.1 Neurological disorders: Spinal Cord Injury and stroke . . . 2
1.1.2 The relevance of rehabilitation and motor learning . . . 4
1.2 Rehabilitation robotics . . . 6
1.2.1 Lower-Limb powered exoskeleton: State of the Art . . . 9
1.3 Electrical Stimulation as a tool for neuromodulation . . . 12
1.3.1 Working Principle . . . 14
1.3.2 Stimulation Parameters . . . 15
1.3.3 Fibers Recruitment . . . 16
1.3.4 Electrodes . . . 17
1.4 Use of ES in Rehabilitation . . . 18
1.4.1 Functional Electrical Stimulation (FES) . . . 24
1.4.2 Sensory Afferent Electrical Stimulation (SAES) . . . 29
1.4.3 Spinal Cord Stimulation (SCS) . . . 31
1.5 Hybrid systems . . . 36
1.5.1 Definition, advantages and disadvantages . . . 36
1.5.2 Control strategies for hybrid systems . . . 38
1.5.3 Hybrid systems in literature: context and limitations . . . 40
1.6 Thesis goal and road map . . . 43

This chapter covers the main themes discussed in my Ph.D. thesis: the use of neuromodulation approaches based on Electrical Stimulation (ES) and of robotics to optimize the rehabilitation of people with Spinal Cord Injury (SCI) and survivors of stroke. Their main objective is to improve subjects' quality of life by restoring motor-sensory functions and social participation.

1.1. Context

1.1.1. Neurological disorders: Spinal Cord Injury and stroke

Neurological disorders are estimated to affect one billion people worldwide, regardless of age and geographical region [1]. Among them, injuries to the Central Nervous System (CNS) are life-disruptive conditions that, besides having a different origin, cause a massive compromise of sensorimotor functions, restricting the functional activities of affected subjects and negatively influencing their independence and quality of life [2, 3]. These injuries include stroke, traumatic brain injury and Spinal Cord Injury (SCI), which represent leading causes of long-term disability [4].

Spinal Cord Injury. Spinal Cord Injury (SCI) is a condition caused by a damage to the spinal cord itself or to the tissue and bones (vertebrae) [5], which affects the conduction of afferent and efferent signals across the sites of lesion. Its main consequence is the loss of motor and/or sensory abilities, whose severity depends on the level and characteristic of the injury [6]. The global incidence of SCI is 40 to 80 new cases per million population per year, which means that every year, between 250 000 and 500 000 people become SCI [7]. It can have either a traumatic or non-traumatic origin but the former is prevalent, representing 90% of cases, and its main causes are road traffic injuries, falls and violence [7]. Nevertheless, in recent years, a trend towards the growth of non-traumatic cases was observed, along with the increase in the age of patients, probably attributable to the ageing population [8]. The age interval in which SCI is most commonly observed is between 33 and 50 years old [9].

A main distinction among SCI cases is made by the expressions tetraplegia and paraplegia: the former is used to refer to the condition consequent to impairments in the cervical segments, resulting in damaged functions in the arms as well as in the trunk, legs and pelvic organs; the latter, instead, considers the condition consequent to injuries at the thoracic, lumbar or sacral segments of the spinal cord, not affecting the arms function but involving, depending on the injury level, the trunk, legs and pelvic organs [6]. Furthermore, according to the Standards for Neurological Classification published by the American Spinal Injury Association (ASIA) [10], a SCI is defined as complete when no motor and/or sensory function exists below the neurological level of injury, while it is defined as incomplete when some of these functions are preserved [11]. The first case is classified as ASIA A, while the second one is classified from ASIA B to ASIA E depending on how impaired the motor and sensory functions are. Even if SCI incidence is low, its physical and psychosocial consequences demand a significant change in the lifestyle of affected individuals [12, 13]. Indeed, this pathology is related to secondary health

complications such as bowel, bladder and sexual problems [14], pressure sores [15], spasticity [16], impaired cardiovascular [17] and respiratory [18] capacities and a higher risk of thrombosis and osteoporosis [19, 20]. In this scenario, lifetime costs of managing SCI pose a significant burden to individuals with SCI, their families, and health-care systems [21, 22]. In the attempt to enhance the quality of life of these patients, rehabilitation plays a crucial role, especially the one aiming at restoring voluntary leg movements and, possibly, gait. In fact, several studies [23–25] analyzed the most relevant functions that SCI individuals wanted to recover and, regardless of the lesion level, the time since injury, or the age, walk restoration was identified as the highest priority objective [24].

Stroke. A stroke occurs when the blood flow to a part of the brain is suddenly interrupted (ischemic) or when a blood vessel in the brain bursts, causing bleeding within the space surrounding brain cells (hemorrhagic). The former causes the deprivation of oxygen and nutrients to the brain cells that, consequently, die within minutes; the latter, generates a high pressure on brain cells, inflicting significant damages [26]. The most common impairment resulting from stroke is the complete or partial paralysis of one side of the body (contralateral to the brain damage), called hemiplegia or hemiparesis respectively. The 80% of stroke patients experience it during the acute phase, while more than 40% in the chronic phase [27]. It leads to limitations in activities such as walking, along with reduced participation in daily life tasks. Other motor impairments include muscle weakness, altered muscle tone, joint laxity, and inability to produce controlled movements [28]. The Global Burden of Diseases, Injuries, and Risk Factors Study (GBD) classified stroke as the third cause of death and disability combined (measured by DALYs = Disability-Adjusted Life-Years) and the second cause of death (with 6.6 million deaths) [29]. Its incidence is continuously growing, with the total number of stroke individuals almost doubled in the past 30 years [30] due to the ageing and growth of the population playing a significant role [31]. This scenario negatively influences the economic impact of stroke, with its cost expected to grow from US$891 billion per year (estimated in 2017) to US$2.31 trillion by 2050 [32]. Part of these costs are attributable to rehabilitation, fundamental in post-stroke recovery for improving lost neuromuscular functions, especially within the acute phase, which has been identified as the period in which intensive exercise therapy yields the most favorable effects on ADLs [33].

The main goal of post-stroke rehabilitation is the regain of patients' independence and their reintegration into social and domestic life [34]. However, in many cases, a complete recovery is not possible. As reported from literature studies, only 20% of stroke survivors recover a normal upper extremity functionality [35]. Focusing on the lower limbs, the main rehabilitation objective is ambulation recovery, but in one-third of stroke

cases, individuals were not able to walk unsupervised when discharged from hospitals [36].

1.1.2. The relevance of rehabilitation and motor learning

The high incidence of these neurological disorders, together with the ageing of the population, is causing a continuous increase in the number of subjects who require assistance and rehabilitation therapies. Their main aim is to induce recovery of physiological and motor functions, which improve independence, community participation and quality of life after stroke and SCI [37].
This, in turn, poses a high economic burden not only to affected individuals and their caregivers but also to healthcare systems [38], limiting their productivity. From the previously reported data about the costs of these pathologies, it is evident the necessity to develop tools and effective strategies to promote the recovery of people with neurological disorders.
Literature studies [39, 40] investigating the general functional recovery of stroke patients stated that it is concentrated in the early months, within the first 3 to 6 months. However, some recovery also continues beyond this time, even if at lower rates.
Therefore, also considering the high economic burden of rehabilitation, it is fundamental to optimize therapy planning and its delivery to patients, to improve users' quality of life and not to waste healthcare resources.
In this work, we will mainly focus on motor rehabilitation, specifically the one of the lower limbs, and thus on the approaches used for retraining gait. We will analyze the existing rehabilitation techniques, paying particular attention to novel approaches, along with their advantages and disadvantages.

Motor rehabilitation takes advantage of *neuroplasticity*, defined as the ability of the nervous system to modify its structure and/or function in response to internal or external stimuli. Plasticity originates from various neurophysiological processes; in fact, *structural* and *functional* plasticity are distinguished [41]. The former comprises a modification in the number of synapses and axonal or dendritic branches; the latter, instead, is related to the change of synapses' strength (increase in neurotransmitters and receptors density). When an injury occurs, this process, usually referred to as injury-induced plasticity, is represented by the spontaneous reorganization of cerebral tissues belonging to the involved brain areas [42]. This process is considered as the primary mechanism underlying functional improvements after stroke, spinal cord injuries, or brain injuries as it allows surviving neurons to modify their innervations and create new synapses in non-damaged

brain regions in order to compensate for lost functions [43]. Thus, the acquisition of motor skills is strictly linked to neuronal plasticity [44].
To facilitate neural plasticity, motor training should be characterized by intense, task-oriented, personalized and repetitive exercises, as these represent key elements of neurorehabilitation and motor relearning. Past studies proved that intensive and task-oriented rehabilitative paradigms, especially when delivered at early stages after the injury, were able to enhance neurological and functional recovery after SCI [45] and stroke [46] and achieve better locomotor outcomes compared to standard therapies [47]. A literature study considering lower limbs reported substantial changes in the walking ability and health-related functional status when providing task-specific interventions [48]; main benefits were obtained with respect to balance, endurance and mobility [49].
Practicing frequent exercises is particularly relevant in the early phases after the injury because plastic changes occur mainly in the first weeks and months after the acute event [50]. The learning process is influenced by different factors. One example is the presence of the patient's volitional contribution [51] that, if possible, should be synchronized with the execution of movements as it provides the link between function and intention which is the best condition for motor relearning. Another important aspect is the motivation of patients while doing the therapy [52], which can be enhanced by therapists defining an adequate therapy goal and providing performance feedback. This also reduces the risk of *maladaptive plasticity* which is a non-genuine brain plasticity occurring when patients learn a wrong movement pattern leading to compensatory movements (i.e., "compensating" affected limbs by using non-affected body parts) [53]. This artifice allows one to accomplish everyday activities besides motor impairments but does not stimulate the functional regain of the affected limb, entering the "learned non-use" condition [54].

Among the wide range of strategies and devices developed for promoting motor recovery by taking advantage of brain plasticity, it is possible to distinguish two different approaches [55]:

1. *Bottom-Up*: those that exploit peripheral (limbs) movements to induce brain structure changes thanks to neural plasticity;

2. *Top-Down*: those that work at the high level to induce brain modifications aiming at regaining peripheral movements.

Top-dow techniques comprise all those strategies that aim at modulating cortical excitability to facilitate neural plasticity and motor relearning. Examples of such techniques are Non-Invasive Brain Stimulation (NIBS) and Transcranial Magnetic Stimulation (TMS), or the use of plasticizing drugs. The active participation of users during the rehabilita-

tion process also represents a *top-down* approach, because the combination of the user's volition and the system's support (assist-as-needed) may facilitate motor learning.
On the other hand, a classic example of *bottom-up* approach is the Conventional Therapy (CT) based on passive maneuvers performed by therapists. These latter are in charge of guaranteeing treatment customization, and patient involvement while providing feedback to him/her. Considering gait training, referred to as Locomotor Training (LT), it is usually performed on treadmills with a Body-Weight Support (BWS) system, whose compensation is adapted based on the capability of the patient to maintain the upright position [47]. In this scenario, one-to-one work between the physiotherapist and the patient is required, unbalancing the cost-effectiveness of this approach, especially in those cases where more than one therapist is needed [56]. This is the main limitation of the CT, together with the limited practice allowed, in terms of training hours per day and number of repetitions, and to the fact that exercises are often boring both for the patient and the therapist. All these aspects concur with slowing down the rehabilitation process.
A possible solution is the integration of technologies within the rehabilitation process to improve its outcomes [57]. One example is the introduction of *Rehabilitation Robotic* into clinical practice which consists of using mechatronic devices in place of therapists to assist the limbs during stepping. Another alternative that has gained particular attention over the past years is *Electrical Stimulation* (ES) to induce beneficial neuromodulations. Depending on its parameters, it can be used to get different outcomes, such as rewiring denervated muscles, reducing spasticity or inducing muscle contractions.
Both technologies will be discussed in detail in the next paragraphs.

1.2. Rehabilitation robotics

Rehabilitation Robotics is a growing research field studying a wide range of devices to support patients' limbs in rehabilitation activities to overcome the main limitations of CT. These latter are the difficulty of guaranteeing prolonged and constant exercises and the mandatory presence of a therapist to accomplish training programs, which has a great impact on the therapy costs and on the amount of available personnel for other treatments. Mechatronic devices represent the modern version of *bottom-up* treatments as they are programmed to deliver a high dosage of task-oriented training to patients affected by different degrees of functional impairments [55]. At the same time, these optimize the time of therapists because, by being alleviated from the labor-intensive aspects of physical exercises, therapists can take care of some more relevant features of rehabilitation [58]. For example, the integration of robots into standard treatments could enable therapists to

provide hands-on postural corrections while the subject is performing robot-assisted tasks.

These systems can be divided into 2 groups, as shown in Figure 1.1 [59]:

1. End-effectors: when the robot applies forces at the distal part without correspondence between anatomical and robotic segments. An example is Gait Trainer [60];
2. Exoskeletons: when robot segments are aligned with the subject's anatomical axes so that the movement of each segment can be directly controlled minimizing abnormal postures. Exoskeletons are named "grounded" or "wearable" depending on whether their structure is fixed or portable. While the former are well established (with Lokomat [61] being the leader of this group), the latter are currently entering the clinical application.

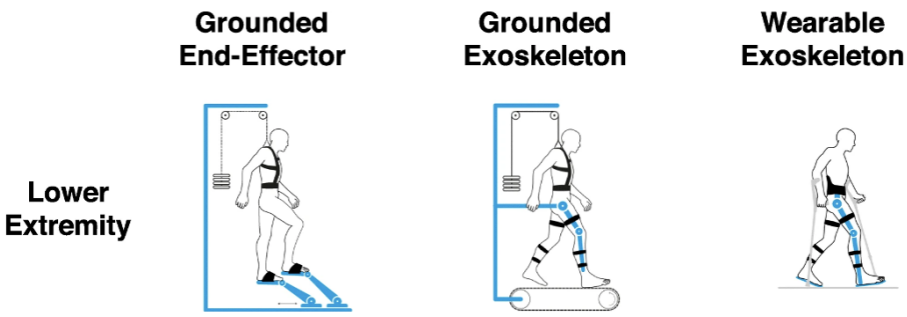

Figure 1.1: Schematic representation of the different types of rehabilitation robots. Adapted from [59].

The control of end-effectors is easier than the one of exoskeletons but the absence of constraints at the proximal joints increases the risk of abnormal movements and trajectories. Consequently, exoskeletons are more used in the early stage of rehabilitation, especially when dealing with highly impaired patients [62].

On the other hand, robotic exoskeletons, whose evolution dates back to the 1970 [63], represent a promising therapeutic approach because they are intended to compensate for reduced motor capabilities of injured patients by addressing the fundamental requirements of rehabilitation and motor relearning [64]. As previously said, the physical practice should be challenging, specific, adaptable over time, intense, task-oriented and engaging for patients [65]. Robotic systems satisfy these aspects because their characteristics can be programmed with a high level of detail. This flexibility is related to their structure and movements, to the implemented exercises and to the number of repetitions. In fact, their movements are usually defined in a parametric way so that they can adapt to the subject's anthropometry. Additionally, many features of the performed exercises, such

as the level of gravity support, the target velocity or trajectory, can be tailored for the specific subject depending on the impairment level and adapted over time based on his or her progress. These devices also increase the users' motivation thanks to technology appeal, Virtual Reality (VR), and gaming [62].
Furthermore, since robotic technology includes sensors (encoders, load cells, ...), it can provide reliable kinematic and kinetic measurements to assess the accuracy in the execution of movements and the patient's improvements over time. Generally, robotic treatment with wearable robots is more expensive (from double to triple) than Conventional Therapy [66]. However, a review [67] examining the expenses associated with both therapies in post-stroke patients revealed a stronger cost advantage for robotic therapy because of the potential cost reduction achieved through optimizing the number of patients treated per robotic session.
Nevertheless, these novel systems also have some limitations and disadvantages. First of all, it must be noted that there has not been conclusive evidence demonstrating a clear superiority of robotic rehabilitation over CT yet. The literature lacks a definitive consensus on this topic. Although it was proved that robotic rehabilitation may be as effective as CT in reducing impairment [56], statistically significant differences between the two approaches were not reported, especially concerning gait training [68]. The question remains whether robot-assisted movements offer unique therapeutic benefits beyond what human therapists can provide [58]. On one hand, some highlighted the diversity of CT as the key aspect making it more effective than robotic therapy [69]; on the other hand, robots allow a significant intensity of practice that would be difficult to get with a therapist-assisted setup. However, robotic therapy at low utilization neither demonstrated particular advantages nor hindered the recovery, and thus there is no reason to assume that robots lead to better results than an equivalent dose of human-delivered therapies [70].
Establishing an overall superiority of one approach over the other is challenging because therapy effectiveness depends on various factors and patient-specific characteristics. For instance, one study [71] noted significant improvements in ADLs with robotic rehabilitation compared to CT, but it also observed an increase in anxiety among participants in the robotic group. In conclusion, further research is necessary to identify significant differences between robotic and conventional treatments, and it should include other dimensions of general health, such as satisfaction and participation [68]. Rather than questioning the usefulness of robotic technologies per se, the focus should be on identifying who would benefit the most from the robotic therapy [71].
From a therapeutic point of view, the main risk of employing robots is the *slacking hypothesis*, which represents an undesired condition in which the patient relies too much on the exoskeleton support without actively contributing to the task, then worsening the

rehabilitation outcome [72]. To avoid this, devices are designed to actively involve patients during therapies and maintain their active attention. This strategy is known as "Assist-As-Needed" (AAN), wherein the individual receives assistance only to the extent necessary to complete the task. One alternative to promote patients' engagement and initiation of movements involves employing a compliant robotic component that permits slight deviations around the desired movement trajectory. Another option is the inclusion of a forgetting factor in the learning algorithm, reducing robotic assistance as performance errors decrease, thus consistently challenging the participant.
From a mechanical point of view, these machines are heavy and bulky due to the presence of actuators, rigid structural components and batteries, and require significant power to generate torques and manipulate limbs. This limits the overall usability of such systems and discourages patients from using them.
Currently, the technological advancement of these structures does not yet allow us to consider their potential application beyond clinical settings. Indeed, their cost is still too high and many times their usage requires the presence of an expert [73]. Consequently, at the moment, exoskeletons are clinical-based devices used by many patients with a rehabilitative purpose rather than an assistive one. Nevertheless, research is moving towards enabling the utilization of these systems outside clinics and thus also for the assistance of injured individuals in practicing ADLs.

1.2.1. Lower-Limb powered exoskeleton: State of the Art

After providing an overview of the existing robotic systems for rehabilitation, this section offers a picture focused on the wearable lower-limbs powered exoskeletons currently involved in the industrialization phase, at the market or pre-market stage. Some of them received clearances, like FDA or CE, while others are going through the process of obtaining a clearance.
The complete list of the considered devices is reported in Figure 1.2, while their detailed individual description is provided as follows.

Atalante (*Wandercraft*) [74] is a CE-marked exoskeleton for the support of paraplegic subjects. It has eight actuators: three in correspondence of the hip in the three planes of movement and one in the sagittal plane of the knee. Additionally, two springs are located at the ankle level. Joints' encoders and three IMUs (one on the torso and two on the ankles) acquire joints' position and velocity, while force sensors measure pressure on the feet. It is the first crutch-less exoskeleton on the market, having solved the frontal balance issue and allowing a stable gait; however, its weight and velocity could be improved.

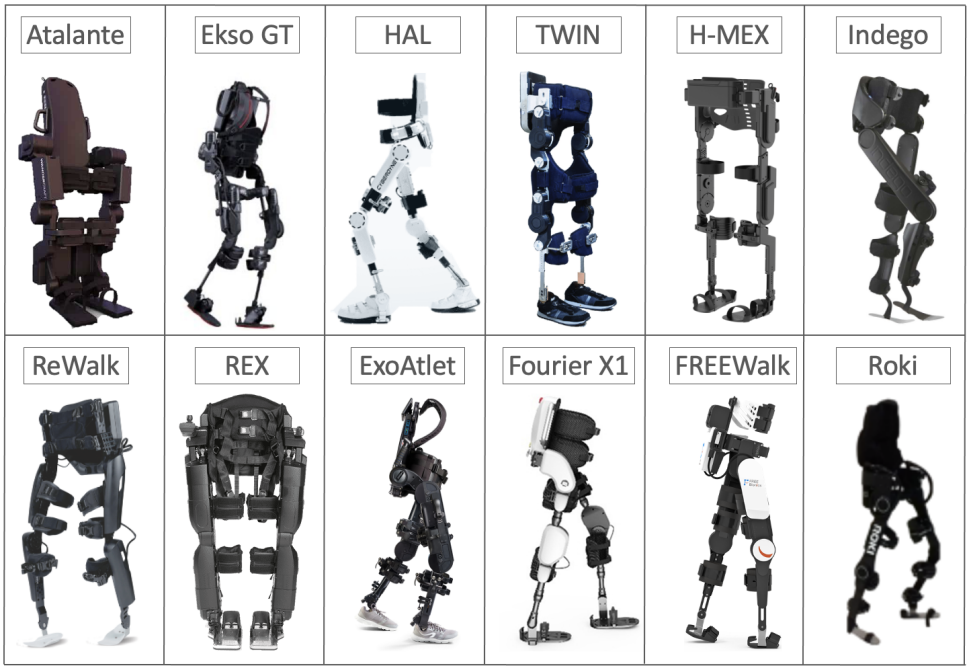

Figure 1.2: Existent commercial Lower-limbs powered exoskeletons.

Ekso GT (*Ekso Bionics*) [75] is a CE- and FDA-marked exoskeleton for the support of post-stroke, SCI and traumatic brain injury patients. It includes four actuated joints in correspondence of both hips and knees and two springs at the ankle level. Sensors of hip and knee angles and feet pressure provide information about the current device state to choose the desired future one through the state automation controlled by a therapist or by the patient. The device does not guarantee sagittal balance, thus the use of crutches is mandatory.

Hybrid Assistive Limb – HAL (*Cyberdine*) [76] is a CE-, PMDA- and FDA-marked exoskeleton for people affected by SCI or other neurological injuries. It consists of four active joints (hips and knees in the sagittal plane). The device control is managed through a Finite State Machine (FSM) that continuously checks the actual system phase by considering joint angles, plantar force and electromyography (EMG) data.

Twin (*Italian Institute of Technology - IIT*) [77] is a CE-approved exoskeleton for both SCI subjects and stroke survivors. It has four active joints (hips and knees in the sagittal plane). The device control consists of a rigid tracking of a target position and is managed through a Finite State Machine (FSM). The triggering of each new step is either manual or automatic: in the former case, it is controlled by the therapist through a tablet; in the

latter, a new step is started every time the subject's bending angle overcomes a threshold.

Hyundai Medical Exoskeleton – H-MEX (*Hyundai Motor Company*) is an MFDS-approved (Ministry of Food and Drug Safety in Korea) exoskeleton to rehabilitate people with low-level SCI or stroke. It includes six active joints for hips' and knee' motion in the sagittal plane and hips' abduction/adduction. Furthermore, ankle springs allow ankle plantar- and dorsiflexion and eversion/inversion movements. Data collected by encoders, force sensors and IMUs are used by the controller to define the next device position in a FSM-based setting. Gait parameters can be customized via tablet and the user can initiate movements using buttons placed on the crutches.

Indego (*Parker Hannifin Corporation*) [78] is a CE- and FDA-approved exoskeleton for assisting gait training and sit-to-stand movements in SCI patients. It incorporates four actuated joints on the sagittal plane of the hip and the knee and an Ankle-Foot-Orthosis (AFO) to provide support at the ankles and prevent foot drop. Joint-level controllers provide a Proportional-Derivative (PD) control managing the joint impedance and are supervised by a FSM that switches between states considering the Center Of Pressure (COP) movements. The use of a walker or crutches is needed for stability while walking.

ReWalk Robot (*Argo Medical Technology*) [79] is a CE- and FDA-approved exoskeleton for paraplegics. It uses four actuators for hips' and knees' sagittal movements. Different locomotion modes are available (walking, standing, climbing, ...), selected by the user through a smartwatch. Gait movements are adapted by the control unit depending on the position of the upper body and the shift in the body weight. These data are retrieved from a tilt sensor on the trunk and force sensors under the feet. It allows real-time control of the gait phases but requires in-depth training of users to ensure correct management of the device through COM movements.

Robotic exoskeleton – Rex (*Rex Bionics*) [80] is an FDA-approved exoskeleton for rehabilitation and assistance of SCI, stroke and brain injury patients during different movements (walking, standing, turning, ...). It is a ten-DOF device with each leg comprising the following actuators: two for the hip sagittal and frontal planes, one for the knee sagittal plane and two for the ankle sagittal and frontal planes. It is a hands-free system allowing user control through a three-button keypad and a joystick as crutches are not required. Its large footplates provide stability but reduce step length and walking speed, resulting in a non-physiological gait.

ExoAtlet I (*ExoAtlet*) [81] is an exoskeleton certified in South Korea, Japan, Thailand, Vietnam, Belarus, Uzbekistan, and Kazakhstan (ISO:13485 certified). This is intended for the assistance of SCI patients during various movements (flat or inclined walking, descending stairs, sitting, ...). It comprises the hips' and knees' sagittal motors. Measurements of relative position and current, angular velocity and foot reaction force are used by the central controller to compute the desired cartesian trajectory, then sent to actuator drivers. Sufficient arms strength is required to manage crutches and balance.

Fourier X1 (*Fourier Intelligence*) [82] is an exoskeleton designed for SCI patients. It includes four actuated joints (hips and knees) and provides four movement patterns. The overall control is carried out by a real-time posture unit using different sensors, such as plantar pressure sensors.

FREE Walk (*FREE Bionics*) [83] is CE- and FDA-approved exoskeleton for walking, standing and sitting, designed for SCI and stroke patients. It includes four active DOFs on the hips' and knees' sagittal plane and two passive DOFs for ankles and hips abduction. Normal functioning in the upper limbs is required for using crutches.

Roki (*Roki Robotics*) [84] is an exoskeleton for SCI patients (inferior to T4 level). It comprises four actuators (hips and knees) and fifteen sensors. The use of this device requires good bone density and arms control for maintaining balance with a walker or crutches. The overall control is operated by the user through buttons placed on the crutches.

1.3. Electrical Stimulation as a tool for neuromodulation

As explained in previous sections, events such as stroke or SCI determine a damage to the nervous system that causes an interruption of descending pyramidal pathways and thus muscles' weakness or, in worst cases, paralysis. This results in the inability of patients to voluntarily produce movements and therefore strongly limits their independence in daily life [85]. A treatment approach proposed in such cases is the use of Electrical Stimulation (ES), which consists of delivering low-energy electrical pulses to either nerves or muscles at different locations in the nervous system. Nerve stimulation is employed in the case of Upper Motoneuron Lesion (UMNL), while muscles are targeted in the case

of Lower Motoneuron Lesion (LMNL), as better explained in Section 1.4. Depending on its characteristics, such as location and parameter setting, ES can be employed across a range of scenarios and intended purposes. In the present thesis, the focus is only on transcutaneous ES, given its easier and wider applicability.
ES is also associated with enhancing the motor learning process and promoting the regain of voluntary movements [86], especially when combined with voluntary motor commands. In such cases, descending signals from the brain reach the corticospinal anterior horn synapse together with the antidromic signals traveling up from peripheral nerves stimulated with ES. This temporal synchronization strengthens the synapse and increases its firing probability [87].
Thus, early interventions with ES in patients with neurological diseases could be beneficial in minimizing their morbidity [88].
Many studies demonstrated the potential benefits that rehabilitation recovery can gain from using different types of ES. Indeed, with ES we refer to an umbrella term including various stimulation strategies that differ in the set of parameters and, consequently, in the expected outcome.
A primary distinction lies in where ES is administered: either peripherally or centrally. When applied to peripheral mixed nerves, the stimulation is generally termed Neuro-Muscular Electrical Stimulation (NMES).

NMES typically denotes a stimulation method employed for motor recovery purposes, targeting structural and functional deficits to enhance a function [89]. Moreover, reducing the impairment level, it may increase patients' participation in voluntary activities [37]. To sum up, it is mainly used to reduce atrophy, to strengthen muscles, to treat spasms, to promote blood circulation, or to improve sensory perception [90].
Furthermore, one of the most used terms in literature is Functional Electrical Stimulation (FES) [91], coined by the scientists Moe and Post in 1962 [92]. The term functional indicates that the stimulation does not aim at inducing a generic muscle contraction but one preceding a functional movement. In fact, it is delivered to completely or partially paralyzed muscles to compensate for their restricted or absent functionality [90]. According to another definition, FES refers to an electrical stimulation synchronized with voluntary movements to assist their execution [93]. There are many literature examples [94, 95] in which the stimulation timing was adapted to mimic physiological activation patterns of either upper or lower limb muscles to generate reaching and grasping tasks or reproduce the human gait, respectively, and thus to overall improve the function of upper and lower limbs. The primary objective of FES is the induction of active movements, obtained by stimulating motor (efferent) nerve fibers with intensities around or above the motor

threshold. However, it also induces central benefits, by triggering sensory (afferent) fibers (explained in section 1.4.1).
The first FES experiment dates back to the 1960s and involved the delivery of current to the peroneal nerve to correct the foot drop in post-stroke subjects [96].
Another type of stimulation is the Sensory-Afferent Electrical Stimulation (SAES), which consists of a peripheral stimulation directed to sensory (afferent) fibers with low amplitudes, usually around the sensory threshold. Its primary goal is to elicit changes in sensorimotor functions [97]. However, SAES has also been used for active and task-oriented therapies, to improve motor abilities and drive cortical plasticity [98].
On the other hand, when applied at the central level, the stimulation is referred to as Spinal Cord Stimulation (SCS). As the name suggests, it is delivered in the posterior region of the spinal cord. At first, afferent nerve fibers contained in the dorsal roots are stimulated then, through the synapses, efferent nerve fibers of the ventral roots are also triggered [99]. This technique is mainly used for spasticity (and eventual pain) reduction. Despite the majority of therapies employing implanted SCS, we hereby only consider its transcutaneous application.
All these stimulation strategies will be explained in detail later in Section 1.4.
Before a general overview of the stimulation working principle is presented together with a description of the stimulation parameters and their effect.

1.3.1. Working Principle

The stimulation is provided by delivering current to a volume of tissue between two electrodes (anode and cathode), with charges moving from the anode (positive electrode) to the cathode (negative electrode), as reported in Figure 1.3. The localized electric field creates an ionic flux through the cell membranes of nearby neurons which influences the

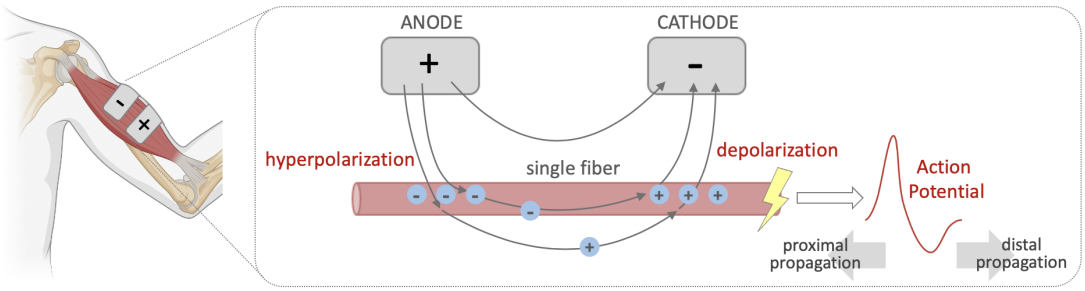

Figure 1.3: Neurophysiological working principle of the electrical stimulation. Considering the zoom over the single fiber, we notice a localized electric field generated by the movement of ions from the anode toward the cathode. This induces a hyperpolarization below the anode and a depolarization beneath the cathode, triggering the Action Potential wave.

transmembrane potential. In particular, membrane hyperpolarization occurs under the anode due to the accumulation of negative ions while depolarization occurs under the cathode as it attracts positive ions [100]. If the depolarization overcomes a critical threshold, the migration of sodium ions from the extracellular to the intracellular space generates an Action Potential (AP) [101], which propagates in both directions away from the site of stimulation: proximally towards the cell body and distally across the neuromuscular junction [100]. Given that the threshold charge needed for generating action potentials in muscle fibers is much higher than the one needed for inducing it in neurons [102], the electrical stimulation generally activates nerves rather than muscles. Consequently, for FES to be effective, it is required to have intact lower motor neurons, from the anterior horns of the spinal cord to the neuromuscular junctions of the target muscles [100]. This condition applies to both SCI and stroke pathologies and therefore electrical stimulation can be used as a therapeutic tool in such cases.

1.3.2. Stimulation Parameters

Electrical stimulation devices deliver pulses in waveform patterns represented by geometric shapes such as square, peaked, or sine waves. Most used ones are square waves, which demonstrated better fibers recruitment compared to other shapes [103]. Additionally, waveforms can be monophasic, biphasic or polyphasic depending on the number of pulses that form the single stimulus. Monophasic and biphasic waveforms are the most common ones: the former consists of repeated unidirectional identical pulses (usually cathodic), while the latter is composed by the repetition of two pulses, a cathodic (negative) one followed by an anodic (positive) one [101]. Both were demonstrated to produce greater torque than polyphasic waveforms when administered to quadriceps muscles of young individuals without disability [104]. Usually, the biphasic balanced pulses configuration is preferred as the positive and negative pulse balance each other, determining a total injected charge of zero that prevents potential damages at the electrode-tissue interface [102, 105].

The pulses' waveform is characterized by three parameters: pulse amplitude A, pulsewidth PW (or pulse duration) and pulse frequency f [37], as shown in Figure 1.4. **Pulse amplitude** is the magnitude of the pulse (usually expressed in mA), while **pulsewidth** is its duration (usually expressed in μs). Their product, called charge, determines the number of recruited muscle fibers. The higher the charge, the higher the number of recruited fibers and thus, for the spatial summation principle, the stronger the resulting contraction. Consequently, an increase in pulse duration may require a lower pulse amplitude to generate the same response, and vice versa [37]. **Pulse frequency**, instead, is the rate at

which stimulation pulses are delivered. By increasing the pulse frequency, the temporal summation of twitches results in a higher mean force [37]. It varies widely depending on the goals of the task or intervention, but optimal clinical results were obtained with 20-50 Hz [106, 107]. On one hand, higher frequencies result in a smoother and more comfortable stimulation as the individual pulses become indistinguishable [108]; on the other hand, higher frequencies boost the appearance of muscle fatigue [101]. Therefore, a trade-off in the definition of the stimulation frequency is required.

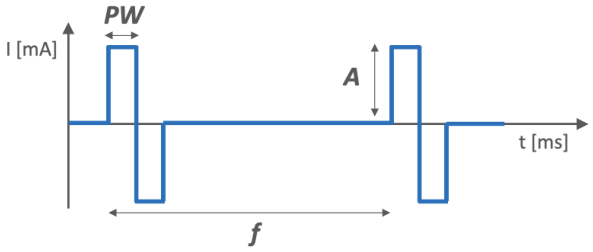

Figure 1.4: Parameters of the typical stimulation square wave: amplitude (A) in mA, frequency (f) in Hz and pulsewidth (PW) in μs.

1.3.3. Fibers Recruitment

The electrical stimulation-induced action potential is indistinguishable from the physiological one. This is due to the nature of the AP which is an *all-or-nothing* phenomenon meaning that, once initiated, it is always identical in terms of shape and duration. Conversely, the recruitment of motor units is significantly different in the two cases, which explains the early fatigue onset induced by FES. The main differences are hereby listed:

- **Recruitment Order**. The physiological recruitment order of motor units follows the Henneman's size principle, wherein smaller and fatigue-resistant motor units are engaged before larger ones [109]. This also helps to postpone the fatigue onset and to accurately modulate force [101]. Conversely, in the electrical stimulation case, this order is reversed. Type IIb fibers (fast-twitch ones and less resistant to fatigue), innervated by larger diameter axons, are activated first, then type IIa fibers (intermediate properties) and, in the end, type I (slow-twitch ones and resistant to fatigue), innervated by smaller diameter axons [100, 110, 111]. This happens because the firing threshold of nerve fibers to externally applied stimuli is inversely proportional to fiber size and proportional to the square of the stimulus-fiber distance [112].
- **Temporal Recruitment**. When using electrical stimulation, muscle fibers are stimulated all at the same time (temporal summation), in contrast to the natu-

ral unsynchronized activation characterized by turn-over among fibers (alternations of recruitment and de-recruitment periods) [113], that reduces the metabolic demand of motor units [114]. Consequently, a stimulation frequency of at least 15-20 Hz is required to get a tetanic contraction, higher than the one needed with the asynchronous physiological recruitment (6-8 Hz) [113]. The higher frequency of the electrically induced contraction increases the rate of muscular fatigue occurrence [101], which represents one of the main limitations when dealing with ES [115–117]. It may also cause uncoordinated and inefficient movement patterns, rather than the smooth force gradation typical of human movements.

- **Spatial Recruitment**. ES-induced motor units' recruitment follows a spatially fixed pattern, from superficial to deep layers with increasing levels of current (geometrical activation) [118, 119]. This occurs because surface-stimulating electrodes direct the current beneath the skin's surface and then it travels through various viscosities of subcutaneous tissue that introduce resistance, leading to a decrease in strength while going deeper.

1.3.4. Electrodes

The delivery of stimulation occurs through a pair of electrodes (cathode and anode) which can be: implanted, percutaneous or transcutaneous (superficial). These three types of electrodes are hereby briefly described; however, the present thesis will only consider transcutaneous ones, being those employed in our tests.
Implanted electrodes are surgically inserted into the body and connected by leads to an implanted stimulator [37], which communicates with an external control unit through a radiofrequency telemetry link [100]. These electrodes can provide a deeper stimulation and with a high repeatability and selectivity (isolated muscular contractions) using low levels of current. However, they require surgery and thus represent an expensive and invasive method, intended for long-term uses and with no possibility of replacing electrodes [37].
Percutaneous electrodes are implanted as well but their leads exit the skin and are connected to an external stimulator, not requiring a surgical intervention [120]. Since in this case leads pass through the skin, smaller wires are necessary [100]. Similarly to implanted ones, percutaneous electrodes enable a highly selective, repeatable and deep stimulation with low levels of current, but they are also associated with a risk of infection for the subject [37].
Transcutaneous electrodes are placed over the skin surface and are connected to an external stimulator [100]. They are localized either over the nerve or over the "motor point",

namely the site generating the strongest and most specific contraction at the lowest current amplitude. In this thesis, self-adhesive disposable pre-gelled (already incorporating a hydrogel layer) electrodes were used. These electrodes are easy to use, inexpensive, reversible and noninvasive and therefore particularly suitable for therapeutic applications. However, on the other hand, they are associated with some disadvantages: i) they do not allow selective and deep stimulation and may induce painful sensations because of cutaneous pain receptors activation [121]; ii) their repeated placement in the same location is complicated; iii) the drying out of their moisture over time deteriorates the skin adherence [122] and decreases the resistivity, which negatively affects the stimulation efficacy and comfort and possibly causes skin irritations; iv) their frequent use may be unhygienic as they are not washable or properly sanitized after use [123].
In this scenario, textile electrodes have been recently proposed as a valid alternative for FES delivery as they can be used for long periods if an adequate conveying of electric signals at the skin/electrode interface is guaranteed [124]. They were demonstrated to increase user comfort and reduce skin irritations, thanks to the good ventilation and flexibility, and they can be easily integrated into clothes and conveniently cleaned [123].

Depending on the relative position of electrodes over the skin area, monopolar and bipolar stimulation techniques are distinguished. The former is delivered in the form of monophasic pulses and is usually associated with two electrodes of different dimensions: a smaller *active* electrode (cathode) located over the target nerve or muscle and a larger *reference* electrode (anode) placed over a remote and less excitable tissue [125]. This configuration is ideal for selective muscle activation over a restricted area [126]. Conversely, in the bipolar one, usually a balanced biphasic pulse is used together with two electrodes of similar dimensions both applied over the target point.
Regardless of the used configuration, positioning of electrodes is a critical issue: identifying the optimal location for electrodes over the skin area requires a good knowledge of the human anatomical structure and sometimes a trial-and-error procedure is needed to verify that the resulting functional movement corresponds to the desired one [37].

1.4. Use of ES in Rehabilitation

As anticipated before, the term ES refers to various types of stimulation that differ in location, parameters, expected outcome and intended use. A schematic representation of the different types of stimulation and their main applications is depicted in Figure 1.5. The definition of the ideal stimulation strategy to be used in rehabilitation depends on the type of lesion. When considering CNS lesions, two macro-categories can be distinguished:

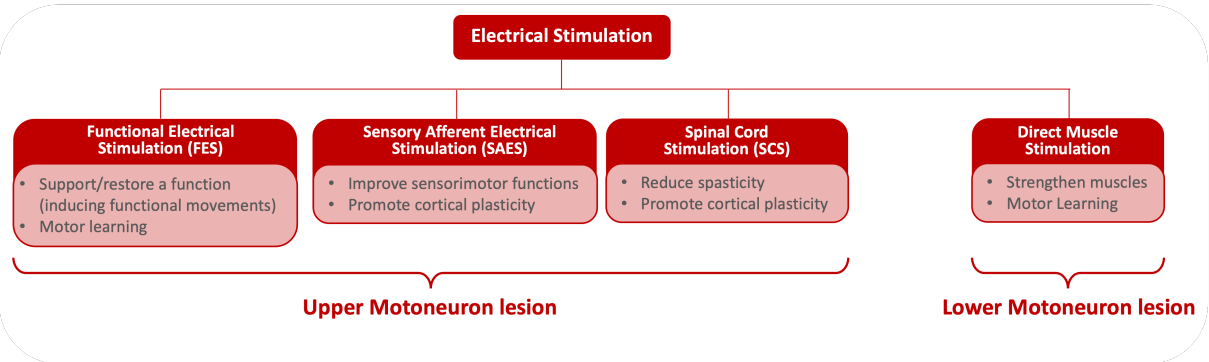

Figure 1.5: ES applications with their main usages. Different strategies are used for Upper and Lower Motoneuron Lesions [127].

Upper Motoneuron Lesion (UMNL) and Lower Motoneuron Lesion (LMNL). The former affects the Upper Motoneuron (UMN) which extends from the cerebral cortex to the motor anterior horn cells in the Spinal Cord (SC); the latter, instead, is localized at the Lower Motoneuron (LMN) level which goes from the anterior horn cells of SC, through peripheral nerves until reaching motor end plates of a muscle (Figure 1.6).
Depending on the localization of the lesion, the stimulation current is transmitted via a muscle or nerve fiber. In the LMNL, as peripheral nerves are not able to conduct signals anymore, direct muscle stimulation is used. In this case we talk about "denervated muscles" and the electric field elicits APs directly on muscle fibers. For the UMNL (more common), instead, nerve stimulation is employed, where cell membranes of neurons are depolarized and APs travel towards muscles, exploiting the residual conduction ability of peripheral nerves [100].

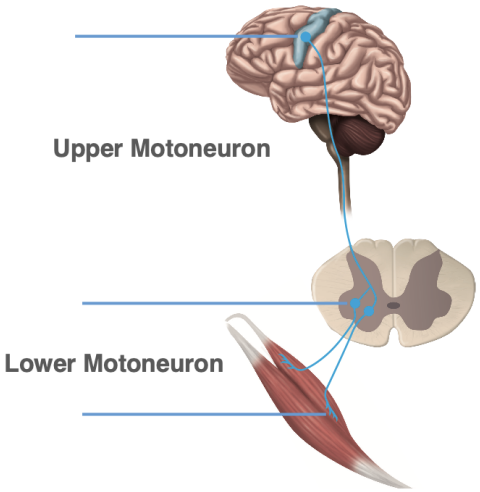

Figure 1.6: Localization of Upper Motoneuron (UMN) between brain and spinal cord and Lower Motoneuron (LMN) between spinal cord and peripheral muscles. Image adapted from [127].

The discrimination between nerve stimulation and direct muscle stimulation relies on the pulsewidth parameter. Specifically, the threshold charge for producing APs in neurons is much lower than that needed for muscles [102]. Given the direct proportionality between charge and pulsewidth, the same trend is observed for the pulsewidth used in the two scenarios. Figure 1.7a reports exemplary square waves for nerve and muscle stimulation respectively. The different excitability of nerve and muscle fibers is depicted in Figure 1.7b, where it is evident that nerve fibers can be activated from very low pulse durations, while muscle fibers require pulses of at least 10 ms.
Typical stimulation parameters for UMNL are pulsewidth of 200-400 μs and frequency within 20-50 Hz; for LMNL, instead, pulsewidth reaches 35-200 ms and consequently frequencies are lower, in the range of 0.25-22 Hz. Amplitudes cannot be defined because they depend on muscle size and subject perception [127]. In the former case, the current waveform is biphasic rectangular, in the latter it is either biphasic rectangular or biphasic triangular. In fact, triangular pulses reduce the perceived discomfort due to the ramped rise compared to rectangular pulses and preferentially activate muscles rather than nerves [128]. This happens because their moderate ramp causes a slow increase of the electrical field strength which determines the maintenance of an equilibrium of diffusion currents in neurons due to their fast-reacting electrical properties; differently, it induces an electrical discharge in the less sensitive membrane of denervated muscle fibers.

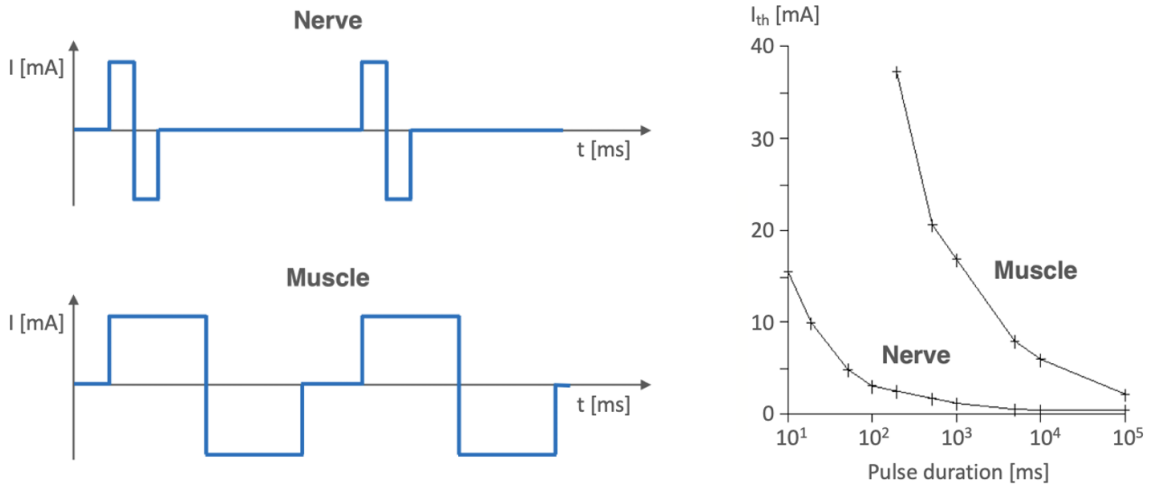

(a) (b)

Figure 1.7: (a) Stimulation square waves with shorter or longer pulsewidth for nerve and muscle stimulation, respectively. (b) Intensity-duration curves for pulses of nerve and muscle stimulation. Image taken from [129].

When the stimulation is administered to peripheral mixed nerves, both motor and sensory

fibers can be engaged. Therefore, electrically induced contractions can be generated by a combination of [130]:

- **Peripheral Recruitment**: activation of motor axons beneath the stimulating electrodes, producing a signal from the stimulation point to the muscle (orthodromic efferent), as depicted in Figure 1.8a. The discharge of the recruited motor units is represented by the M-wave in the electromyographic (EMG) signal.
  Additionally, the movement resulting from the muscle contraction generates sensory feedback traveling toward the center;
- **Central Recruitment**: activation of sensory axons producing a signal from the stimulation point to the CNS (orthodromic afferent), as depicted in Figure 1.8b. This sensory volley can contribute to the electrically evoked contraction because it reaches the spinal cord and there, through synapses, recruits motor neurons [131]. This recruitment generates a discharge of motor units (orthodromic reflex response) through the Hoffmann- or H-reflex pathway, which manifests as the H-wave in the EMG signal. This latter exhibits a higher latency compared to the M-wave, attributable to the longer pathway the signal takes through the spinal cord.

However, the coexistence of M-wave and H-wave is only visible in a small amplitude range. As sensory fibers are characterized by larger diameters, these present a lower firing threshold compared to motor ones and thus H-waves typically precede M-waves in the EMG signal. When using higher amplitudes, a greater number of motor fibers are activated, causing stronger contractions but at the same time increasing the antidromic transmission in motor axons. This latter collides with the descending reflex response, blocking its movement towards the periphery, as shown in Figure 1.8c. This phenomenon is known as *Collision Block* [133, 134]. Figure 1.9 reports the EMG signal obtained from a Tibialis Anterior muscle under electrical stimulation with growing intensity. At lower amplitudes only the H-wave is present, indicating a preferential activation of sensory fibers; then, as the amplitude increases, the M-wave also appears and we observe the progressive growth of the M-wave and shrinkage of the H-wave, until it disappears.

Therefore, to enhance the central contribution and exploit the advantages of afferent brain inputs, stimulation amplitude should be low enough to minimize the antidromic block, but sufficient for inducing stable contractions, useful for restoring movements [130].
Taking into account the influence of pulsewidth, shorter values (0.05–0.4 ms) preferentially activate motor axons [135], while longer ones (0.5–1 ms) recruit more sensory axons [136–138]. Lastly, stimulation frequency is directly proportional to the smoothness and strength of evoked contraction due to the temporal summation of M-waves. Nevertheless, it has

the opposite effect on central recruitment, which decreases at higher frequencies. This happens because H-reflexes are progressively attenuated by the post-activation depression of the synaptic transmission [139].

The recruitment of motor units through central pathways induces a sensory volley directed toward the center (i.e., the brain), determining the following benefits:

- Augmentation of contractions generated by peripheral pathways, leading to greater torques and to more fatigue-resistant contractions because central recruitment follows the size principle;
- Increase in sensorimotor cortex excitability and changes in motor cortical network activity [140], facilitating long-term and short-term neuroplasticity;

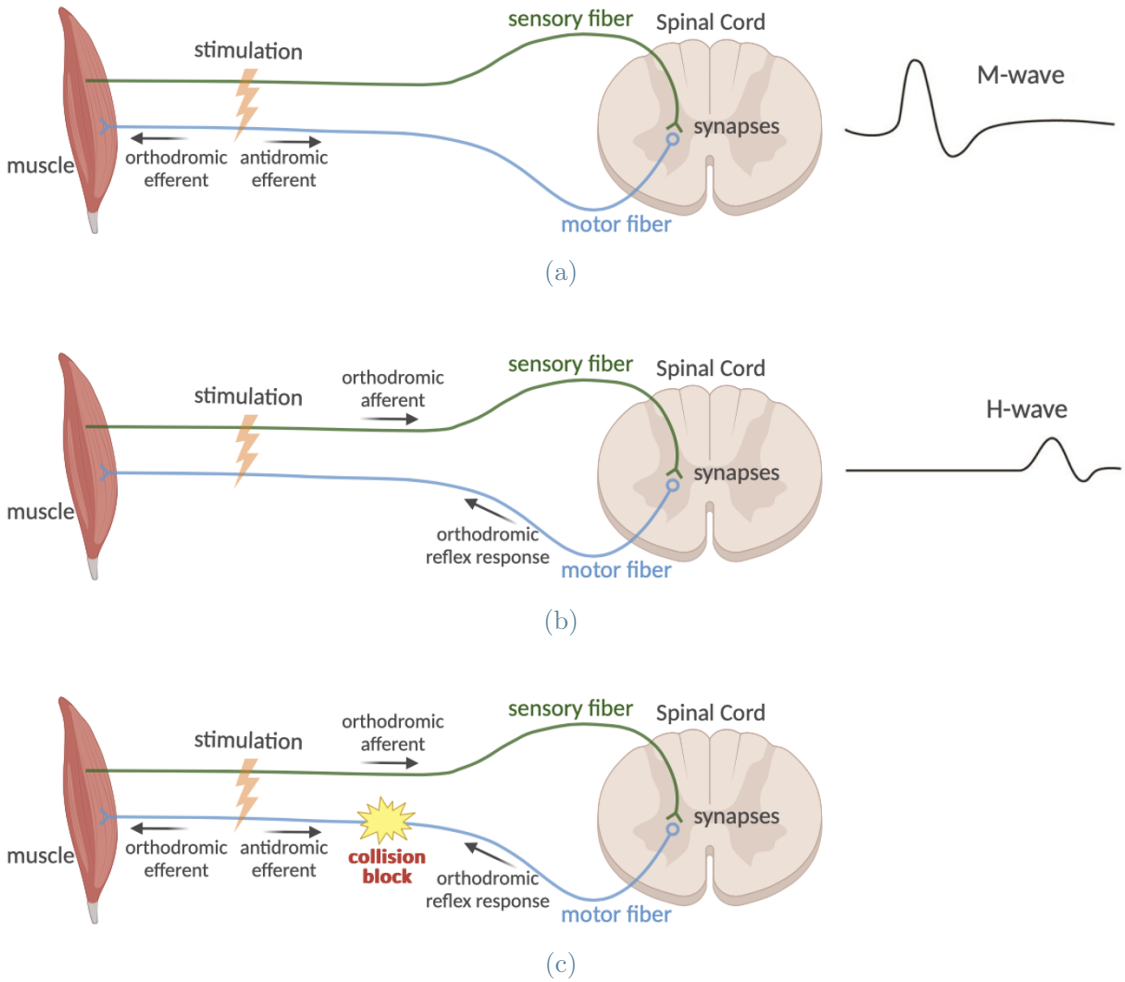

Figure 1.8: Schematic representation of the signal traveling along motor (panel a) and sensory (panel b) fibers after the stimulation and correspondent induced waves in the EMG signal. Panel c illustrates the *Collision Block* phenomenon occurring when opposite signals collide. Image adapted from [132] and drawn on *BioRender.com*.

- Possible enhancement of the NMES capability of reducing muscle atrophy and improving muscle quality [130].

All these processes could be summarized with the term **Neuromodulation** which is defined as "an intervention within the central or peripheral nervous system that alters electrical or chemical activities to modulate or improve a function" [141]. As previously said, we can differentiate between *Sensory* (afferent neurons), *Motor* (efferent neurons) and *Spinal Cord* stimulation, but all share the aim of retraining the nervous system and promoting *neural plasticity*, namely the reorganization of existent neuronal connections and the formation of new ones [141].
These aspects are particularly relevant when dealing with spinal cord injured patients as the decreased activity in their neural circuits reduces the CNS excitability [142], leading to weak brain-muscle pathways which could be enhanced by exploiting central inputs coming from the stimulation. Indeed, the idea that "neurons that fire together, wire together", coming from the Hebbian Theory [143], is always valid [144], regardless of the neural input origin (either physiological or electrically-induced).

Key elements for neuromodulation and neural plasticity are:

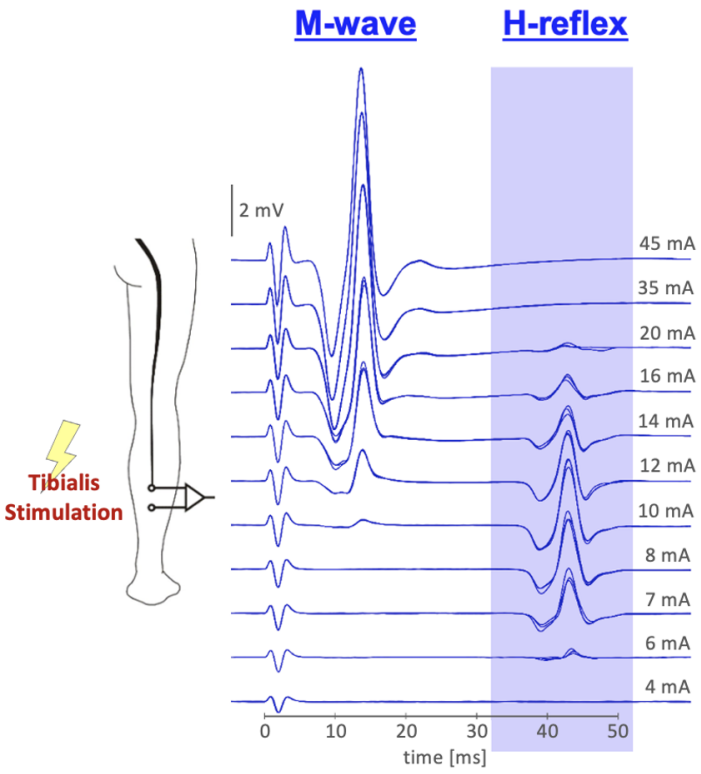

Figure 1.9: M-waves and H-waves induced on the Tibialis Anterior muscle during its stimulation at different amplitudes. Image realized by Matthias Krenn and used with his permission.

- Early start: as soon as possible after the lesion;
- Training intensity: neural circuits demonstrate use-dependent plasticity;
- Active subject participation;
- Repetitive and task-specific movements;
- Combination with conventional rehabilitation modalities.

1.4.1. Functional Electrical Stimulation (FES)

FES: Definition and Benefits

As previously anticipated, Functional Electrical Stimulation (FES) consists of delivering low-energy electrical pulses to the excitable tissue of muscles to induce an artificial contraction. This is usually used with neurologically impaired individuals to enhance or replace lost motor functions [145, 146].
Being applied in the case of UMNL, its typical pulsewidth and frequency are 200-400 μs and 20-50 Hz respectively, while its amplitude is above the movement threshold (to induce a functional task). The low pulsewidth suggests that, in this case, peripheral recruitment is predominant.
By coordinating the stimulation of different muscles, functional movements are obtained, implying that rehabilitation scenarios can derive significant advantages from FES-based treatments. As said, the primary benefit of FES lies in its ability to induce active muscle contractions and thus facilitate the practice of motor activities that would otherwise be hindered by paralysis. Besides this, FES is also associated with peripheral advantages. It was proven to strengthen muscles, thereby preventing disuse and atrophy, improve bone density, associated with a diminished risk of osteoporosis, and decrease spasticity and spasms [95]. Moreover, it improves general cardiovascular fitness and oxidative capacities [147], inducing the conversion of type IIB fibers, predominant in spinal cord injured patients, to type IIA and type I [148]. By increasing muscular blood flow and muscle mass [149], it also prevents pressure ulcers. In some cases, also benefits at the bladder, bowel, and sexual level were reported [150]. Furthermore, FES can engage users' attention, be repetitive and challenging, and provide sensory and visual movement feedback to participants, which are essential attributes for an intervention aimed at effectively promoting motor recovery [151].
Although being applied at the peripheral level, it was also demonstrated to induce central neurological changes. Indeed, FES targets the mixed nerve trunk and thus synchronously depolarizes motor and sensory axons (as shown in Figure 1.8a): the first (direct descend-

ing pathway) generates a contraction by depolarizing motoneurons; the second (indirect ascending pathway) provides afferent excitatory inputs to the center. This latter promotes neural plasticity and motor relearning by strengthening existent neural pathways or inducing the sprouting of new axons [152–155]. In fact, some key aspects of *Motor Learning* are encouraged by FES: high repetition, active practice, motivation, goal-oriented and task-specific training [156]. Thus, FES-induced repetitive movements increase the motor cortex excitability (following the Hebbian principle of activity-dependent neuroplasticity) and facilitate motor-evoked potentials [157].

This phenomenon is enhanced when FES is coordinated with the residual volitional activation of patients [153] because the proprioceptive information mediated by FES (through sensory fibers) determines an increased excitation of primary sensorimotor areas which produces long-lasting motor improvements [158]. Specifically, the combination of the volitional effort and the perception of successfully completing the movement (through FES) provides somatosensory feedback that facilitates Hebbian-like plasticity [159]. This combination also induces a sense of agency because the predicted sensory consequences of a movement align with the actual consequences, allowing patients to perceive the action as self-generated.

Additionally, this combination was proved to facilitate the *carry-over effect* as this latter was demonstrated to be mediated through movement prediction and sense of agency [160]. The *carry-over effect* is defined as the long-lasting persistence of stimulation's effects on the participants' abilities even after the treatment has concluded. It was observed in the study by Liberson and colleagues [96], which represents one of the first attempts to include FES in rehabilitation. They used FES to correct the foot drop, a common motor deficit in neurological patients [161] given by their inability to contract the tibialis anterior muscle and thus to lift the foot tip, making it difficult or impossible to walk. In such application, FES was triggered during the *toe-off* gait phase and then delivered throughout the whole swing to the peroneal nerve innervating the tibialis anterior muscle. Interestingly, they noticed that after stopping the stimulation, some patients were able to dorsiflex the foot by themselves.

The mechanism behind the *carry-over effect* is still unclear but Rushton's hypothesis is the most accredited explanation [87], based on the previously introduced concepts about FES. It states that the afferent input sent back to the brain allows to reinforce synapses and encourages neuroplasticity [101].

In conclusion, FES exerts a double rehabilitative effect [162]: the "orthotic" effect refers to the practice of lost movements and functions, enabled by the use of FES; the "therapeutic" effect, instead, considers the long-term recovery of functions and voluntary movements, observed also in the absence of FES [163]. This latter is associated with the activation

of cortical motor areas and residual efferent corticospinal pathways [164], and can be achieved after daily long-term use of FES for at least 6 months [165].

FES: Clinical Application

Before proceeding to the clinical application of FES, some precautions must be considered. As electrical pulses may affect tissues beyond the intended muscles, subjects should be excluded in the case of [37]:

- Poor skin conditions (pressure sores or irritations prevent the use of self-adhesive electrodes);
- Poorly controlled epilepsy;
- Significant autonomic dysreflexia;
- Pregnancy;
- Active implants (e.g., cardiac pacemakers, electric pump);
- Passive implants (e.g., orthopedic plates and screws)
- Cancerous tumor;
- Unhealed fractures;
- Suspected or uncontrolled cardiovascular conditions;
- Botulinum toxin therapy (subjects may not respond to stimulation).

Clinical applications of FES include assistive or therapeutic interventions that range from improving hand function and ambulation for achieving ADLs to restoring bladder or bowel control and respiration [100].
The term *Neuroprosthesis* is used to refer to these techniques, mainly implemented in individuals with stroke and SCI, that interface with their nervous system to restore impaired neurological functions and joint movements [166]. The basic components of a neuroprosthesis are: an electrical stimulator for generating electrical discharges, electrodes to deliver pulses, sensors for stimulation control and an orthosis to provide movement assistance [167]. The stimulator can have multiple stimulation channels, each of which consists of a pair of electrodes (cathode and anode) and can stimulate individual muscles [37].

Upper limb neuroprostheses are intended to facilitate grasping and reaching tasks. Within

grasping tools, the *Handmaster* (NESS Ltd., Ra'anana, Israel) [168] is one of the available options. It consists of a wrist-hand orthosis delivering a predefined opening/closing stimulation pattern to finger muscles at different amplitudes when the user pushes a button. In other systems, like *Bionic Glove* (University of Alberta) [169] or *Freehand* (Neuro-control Corporation) [170], the user directly controls the stimulation through his/her movements. The former includes a fingerless glove and a forearm sleeve, integrated with a displacement transducer recording wrist movements: wrist extensions trigger grasp while wrist flexions trigger hand opening, with an on/off stimulation pattern. Similarly, the latter uses motion sensors to detect wrist movements and subsequently provide stimulation to eight epimysial electrodes for fingers' flexion/extension. Other systems were designed to implement both reaching and grasping movements that could be obtained with surface electrical stimulation. Examples are *COMPEX Motion Neuroprosthesis for reaching and grasping* (ETHZ) [171] and *MyndMove* [172]. Both offer a fully programmable stimulation pattern that allows them to match users' needs.

Considering lower limb technologies, their main focus is on supporting standing and walking tasks. An example of a standing device is offered in [173] where a 16-channel implanted stimulator is used in combination with bilateral activation of thighs, hip, and trunk to allow paraplegics to stand upright. Considering walking, the simplest and oldest neuroprostheses are those for foot drop correction. They envision the stimulation of the peroneal nerve innervating the tibialis anterior muscles, triggered during the swing phase of gait by a foot switch. In the literature, there are examples using transcutaneous electrodes, such as in *Odstock* (Odstock Medical Limited) [174] or *Footlifter* (Elmetec A/S, Arhus, Denmark) [175], and others using implanted ones, like *STIMuSTEP* (University of Twente) [176] or *ActiGait* (Ottobock SE & CO. KGAA) [177]. Some other walking neuroprosthesis, instead, are designed for greater lower limb impairments and thus include a higher number of stimulation channels. Typically, in these cases, the user initiates the stimulation (e.g., by pressing a button), such as in the *COMPEX Motion FES system for walking* [178] or in *Parastep* (Sigmedics, Inc., Fairborn, Ohio) [179]. This latter enabled paraplegic individuals to walk for limited distances with a walker. Once initiated, the stimulation is then delivered to each leg according to the specific gait phase [180]. A more recent example is *NeuroSkin* (Kurage, Lyon, France) [181] which includes 12-channel bilateral stimulation and, with an AI-based controller, allows the definition of personalized muscle contraction sequences, resulting in a variety of functional movements. Many times these neuroprosthesis are used in combination with a passive [178] or active [182] orthosis, as in the *Hybrid Assistive System (HAS)*, to satisfy the requirement for high stability during waking.

Nevertheless, lower limb neuroprostheses still face limitations due to the rapid onset of muscle fatigue and the high effort demanded from the upper body to maintain balance [88].

The therapeutic effects of FES correspond to an improved capacity of users to voluntarily control their muscles, which persists even after discontinuing the use of the neuroprosthesis. In this scenario, FES may be used as part of a short-term intervention with the aim of inducing the carry-over effect, restoring patients' ability to move independently, without neuroprosthetic assistance.
After the earliest report of the carry-over effect, related to the use of a neuroprosthesis for the foot drop correction [183], further studies followed to formally examine this phenomenon. By comparing the effects of producing ankle dorsiflexion with the peroneal nerve stimulation against the traditional physiotherapy treatment, a torque three times higher was obtained in the first case compared to the second [184]. An improved plantar flexion after training with a walking neuroprosthesis was also reported in [185]. In a separate investigation [178], five patients with cervical and thoracic injuries underwent a 12- to 18-week intervention using the previously mentioned *COMPEX Motion FES system for walking*. Among them, four participants experienced improvements in both stride length and stepping frequency, leading to an overall increase in walking speed. The first concrete evidence of the FES ability to improve upper limb functions was reported by Popovic and colleagues [186] after applying a 6-month therapy with the Bionic Glove to cervical SCI subjects. Furthermore, the FES-mediated therapy was shown to yield significantly greater enhancements in hand functions of cervical SCI subjects compared to the conventional therapy [187, 188]. Notably, in some individuals these effects endured, and sometimes improved, months after the intervention.

FES: Limitations

The primary drawback of FES is the early onset of muscle fatigue [115–117], which prevents long-lasting rehabilitation sessions and complicates the modulation of muscle contractions. As previously pointed out, this is due to the inversion of the physiological motor fibers recruitment order [100, 111], the synchronous activation of fibers [113, 114] and the limited activation of deep structures when using superficial electrodes [91, 189]. A second limitation is the complex control of the electrically induced movements due to the non-linear relation between the generated current and the produced torque [190–192], strongly dependent on the specific subject. This may cause insufficient joint torques to generate reliable limbs movement and body support [63]. The difficulty of accurately

modeling the response to muscle activation is particularly evident in multi-joint motions, where it is further complicated by the physiological delays in muscle response to applied stimulation [193].

1.4.2. Sensory Afferent Electrical Stimulation (SAES)

SAES: Definition and Benefits

Sensory Afferent Electrical Stimulation (SAES) consists of stimulating sensory nerve fibers and triggering afferent APs, which lead to an increased sensory input to the brain sensorimotor centers that enhances changes in sensorimotor functions [97]. SAES has been used in active and task-oriented therapies, to improve motor abilities and drive cortical plasticity [98]. Indeed, even if targeting sensory nerves, this stimulation also determines the trans-synaptic activation of motor nerves. This is the H-reflex response induced in motor fibers (explained in Section 1.4), which can be observed in the EMG activity of peripheral muscles when stimulating their nerves at low amplitudes. Then, if the amplitude is increased, also the M-wave appears, resulting from the direct motor fibers stimulation. This technique induces neuromodulatory effects in the area of short-term plasticity, long-term plasticity and structural neuroplasticity with the sprouting of new synapses (*synaptic sprouting*) and the formation of new anatomical connections (*wiring*) in the nervous system [194].
If the stimulation lasts 30 minutes, the duration of the neuromodulatory effects is in the range of a few hours [195, 196], while with prolongation and repetition of the stimulation, longer-lasting effects are possible.
It usually employs standard self-adhesive electrodes, but the sensory afferent input can be increased by using anodes in the form of electrode gloves or socks, due to the larger stimulated area [194].
In these practices, the current is usually delivered with an amplitude equivalent to 120% of the sensory threshold, a duration of 30-60 minutes and a frequency between 10 and 50 Hz [196]. However, the optimal parameters and stimulation patterns for SAES are not yet exactly known [197]. Based on the literature, stimulation frequency and intensity seem to have the greatest influence on neuromodulation; in fact, similar neuromodulatory effects were obtained with lower frequencies but higher amplitudes.

SAES: Clinical Application

In literature, neuromodulatory effects through SAES were demonstrated in an fMRI study involving a finger-to-thumb tap paradigm (Test Motor Task, TMT) [195]. Specifically, the brain activity of both hemispheres during the tapping was increased when performed after 30 minutes of SAES and this increase lasted for two hours after the stimulation. The reason is that SAES enhances the Local Field Potential (LFP) of the sensorimotor cortex and changes its excitability. Consequently, this facilitates the recruitment of the motor neurons involved in finger-to-thumb tapping, thus getting an additional functional gain, through the transformation of pre-existing silent synapses into functional ones.
This neuroplastic effect is confirmed by the fact that SAES was also observed to increase the amplitude of Motor Evoked Potentials (MEPs) of the stimulated muscle, which is a typical manifestation of plastic changes in the motor cortex [198].
Considering that increased motor excitability in a muscle typically correlates with enhanced muscle functionality, this phenomenon may be particularly effective in treating muscle weakness resulting from stroke, as demonstrated by Ridding and colleagues [155]. Their idea was that in case the motor cortical projection to a muscle has been damaged by stroke, then its size and excitability can be altered by stimulating the muscle afferently. Specifically, adjacent areas of the motor cortex take over some functions of the damaged area, thereby increasing the functionality of the weakened muscles.
SAES was also used in combination with daily motor therapy in stroke patients with sensorimotor paresis both in the subacute and chronic phase [197]. Higher functional benefits were observed in patients treated with the stimulation combined with the motor therapy, compared to those treated with the sole motor therapy [199]. One study [200] demonstrated that SAES significantly improved the maximum torque of the affected hand during dorsiflexion and also the performance in the Timed up-and-go test. The Ashworth score for spasticity was also reduced, but not significantly. This conclusion was confirmed by other studies testing repetitive motor training in two cases: with and without a preceding phase of SAES. They demonstrated that the former condition induced a better motor and somatosensory performance and facilitated training-induced effects [201, 202]. These findings were particularly relevant in those subjects with partially preserved voluntary movements and when the stimulation treatment was repeated daily [203].
Another reported application for SAES is in the therapy for neglect reduction [204].

SAES: Limitations

In addition to the general limitations related to the ES application, SAES presents a specific drawback related to the type of stimulated fibers. In fact, as previously explained, SAES targets sensory fibers as it exploits the advantages coming from afferent signals directed to the brain. However, as SAES is applied to peripheral mixed nerves, it also triggers motor fibers, generating the M-wave potential. SAES efficacy may be reduced by this motor fibers excitation, due to the collision block phenomenon among stimulated fibers. To limit this issue, more precise guidelines about the optimal electrode location that maximizes the stimulation of sensory nerve fibers are needed.

1.4.3. Spinal Cord Stimulation (SCS)

SCS: Definition and Benefits

Spinal Cord Stimulation (SCS) is a form of stimulation that targets spinal circuits by placing electrodes over the spinal cord. It is a neuromodulation technique capable of inducing neuroplastic changes, mainly used to treat spasticity and pain and to improve or facilitate motor functions [205].
An under-threshold continuous SCS modulates the excitability of spinal circuits, moving the central state of excitability closer to the motor threshold. By decreasing their activation threshold, it eases the processing of incoming inputs so that weak residual volitional signals become strong enough to induce an action potential on motor neurons (Figure 1.10).

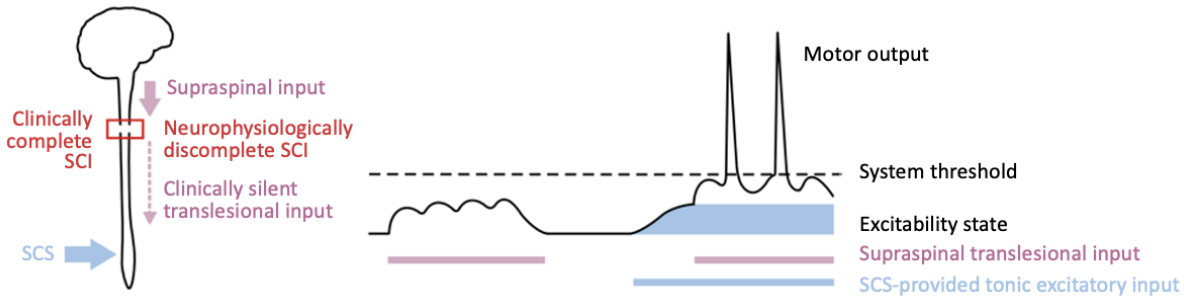

Figure 1.10: SCS-provided excitatory input moves the central state of excitability closer to the threshold and enables an otherwise ineffective supraspinal input to generate a motor output. Figure from Minassian et al., 2016 [206].

This would be helpful in many SCI patients, usually referred to as "*discomplete*" [207], where undamaged axons extending through the lesion are still present but unable to pro-

vide a voluntary signal strong enough to trigger lower motor neurons [208]. In such cases, the addition of the SCS input, lowering the neurons firing threshold, could enable residual voluntary signals to generate APs and therefore produce voluntary motor activities.
The SCS-related assistive effect is distinct from the one induced by FES. Rather than directly producing a movement, SCS facilitates the ability of residual propriospinal and supraspinal inputs to activate spinal motoneurons, thereby enabling volitional movement in previously paralyzed subjects [209, 210]. Thus, SCS rehabilitation has the potential to strengthen residual spinal pathways, both at the spinal and cortical levels.
It has been suggested that the combination of electrical stimulation with descending motor commands is essential for beneficial neuroplastic changes, resulting in a Hebbian-type learning effect [211]. In some cases, the obtained benefits and the recovery of voluntary movements persisted also in the absence of stimulation, after the end of the protocol [210, 212].
Previous studies [211] proved that SCS works similarly to peripheral NMES, with the difference that it targets the neuralgic center of motor neurons rather than the peripheral CNS. Specifically, being applied on the dorsal roots, it targets sensory afferent fibers, which have the lowest activation threshold due to their large diameter and to the myelin sheet [213]. Then, sensory fibers elicit an action potential in the efferent motor fibers by inter-synaptic excitation within the spinal cord, and the activation of motor fibers facilitates the muscular contraction (Figure 1.11).

Therefore, motor fibers are activated through a reflex activity [99], which is referred to as Posterior Root Muscle Reflex (PRM reflex) and represents the distinctive element of

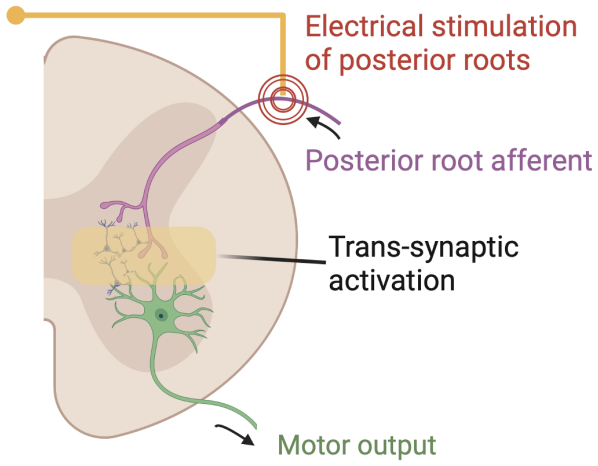

Figure 1.11: PRM reflex: the electrical stimulation causes an action potential in the sensory afferent fibers, which elicit the motor fibers through trans-synaptic activation, resulting in a short-latency muscular contraction (figure drawn on *BioRender.com*).

spinal stimulation. It can be observed in the EMG recordings of the main leg muscles, being the motor response to single pulses of current. The PRM reflex and the H-reflex are elicited by the same afferents but stimulated at different locations in the afferent reflex arc, either in the posterior roots of the SC or in the mixed peripheral nerves [214]. This was demonstrated in literature for the Triceps Surae muscle [215].
Furthermore, both signals show the Post-activation Depression (PaD) phenomenon, typical of reflex-mediated responses. It is defined as a reduction in Monosynaptic Excitatory Postsynaptic Potential (EPSP) which refers to the reduction of the potential induced in a postsynaptic motor fiber trans-synaptically stimulated by a sensory fiber, due to the previous activation of the same fiber [216]. Practically speaking, it means that when two close stimuli are delivered to the spinal cord, the EMG response to the second stimulus is either absent or much smaller in amplitude (depending on the Inter-Stimulus-Interval) compared to the one to the first stimulus [206, 214], as shown in Figure 1.12. This method was used in multiple studies to verify that the recorded EMGs are, in fact, due to SCS stimuli.
The main similarities and differences between the two reflexes are better detailed in the *State of the Art* section of Chapter 5 5.1.

Both Epidural SCS (eSCS) and Transcutaneous SCS (tSCS) exist, which are the invasive and non-invasive approaches respectively. The former uses implanted electrodes to deliver an electric current through percutaneous leads or an implanted device; the latter, instead, employs paravertebral and abdominal surface electrodes to stimulate the spinal

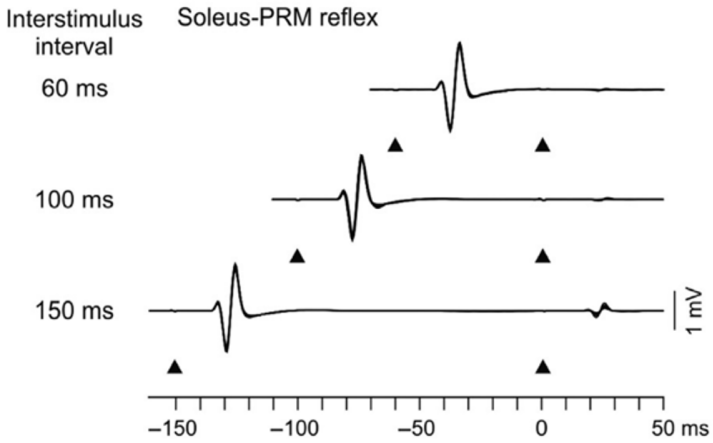

Figure 1.12: Post activation depression in the soleus muscle with PRM reflex elicited from transcutaneous SCS. Black triangles indicate the stimuli while waves represent the EMG response recorded on the soleus muscle. It is easily observed that the second stimulus does not generate a muscle response at all in the case of 60 ms interval, or a very low amplitude response in the case of 100 ms and 150 ms intervals. Figure from Minassian et al., 2007 [214].

circuitries, generating a current flow through the lower trunk.
In this work, we will focus on the second one because of its numerous advantages: non-invasiveness, affordability, suitability for short-term protocols, and compatibility with conventional and commercially available stimulation devices. Indeed, many complications are associated with epidural stimulation, such as the loss of electrodes' efficacy over time, the formation of masses around electrodes and the migration of the latter in 13 to 22% of implantation reports [217]. These latter lead to a loss of therapeutic efficacy as well as to neurological complications and infections, requiring additional clinical interventions. Hence, tSCS emerges as a safe and more accessible modality of SCS.
Additionally, many literature studies demonstrated that tSCS can increase limbs' function to a degree comparable to the implanted version [218–220]. Hofstoetter and colleagues [221] also compared the EMG responses of both methods for lumbar stimulation in SCI subjects and proved that the PRM responses were very similar in terms of EMG waveforms and onset latencies.
Nevertheless, due to the different electrode positions, the current flows and electric potentials induced by the two methods are different, with a higher selectivity in the epidural setting compared to the transcutaneous one. In the former case 80 to 90% of the current flows in the highly conductive cerebrospinal fluid, in which the posterior roots are immersed, generating a localized electric field. Conversely, in the latter case, the current flow is influenced by the conductivity properties of the numerous tissues between the skin and the posterior roots. At first, the current is directed below the electrodes, causing brief contractions of paraspinal and abdominal muscles, and then around the spine, with some current crossing the spine via soft tissues.

SCS: Clinical Application

The first applications of SCS date back to the 1960s', when Drs. Shealy and Mortimer [222] used it for reducing and modulating chronic neuropathic pain, given its ability to block pain signals traveling through nociceptive nerve fibers entering the dorsal horns of the spinal cord [223].
Then, as SCS was observed to modulate spinal circuits and induce neuroplastic changes, it was used to treat neurological discomforts and decreased motor abilities, typical of neuromuscular diseases, with positive results for the functional recovery of movements [99, 211, 215, 220, 224], reduction of spasticity [220, 225–227] and improved bladder function [228].
Additionally, multiple studies discussed the ability of SCS to exploit the capability of

residual spinal circuits, unaffected by neuromuscular damages [218, 229]. This is particularly relevant for those circuits involved with standing and walking because SCS is applied at the lumbar level, where the Central Pattern Generator (CPG) is located. This comprises biological neural circuits that produce rhythmic outputs in the lower limbs in the absence of rhythmic inputs [230]. Complex neural interactions participate in walking, making the weight shift from one leg to the other almost automatic and controlling the arms' oscillation during progression [229]. As these interactions are often unaffected by neurological injuries, SCS may engage them and exploit their residual functionality.
Minassian and colleagues [206] showed that epidural SCS at 22-50 Hz can generate locomotor-like EMG activity and induce leg flexion-extension movements in individuals with chronic, motor-complete SCI lying supine. In general, the use of spinal neurostimulation during cyclic movements has shown increased activation of CPG circuits and perceived motor facilitation both in walking [218, 231] and cycling [232]. Involved current intensities are quite high: from 30 to 200 mA [218], from 20 to 80 mA [231] and up to 180 mA [232].
Further literature studies reported that, thanks to epidural SCS, some patients were able to pass from using a wheelchair to maintaining the upright position without any external help [233]. Less severe cases also recovered part of lost movements due to the injury [210]. In another study [234], the positive combination of gait training and tSCS proved beneficial for regaining voluntary gait movements, with current intensity ranging from 80 to 180 mA.
The SCS application will be further discussed in Chapter 4, with a focus on the optimal settings (electrode position and stimulation parameters) to induce the PRM reflex and obtained effects.

SCS: Limitations

Practical limits for the application of the tSCS are i) the impossibility of using this technique on patients with a spinal metal implant (common in SCI patients); ii) the fact that patients are not able to position back electrodes by themselves but need the presence of a second person; iii) the higher risks associated with the delivery of this stimulation due to the high amplitudes involved.
A further limitation of tSCS is the fact that there is no clear consensus on its effects and benefits, in particular when considering recovery in terms of neuroplasticity. Neuroplastic changes were demonstrated after repeated sessions of tSCS and specific training, and they seemed greater when the stimulation was phasic, adapting the different stimulation

parameters to the different phases of the stride [212]. Nevertheless, further research is needed to better understand where and how these neuroplastic alterations occur. Furthermore, another aspect to be taken into account is the fact that the neuroplastic recovery may be reduced by the collision block of action potentials on sensory fibers. As previously explained in Section 1.4, when a nerve fiber is electrically stimulated, APs are generated in both the orthodromic and the antidromic directions. Those in the antidromic direction of sensory fibers (efferent) may collide with those that transmit proprioceptive information (afferent), preventing their propagation to the SC and the brain, which is fundamental for locomotion [235]. The probability of these collisions is proportional to the stimulation frequency but the percentage of erased proprioceptive information is proportional to its amplitude. One proposed solution is to exploit the temporal summation of APs, using instead low-amplitude stimuli with high-frequency that enable the same level of excitability as high-amplitude stimuli [235].
The collision block phenomenon is more pronounced in SCS compared to FES because of the higher involvement of sensory fibers [211], as SCS is directly applied to the SC where these fibers branch.

1.5. Hybrid systems

1.5.1. Definition, advantages and disadvantages

Previous sections introduced robot-assisted devices and electrical stimulation as rehabilitation tools that support the functional recovery and motor learning processes. However, it was also highlighted how their intrinsic limitations decrease the rehabilitation efficiency. The drawbacks of both approaches are hereby briefly recalled, as retrieved from literature reviews on this topic [63, 64] (refer to Sections 1.2 and 1.3 for higher details). Robotic devices provide support to the execution of movements and allow an intense and customized treatment. However, their excessive weight and encumbrance increase the system's energy demand for movement execution and discourage patients from using them. Additionally, it was proved that the induced functional improvements are not significantly higher than those of conventional therapies and do not necessarily translate into improvements in ADLs [236, 237]. On the other hand, electrical stimulation, in particular FES, enhances functional improvements, general physiological benefits and cortical reorganization. However, it is associated with the early onset of muscle fatigue [115–117] because, inducing a non-physiological fibers' recruitment [110], it increases the metabolic cost of movements that makes it unsuitable for long-lasting applications. Additionally, the management of

stimulation-induced movements is complicated by the non-linear relation between the injected current and the produced torque [190–192].
In this context, the cooperation of these two components into a single system, usually referred to as a hybrid system, has arisen as a promising approach for robotic rehabilitation. The rationale of this research lies in the idea that robotic systems have the potential to complement FES by supplying power and mitigating discomfort and fatigue [57]. Hybrid systems are defined as structures designed to facilitate motor function compensation and rehabilitation [63], offering a promising avenue to enhance the efficiency of rehabilitation therapies. They present a novel approach to rehabilitation that modulates the torque produced by stimulated muscles with the one coming from the robotic actuation so as to achieve the desired movement. At the same time, they address the limitations inherent in standalone robot-assisted training devices and FES applications [63, 64] and were in fact proved to be more beneficial than using FES or robotic assistance only [64].
These systems enable smooth and controlled limb motion and offer a more comprehensive sensorimotor experience compared to the sole robotic therapy because they trigger additional mechanoreceptors and muscle activity through stimulation [57].
Zhang et al. [238] stressed the urgent demand to combine the action of FES with the one of exoskeletons because the use of the sole robotic therapy produces an assistive torque, but only generates a passive limb movement. Consequently, it could induce the slacking effect (previously explained in Section 1.2), which can be instead avoided through the application of FES [57].
The primary advantage of hybrid solutions lies in the incorporation of stimulation, which imparts both physiological and functional benefits. Besides this, other advantages are connected to such devices [63]. By incorporating FES-induced torque input, they enable a reduction in the torque, and thus power, demand on actuators [239]. In the future, this could potentially enable the use of smaller motors and batteries, promoting the development of lighter systems that enhance the comfort and wearability for users. Furthermore, the mechanical support provided by these solutions determines smoother and more precise joint trajectories and lower current levels, thereby delaying the onset of muscular fatigue. This permits to extend the training duration and the number of repetitions, which is critical for rehabilitation.
Existing hybrid systems are categorized into orthotic and non-orthotic ones [64]:

1. **Orthotic-based**: further distinguished into semi-active and active [240]:

    a. Semi-active: the stimulation is the only power source for producing joint torques, while the robotic system just dissipates energy, generated by FES and gravitational forces, through brakes or clutches. The lack of active ele-

ments allows for low-weight and energy-efficient systems but also determines limited joint control and poor-quality trajectories. Indeed, these exoskeletons provide a correction only when FES-induced torques overcome those needed to accomplish the desired trajectory. So, they lose their efficacy when the patient is unable to supply muscle forces sufficiently high to perform the whole movement, which is common after some time when fatigue appears.

b. Active: both the stimulation and the robotic component are torque-generating devices because motors can either dissipate or deliver power to joints. In these solutions, a lack of muscular response or fatigue can be compensated, increasing the system's efficacy. However, the presence of actuators and their power supplies leads to cumbersome and energetically inefficient systems.

In both classes, orthotic robots need to transfer power to users' limbs and give mechanical support while adapting to the user's anatomy and guaranteeing his/her safety [64]. Moreover, the provided support should not be exaggerated; instead, rehabilitation should follow an "assist-as-needed" and "challenged-based" approach to observe improvements in cognitive and motor functions [72].

2. **Non-orthotic**: systems such as robotic footplates, mobile platforms or cycling systems.

1.5.2. Control strategies for hybrid systems

In hybrid systems, the joint activity of muscles and actuators contributes to the final movement, thus exoskeletons should be compliant structures that allow an active participation from the subject rather than imposing a rigid control. This "soft" behavior can be achieved by acting on the mechanical components of the robot or adopting particular control strategies. In the former case, this characteristic is attained by using soft structures based on textile technologies or by means of compliant actuators, such as Serial Elastic Actuators (SEA) or Variable Stiffness Actuators (VSA). SEAs include elastic components with fixed stiffness in series with the motor while VSAs allow them to modulate their stiffness according to the gait phase, simulating a more realistic behavior. The latter case, instead, is adopted when rigid actuators and structures are comprised in the system (which is the case of the present work). Here, the soft characteristic is achieved at the software level, implementing compliant control strategies that shape the mechanical impedance of the robot (i.e., the dynamic relationship between the robot position and/or velocity and external forces). Rather than controlling a position or a force, it acts on the

power transferred to the environment [241], virtually modifying the system stiffness.

Concerning the motor control of robots, this is based on closed-loop strategies, using torque or position feedback signals. In particular, two opposite control strategies are most commonly implemented in robots, namely the impedance and the admittance control [242]. The **Impedance control** requires a target kinematic trajectory and returns a force as output. It is composed of an inner force loop with a softening role, promoting mechanical user-robot compliance, and an outer position loop with a stiffening action that corrects trajectory errors. It deals with three possible formulations: the 0^th *order* one (pure stiffness control) which corresponds to a proportional (P) position controller, the 1^st *order* one which is a proportional-derivative (PD) position controller and the 2^nd *order* one equivalent to a proportional-integral-derivative (PID) velocity controller. The 1^st *order* impedance controller is the most used in rehabilitation robotics because, differently from a rigid position controller, it does not aim for the exact tracking of the desired trajectory but rather for a trade-off between trajectory errors and interaction forces.
On the other hand, the **Admittance control** represents the counterpart of the Impedance control as it provides a desired force profile as input and returns a position as output. Here, the force loop (softening the control) is the outer one, whereas the position loop (stiffening the system) is the inner one.

Concerning stimulation control, it features both open-loop and closed-loop approaches [63, 64].
The open-loop strategy consists of delivering a predefined stimulation pattern in feedforward to muscles, according to the task to be performed, usually triggered by a Finite State Machine (FSM) [238, 243–246]. This strategy is easier to implement but it does not allow any balancing between FES and exoskeleton power because the two systems work independently. Furthermore, it does not adapt to the varying performances of the user over time and thus it is prone to the risk of overstimulation causing early fatigue or exaggerated gait pattern. These factors negatively impact the overall equilibrium control of the subject and potentially threaten his safety.
An example of this control strategy is represented by the hybrid neuroprosthesis proposed by Kobetic et al. [247], based on implantable electrodes for muscular stimulation and a passive structure. To get the best trade-off between the stability required during standing and functional movements of the lower limbs during walking, they proposed a pre-defined stimulation pattern together with a Variable Constraint Hip Mechanism (VCHM). Depending on the gait phase, both the FES amplitude and the mechanical impedance were varied, with the whole system working with a Finite-State Machine (FSM) where phase

identification was performed thanks to force and position sensors. However, since FES was delivered through an open-loop control strategy, it was not possible to adapt stimulation parameters taking into account the onset of muscular fatigue.
The closed-loop strategy, instead, continuously modulates FES by optimizing a muscle performance indicator to track a desired joint torque or position. This is more promising and efficient than the open-loop strategy but also deals with a higher computational cost, considering the difficulty of obtaining reliable indicators of muscles' performance. In most of the cases reported in the literature, indirect measures were utilized.
One example is represented FES controllers aimed at minimizing the human-robot interaction torque while motors are entitled to ensure the tracking of the target trajectory [240, 248]. In the study by Ha and colleagues [239], instead, the muscle-generated torque was estimated as the difference between the torque exerted by the motor when walking without and with the FES assistance. This estimated muscle torque was then compared to the desired muscle torque and the minimization of their difference was the cost function used to shape the FES of the following step. Lastly, more recent studies [189, 249] managed stimulation with the sole joint position feedback, minimizing the tracking error between joints' actual and target trajectory.

1.5.3. Hybrid systems in literature: context and limitations

The first attempts of combining FES and powered devices date back to the 90's, with the work by Popovic and colleagues [182] representing one of the first examples Their evolution primarily occurred within the framework of lower-limb applications. This is given by the repetitive nature of typical lower-limb movements, such as walking or cycling, which makes them suitable for replication through FES-assistive patterns. Upper-limb movements, instead, being less stereotyped, are more difficult to perform with FES. This is caused by the fact that, regardless of adopting an open-loop or closed-loop strategy, the knowledge of the target movement trajectory is a prerequisite for the majority of FES controls. Indeed, open-loop approaches usually deliver FES through a predefined activation sequence, tailored to induce a specific target movement; closed-loop ones, instead, iteratively adjust stimulation parameters based on one indicator of the subject performance in executing the target motion.
However, the first examples of hybrid devices were simply applying the two components together but with independent controls, rather than developing cooperative strategies with a real integration between them.
Indeed, the main challenge of hybrid systems is the definition of a shared control able

to reduce the motor torque demand while increasing patients' participation. Various approaches were attempted, dealing with a different number of stimulation channels and motors [63]. Nevertheless, when considering complex functional and multi-joint movements, such as walking, the implementation of a hybrid cooperative system is still challenging.
The main difficulty is given by actuation redundancy, which refers to the condition where a double power source (FES and motor in this case) work on the same joint. A further challenge when developing hybrid devices is the complex muscle activation dynamics. This comprises the electromechanical delay (EMD), muscle fatigue, nonlinear and time-varying dynamics model, and uncertainties of muscle physiology parameters [250].
Many times researchers circumvented these problems by reducing the system's dimensionality or complexity. With regards to lower-limb examples, the redundancy problem was avoided either by superimposing the two technologies without any interaction among them [247], or by using the two actuations on different joints [251].
A further alternative, defined *muscle-first approach* was proposed by Nandor and colleagues [246]. It consisted of a control system where most of the kinetic energy was injected from FES-stimulated muscles while motors only provided assistance to guarantee task accomplishment.
Considering instead upper limb examples, in most cases, developed hybrid systems did not define a shared control strategy between the robotic and the FES components, but rather combined the two technologies through one of the following alternatives:

- The FES component is used for assistance, while the robotic one is only intended for gravitational support [252, 253], enabling muscles to relax and preventing fatigue, or to lock degrees of freedom [254];
- The robotic and the FES components are employed to actuate distinct sets of degrees of freedom thereby influencing the motion of different joints [252, 255]. Typically, the robot handles motions that need precision or substantial support, while FES is used for coarse movements.

The definition of non-integrated hybrid systems reduces their potential advantage, previously presented in Section 1.5.1 Recent research has thus shifted towards defining cooperative strategies where the FES and motor components share the same control loop and are thus aware of each other's state. This allows each component to respond to any inefficiencies of the other, compensating as needed to maintain optimal movement performance. One of the first examples of a hybrid cooperative system for the lower limbs is the one developed by del Ama et al. [240], while for the upper limbs the one of Wolf and colleagues [256].
An overview of the current state of the art about hybrid cooperative systems is provided

in the next chapter (Section 2.1), considering that they represent the main target of the presented research.
Despite the aforementioned benefits of hybrid solutions, the discussion on whether these systems provide significant improvements with respect to conventional therapies is still open (as explained in Section 1.2). Future research on the design and implementation of such devices is needed to drive stronger conclusions. Additionally, it would be particularly relevant to extend their testing to disabled subjects because current literature faces a limited number of studies involving SCI or stroke patients, the majority of which considered small sample sizes [239, 257].

1.6. Thesis goal and road map

In the context of neuromotor disorders, such as stroke and SCI, rehabilitation plays a main role in the lifes of affected subjects. Indeed, given the importance of brain plasticity and relearning processes, it supports the regain of fundamental functionalities for carrying out ADLs and increases patients' independence, ameliorating their quality of life [37]. Besides conventional therapies, different strategies were attempted over the years in the clinical setting, with the final objective of modulating patients' nervous system, and enhancing their physiological and physical functions [42]. This thesis discusses various applications of electrical stimulation, employing different parameters depending on the intended outcome, whether to attain general physiological benefits (such as spasticity and pain reduction) or to elicit functional movements. The central goal of this work lies in analyzing the different types of ES, with their usages and advantages, in the context of rehabilitation and neuromodulation, which aids the strengthening of residual neural connections and promotes the formation of new ones [43].

This goal was pursued through two research questions:

- "Is it possible to realize *hybrid* systems that integrate the use of FES with a robotic device?".
  Related to this, the first aim is to define a cooperative controller able to enhance the advantages of the two components while mitigating their disadvantages. Indeed, from the literature, it is known that the addition of robotic support may be promising in delaying stimulation-induced muscle fatigue, which is the main limit to prolonged stimulation training.
  However, stimulation-based neuroprostheses often deal with low usability due to their complex fit and the necessary presence of a therapist to accurately position the electrodes. Thus, the second objective is to enhance the usability and acceptability of stimulation-based systems by studying alternative solutions based on textile electrodes. Indeed, these latter are promising because, given their possible integration into clothes, they would ease the usability of the stimulation system, in particular the donning and doffing processes. This would also support the shift of rehabilitation from a clinical-based setting to a home-based one. This transition represents a growing trend in recent years as it simplifies the handling of the therapy for patients, not requiring them to reach the clinic or the hospital to get it.
- "How can alternative non-invasive ES solutions targeting afferent neural circuits enhance neuromodulation effects to their fullest potential?".

To address this question, two sub-studies were carried out: one applying the stimulation at the spinal level (SCS) and the other at the peripheral level (SAES).
From the literature, it is known that SCS, by triggering sensory afferent fibers, acts on the central state of excitability of the nervous system. Specifically, providing additional inputs to the spinal cord increases its activity level with the potential of strengthening existing connections or creating new ones. Previous studies [226] demonstrated the SCS ability to reduce spasticity by inhibiting the hyperactivity of antagonist muscles. Furthermore, considering the beneficial combination of electrical stimulation and descending motor commands, the increased excitatory level enabled by SCS could strengthen eventual weak residual signals and facilitate the firing of fibers to produce voluntary movements. We hereby aim to verify these observations and better understand their working principle.
Despite demonstrating advantages in the treatment of neuromuscular injuries, SCS is still difficult to apply outside the clinic. This is due to the high currents involved in this strategy with respect to peripheral ones, increasing the risks for the subject's safety, and the need for a second person to position electrodes on the spine. For this reason, the study of afferent stimulation was expanded to peripheral sensory stimulation (SAES). The rationale behind this research is to understand whether SAES could substitute SCS, considering that both are based on a reflex-mediated activity.
In this thesis, we do not demonstrate that the two types of stimulation prompt the same benefits, but we verified that they trigger the same spinal circuits. Despite being preliminary, this study paves the way for future studies on the therapeutic effects of the two strategies. In fact, demonstrating their interchangeable use would be relevant considering that SAES requires a less demanding application than SCS and thus allows a higher independence for the patient. This would also facilitate the transition from hospital-based to home-based settings, strongly promoted in recent years [258, 259].

The first research question was addressed by realizing a hybrid prototype, integrating two commercial electrical stimulators into a lower-limb exoskeleton, both at the hardware and software level, to generate a functional walking movement. Particular attention is given to the implemented control strategy, whose novelty lies in the fact that the two components are integrated into a shared loop, rather than simply summed on top of each other. A double validation of this hybrid control system was carried out: at first, it was tested on non-disabled subjects at the laboratory of the Politecnico di Milano; then it was applied to target users, namely individuals affected by neuromuscular diseases (complete/incomplete

SCI and stroke), recruited at Villa Beretta rehabilitation center. Significant advantages were demonstrated for the FES-robotic integration with respect to using the sole exoskeleton. In particular, the addition of FES allowed similar movement performances to the robotic-only condition, despite a significant motor torque reduction. Additionally, by engaging subjects' muscles in the movement execution, it increased the device's usability, as reported by users. Nevertheless, the developed system was also associated with some limitations, introducing possible improvements to be realized in the future.
Among these limitations, overall users reported low device usability ratings, despite the previously mentioned improvements in the condition with stimulation. The second study included in this research question addresses this topic by investigating the possibility of using textile electrodes in place of standard hydrogel ones, considered the gold standard for delivering stimulation. In particular, a new set of textile electrodes, obtained by integrating commercial screen-printed electrodes into textile strips, was validated. These latter were compared to hydrogel electrodes with the aim of understanding whether the two are comparable in terms of electrical properties and induced stimulation performances and comfort. Conducted tests, involving fourteen non-disabled subjects, demonstrated a similar behavior for the two types of electrodes. This result is promising for the possibility of substituting hydrogel electrodes with textile ones, particularly relevant when coming to home-based setups.
The second research question, instead, is addressed by developing an SCS cycling-based protocol, then tested on four SCI individuals. Results reported SCS-induced modulatory effects in the EMG signals, together with further non-motor SCS consequences. Besides being preliminary, given the low number of tested subjects and performed sessions, these observations are promising and in the same direction as literature ones.
The second aim of this research question, relative to the possibility of using SAES in place of SCS, is addressed by juxtaposing the two stimulations. In particular, the reflex waves induced in the muscles' EMG by the central and peripheral stimulation are compared in terms of shape, amplitude and latency. This work was carried out during the 6 months I spent at the Medical University of Vienna, where I collaborated with the group of Professor Winfried Mayr. This preliminary study proved a similar working principle for the two stimulations that trigger the sensory axons but at different locations along them. It paved the way for future works investigating whether the two stimulations also induce the same neuromodulation effects.

2 | Development and validation of a Hybrid system for walking

Chapter Highlights

The introduction about hybrid systems presented in the previous chapter (Section 1.5) highlighted the relevance that such systems could have in the rehabilitation of individuals affected by neuromotor disorders. However, it also pointed out that only a few studies in literature carried out cooperative controllers with a real interdependence of the two components.

Starting from this assumption, we developed a novel controller for a lower-limb hybrid exoskeleton with two actuated joints (hip and knee) and four stimulated muscles. In particular, a cooperative FES-motor component was developed at the knee level, which represents the main focus of the following study. This was then tested both on a group of non-disabled subjects and on target users (complete/incomplete SCI and post-stroke individuals).

The complete work is presented in this Chapter as follows. Section 2.1 presents the actual state of the art about hybrid cooperative devices, focusing on their control strategy. Then, Section 2.3 contains the development of our system, including a description of the used materials and the implemented control. Sections 2.4 and 2.5, instead, regard the two testing procedures with a description of the recruited subjects and of the experimental protocol, and a presentation of gathered results with their respective discussion. Finally, Section 2.7 summarizes the main conclusions of the study, along with its main limitations.

Chapter Contents

2.1 State of the Art 48
2.2 Objective of the study 58
2.3 Materials and Methods 59

2.3.1 Experimental Setup . . . 59
2.3.2 Calibration . . . 62
2.3.3 TwinFES control . . . 62
2.4 Testing on non-disabled subjects . . . 66
2.4.1 Experimental Protocol . . . 66
2.4.2 Data Analysis and Statistics . . . 67
2.4.3 Results . . . 67
2.5 Testing on target users . . . 74
2.5.1 Experimental Protocol . . . 74
2.5.2 Data Analysis and Statistics . . . 75
2.5.3 Results . . . 75
2.6 Discussion . . . 85
2.7 Conclusions . . . 87

2.1. State of the Art

As previously discussed in the introduction of this thesis, the integration of FES and robotic devices in the rehabilitation process can facilitate motor and functional recovery. Specifically, in recent years, increasing interest has grown around the possibility of combining these two technologies into hybrid structures to avoid the inherent limitations of standalone systems. As introduced in Section 1.5.1, the FES addition, besides providing the stimulation-related physiological advantages, allows the reduction of the power required from actuators and thus the creation of lighter systems with better usability. Additionally, the presence of mechanical support determines precise joint trajectories and lower current levels that delay the onset of muscular fatigue and prolong the training duration. Nevertheless, these advantages are obtained only in case of hybrid systems implementing FES-motor cooperative controllers, where the two technologies are not simply summed one over the other but integrated in a single control loop. Considering that these represent the focus of this research, the current state of the art about hybrid cooperative systems is hereby provided. It is presented by dividing the devices according to their FES control strategy, which is described along with its main advantages and disadvantages. In particular, four different approaches can be distinguished: open-loop control, Proportional Integrative Derivative (PID) control, Iterative Learning Control (ILC) and Model-Based control.

- **Open-loop control**. In this case FES follows a predetermined control pattern, without receiving any feedback on the state of the system or the user's performance. This represents the simplest control strategy, not requiring any muscle modeling process or extra force/torque sensors. However, its control performance is strongly limited by not accounting for the high variability of FES-induced muscle responses, in particular when considering muscles affected by fatigue. This control mainly relies on the muscle-generated torque to produce movements and employs the motor torque component only to compensate in the case of insufficient muscle power with the aim of ensuring good target trajectory tracking. To this end, it is commonly paired with a PID motor control, given its low computational effort and high robustness.

- **Proportional Integrative Derivative (PID) control**. This represents the most straightforward, yet effective approach to address a closed-loop strategy. It continuously adjusts the output with the aim of minimizing the error between the system's actual state and a reference, determining a real-time correction of deviations. Specifically, the Proportional component (P) takes into account the present error, the Derivative (D) its trend over time and the Integral (I) a prediction of its future behaviour.
  This control strategy is particularly suitable for motor management, while researchers claimed that it is not ideal in FES applications. This is due to the slow nature of FES-induced muscle responses [191, 239], where the relationship between the injected current and the resulting movement is non-linear and highly variable over time, while the PID hypothesizes a linear input-output connection. Indeed, the real-time and punctual correction of this controller may produce sharp current variations, which are not effective given the slow muscles' dynamics and may determine over-stimulation and uncomfortable sensations. Sometimes, muscle-joint models [260] were employed to define the relationship between the injected current, the recruited fibers, the produced torque and the final generated movement. However, the modeling process does not have any control duty, since it only manages the relationship between required torque and stimulation parameters.

- **Iterative Learning Control (ILC)**. It is a resilient close-loop strategy that continuously adjusts the system performance by incorporating insights from previous iterations. It involves strategic adjustments to the input variable with the primary objective of minimizing a cost function, evaluated at the end of each iteration [261, 262]. In this way, it avoids the real-time correction of the deviations from the target movement, which is complicated by the slow and highly variable nature of

FES-induced muscle responses [239]. Its iterative nature renders ILC exceptionally well-suited for cyclic activities, common in lower-limb movements (such as walking or cycling) [249].
All considered works developed a single-joint ILC FES-motor cooperation, even if dealing with multi-joint movements, such as walking [239, 240], sit-to-stand [249] or elbow flexion/extension movements [263]. Studies differ in the control variable to be minimized, used as ILC input; it could be the motor torque required to accomplish the movement [239], the interaction torque at the leg/exoskeleton interface [240] or the error between real and target positions [249, 263].

- **Model-Based control**. These controls were investigated to address non-cyclic movements, particularly common when dealing with the upper limbs. Recent model-based works focused on Model Predictive Control (MPC) algorithms [264, 265]. Given an a priori cost function to be minimized, the MPC can solve the optimal control problem. In particular, it uses the mathematical model of a system (the musculoskeletal system in this case) and its actual state (as an initial condition) to predict how it will behave over a finite time horizon. The control signals over the defined time period are numerically computed by minimizing a user-defined cost function. At each time step, it computes the torque requirement of the system by minimizing a user-specific cost function and successively divides it among the various actuators (FES, motors, etc.). The primary advantage of this approach is the fact that it does not require the previous estimation of the torque requirement needed to execute the movement. However, the presence of a pre-defined model required by model-based controls and the long-lasting calibrations associated with it represent their main disadvantage. In fact, subject- and session-specific tunings make such solutions not suitable for clinical applications that instead require rapid and automated calibrations. System models can be either linear or non-linear; the main disadvantage of using a linearized musculoskeletal model is that it may decrease its performance outside the linearization region [265].

In the following paragraph, the most relevant lower-limb literature examples are reported. Some works [238, 245] implemented the open-loop strategy for stimulating the Quadriceps during knee flexion/extension movements, paired with a model-based [245] or PID [238] motor control. In [245] the testing procedure was only carried out in simulation and on one subject without disability while in [238] the testing was more consistent, including four non-disabled subjects and five SCI individuals. Both cases reported a satisfying controller capability of tracking the desired trajectory.
The ILC approach, instead, was adopted by Molazadeh et al. [249] for carrying out sit-to-

stand movements. In particular, by testing it on 4 non-disabled users and 1 SCI subject, they demonstrated better trajectory tracking performance for this control when compared to a PID strategy.

Moreover, Ha et al. [239] implemented such control for the stimulation of Quadriceps and Hamstrings muscles combined with the PID actuation of hip and knee motors, with the final aim of generating walking movements. In particular, they combined the knee motor and the Quadriceps stimulation during the swing phase, while the hip motor and the Hamstrings stimulation during the stance phase.

A similar strategy was carried out by del-Ama et al. [240] with the difference that they only handled knee flexion-extension movements during walking by actuating the knee joint (PID control) in combination with Quadriceps and Hamstrings. Specifically, two different FES control strategies were carried out on the pulsewidth parameter: PID to stimulate Quadriceps (knee extension) during stance and ILC to stimulate Hamstrings (knee flexion) during swing. The aim of using a PID control was to stabilize the knee joint in the extended position, increasing pulsewidth in case of a non-complete extension (identified by a higher interaction torque), hypothesizing a linear relationship between interaction torque and FES amplitude. The risk of over-stimulation was avoided because the main joint stability was guaranteed by a rigidly PID-controlled knee motor, running in parallel to the FES PID, while the stimulation-induced torque was participating in the movement only to a small extent.

Both walking movement controls [239, 240], even if differing in the considered joints, muscles and gait phases, achieved satisfying results when tested on four non-disabled volunteers [240] and three SCI subjects [239], respectively. In particular, good trajectory tracking at both joints together with a reduction of the torque required from motors to execute the movement. The reduction of the motors' contribution demonstrates that the added input (i.e., the FES-induced muscle torque) positively participates in the movement.

Despite being preliminary, because of the limited number of tested subjects, their results are promising and should be followed by future research on this topic. In particular, by demonstrating the possibility of reducing the energy demand to motors, they pave the way for the future fabrication of exoskeletons with less powerful motors that, being smaller and lighter, could improve the wearability and acceptability of such structures.

The model-based approach was employed, both for the FES and motor component, by Chang and colleagues [266] who developed a full-body hybrid system for locomotion. In particular, they combined knee motor actuation with the stimulation of Hamstrings and Quadriceps to induce knee flexions and extensions respectively. The cooperative strategy used kinematic and stiffness controllers to manage motors and FES respectively, allowing

a dynamic allocation of actuation to motors and FES.
The system, tested on three non-disabled users, demonstrated repeatable and consistent joint trajectories. Nevertheless, the knee joint tracking performance was negatively influenced by the muscle activation input delay, such that authors highlighted the necessity of estimating it to implement delay-free controllers. Furthermore, they pointed out that also the influence of fatigue should be included in the control design, as this would be particularly relevant when using the system with its target population, represented by individuals with movement disorders.
Other literature works [264, 265] adopted the MPC approach to perform single-joint flexion-extension movements by integrating the Quadriceps stimulation with the knee motor actuation. In the former study, the hybrid condition was compared with the only-motor and only-FES ones. It reported better tracking performance with respect to the only-FES one and similar to the only-motor one, which, however, required higher motor torque. In the latter, instead, a PD motor controller was added in parallel to the MPC one to overcome possible model-related uncertainties, which represent an intrinsic characteristic of MPC models. By comparing the with- and without-PD alternatives, the first one resulted in better tracking performance, suggesting that model imperfections may inhibit system usability.
In [264] the control strategy was employed during stair ascent and descent while in [265] it was used for tracking single-joint time-varying trajectories within a test bench knee exoskeleton. The adoption of the single-joint approach, besides being easier to control includes fewer complexities for the subject as it does not involve the stability of the whole body. In fact, one big issue of dealing with the gait activity is the fact that a control failure not only results in a wrong movement execution but also attempts the safety of the user.
Future studies on this approach should extend to other movements and also increase the number of tested subjects as both cited works only considered one non-disabled subject and one SCI.
Moving to model-based applications in multi-joint movements, synergy-based controllers were recently proposed as a promising alternative to overcome actuators' redundancy. They reduce the system's dimension by solving low-dimensional problems which enable the use of few control signals for multiple actuators. The inspiration comes from the Central Nervous System (CNS) which handles the over-actuated musculoskeletal system by activating muscle fibers not individually but in groups called synergies to simplify the task.
This approach was first attempted by Alibeji et al. [189, 257] who reported satisfying results even if preliminary as only testing one non-disabled subject. Nevertheless, the

resulting controller was difficult to interpret because synergies may not have a direct physical meaning. Additionally, it required extensive system identification experiments to find subject-specific model parameters and recruitment curves, that strongly limit the system's usability.
Interestingly, some of the previously mentioned works also included a fatigue estimation strategy, given that it represents the primary cause hindering the long-term usability of such structures in particular when dealing with disabled individuals. The management of muscle fatigue aims at maintaining the desired muscle torque output, enabling the correct task execution, also in the presence of fatigue.
In [239, 240], a reduction of the FES-produced torque was adopted as an indicator of muscle fatigue. Once it appeared, it determined either a modification or cessation of the FES delivery for a certain time, to let muscles recover. Actually, as the direct measure of the torque generated by muscles is not available, an estimate of it was adopted: either the interaction torque at the human-exoskeleton interface [240], or the total torque difference among only-motor and hybrid trials [239]. Both studies considered a uniform effect of fatigue for all muscles, while future studies should try to monitor each muscle independently.
In [238], even if not directly addressing muscle fatigue, they defined variable stimulation and motor gains, adjusted depending on torque variations. As soon as registering a reduction in the total torque compared to the target one (attributed to a decrease in the FES-generated torque), the exoskeleton gain was increased to compensate for this reduction and guarantee the correct movement execution. Given the variable nature of muscle-induced contractions, the modulation of the FES and motor participation in the movement is ideal as it allows to establish real cooperation between the two components, where one compensates the other.
Additionally, they mitigated the fatigue appearance by reducing the periods in which FES was provided, using it only during the active phases of the movement. In particular, FES was delivered only during the swing phase of walking. During the stance phase, instead, brakes or other locking systems were used to guarantee the subject stability. In this way, the total amount of injected current was reduced and, consequently, the muscle fatigue onset was delayed. A similar approach was also employed in [189].

Considering that the present study deals with a lower-limb hybrid system, a schematic summary of the most relevant studies developing cooperative controllers intended for lower-limbs hybrid systems is reported in Table 2.1.
Overall, the state of the art highlights the relevance of lower-limb hybrid systems for walk-

ing and demonstrates an increasing interest towards them. In the present study, starting from the reviewed literature, we developed a system where real FES-motor cooperation is present and particular attention is given to evaluating the motor torque reduction enabled. Differently from many literature studies comprising small sample sizes, a wide evaluation procedure was carried out involving twelve non-disabled participants and eleven users with neuromuscular disorders. Furthermore, being non-model-based, the novel device enables fast calibration procedures which are mandatory when considering a possible clinical application.

In the following paragraph, some upper-limb literature examples are reported.
In [256, 267], FES was integrated with the elbow motor (PID control) to produce its flexion/extension. The FES component implemented either an open-loop strategy [267] or a combination of open-loop and model-based ones [256]. In [256] seven non-disabled subjects were tested, while in [267] only simulation experiments were carried out. In both cases, this control strategy was identified as not appropriate for the FES control, highlighting the need to adopt closed-loop strategies or incorporate the motor component to refine movements and minimize trajectory errors. To this end, Burchielli et al. [267] introduced the possibility of varying the torque allocation between FES and the motor. However, the allocation update was done at the end of an exercise repetition and did not strongly affect the FES ability to react to trajectory tracking inaccuracies.
An elbow hybrid exoskeleton, combining an electric motor with FES to assist flexion/extension movements, was also developed by Stewart et al. [268]. They implemented a model to express the elbow angular position as a function of the stimulation parameters and defined two control loops: one relative to the user contribution (both the volitional and the FES-induced one) and dealing with position feedback; the other dedicated to the motor and considering the support percentage allocated to it, whose update depends on trajectory tracking performance. While the support percentage update was fast, stimulation parameters were gradually updated to comply with the slow dynamics of muscles. This allowed the motor to provide its contribution to the movement only when the user's one was not enough to fulfill precise trajectory tracking (in a range from no assistance to gravity compensation to active arm manipulation). The main limitation of this study was its small sample size, only comprising one non-disabled user.
A greater number of subjects (15 non-disabled individuals) was instead included in the work by Cazenave et al. [57], where the stimulation of wrist flexor/extensor muscles was integrated in a one-DOF wrist robotic interface. Here the use of muscle models was avoided by handling the FES control with a linear mapping of the current amplitude between a minimum and a maximum value. Different types of assistance were tested and

the hybrid condition exhibited superior tracking performances and movement smoothness with respect to the sole FES and comparable to those of the only-motor one. The hybrid alternative also demonstrated a significantly higher muscle effort, attributed to the presence of stimulation, which enhances muscle contraction, voluntary contribution and user engagement. Additionally, it was proven to reduce mental demand, promoting the recovery process.

With regards to the ILC strategy, the only work found in the literature is the one by Dalla Gasperina et al. [263] (from our laboratory) who implemented the FES-motor cooperation during elbow flexion/extension movements. Differently from other works [57, 269], this is also the first example among upper-limb systems where fatigue was explicitly addressed. Despite being only tested on 12 subjects without disability, this study reported promising results both in terms of reducing energy consumption and delaying the onset of fatigue. Moreover, satisfying trajectory-tracking performances were reported by this novel controller, which just employed the motor to partially compensate for the arm's weight and to refine significant trajectory errors with a low-stiffness impedance controller.

A similar control was used by Ferrari et al. [270] who managed knee flexion/extensions with an EMG-triggered FES strategy. Additionally, they addressed the voluntary contribution as an actual torque component in the control loop, shaping the FES and motor contributions accordingly.

A model-based control was implemented by Dunkelberger et al. [193] within a powered 4-DOF forearm exoskeleton intended for both wrist and elbow trajectory-tracking tasks. Similarly to [264], they also included a PID loop at the motor level, in parallel to the main MPC controller, to limit model-related imperfections. Their tests comprised 10 non-disabled users performing elbow and wrist flexion/extension independently. By comparing the hybrid condition with the only-motor one, the former demonstrated better performances in terms of trajectory tracking and torque reduction.

A more recent study from the same group [269] attempted to develop a synergy-based controller for the management of multi-joint movements, as previously done in [189].

Study	Materials		Control	Testing	Results
	motor	**FES**			
Hybrid FES-robot cooperative control of ambulatory gait rehabilitation exoskeleton *del-Ama et al., 2014* [240]	Knee-ankle-foot Exo (Kinesis) with knee motor	knee extensors (rectus+vastus) and flexors (biceps femoris + semitendinosus)	Single-joint cooperative control. i) Stance: knee motor + extensors ii) Swing: knee motor + flexors **Motors**: impedance control **Stimulation**: ILC for flexors; PID for extensors	4 non-disabled Walking 6 minutes	Good trajectory tracking (despite decrease in motor stiffness) Lower motor torque in hybrid case
An approach for the cooperative control of FES with a powered exoskeleton during level walking for persons with paraplegia *Ha et al., 2016* [239]	Exo with Hip and Knee motor (Indego)	Quadriceps and Hamstrings	Single-joint cooperative control. i) Stance: hip motor + hamstrings (hip extension) ii) Swing: knee motor + quadriceps (knee extension) **Motors**: PD control **Stimulation**: ILC on target torque	3 cSCI Walking 10 minutes	Joints position consistent with/without FES Torque reduced in hybrid case
Cooperative control for a hybrid rehabilitation system combining functional electrical stimulation and robotic exoskeleton *Zhang et al., 2017* [238]	Single-joint Exo with Knee motor	Quadriceps and Hamstrings	Single-joint cooperative control. Target torque split between exo and FES (δ_{EXO} and δ_{FES}) **Motors**: FB control **Stimulation**: FF control	5 non-disabled + 4 SCI Knee flexion/extension	Reached angle not influenced by δ_{FES} Exo torque decreases as δ_{FES} increases
Model-based dynamic control allocation in a hybrid neuroprosthesis *Kirsch et al., 2017* [265]	Single-joint Exo with Knee motor	Quadriceps	Single-joint cooperative control **Motors**: Close-loop on target position **Stimulation**: intensity modeled from current amplitude	1 non-disabled + 1 SCI i) Parameters estimate ii) Knee extensions in various conditions	Better tracking performance in hybrid than FES-only Lower motor torque in hybrid than motor-only.

An adaptive low-dimensional control to compensate for actuator redundancy and FES-induced muscle fatigue in a hybrid neuroprosthesis *Alibeji et al., 2017* [189]	Hybrid Exo with Hip and Knee motors	Quadriceps and Hamstrings	Full-Body hybrid system (cooperative only in swing) Synergy-based model for target position tracking. Electro-Mechanical Delay (EMD) and FES-related fatigue dynamics are considered.	1 non-disabled i) Parameters estimate ii) Walking 6 steps	Good gait reproducibility Better tracking performances compared to other controllers
A tube-based model predictive control method to regulate a knee joint with functional electrical stimulation and electric motor assist *Bao et al., 2020* [264]	Single-joint Exo with Knee motor	Quadriceps	Single-joint cooperative control. Tube-based NMPC (to constrain error between actual and target position to a small region) + FB control for motors.	1 non-disabled + 1 SCI i) Parameters estimate ii) Knee extensions (NMPC-only and NMPC + FB)	Better position tracking with FB compared to without FB
Closed-loop torque and kinematic control of a hybrid lower-limb exoskeleton for treadmill walking *Chang et al., 2022* [266]	Exo with Hip and Knee motor	Quadriceps and Hamstrings	Single-joint cooperative control **Motors**: current under kinematic (hip) or stiffness controller (knee) **Stimulation**: kinematic controller on stimulation PW	3 non-disabled Walking 3 minutes	Repeatable and consistent kinematic joint trajectories
An Iterative Learning Controller for a Switched Cooperative Allocation Strategy During Sit-to-Stand Tasks with a Hybrid Exoskeleton *Molazadeh et al., 2022* [249]	Exo with Hip and Knee motor	Quadriceps	Single-joint cooperative control NN-based Iterative Learning Controller (NNILC) to minimize position error Input dynamically allocated to FES and motors	4 non-disabled + 1 cSCI 4 sessions of 20 sit-to-stand movements	Trajectory RMSE reduced by 46.20% (knee) and 53.34% (hip) after 4 iterations

Table 2.1: Schematic table of main cooperative controllers developed in the literature for the control of lower-limbs hybrid approaches. Each study's characteristics are reported in terms of materials, methods (control), carried-out testing and key results.

2.2. Objective of the study

The aim of this work was to develop a hybrid cooperative control modulating FES and motor assistance based on trajectory tracking errors. It was implemented in a four-degrees-of-freedom (DOFs) exoskeleton integrated with an 8-channel neuroprosthesis, both controlled with a closed-loop strategy. The final device was defined as *TwinFES* and was intended to support locomotion.
The main advantage of this system lies in its capability of iteratively adapting to subjects' performance, without requiring a pre-defined model. Indeed, few non-model-based literature studies exist [239, 240] and their validation was limited to non-disabled subjects or a few individuals with disability. Here, instead, we provide an extensive testing procedure both on non-disabled subjects and on target users. These latter comprised complete and incomplete SCI and post-stroke individuals. Former tests on subjects without disability aimed at proving the developed system's feasibility and its ability to reduce motor torque, thanks to the FES addition, while preserving safe walking. These experiments were carried out both during knee flexion/extension movements (single-joint setup), which represent a simplified condition, and during walking (whole-body gait setup). Latter tests on target users, instead, had a double objective: demonstrating the ability of the *TwinFES* system to reduce motor torques compared to the *Twin* one, also in case of people with weakness and poor control of their muscles, and comparing the two devices in terms of system usability, acceptability, user experience and human-exoskeleton interaction.
Given the intended clinical use of the device, a further objective was the development of a fast calibration procedure, leveraging on the fact of dealing with a non-model-based device.

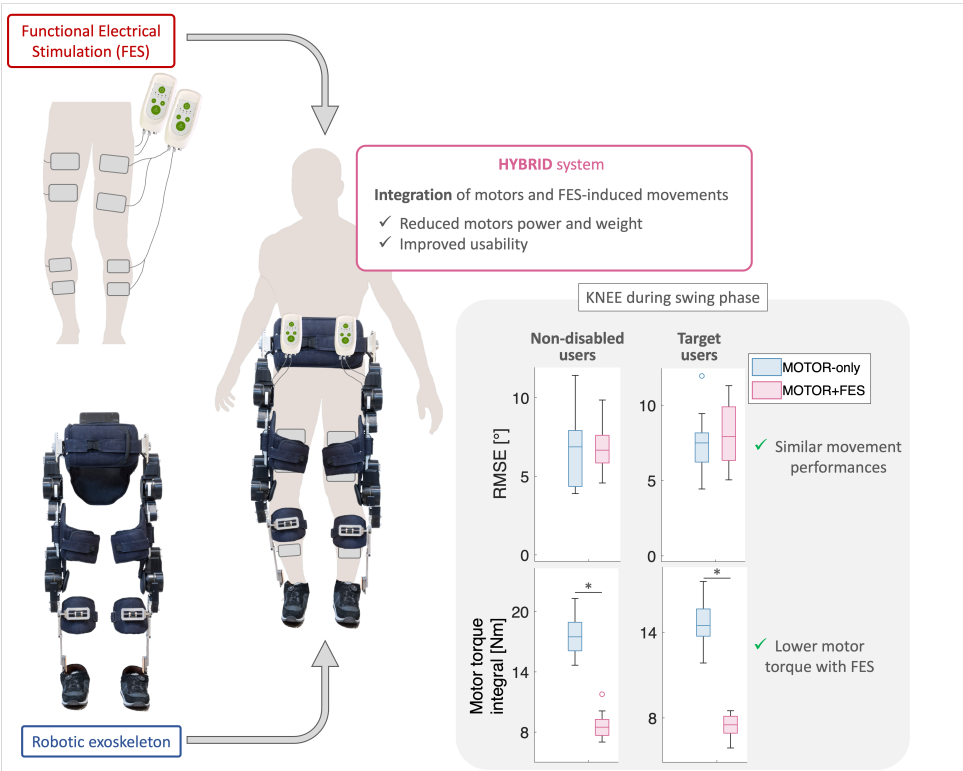

Figure 2.1: Graphical representation of the work: the rationale and the objective of realizing a hybrid system, together with the main results.

Lastly, preliminary considerations on the eventual muscular fatigue induced while using the *TwinFES* system were also carried out.
A graphical abstract of this work is offered in Figure 2.1 where the integration of FES and the robotic exoskeleton is shown, together with the key obtained results.

2.3. Materials and Methods

2.3.1. Experimental Setup

The Central Control Unit (CCU) of the *TwinFES* device is an ARM Cortex-M4 microcontroller programmed in C++, running at 500 Hz. It integrates the robotic and stimulation components of the system, which are reported in Figure 2.2 and hereby described.

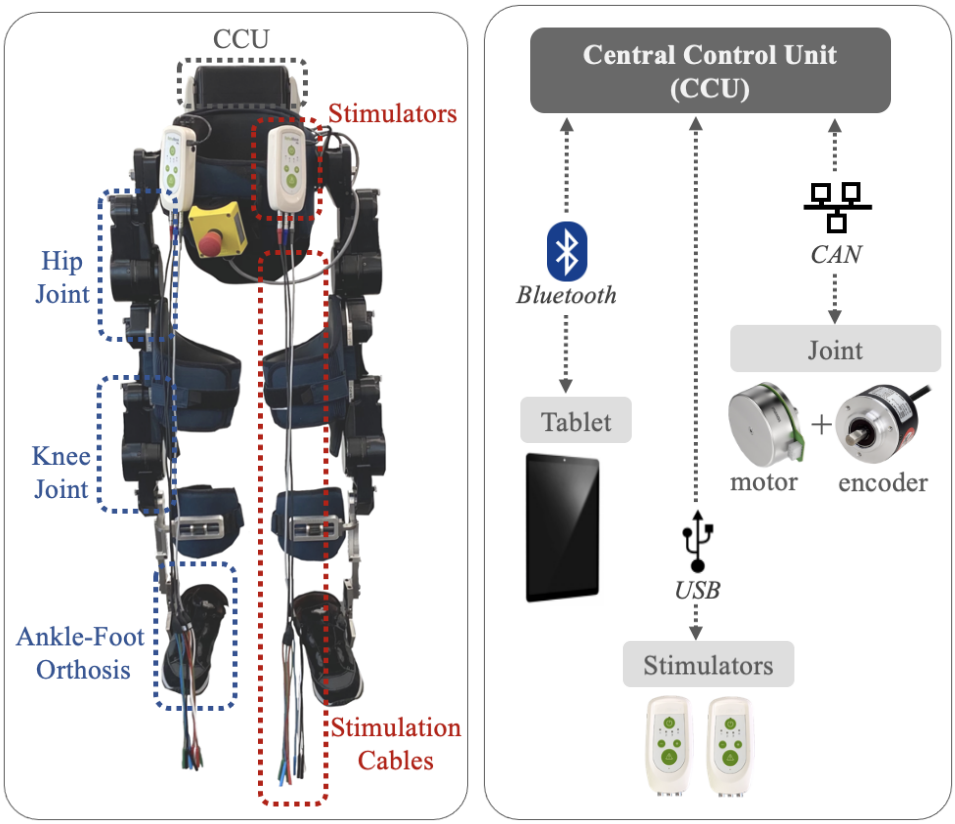

(a) (b)

Figure 2.2: (a) Hardware components of the TwinFES hybrid device: the Twin exoskeleton and the two RehaMove3 stimulators with their cables. (b) A scheme of the connections between components.

Robotic component

The *Twin* exoskeleton is employed in this work. It is a motorized lower-limb exoskeleton developed by the IIT-INAIL Rehab Technologies Lab of the Italian Institute of Technology (IIT) [77, 271], in collaboration

with the INAIL Prosthesis Center.
It was designed for the neuromotor rehabilitation of gait in subjects with lower limb mobility deficits, specifically SCI or stroke, as they experience a partial or complete loss of muscle functions in their lower limbs, preventing normal walking [271].
Its structure comprises four actuation modules positioned at the hip and knee joints of both legs and five rigid connecting links: a pelvic component and four separate segments for the femur and tibia of the right and left side respectively. Movement transmission between the structure and the subject's limbs is achieved through five ergonomic fabric interfaces (braces) attached to the his/her pelvis, thighs and lower legs on both sides. At the ankle level, two passive Ankle-Foot Orthoses (AFOs) are connected to shoes. These can be either locked at 90° or unlocked with a Range Of Motion (ROM) of ±20°. Both links and braces come in various sizes to easily adapt to individuals with different anthropometric characteristics.
Each actuation module includes a motor unit and a sensing unit, working at 2 kHz. The former comprises a BLDC Maxon motor EC90 Flat, with a gearbox ratio of 100:1 and a driver board controlling it; the latter, instead, includes an incremental encoder for the acquisition of the joint angular position.
At the trunk level, the exoskeleton is equipped with a backpack containing batteries, IMUs, the emergency button and the CCU of the exoskeleton. The used batteries are Lithium batteries (Accutronics CMX820P Li-ion batteries) with a nominal voltage of 28.8 V and a maximum current peak of 15 A. The emergency button is used in case of dangerous situations for the user. Once pressed, it cuts the power to the actuation units and thus all joints are released slowly (due to friction), allowing an operator to assist the user on time. The CCU is the exoskeleton's motherboard, referred to as SMEx (*Scheda Madre Exo*), which is the same ARM Cortex-M4 microcontroller we used for the *TwinFES* device. It receives information from sensors and sends signals to motors, based on what is defined by the therapist. This latter is in fact responsible for handling the overall session by defining the activities that the exoskeleton should perform through a custom application running on an Android tablet.
The communication of the CCU with the actuation unit is based on the CAN protocol, the one with the batteries on the I^2C protocol and the one with the tablet on the BLE (Bluetooth Low-Energy) protocol.
Given that the exoskeleton structure is not self-balancing, users are required to maintain balance through their upper limbs by using walking aids such as crutches or walkers. Consequently, users must have sufficient trunk and upper limb function (listed as inclusion criteria) and learn to balance and shift their weight to achieve an efficient walking pattern.
Twin is intended for rehabilitative use only and thus is confined to dedicated facilities, under the close supervision of healthcare professionals that must assist users during the whole activity. A session with the device requires at least two operators, one ensuring user safety and the other managing the overall training through the tablet.

Stimulation component

Two commercial neuromuscular current-controlled electrical stimulators (RehaMove3, Hasomed GmbH), one per leg, were integrated into the exoskeleton CCU. Each of them includes four stimulation channels, enabling the simultaneous stimulation of four different muscle groups, which in our case were: Quadriceps, Hamstrings, Gastrocnemius, Tibialis Anterior. Each channel was connected to a pair of surface self-adhesive electrodes (Pals®from Axelgaard Manufacturing Ltd.) with a rectangular shape of 5x9 cm, placed on the target muscle. The stimulation waveform was defined as rectangular biphasic because it is charge-balanced, and thus it does not induce net polarization, and it promotes an efficient muscle fibers

recruitment [105].
Stimulators were connected via USB to the CCU, which set the following stimulation parameters: frequency in Hz, pulsewidth in μs and amplitude in mA.
The stimulators' integration was not only at the physical (hardware) level but also at the software one. In fact, the exoskeleton software was modified accordingly to include the control of the stimulators.

Inclusion Criteria	Exclusion Criteria
• Age > 18 years	• Pregnancy or breastfeeding
• Height range: 150 - 192 cm	• Previous or present malignant neoplasia
• Weight: maximum 90 Kg	• Previous severe neurological damage
• Femur length: 355 – 475 mm, Tibia length: 405 – 485 mm	• Chronic inflammatory diseases affecting lower limb joints
• Hip circumference: 690 - 990 mm	• Severe osteoporosis of hips or spine
• Shoe size: 36 - 45	• Pelvic fractures or unstable spine
• SCI: complete and incomplete, acute and chronic, injury level <T4	• Significant limitations in the range of motion of hips and knees
• Stroke: ischemic and hemorrhagic, acute, able to ambulate (FAC* level >2)	• Severe or uncontrolled spasticity and autonomic dysreflexia
• Spasticity: Modified Ashworth <= 2	• Presence of a cardiac pacemaker
• Sufficient upper limb strength to use crutches or a walker safely	• Skin integrity problems at the interface with the device or stimulation electrodes
• Ability to use FES	• Complete lack of response to FES
• Ability to provide the informed consent	• Inability to provide the informed consent

*Functional Ambulation Categories (FAC) is a 0-5 scale to evaluate the ambulation capacity, with 0 meaning "non-functional ambulator" and 10 meaning "independent ambulator".

Table 2.2: Inclusion and exclusion criteria for the experimental protocol

The inclusion/exclusion criteria defined for the *TwinFES* device are listed in Table 2.2.

Walking sessions with the *TwinFES* device were supervised by two therapists, one in charge of physically supporting the user and the other managing the overall session. His interface with the device was facilitated by a custom application running on the Android tablet, obtained by modifying the original *Twin* application. This App allowed the configuration of subject-specific parameters, the calibration of the stimulation (better explained in Section 2.3.2), the selection of the operating mode and settings (e.g., stimulation and step parameters) and the saving of users' progress over time.

2.3.2. Calibration

Before starting a therapeutic session with *TwinFES*, a calibration of the subject-specific and session-specific stimulation parameters was carried out. This only involved current amplitude because during all tests both frequency and pulsewidth were kept constant at 40 Hz and 400 μs, respectively. During the calibration phase, the user is seated without wearing the exoskeleton and with his/her feet not touching the ground, allowing free knee flexion/extension movements. This procedure is performed through the *TwinFES* application, for one muscle at a time and repeated identically for all stimulated muscles. The minimum stimulation amplitude delivered by the device is fixed a priori to 4 mA. Then, starting from this value, the subject receives a stimulation ramp of increasing current and two intensity levels are defined:

- Level 1 – I_{L1} (Movement threshold): the value that produces a first limb movement;
- Level 2 – I_{L2} (Maximum threshold): the minimum value between the one producing a full joint movement and the highest one tolerated by the subject.

These levels define the ranges of stimulation amplitude used by *TwinFES*.
The calibration procedure was repeated before each session because, even if dealing with the same subject, different calibration values could be identified as they depend on the specific electrode placement and on the highly variable muscles' response.

2.3.3. TwinFES control

A model-free strategy was defined to iteratively modulate motor and FES inputs while easing and accelerating calibration procedures, which is an essential requirement for the clinical usability of the device.
Figure 2.3a offers an overview of the control strategy implemented in *TwinFES*, with different controllers implemented for joints and muscles depending on the gait phase. For safety issues, during the stance phase a rigid control was implemented for both joints and FES was superimposed to motors and managed with an open-loop modality. The same approach was applied to the hip during the swing phase, given the difficulty of getting FES-induced movements from hip flexors. This hybrid control was defined as *synchronized* because the two components share the same timing but operate independently.
Differently, the hybrid control developed for the knee during the swing phase was named *cooperative* because a shared input signal modulated the two components to actively collaborate in the movement generation.
Both cases did not consider any volitional contribution from subjects.

Synchronized Control
At the motor level, a rigid position control was implemented, based on a Proportional Integral (PI) strategy that computed the PWM (Pulse-Width Modulation) duty cycle to minimize position errors (i.e., the difference between target and actual angular positions). It resulted in a precise tracking of the target walking trajectory, not comprising any voluntary participation from the subject.

Regarding FES, frequency and pulsewidth were maintained constant while current was modulated in open-loop following a biomimetic stimulation timing to mimic muscles' activations during a physiological

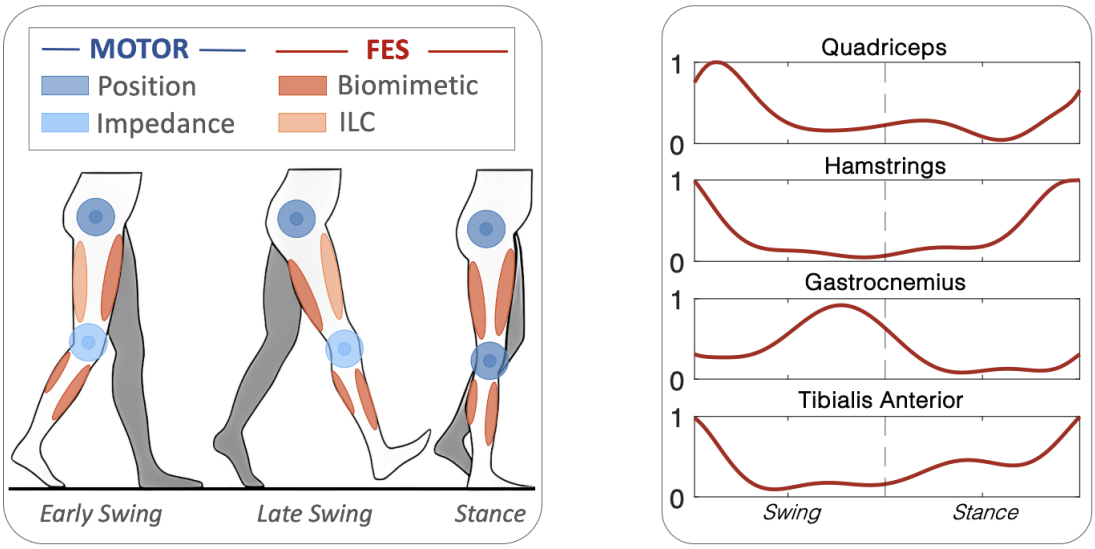

(a) (b)

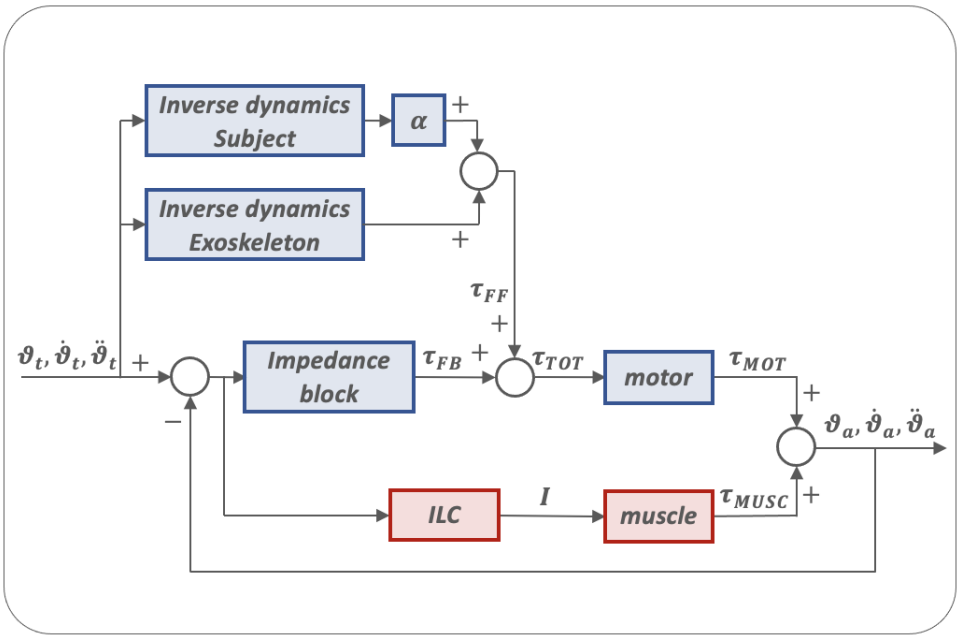

(c)

Figure 2.3: (a) Overall FES and motor control strategies for locomotion. Depending on the gait phase, joint motors are controlled either in position or impedance, while muscles are controlled either with biomimetic or ILC strategy. (b) Biomimetic stimulation profiles derived from literature EMG recordings [272, 273] and used for the synchronized control. (c) Cooperative control scheme. θ_t, $\dot{\theta}_t$, $\ddot{\theta}_t$ and θ_a, $\dot{\theta}_a$, $\ddot{\theta}_a$ are target and actual position, velocity and acceleration. τ_{FF}, τ_{FB} and τ_{TOT} are the feedforward, feedback and total torque components computed. τ_{TOT} is transferred to the motor and τ_{MOT} is the real exerted motor torque. α is the percentage of the subject's shank weight compensated by the motor. I is the FES current computed by the ILC block and delivered to muscles, generating the muscle torque τ_{MUSC}.

gait, retrieved from literature EMG recordings [272, 273]. Essentially, this represents a position control as muscle contractions were coordinated based on the gait timing and thus on the joints' position.
For Quadriceps and Hamstrings, the amplitude is always below the movement threshold because any induced movement would collide with the rigid control of the motor. In this case, the aim is to exploit the stimulation advantages and the neuroplastic benefits coming from sending sensory inputs to the brain, coordinated with the executed movement.
Differently, for Gastrocnemius and Tibialis Anterior, as they do not directly act on a motorized joint, the current level can be either above or below the movement threshold. In the former case, the AFO must be unlocked to allow functional movements ("push off" for Gastrocnemius and "foot clearance" for Tibialis Anterior).
For each channel j, at sample i, Eq. 2.1 defines the delivered current amplitude:

$$I_j(i) = I_{min,j} + (I_{max,j} - I_{min,j}) \cdot act_j(i) \tag{2.1}$$

where $I_{min,j}$ is the minimum current for the j^{th} channel (fixed to 4 mA for all channels) and $I_{max,j}$ is the maximum current for the j^{th} channel, equal to either $I_{L1,j}$ or $I_{L2,j}$, depending on whether the under- or over-movement threshold case is considered. $act_j(i)$ is a [0,1] value indicating muscles' activity level at each sample i of the gait cycle, retrieved from physiological activation patterns (Figure 2.3b).
The final result was a predefined current profile over the gait cycle, specific for each muscle, aiming at coordinating the delivered current with the executed movement.

Cooperative Control

The cooperative control (Figure 2.3c) simultaneously modulates the knee joint motor assistance and the current amplitude delivered to either Hamstrings (early swing) or Quadriceps (late swing). Motor and FES share the same input (i.e., angular signal) to carry out a dual task: FES primarily contributes to movement generation while reducing the motor torque; conversely, the faster motor component guarantees the correct task execution. Thus, it considers the co-participation of muscles and motors in the generation of the overall movement, which results in a "softer" tracking of the target trajectory.
The choice of not using this control at the knee and hip level during the stance phase was due to the high rigidity demanded from the stance leg in that phase, to guarantee subjects' stability. This aspect is particularly relevant when dealing with complete SCI individuals who do not present any residual muscle activation in the lower limbs. Additionally, this control was not used for the hip joint during the swing phase because a multi-joint cooperative control was not feasible as both Quadriceps and Hamstrings are bi-articular muscles (acting on the hip and knee joints) with an opposite effect and thus it was not possible to use them to induce at the same time a hip and knee flexion (1st half of swing) and extension (2nd half of swing). For example, to induce hip flexion at the beginning of the swing, Quadriceps stimulation would be needed, but this would also induce a knee extension that is not appropriate in this phase. The opposite occurs in the second part of the swing phase when hip extension would require Hamstrings stimulation, which would also determine an undesired knee flexion. Thus, the only possible solution was to use this system only for the swing knee joint.

At the motor level, a 1st order implicit impedance controller is implemented which guarantees compliant actuation of the knee motor and performs a trade-off between target trajectory tracking and human-robot interaction forces. Thus, instead of forcing precise tracking, as in rigid position control, impedance-based

strategies promote a more compliant behaviour (virtual spring-damper correction), which permits deviations from the target trajectory [242]. The impedance control is defined as implicit because the system is not equipped with torque sensors at the joint level and therefore it was not possible to measure the actual torque generated at the output shaft of the joint [242]. Consequently, the torque control was implemented through an open-loop control based on the motor's current flow.
Its architecture shows two nested loops: an internal torque loop and an external position-feedback loop. The former one computes the torque needed to support the movement (τ_{FF}), considering inertia and gravity contributions of both the exoskeleton and the subject's shank. This is then adjusted by an allocation index $\alpha \in [0, 1]$, indicating the proportion of the subject's shank weight compensated by the motor (Eq. 2.2) [274]. When $\alpha = 100\%$ both the exoskeleton and the user component are compensated, when $\alpha = 0\%$, instead, only the exoskeleton one. α is defined at the beginning of the trial and then maintained constant. The position-feedback loop, instead, accounts for trajectory-tracking errors by calculating the corrective torque (τ_{FB}) with a Proportional-Derivative (PD) controller based on position and velocity errors (Eq. 2.3).

$$\tau_{FF} = (J_E + J_S\alpha)\ddot{\theta}_t + (m_E + m_S\alpha)g\frac{l}{2}\sin(\theta_t) \tag{2.2}$$

$$\tau_{FB} = K_s(\theta_t - \theta_a) + K_d(\dot{\theta}_t - \dot{\theta}_a) \tag{2.3}$$

θ_t, $\dot{\theta}_t$, $\ddot{\theta}_t$ and θ_a, $\dot{\theta}_a$, $\ddot{\theta}_a$ are target and actual position, velocity and acceleration. J_S, m_S and J_E, m_E are the subject and exoskeleton's moments of inertia and masses. l is the shank length and g the gravitational constant. K_s ($5\frac{Nm}{^\circ}$) and K_d ($2\frac{Nm*s}{^\circ}$) are stiffness and damping gains defining the system's rigidity and viscosity. They were identified during preliminary tests and maintained identically across all subjects. The sum of τ_{FF} and τ_{FB} yields the overall torque (τ_{TOT}) transmitted to the motor and converted in the duty cycle of the Pulse Width Modulation (PWM) used to drive it.

Considering FES, it was delivered to the Hamstrings during the first half of the swing movement (flexion phase) and to the Quadriceps during the second half (extension phase). Its frequency and pulsewidth were maintained constant to 40 Hz and 400 μs, while the current amplitude was stride-by-stride adapted through an *Iterative Learning Controller* (ILC) [261, 262, 275]. This approach involves iterative adjustments of the current amplitude to minimize trajectory tracking errors evaluated in the previous step [261]. Thus, the signal is updated only at the end of a complete iteration (i.e. step), making this approach well-suited for repetitive movements like walking [262].
In particular, amplitude modulation was carried out such that positive tracking errors (under-tracking of the target trajectory) resulted in a current increase, while negative tracking errors led to its decrease. The current range was limited by user-specific thresholds I_{L1} and I_{L2}, determined during calibration.
For each stride k, the current for channel j at sample i was defined as:

$$I_j^k(i) = I_{L1,j} + K_{FES} \cdot u_j^k(i) \tag{2.4}$$

where K_{FES} ($4[\frac{mA*ms}{^\circ}]$) represents the stimulation gain, experimentally identified and maintained identical across all subjects. The resulting current is saturated to $I_{L2,j}$ which is the maximum value established

for the j^{th} channel during calibration. u_j^k is the control vector (i.e., cost function), initialized as zero and updated at each k as:

$$\mathbf{u^k} = \mathbf{u^{k-1}} + f(\mathbf{e^k_{pos}}) \tag{2.5}$$

where $f(\mathbf{e^k_{pos}})$ is a function of the position errors vector for the k^{th} swing. Errors during the early and late swing are considered for the Hamstrings and Quadriceps control vector, respectively. These errors are the same given as input to the impedance block.
It was computed as:

$$f(\mathbf{e^k_{pos}}) = \lambda Q \mathbf{e^k_{pos}} \tag{2.6}$$

where λ ($1.25\frac{1}{ms}$) is the error gain, experimentally identified and maintained identical across all subjects, and Q a Gaussian window filter [262], defining the amplitude of the considered errors window. In fact, this function at the instant i does not only take into account the i^{th} error, but a symmetric interval of errors centered around it. As the length of the window increases, the convergence towards the desired trajectory accelerates; however, there is a simultaneous sharper increase in current. To achieve good convergence in a few repetitions while avoiding current spikes, the filter window length was set to 5 samples.

2.4. Testing on non-disabled subjects

2.4.1. Experimental Protocol

A first testing session was carried out on non-disabled volunteers. This experimental procedure conforms to the Helsinki Declaration and was approved by the Ethical Committee of *Politecnico di Milano* (*Nr 13/2021*). Individuals provided their written informed consent before starting.
At the beginning of any experimental session, the calibration procedure was carried out.
This experimental procedure was divided in two parts: single-joint tests and tests during walking. Former ones were preliminary trials intended to verify the proper functioning and feasibility of the developed control system, before moving to the latter tests in which the complete device was tested during the target task (gait).
During single-joint tests, subjects were seated while wearing the *TwinFES* system with only one motor (right knee) active and FES delivered to the right Quadriceps. They were instructed to remain passive while performing knee extension movements, from -90° (flexed-knee position) to 0° (extended-knee position), shaped as a beta function lasting 2 seconds. These represent a simplified testing condition, easier to control as, having the subject in a seated position, it does not involve the stability of the whole body. Three conditions were tested:

- $MOT_{100\%}$: stimulation OFF and maximum motor assistance ($\alpha = 100\%$) - 50 repetitions;
- $MOT_{0\%} + FES$: stimulation ON and reduced feed-forward motor assistance ($\alpha = 0\%$) - 50 repetitions. Since α is the percentage of the subject's shank weight compensated by the motor, in this

case the sole exoskeleton's shank weight was compensated and this is the reason why we talked about "reduced feed-forward motor assistance" for this condition;

- $MOT_{0\%}$: stimulation OFF and reduced feed-forward motor assistance ($\alpha = 0\%$) - 50 repetitions;

$MOT_{0\%}$ represents a proof-of-concept condition where the total system input was reduced, thus not intended to be used during walking but just to drive theoretical conclusions.
During walking tests, subjects were instructed to remain passive and walk with *TwinFES* using the joint-space trajectory implemented by the *Twin* exoskeleton [77] but slowed down to a step duration of 4s, instead of 2s. Stimulation was only delivered to Quadriceps and Hamstrings, while Gastrocnemius and Tibialis Anterior were excluded for simplicity.
Here only two conditions were tested, the $MOT_{100\%}$ and $MOT_{0\%} + FES$ one. As previously anticipated, the $MOT_{0\%}$ case was excluded here because, reducing the total input to the system, it does not allow performing the correct walking trajectory and thus it is unsafe to test. The $MOT_{100\%}$ condition comprised 20 steps, while the $MOT_{0\%} + FES$ one 50 steps. The extended duration of the latter condition was intended to evaluate muscle fatigue.

2.4.2. Data Analysis and Statistics

Kinematic and dynamic data plus current amplitude were continuously recorded at a frequency of 100 Hz and 40 Hz, respectively. Data were organized into repetitions. For single-joint experiments, these were the different extensions; for walking tests, instead, these were the swing and stance phases.
For both testing procedures, the following data were considered: angular trajectory [°], motor current [A], motor torque [Nm] and FES current [mA]. Then, to assess trajectory tracking performance, the Root Mean Squared Error (RMSE) between the target and the actual angular positions was calculated. To quantify motor assistance, integrals of both motor current and total estimated motor torque were computed. To quantify FES assistance, the integral of the delivered current amplitudes was computed. For the sole $MOT_{0\%} + FES$ condition of walking tests, metrics were also averaged in blocks of 5 consecutive steps to assess the onset of muscle fatigue.
The mean and Standard Deviation (SD) across all performed movements (either step or extension) were extracted for all data. The only exception is the FES current for which the median and Inter-Quartile Range (IQR) were considered.
All data analyses were conducted using MATLAB (R2021b version).
Finally, a non-parametric test for correlated samples was defined in SPSS Statistics (IBM) to compare the two tested conditions (*Twin* and *TwinFES*) in terms of exoskeleton metrics. Specifically, their mean values were considered for each subject, condition, step phase and side.

2.4.3. Results

Single-joint tests
Six non-disabled participants (3 M and 3 F, mean age 24.3±2.4 years, average height 165 cm and weight 60 kg) were recruited for single-joint tests. Calibration results for the six subjects who participated in the single-joint tests, together with some other general information, are reported in Table 2.4.

Figure 2.4(a) displays, for a representative subject (ID 1), the angular position [°], the motor current [A] and torque [Nm] and the stimulation current [mA] delivered to the Quadriceps for the three tested

Generalities			RIGHT Quadriceps current [mA]	
ID	**Sex**	**Age**	I_{L1}	I_{L2}
1	M	24	16	26
2	F	27	16	23
3	F	20	10	17
4	M	25	17	30
5	F	26	15	30
6	F	24	17	28

Table 2.3: Data of the 6 subjects who took part in single-joint tests. General information (ID, Sex and Age) are reported together with the I_{L1} and I_{L2} calibration amplitudes for the Quadriceps of the right leg (only stimulated muscle group).

conditions during knee extension movements ($MOT_{100\%}$, $MOT_{0\%} + FES$ and $MOT_{0\%}$). For the angular position, the $MOT_{100\%}$ case (blue line) shows a good trajectory tracking with an end-point position (reached at t=2s) of -0.6°(±1.9°), closely approaching the target of 0°, and an overall RMSE of 13.3°(±1°). For the two conditions with $\alpha = 0\%$, movement performances remained good when FES was applied (pink line), while they decreased when FES was OFF (green line). Registered end-point positions were -8.7°(±7.8°) and -43.6°(±0.5°); overall RMSEs were 11.4°(±4.4°) and 30.9°(±0.5°).
Considering the motor current and torque, higher values were observed for $\alpha = 100\%$ compared to $\alpha = 0\%$, due to the different feed-forward contribution, with a maximum of 20.1 Nm in the former case and 6.9 Nm in the latter. Surprisingly, even though they receive the same feedforward input, $MOT_{0\%} + FES$

Generalities			LEFT leg currents [mA]				RIGHT leg currents [mA]			
			Quadriceps		*Hamstrings*		*Quadriceps*		*Hamstrings*	
ID	**Sex**	**Age**[years]	I_{L1}	I_{L2}	I_{L1}	I_{L2}	I_{L1}	I_{L2}	I_{L1}	I_{L2}
1	F	24	34	44	17	26	24	29	23	34
2	F	22	15	27	19	26	15	26	21	28
3	F	23	15	29	18	27	16	28	15	22
4	F	40	8	25	11	30	8	25	9	25
5	F	26	12	24	10	15	13	23	15	18
6	F	24	29	35	23	29	27	37	19	25
7	F	23	17	28	30	41	18	27	26	32
8	F	23	26	35	30	41	27	33	30	39
9	F	26	24	40	23	33	27	34	20	27
10	F	22	18	27	21	32	21	32	21	29
11	M	24	13	25	27	30	21	28	27	35
12	M	26	33	40	16	23	29	39	17	27

Table 2.4: Data of the 12 subjects who took part in walking tests. General information (ID, Sex and Age) are reported together with the I_{L1} and I_{L2} calibration amplitudes for Quadriceps and Hamstrings of left and right leg.

and $MOT_{0\%}$ exhibit distinct total torque outputs, with the latter registering higher values, indicating an increased corrective torque. Finally, current values were reported for the $MOT0\% + FES$ condition. An initial rapid increase is displayed, followed by an almost constant value, before a final decrease at the end of the extension phase.

The same results were confirmed when considering all tested subjects, displayed in Figure 2.4(b). Here the angular RMSE [°], the motor current integral [A] and motor torque integral [Nm] are reported. Sim-

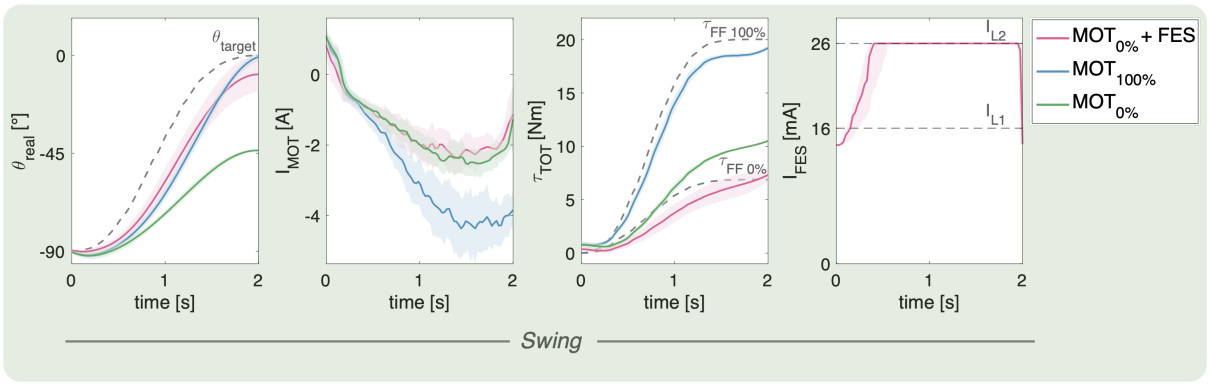

(a)

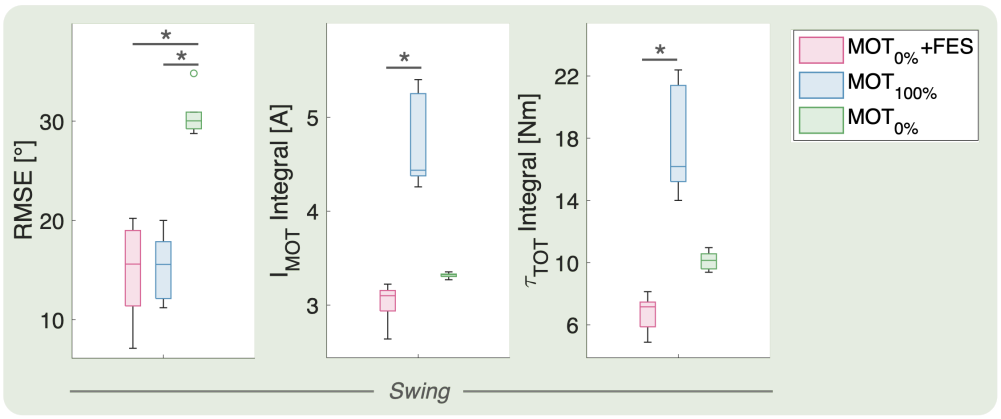

(b)

Figure 2.4: Panel (a) reports single-joint experiments of one representative subject (ID 1) for the three tested conditions: $MOT_{0\%}+FES$, $MOT_{100\%}$ and $MOT_{0\%}$. Reported variables are angular position (θ_{real} in [°]), motor current (I_{MOT} in [A]), total motor torque (τ_{TOT} in [Nm]) and Quadriceps stimulation current (I_{FES} in [mA]). Data of all extensions were averaged and are here displayed in terms of mean±SD (Standard Deviation) as a function of time (with 2s being the extension duration), except for the stimulation current, presented for the sole condition with FES in terms of median±IQR (Inter-Quartile Range). The dotted grey line in the first graph represents the target trajectory θ_{target}, those in the third graph the feedforward torque in $\alpha = 100\%$ and $\alpha = 0\%$ cases and those in the fourth graph I_{L1} and I_{L2} subject-specific calibration values. Panel (b) displays the boxplots of the single-joint metrics over the 6 subjects for the same conditions. Position RMSE (RMSE in [°]), motor current integral ($I_{MOT}Integral$ in [A]) and motor torque integral ($\tau_{MOT}Integral$ in [Nm]) are reported. The green background indicates that the cooperative control modality was applied in this case. Differences were considered statistically significant when p-value$<$0.05.

ilarly to before, a comparable RMSE is observed for $MOT_{0\%} + FES$ and $MOT_{100\%}$ (median of 15.6° in both cases), while it is significantly higher ($p<0.01$) for $MOT_{0\%}$ (median of 30°). Additionally, the integral of both motor current and total torque follows the same trend observed for the single-subject case, with the highest median values displayed by $MOT_{100\%}$ (4.4 A and 16.2 Nm), followed by $MOT_{0\%}$ (3.3 A and 10.2 Nm) and $MOT_{0\%} + FES$ (3.1 A and 7.2 Nm). Significant differences were registered in both cases among $MOT_{100\%}$ and $MOT_{0\%} + FES$ ($p<0.01$).

Walking tests

Twelve non-disabled participants (2 M and 10 F, mean age 25.3±4.9 years, average height 166 cm and weight 57 kg) were recruited for the tests during walking.

For all subjects, calibration was completed within 10 minutes.

Calibration data for the twelve subjects who participated in the walking tests, together with some other general information, are reported in Table 2.4.

Figure 2.5 displays data acquired from a representative subject (ID 4) during walking tests with *TwinFES* in $MOT_{100\%}$ and $MOT_{0\%} + FES$. Panel (a) reports the angular position [°] in terms of mean±SD over a complete stride for both hip and knee joint; panel (b) displays FES current amplitude [mA] in terms of median±IQR over a complete stride for the two stimulated muscles (Quadriceps and Hamstrings). The figure pertains to the left leg but a similar behavior can be assumed for the other side since both legs implement the same control strategy. Looking at panel (a), for the hip joint during both gait phases and for the knee joint during stance, the real trajectory of the two conditions is perfectly superimposed on the target one. This was expected considering that in these cases the synchronous modality is implemented, where the same motor control is carried out in the two conditions. For the swing knee, instead, greater deviations from the target position are noticeable under both conditions, with an overall position RMSE of 5.1°(±1.4°) for $MOT_{100\%}$ and 6.7°(±1.3°) for $MOT_{0\%} + FES$. Considering current levels depicted in panel (b), a variable current trend is reported for the Hamstrings during early swing and for the Quadriceps during late swing, as their current is iteratively updated by the ILC over the $[I_{L1}, I_{L2}]$ range. During all other phases, both muscles follow the imposed biomimetic trend in the $[min, I_{L1}]$ range.

For the same representative subject (ID 4) walking data were also reported for the knee joint during selected swing movements (Figure 2.6), to observe their trend over time. In particular, 6 swing movements were considered, those from 3 to 5 and those from 17 to 19, to display the system behaviour at the beginning and the end of the test. In panel (a), the $MOT_{100\%}$ case (blue line) shows good trajectory tracking, comparable among all swings. Differently, the case with FES has a worse tracking at the beginning that then improves over time. Indeed, while a big difference between the two conditions is noticed in the RMSE of the 3rd swing (9.96° for $MOT_{0\%} + FES$, 5.63° for $MOT_{100\%}$), this difference decreases over time with comparable values for the 19th swing (5.02° for $MOT_{0\%} + FES$, 5.29° for $MOT_{100\%}$). This may also be related to the fact that the ILC control takes some time to adapt.

Interestingly, this improvement in the condition with FES occurs with a contemporary decrease of the associated total torque. The computed total torque integral for the 3rd swing is 11.01 Nm (minimum torque of -7.03 Nm and maximum torque of 3 Nm), while it decreases to 9.03 Nm for the 19th swing (minimum torque of -6.15 Nm and maximum torque of 2.5 Nm). Differently, for the condition without FES, the total torque remains almost constant over time, with an integral of 18.2 Nm in the 3rd swing and 17.9 Nm in the 19th swing. Additionally, the total torque is always higher in the $MOT_{100\%}$ case, because a larger motor participation is required in this case ($\alpha = 100\%$). Thus, the $MOT_{0\%} + FES$

case allows a reduction in the total torque exerted by the motor, with a percentage decrease of the total torque integral of 39% at the beginning (3rd swing) and 49% at the end (19th swing). Considering the

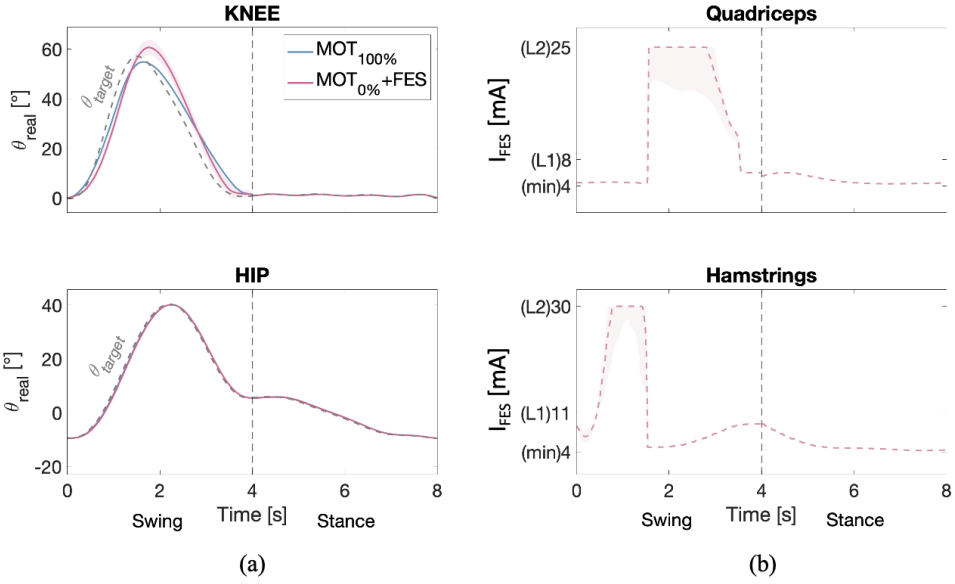

Figure 2.5: Data from one subject (ID 4) over a complete gait cycle, averaged across all performed cycles. Panel a reports the mean±SD of the target trajectory (θ_{target}, dotted grey line) juxtaposed to the actual one (θ_{real}) under two cases: $MOT_{100\%}$ (solid blue line) and $MOT_{0\%} + FES$ (solid pink line) for the knee and hip joint (upper/lower panel). Panel b illustrates the median±IQR of the current levels (I_{FES}) administered to Quadriceps and Hamstrings (upper/lower panel) in $MOT_{0\%} + FES$.

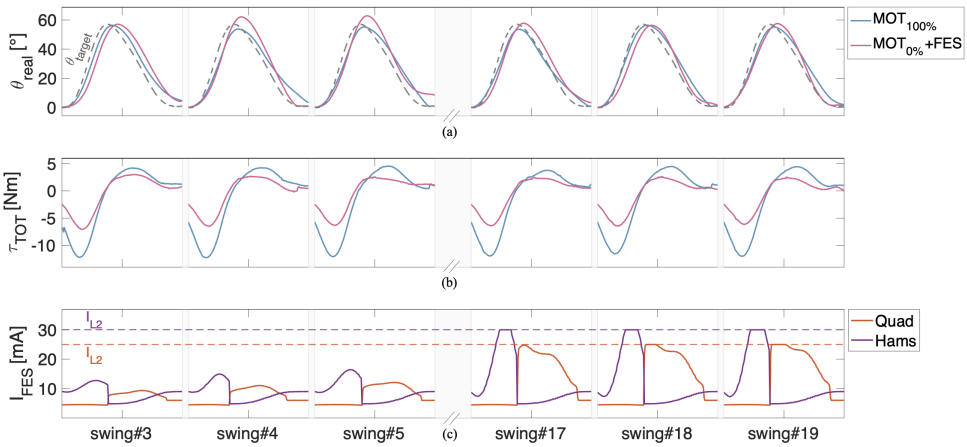

Figure 2.6: Results of the knee joint during selected swing movements of walking experiments on one representative subject (ID4) for the two tested conditions: $MOT_{0\%} + FES$ and $MOT_{100\%}$. Reported variables are the angular position (θ_{real} in [°]) in (a), the total motor torque in (τ_{TOT} in [Nm]) in (b) and the Quadriceps and Hamstrings stimulation current (I_{FES} in [mA]) in (c) for the sole condition with FES. Data are displayed for 6 swings, those from 3 to 5 and those from 17 to 19. The dotted grey line in (a) represents the target trajectory θ_{target}; the orange and purple ones in (c), the I_{L1} and I_{L2} subject-specific threshold values defined during calibration for the Quadriceps and Hamstrings respectively.

delivered current to the Quadriceps and Hamstrings (c), we notice an increase in its amplitude over time for both muscle groups, with the saturation value (I_{L2}) reached in the last swings. Based on these observations, we can conclude that the growing current input allows the $MOT_{0\%} + FES$ condition to attain a comparable movement performance (in terms of trajectory tracking) as the $MOT_{100\%}$ condition, despite requiring a significantly lower total motor torque. This demonstrates the FES capability of compensating for decreases in motor torque inputs.

Figure 2.7 displays the metrics retrieved from walking experiments under the two different conditions, considering all tested subjects and strides (both the left and right side). For the hip and knee motors, boxplots are relative to the position RMSE [°] and the motor current integral [A]. Additionally, for the knee motor during the swing phase, the total torque integral [Nm] and the Quadriceps and Hamstrings current integral [mA] are displayed.
Considering the knee joint during the swing phase (d), it displays a similar RMSE for $MOT_{100\%}$ (median of 6.9°) and $MOT_{0\%} + FES$ (median of 6.7°). Differently, significantly higher motor current and motor torque are reported for $MOT_{100\%}$ ($p<0.01$). Median motor torques are 17.5 Nm for $MOT_{100\%}$ and 8.5 Nm for $MOT_{0\%} + FES$.
On the other hand, the hip joints during stance (a) and swing (b) and the knee joint during stance (c) display similar values between $MOT_{100\%}$ and $MOT_{0\%} + FES$ for all metrics because, being under the synchronous strategy (yellow background), they implement the same motor control in the two conditions. Despite this, a significant difference was observed for the RMSE of the hip in swing which can be justified by a tendency of data because actual differences were very small: 0.703° versus 0.704° in the $MOT_{100\%}$ and $MOT_{0\%} + FES$ condition respectively. The low RMSE values are justified by the fact that the motor control is a rigid position control. The median FES amplitudes are 63.1 mA for Quadriceps and 65.8 mA for Hamstrings.
When averaging metrics every 5 repetitions (Figure 2.7(e)), the RMSE exhibits a decreasing trend with a slight increase in the last block. Nevertheless, no significant differences were reported among blocks. Motor torque remains almost constant throughout blocks, with only one significant difference among blocks 11-15 and 36-40 ($p=0.045$). Significant differences for the motor current integral and Quadriceps and Hamstrings current integrals are reported in tables in Figure 2.8 with their p-values. The motor current integral displays a similar trend in between swings, with a slight decrease at the beginning followed by an increase, as depicted in the table where in the majority of identified significant differences previous blocks have lower values (downward arrow in Figure 2.8) than latter ones. The FES current delivered to Quadriceps and Hamstrings showed an increasing trend over time, as indicated in all significantly different pairs where previous blocks have lower values (downward arrow in Figure 2.8) than latter ones.

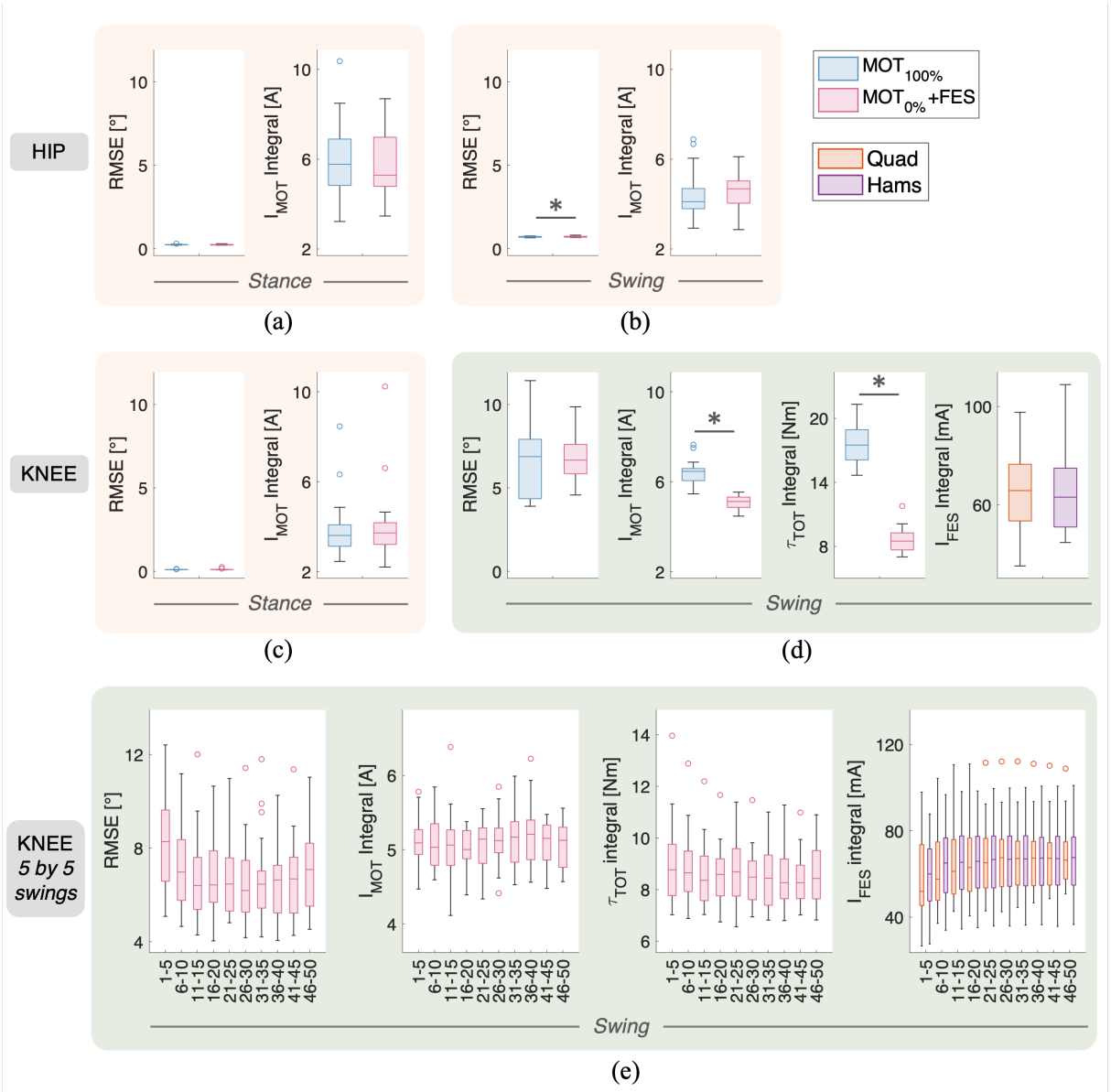

Figure 2.7: Results of the walking experiments under the two conditions ($MOT_{100\%}$ and $MOT_{0\%}+FES$) considering all tested subjects and strides of both sides. Boxplots report position RMSE ($RMSE$ in [°]) and integral of the motor current ($I_{MOT}Integral$ in [A]) for the hip joint during the stance (a) and swing (b) phase and for the knee motor during the stance phase (c). The yellow background indicates that these joints are under synchronous control. Panel (d) displays, in addition to the position RMSE and motor current integral, the motor torque integral ($\tau_{MOT}Integral$ in [Nm]) and Quadriceps and Hamstrings FES current integral ($I_{FES}Integral$ in [mA]) for the knee motor during swing. The same metrics are reported in panel (e) but averaging data into blocks of 5 consecutive steps for each subject and then mediating them for all subjects and sides. The green background of panels (d) and (e) indicates that these joints are under cooperative control. Differences were considered statistically significant when p-value$<$0.05.

Quadriceps current integral

	(1-5)	(6-10)	(11-15)	(16-20)	(21-25)	(26-30)	(31-35)	(36-40)	(41-45)	(46-50)
(1-5)				0.025 ↓						
(6-10)								0.036 ↓		
(11-15)								0.008 ↓	0.04 ↓	
(16-20)						0.004 ↓	0.003 ↓	<0.001↓	0.001 ↓	0.004 ↓
(21-25)								0.022 ↓		
(26-30)										
(31-35)										
(36-40)										
(41-45)										
(46-50)										

Hamstrings current integral

	(1-5)	(6-10)	(11-15)	(16-20)	(21-25)	(26-30)	(31-35)	(36-40)	(41-45)	(46-50)
(1-5)				0.032 ↓	<0.001↓	<0.001↓	<0.001↓	<0.001↓	<0.001↓	<0.001↓
(6-10)					0.005 ↓	0.001 ↓	<0.001↓	<0.001↓	<0.001↓	<0.001↓
(11-15)							0.003 ↓	0.001 ↓	<0.001↓	<0.001↓
(16-20)							0.012 ↓	0.003 ↓	<0.001↓	<0.001↓
(21-25)									0.028 ↓	0.013 ↓
(26-30)										0.04 ↓
(31-35)										
(36-40)										
(41-45)										
(46-50)										

Motor Current Integral

	(1-5)	(6-10)	(11-15)	(16-20)	(21-25)	(26-30)	(31-35)	(36-40)	(41-45)	(46-50)
(1-5)			0.028↑		0.025 ↓	0.004↓	<0.001↓	0.006↓		0.028↓
(6-10)							0.006↓			
(11-15)										
(16-20)							0.008 ↓			
(21-25)										
(26-30)										
(31-35)									0.032↑	
(36-40)										
(41-45)										
(46-50)										

Figure 2.8: p-values for the 5-by-5 swings comparisons. Tables must be read row by column and the arrow indicates whether the row value was higher or lower than the column value. Differences were considered statistically significant when p-value$<$0.05.

2.5. Testing on target users

2.5.1. Experimental Protocol

A schematic representation of the testing procedure used for target users is reported in Figure 2.9.
The study conforms to the Helsinki Declaration and was approved by the Ethical Committee of Politecnico di Milano (*Nr 0314/10/2022*). Once recruited, individuals were required to provide their written informed consent and inclusion/exclusion criteria were verified.
At the *T0 evaluation* (before starting the tests), subjects' anamnestic and anthropometric data are collected. These include age, sex, height, weight and previous experiences with FES and/or lower-limb exoskeletons. Additionally, for SCI subjects, the lesion type and level, the time since the lesion and the ASIA scale, while for post-stroke individuals the ictus type and location, the time since the event, and the FAC scale. The Functional Ambulation Categories (FAC) is a 0-5 scale to evaluate the ambulation capacity, with 0 meaning "non-functional ambulator" and 10 meaning "independent ambulator".
At T0, it was checked that the user could undergo the testing procedure by verifying the absence of spasticity and pain and good autonomic functionality. Then, the following baseline evaluations were carried out:

- Bristol scale [276] and NBD [277] score for bowel and bladder functionality;
- Modified Ashworth scale for spasticity [278];
- Numeric Rating Scale (NRS) for pain level [279], a 0–10 scale to evaluate pain, with 0 meaning "no pain" and 10 meaning "worst imaginable pain";
- Psychological General Well-Being Index (PGWBI) [280].

After that, the subject starts the training. The first phase is the familiarization with the *Twin* exoskeleton, during which the subject walks with the sole *Twin* exoskeleton without FES (corresponding to the

$MOT_{100\%}$ condition: stimulation OFF and maximum motor assistance). This phase lasts for a maximum of 10 sessions (1 hour each), until the subject can walk for at least 10 meters and perform sit-to-stand transitions. If this condition is not met the subject is excluded, otherwise the *T1 evaluation* is carried out. This includes an evaluation of the outcomes (acceptability, usability, user experience and interaction with the system) for the *Twin* device, performed through the following questionnaires:

- System Usability Scale (SUS) [281];
- Technological Acceptance Measure 3 (TAM-3) [282];
- User Experience Questionnaire (UEQ) [283].

After T1, the second phase of the training takes place, which is the testing of the *TwinFES* device, during which the subject walks with the *Twin* exoskeleton integrated with FES (corresponding to the $MOT_{0\%} + FES$ condition: stimulation ON and reduced feed-forward motor assistance). In this case, a maximum of four sessions are performed (1 hour each). The currents calibration (definition of I_{L1} and I_{L2}, as explained in Section 2.3.2) is carried out in the first session and then is maintained identical for the following ones, unless the subject specifically requires to modify it.
Lastly, the *T2 evaluation* takes place, during which the same questionnaires of the *T1 evaluation* are filled out by subjects but this time focusing on their experience with the *TwinFES* device.
Similarly to the tests on non-disabled subjects, the joint-space walking trajectory implemented in the *Twin* exoskeleton was used [77], but with a step duration of 3s in this case. Differently from the tests on non-disabled subjects, instead, FES was here delivered to all four muscle groups per leg, each one with its specific control, as explained in Section 2.3.3.

2.5.2. Data Analysis and Statistics

The analysis of dynamic and kinematic data extracted from the *TwinFES* device followed the same procedure used for the data of non-disabled individuals (explained in Section 2.4.2). As here multiple sessions were performed for the same conditions, all steps belonging to the same condition were considered together.
Additionally, these tests included the collection of questionnaires' data, analyzed according to each questionnaire's guidelines, as will be detailed in the results section.
All data analyses were conducted using MATLAB (R2021b version).
Finally, a non-parametric test for correlated samples was defined in SPSS Statistics (IBM) to compare the two tested conditions (*Twin* and *TwinFES*), both for the questionnaires' answers and for the exoskeleton metrics. For these latter, their mean values were considered for each subject, condition, step phase and side.

2.5.3. Results

Thirteen subjects (12 M and 1 F, mean age 40.7±8.3 years) were recruited at Villa Beretta rehabilitation center (Costa Masnaga, Lecco).
They were subdivided into three categories based on their pathologies: four suffered from a complete SCI (cSCI), four from an incomplete SCI (iSCI) and five from a stroke (stroke). Not all subjects could complete the experimental protocol and, in fact, we had two dropouts. In particular, one cSCI subject

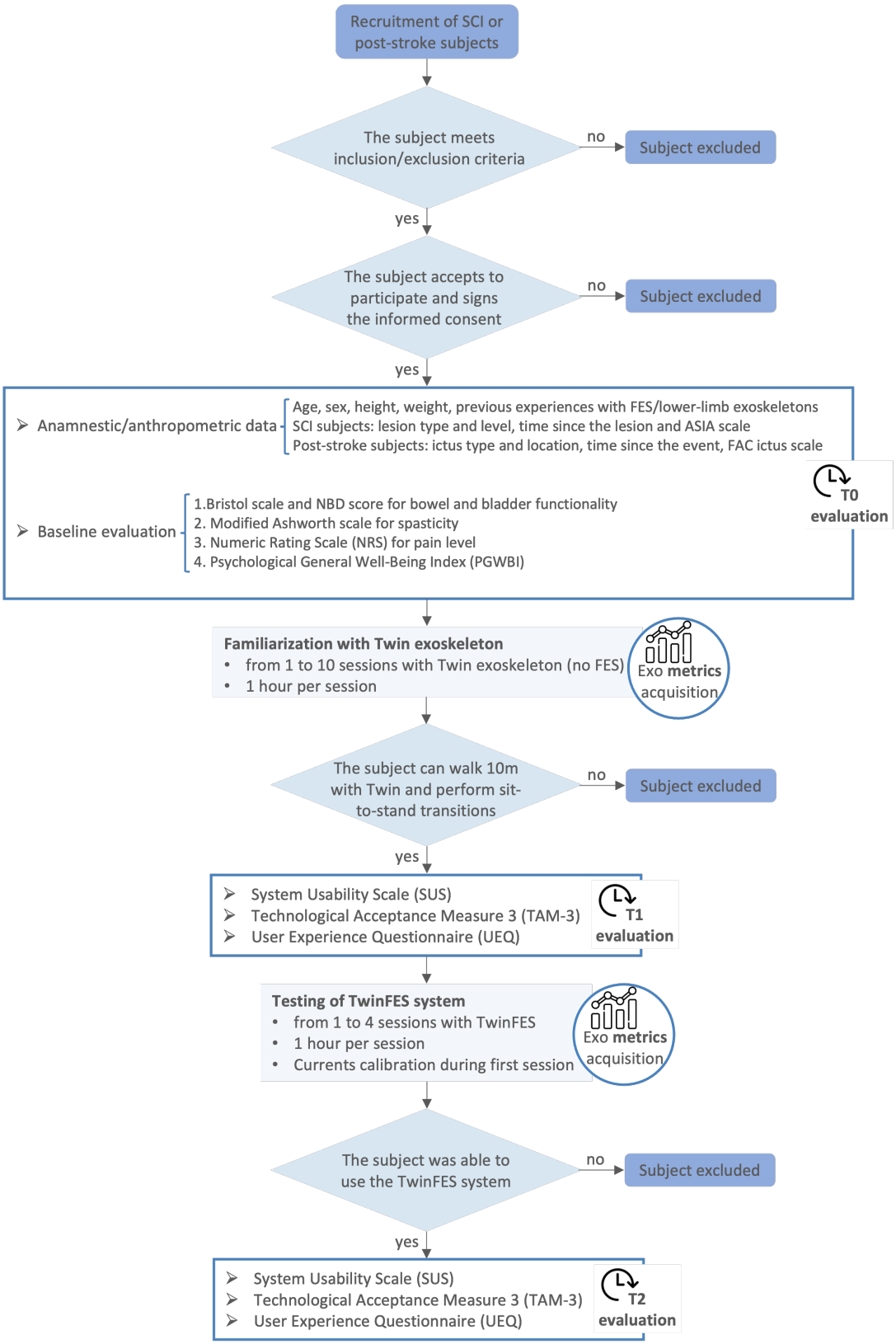

Figure 2.9: Flowchart of the protocol used for tests on target users.

interrupted the testing procedure as he did not feel well during the second session (for a reason not related to the ongoing tests) and further sessions could not be scheduled due to incompatibility of his availability and the end of the project. One iSCI subject, instead, was not able to use the system due to the mismatch between his availability and the project's conclusion.
General characteristics of recruited subjects are reported in Tables 2.5 and 2.6.
Figure 2.10, instead, shows the results of the Psychological General Well-Being Index [280] (conducted at T0). This questionnaire asked subjects to answer 22 questions about their general psychological condition, on a scale from 0 (low) to 5 (high). Then questions are grouped into six categories: health, positivity, anxiety, depression, self-control and vitality. The scores for questions within each category are totaled, and then the response for each category is presented as a percentage relative to the maximum possible score for that category (taking into account the number of questions within it and 5 as the maximum score). For all categories, a higher score indicates a better psychological condition, with the exception of anxiety and depression ("negative" feelings) for which low values are better.

ID	Sex	Age [years]	Lesion level	ASIA	Complete/ Incomplete	Time since the event [months]	Comments	Spasticity (Modified Ashworth Scale)	Pain level (NRS)	Performed tests
P1	M	35	T7	A	Complete	32	Non-ambulatory user	Spasticity level between 2 and 3, symmetrical between right and left	4	10 sessions: 6 $MOT_{100\%}$ 4 $MOT_{0\%} + FES$
P2	M	38	L3	D	Incomplete	79	Ambulatory user with 2 Canadian canes and left Peroneal Electrical Stimulation ($>$ 194m in 6 min)	Spasticity level between 0 and 2, greater on the left	0	6 sessions: 3 $MOT_{100\%}$ 3 $MOT_{0\%} + FES$
P3	M	38	D2	B	Incomplete		Non-ambulatory user	Spasticity level between 0 and 1, symmetrical between right and left		0 sessions $\rightarrow$ **dropout**
P4	M	42	T5	A	Complete	61	Non-ambulatory user	Spasticity level between 0 and 2, symmetrical between right and left	10	4 sessions: 2 $MOT_{100\%}$ 2 $MOT_{0\%} + FES$
P5	F	42	D4	C	Incomplete		Ambulatory user with tibia orthosis	Spasticity level between 0 and 1, symmetrical between right and left	0	3 sessions: 1 $MOT_{100\%}$ 2 $MOT_{0\%} + FES$
P6	M	30	T3	A	Complete	25	Non-ambulatory user	Spasticity level between 0 and 1, symmetrical between right and left	3	5 sessions: 2 $MOT_{100\%}$ 3 $MOT_{0\%} + FES$
P12	M	66	D8	A	Complete	47	Non-ambulatory user	Spasticity 2 on Triceps	5	1 session: only 1 $MOT_{100\%}$ $\rightarrow$ **dropout**
P13	M	38	Sacral	A	Incomplete	43	Ambulatory user with tibia orthosis	No spasticity	0	2 sessions: 1 $MOT_{100\%}$ 1 $MOT_{0\%} + FES$

Table 2.5: Characteristics of SCI subjects.

ID	Sex	Age [years]	Type of stroke	More impaired side	Stroke scale (FAC)	Time since the event [months]	Spasticity (Modified Ashworth Scale)	Pain level (NRS)	Performed tests
P7	M	41	Ischemic	Left	4	19	Quadriceps Ash 2	0	4 sessions: 2 $MOT_{100\%}$ 2 $MOT_{0\%}+FES$
P8	M	41	Ischemic	Right	4	26	No spasticity	0	4 sessions: 2 $MOT_{100\%}$ 2 $MOT_{0\%}+FES$
P9	M	48	Hemorragic	Right	4	8	Quadriceps Ash 1	0	3 sessions: 1 $MOT_{100\%}$ 2 $MOT_{0\%}+FES$
P10	M	42	Ischemic	Right	4	303	Triceps Ash 1+	0	3 sessions: 1 $MOT_{100\%}$ 2 $MOT_{0\%}+FES$
P11	M	48	Ischemic	Left	4	98	No hypertonicity	0	3 sessions: 1 $MOT_{100\%}$ 2 $MOT_{0\%}+FES$

Table 2.6: Characteristics of stroke subjects.

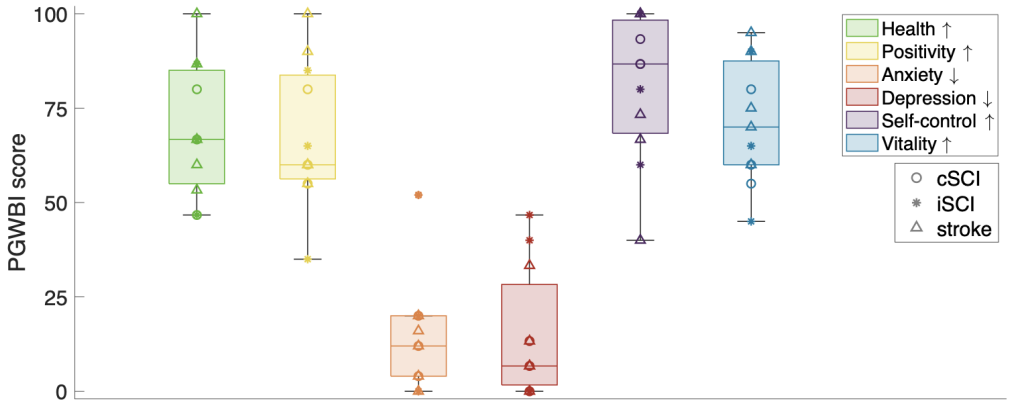

Figure 2.10: Results of the Psychological General Well-Being Index (PGWBI) for all individuals. Single-subject data are reported, with a different marker depending on the pathology as detailed by the legend. Scores are reported on a 0-100 scale, with a higher value indicating a better psychological condition, except for anxiety and depression ("negative" feelings) for which the opposite occurs.

Similarly as done for tests on non-disabled subjects, Figure 2.11 displays the metrics retrieved from walking experiments under the two different conditions, considering all eleven tested subjects and strides (both the left and right side). For both conditions, the steps of all sessions were considered together. For both joints boxplots are relative to the position RMSE [°] and the motor current integral [°]. For the knee during swing also the motor torque integral [Nm] and the Quadriceps and Hamstrings current integral [mA] are displayed.

The hip joints during stance (a) and swing (b) and the knee joint during stance (c) share the same motor control in the two conditions (as indicated by the yellow background for synchronized control) and this explains why all metrics display similar values between $MOT_{100\%}$ and $MOT_{0\%} + FES$ for such joints. Despite this, significant differences were observed for the RMSE of the hip in swing and the motor current integral of the knee in stance. Nevertheless, this can be justified by a tendency of data but actual differences were very small: 1.024° versus 1.006° for the RMSE and 5.49 A versus 4.86 A for the motor current integral, in the $MOT_{100\%}$ and $MOT_{0\%} + FES$ condition respectively. Given that the motor control is a rigid position control, negligible values were obtained for the RMSE.

Considering instead the knee joint during the swing phase (d), more interesting observations arise as this is when the FES-motor cooperation takes place (as indicated by the green background for cooperative control). A slight increase in the RMSE is noticed between the $MOT_{100\%}$ condition (median of 7.92°) and the $MOT_{0\%} + FES$ one (median of 7.50°), but this increase is not significant ($p = 0.053$). Such a small increase is not relevant when compared to the extensive angular Range Of Motion (ROM) of 57.2° travelled by the knee during the swing phase. Indeed, the RMSE percentage values relative to this excursion are 13.8% and 13.1% for the $MOT_{100\%}$ condition and $MOT_{0\%} + FES$ one respectively.

At the same time, the knee motor during swing displays a significantly lower ($p < 0.001$) motor current integral and motor torque integral in the $MOT_{0\%} + FES$ condition. Their values decrease from 5.56 A to 4.44 A and from 14.47 Nm to 7.52 Nm respectively.

The median FES current amplitudes during the swing phase (when ILC is implemented) were 61.9 mA for Quadriceps and 59.3 mA for Hamstrings.

These observations demonstrate how the FES addition allows a significant reduction of the motor power and, at the same time, small variations of the position error that do not alter the walking trajectory.

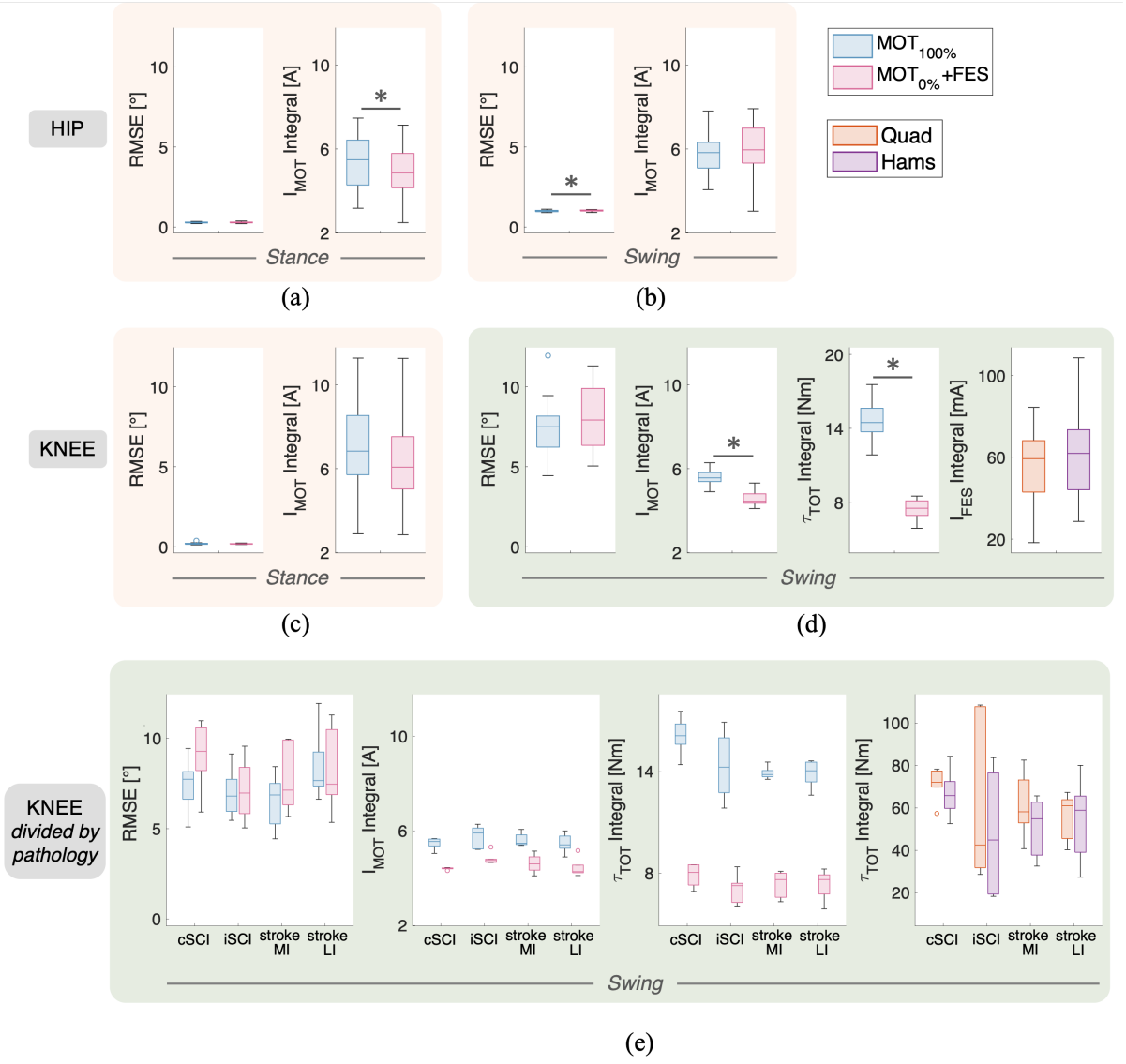

Figure 2.11: Results of the walking experiments under the two conditions ($MOT_{100\%}$ and $MOT_{0\%} + FES$) considering all eleven tested subjects and strides of both sides. For both conditions, the steps of all sessions were considered together. Boxplots report position RMSE ($RMSE$ in [°]) and integral of the motor current ($I_{MOT}Integral$ in [A]) for the hip joint during the stance (a) and swing (b) phase and for the knee motor during the stance phase (c). The yellow background indicates that these joints are under synchronous control. Panel (d) displays, in addition to the position RMSE and motor current integral, the motor torque integral ($\tau_{MOT}Integral$ in [Nm]) and Quadriceps and Hamstrings FES current integral ($I_{FES}Integral$ in [mA]) for the knee motor during swing. The same metrics are reported in panel (e) with a focus on the knee joint where users are separated based on their pathology: complete SCI (cSCI), incomplete SCI (iSCI), stroke - More Impaired side (stroke MI) and stroke - Less Impaired side (stroke LI). The green background of panels (d) and (e) indicates that these joints are under cooperative control. Differences were considered statistically significant when p-value$<$0.05.

Panel (e) reports the same results of panel (d) but separately for the type of pathology. Specifically, the following four categories were distinguished: complete SCI (cSCI), incomplete SCI (iSCI), stroke - More Impaired side (stroke MI) and stroke - Less Impaired side (stroke LI). The statistical analysis was not carried out in this case due to the small sample size of each category.
For all metrics, the observed trends resemble those previously commented for panel (d). In fact, for all categories, significant decreases in the motor current and torque are observed when adding FES (condition $MOT_{0\%} + FES$), with contemporary small alterations in the RMSE value. In particular, when passing from the $MOT_{100\%}$ to the $MOT_{0\%}+FES$, the RMSE variations are as follows (expressed both as absolute values and as percentage of the knee ROM): from 7.74° (13.5%) to 9.29° (16.2%) for cSCI, from 6.81° (11.9%) to 6.97° (12.2%) for iSCI, from 6.87° (12.0%) to 7.13° (12.5%) for the more impaired side of stroke and from 7.67° (13.4%) to 7.47° (13.1%) for the less impaired side of stroke.

Figure 2.12 still focuses on the metrics of the knee joint during the swing phase but, in this case, reported only for one representative subject (ID1 - cSCI) and separately among sessions. The aim of this figure was to show the metrics trend over time and user ID1 was selected being the one who performed the highest number of sessions.
Looking at panel (a), it can be noticed that the RMSE decreases over time during sessions without FES. Then, it suddenly grows during the first session with FES but then it continues to follow a decreasing trend, until reaching similar values to the condition without FES. In parallel, for both conditions, the motor current integral stays constant over time, while the motor torque integral shows a decreasing trend.

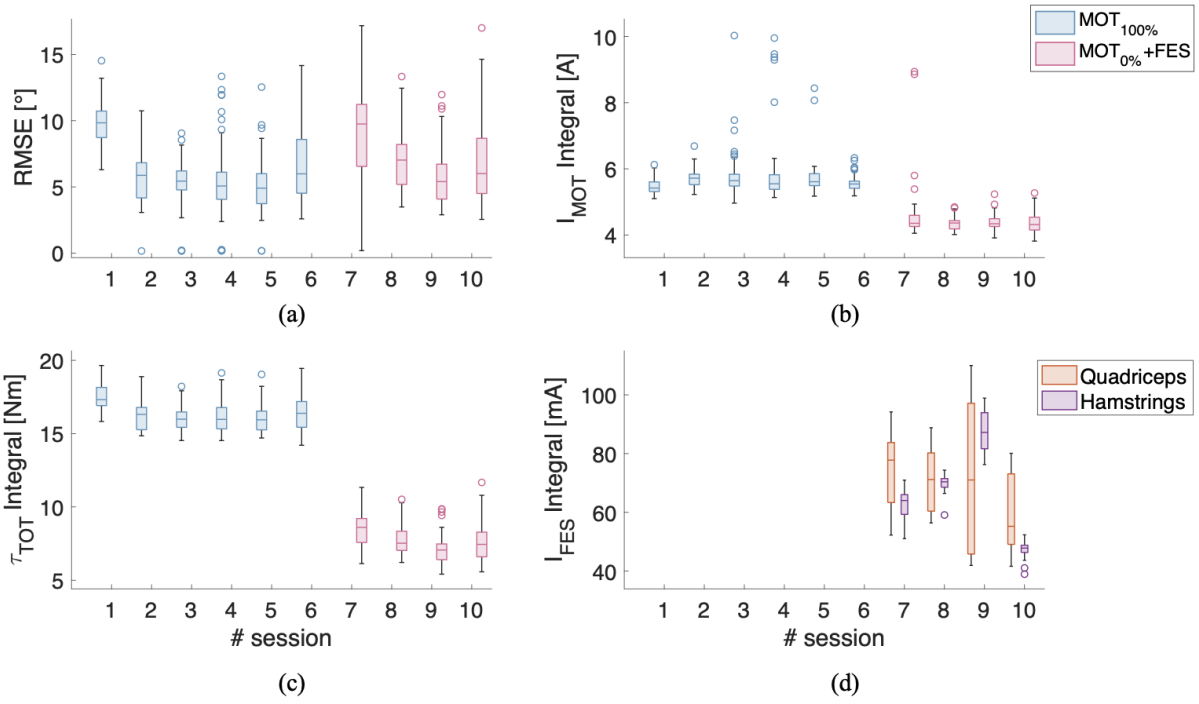

Figure 2.12: Focus on the swing knee joint during walking experiments of one representative subject (ID1 - cSCI) under the two tested conditions ($MOT_{100\%}$ and $MOT_{0\%} + FES$). Results are reported separately for each session. Boxplots report the position RMSE (a), the integral of the motor current (b), the integral of the total torque (c) and the the integral of the Quadriceps and Hamstrings current amplitude (only for those conditions including FES) (d).

For both these metrics, the condition with FES assumes significantly lower values, as expected. By comparing the last session in the $MOT_{100\%}$ condition (session 6) and the last one in the $MOT_{0\%} + FES$ condition (session 10), it can be noticed that the RMSE assumes the same median value of 6°, while the motor torque integral is more than halved, decreasing from 16.4 Nm to 7.4 Nm (55% decrease). Lastly, the FES current assumes a decreasing trend for the Quadriceps while it increases for Hamstrings, with a sudden decrease in the last session.

This section presents the results of the questionnaires filled out by users at T1 and T2.

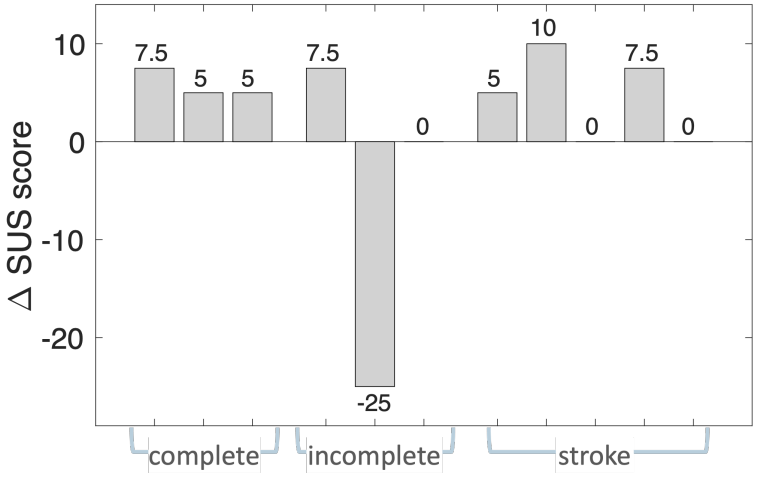

Figure 2.13: Results of the System Usability Scale (score between 0 and 100) reported subject-by-subject as the difference between the value given to the TwinFES system (T2 evaluation) and the one to the Twin system (T1 evaluation), computed as $SUS_{T2} - SUS_{T1}$.

Figure 2.13 reports the result of the System Usability Scale (SUS) [281]. This questionnaire includes 10 items with a rating scale from 1 to 5 for the subjective evaluation of the system's usability. Then all ten answers are summed up and the final score is expressed on a 0-100 scale, where a higher value corresponds to better device usability. In particular, 4 rankings are distinguished: "awful" from 0 to 51, "poor" from 51 to 68, "good" from 68 to 80 and "excellent" from 80 to 100.
This questionnaire is filled out by users both at T1 (evaluating *Twin*) and at T2 (evaluating *TwinFES*) and the presented figure reports the difference between the usability of the two systems subject by subject. From this, it can be noticed that the *TwinFES* device reported higher scores with respect to the sole *Twin* for all subjects, except one (ID5 - iSCI). Indeed, the median usability increases from 47.5 (25.6) for *Twin* to 55 (35.6) for *TwinFES*, with an overall median difference of 5 (7.5). This suggests that the presence of stimulation is beneficial for the overall system usability.

Figure 2.14 reports answers to the Technological Acceptance Measure 3 (TAM-3) [282] which asks subjects to evaluate how much they agreed with 46 statements, then grouped in 13 categories, on a scale from 1 (totally disagree) to 5 (totally agree).
As results are reported as the difference between the *TwinFES* evaluation and the *Twin* one, data above

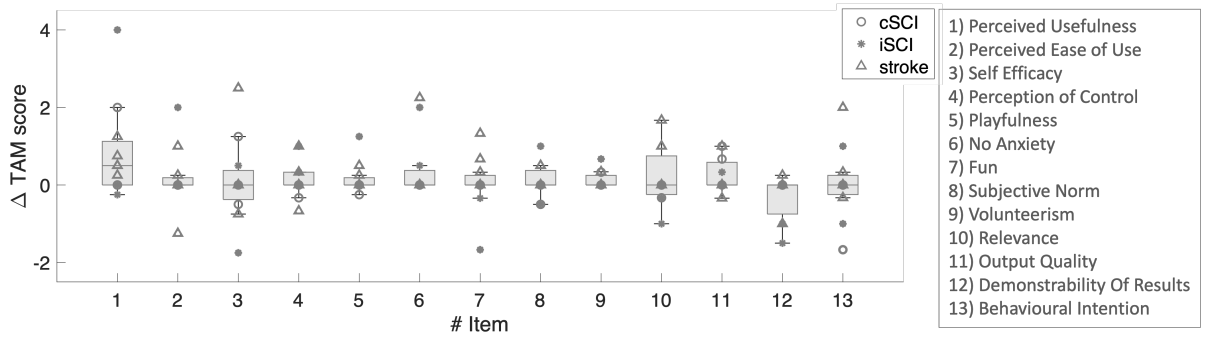

Figure 2.14: Results of the Technological Acceptance Measure 3 (score between 1 and 5) reported subject-by-subject as the difference between the value given to the TwinFES system (T2 evaluation) and the one to the Twin system (T1 evaluation), computed as $TAM_{T2} - TAM_{T1}$. Answers to the 46 questions are divided into 13 categories. For all categories, a higher score corresponds to a better device evaluation. Single-subject data are superimposed to the boxplots, using a different marker to indicate the pathology (reported in the legend).

0 indicate better acceptability for the condition with FES. Additionally, single-subject data are superimposed to the graph, using a different marker to indicate the pathology (square for cSCI, star for iSCI and triangle for stroke).
Overall, no relevant differences can be observed between the two systems, with all median scores around zero. The statistical analysis was conducted to compare the condition with and without FES across all individuals, considering differences statistically significant when p-value$<$0.05. The only significant difference was found for the "Perceived Usefulness" item ($p = 0.02$), with a median of 3.5 for the *Twin* system and 4 for the *TwinFES* one.

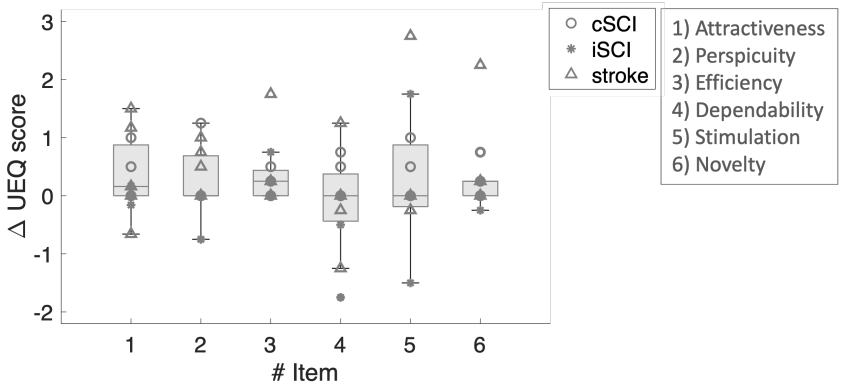

Figure 2.15: Results of the User Experience Questionnaire (UEQ) reported subject-by-subject as the difference between the value given to the TwinFES system (T2 evaluation) and the one to the Twin system (T1 evaluation), computed as $UEQ_{T2} - UEQ_{T1}$. The questionnaire asks subjects to rate, on a 1-7 scale (then rescaled between -3 and 3), 26 device characteristics then grouped into six categories. Single-subject data are superimposed to the boxplots, using a different marker to indicate the pathology (reported in the legend).

Figure 2.15 depicts the results of the User Experience Questionnaire (UEQ) [283] where subjects are asked to rate, on a 1-7 scale (then rescaled between -3 and 3), 26 device characteristics, then grouped into six categories. These latter are: attractiveness, perspicuity, efficiency, dependability, stimulation and novelty. Additionally, single-subject data are superimposed to the graph, using a different marker to indicate the pathology (square for cSCI, star for iSCI and triangle for stroke).
Also in this case, data above 0 indicate a better user experience for the condition with FES. Overall, the two systems received a similar average evaluation from all users, with all median scores around zero. The statistical analysis was conducted to compare the condition with and without FES across all individuals, considering differences statistically significant when p-value$<$0.05. The only significant difference was found for "Efficiency" ($p = 0.03$), with a median of -0.5 for the *Twin* system and -0.25 for the *TwinFES* one.

2.6. Discussion

The primary goal of this study was to design and validate a cooperative control system for a hybrid device (named *TwinFES*) integrating FES within a motorized lower-limb exoskeleton to support locomotion in neurological impaired subjects. The novel controller decreases the motor power and iteratively adapts FES to compensate for these reductions. Nevertheless, the fast-reacting motor component continuously monitors the task accomplishment and intervenes in case of stimulation inefficiencies.
An extensive experimental procedure was carried out in two stages: the former encompassed 18 non-disabled subjects who underwent either full-body or single-joint tests; the latter involved 11 users (either complete/incomplete SCI or stroke) who performed walking tests with the system.
The gathered results proved the feasibility of the hybrid system and demonstrated that FES assistance could compensate for lower motor contributions while guaranteeing the system's safety. In fact, the cooperative controller implemented by the knee joint during the swing phase allowed a similar RMSE for $MOT_{0\%} + FES$ and $MOT_{100\%}$, with both conditions displaying a median RMSE $<7°$ for non-disabled subjects and $<8°$ for target users. This occurred together with a significantly lower estimated motor torque in the condition with FES, which was reduced by 51.5% across non-disabled subjects and 48% across target users. These observations demonstrate that exchanging a reduction in motor contribution for the addition of FES did not impact the controller's ability to track the target trajectory and thus guarantee the users' safety. This represents a promising result for the development of future devices with smaller and lighter motors and batteries and thus with increased usability.
This conclusion is confirmed by the fact that reducing the motor torque without including FES generates bad trajectory tracking, as observed in the $MOT_{0\%}$ case of single-joint tests on non-disabled individuals. This condition was not tested during walking and on impaired individuals for safety issues.
The $MOT_{0\%} + FES$ condition also provoked a decrease in the motor current for the knee joint during swing, reduced by 20.7% and 20.1% for non-disabled subjects and target users, respectively. The same trend followed by the motor torque and current proves the validity of using the estimated motor torque as a proxy of the motors' real exerted output. Few other studies with FES-motor cooperative actuation in lower-limb exoskeletons included a clear quantification of the motor torque reduction [239].
The higher motor current and torque of $MOT_{100\%}$ are due to the greater feedforward torque required from motors in this condition ($\alpha = 100\%$). Interestingly, a significant difference in motor current and torque was observed between $MOT_{0\%}$ and $MOT_{0\%} + FES$ of single-joint tests. Even if they share the same feedforward contribution, the former case deals with a larger feedback component. In fact, while

the $MOT_{0\%} + FES$ condition overcomes motor torque reductions through FES-induced movements, the $MOT_{0\%}$ one, not including FES, relies on the feedback portion to compensate for reduced motor inputs. Nevertheless, the feedback component is not enough to achieve good tracking due to the weak gains of the impedance controller (K_s and K_d). These were set to low values to avoid having a strong and fast feedback contribution, overpowering the stimulation slow effect in the condition including FES.
The use of low impedance gains allows a "soft" tracking of the target trajectory but not very precise at the same time. In fact, considering the average position tracking for one representative subject, reported both in the walking and single-joint case, it can be noticed that it is not perfect. Actually, it is not ideal also in the $MOT_{100\%}$ case and this can be attributed to imperfections of the modeled feedforward torque provided as input. Nevertheless, considering that the system is designed for walking movements, small deviations from the target trajectory are admitted.
On the other hand, for joints undergoing synchronous control, no significantly divergent metrics were observed, as both conditions implemented the same motor control in this case. Specifically, given that it was a rigid position control, negligible RMSEs were retrieved. In this circumstance, FES was intended not to induce movements, but rather to deliver a beneficial therapeutic effect. It was also observed that it did not alter in any way the system functioning.
Taking into account the subjective assessments provided by target users, it can be concluded that, overall, the system was accepted and received a medium rating, regardless of including the stimulation. Interestingly, when considering the usability score, a difference was instead observed between using the system with FES (*TwinFES*) or without (*Twin*), with the former receiving a higher evaluation across all users, except one. Such a result demonstrates that the FES addition improves the system's usability. This finding is not obvious considering that the *Twin* exoskeleton is already a complex system, exacerbated by the added complexity of the FES integration that reduces the system's wearability. Nevertheless, this observation indicates that impaired subjects indeed found the inclusion of FES beneficial for the system's usability, despite the aforementioned limitations. Additionally, it is worth emphasizing that all *TwinFES* sessions were carried out after *Twin* ones, which could have potentially reduced the users' willingness to utilize it.

Differently from other studies [251], here FES and motor cooperation acted on the same joint and aimed at reducing the trajectory tracking error, without the need for sophisticated FES-torque models and time-consuming FES calibrations [189, 193, 265]. The objective was to use FES as a coarse position controller, with the motor impedance control serving to fine-tune the movement. The fast calibration procedure, lasting no more than 10 minutes and not requiring further repetitions, makes this approach suitable for clinical applications.
Hybrid systems also claimed to postpone the onset of muscle fatigue compared to the use of FES alone. In our case, we could not test the FES-only condition, being not safe during walking, in particular for non-ambulatory users. Anyways, when considering 50 consecutive strides performed by non-disabled subjects (Figure 2.7(e)), we did not observe an increase in both RMSE and motor torque demand in the last steps, which would have indicated a clear onset of muscle fatigue. Nevertheless, we cannot definitively assert that fatigue was delayed since the number of steps should be increased to identify its clear onset.

This study faced some limitations. The cooperative control was only implemented for the knee in swing, as in previous studies [189]. The limited scalability to the stance phase and to the hip joint was due to multiple factors: the need to guarantee subjects' stability during the stance phase (particularly relevant

for non-ambulatory users), the fact that Quadriceps and Hamstrings have opposite effects on the hip and knee joint, and the depth of hip flexors which prevents their transcutaneous stimulation [189].
Nevertheless, future studies should consider the possibility of integrating knee locking systems, such as brakes, to support the knee extension during the stance phase. Indeed, from the tests on target users, we observed higher values for the motor current integral with respect to those registered with non-disabled individuals. This is probably due to the fact that a greater effort is needed to sustain those individuals that are not completely able to maintain the standing posture by themselves. In the direction of decreasing the motors power, the inclusion of locking devices could enable to alleviate the load on motors.
Additionally, the implemented impedance controller was implicit due to the absence of torque sensors measuring user-robot interaction forces. Future studies should include direct torque sensing to reject friction disturbances and improve back-drivability [242].
Concerning the testing, users with and without disability were included, but for both groups only a single walking speed was considered and this was quite slow. Future studies should evaluate the feasibility of the proposed approach at faster walking speeds, which would be particularly beneficial for impaired subjects by reducing their challenges in maintaining balance.
Furthermore, the presence of a volitional contribution in addition to FES and motor assistance was not considered. Nevertheless, given the adaptability of the control system and its independence from a priori models, we can assume that this contribution would be integrated into the loop. Specifically, if this tends to reduce tracking errors, then either FES, motor assistance, or both could be decreased. Additional tests are needed to demonstrate the feasibility of this three-fold cooperation but it seems promising for future advancements in cooperative controllers for robotics.

2.7. Conclusions

This study proposes a novel hybrid FES-motorized gait system comprising 4 DOFs and up to 8 stimulated muscles. The developed cooperative controller modulates FES amplitude and motor torque to potentially delay the appearance of muscle fatigue and reduce the motor power demand while ensuring good tracking performance and not compromising the user's safety.
Preliminary tests on non-disabled participants proved the feasibility of the FES-motors integration and then the system's functionality was validated both on non-disabled participants and on target users. Specifically, the following *take-home messages* could be extracted:

- when FES is integrated with the aim of inducing a functional movement (cooperative control), there is a significant reduction in the motor's workload with a simultaneous negligible alteration of the angular profile;
- when FES is introduced as a *proprioceptive* factor, it acts independently from the robotic component to potentially induce therapeutical benefits, without altering the system's control and security;
- the presence of FES increases the system's usability, indicating that subjects found beneficial the use of an exoskeleton in which their muscles contribute to the movement;
- the device is suitable to be transferred to clinical settings thanks to the small calibration time required.

These conclusions pave the way for the realization of exoskeletons incorporating smaller and lighter motors and batteries. This trend is in line with the recent shift towards the development of "soft" robots, which hold promise for enhancing the overall system's comfort and acceptance.

3 | Investigation of textile electrodes for delivering transcutaneous electrical stimulation

Chapter Highlights

As previously explained, when talking about the use of electrical stimulation in the clinical field we refer to the delivery of current to a volume of tissue between a pair of electrodes (cathode and anode). These latter can be implanted, percutaneous or transcutaneous (superficial), as detailed in Section 1.3.4.
With respect to the clinical application the most used type of electrodes are the superficial ones, ideal for temporary applications as they can be easily placed and removed. Nevertheless, these electrodes are also associated with some disadvantages such as the risk of inducing skin irritations and their non-reusability. Starting from this, research is now moving toward the development of textile-based electrodes, which could be a valid alternative for long-time and domestic use of FES. They seem to reduce the risk of skin irritations, due to their good ventilation and flexibility, and could be easily integrated into clothes, improving the overall efficacy of wearable FES systems.
In the present Chapter, a study is presented in which a novel set of ink-based printed textile electrodes for FES was developed in collaboration with the Department of Design of Politecnico di Milano.
This study was accepted for publication on Artificial Organs.

The Chapter is organized as follows. Section 3.1 presents the actual literature about existent textile-based electrodes and their validation. Based on this, Section 3.2 explains the rationale that prompted the present investigation. Section 3.3 details the procedure we followed both for realizing the electrodes and for validating them in comparison to standard hydrogel electrodes. Then, Section 3.4 exposes the study results and the discussion around them. Finally, Section 3.5 summarizes the main findings of the study and highlights its limitations.

Chapter Contents

3.1 State of the Art 90

3.1.1 Electrodes characteristics . . . 91
3.1.2 Production Methods . . . 92
3.1.3 Evaluation Methods . . . 92
3.1.4 Examples . . . 94
3.2 Objective of the study . . . 95
3.3 Materials and Methods . . . 96
3.3.1 Ink-based printed textile electrodes . . . 96
3.3.2 Self-adhesive hydrogel electrodes . . . 97
3.3.3 Skin-electrode impedance . . . 97
3.3.4 Tests on non-disabled subjects . . . 98
3.4 Results and Discussion . . . 106
3.4.1 Skin-electrode impedance . . . 106
3.4.2 Tests on non-disabled subjects . . . 107
3.4.3 Limitations . . . 111
3.5 Conclusions . . . 111

3.1. State of the Art

When dealing with the rehabilitative field, ES is usually delivered through transcutaneous electrodes, which can be easily placed and removed and are thus suitable for temporary applications. Conventionally, these electrodes are represented by self-adhesive, disposable Ag/AgCl pads, interfacing with the skin through a hydrogel layer which improves the skin contact and assures a homogeneous current flow [122, 284].

These standard electrodes are widely available at a moderate cost and allow an easy and ad-hoc positioning [285]; moreover, they are advantageous for fixation and good contact with the skin [123]. However, they are unable to retain moisture for long periods, resulting in a deterioration of skin adherence after a few applications [122]. The decrease in resistivity due to the drying out of their hydrogel layer causes a decrease in resistivity that negatively affects the stimulation efficacy and comfort. Additionally, they can cause skin irritation and allergic reactions in users over time and they cannot be used with different subjects as it would be completely unhygienic, considering that they cannot be properly sanitized [123, 286].

A further critical aspect lies in the placement of these electrodes because it strongly influences the stimulation outcomes but, on the other hand, ensuring a precise and repeatable positioning across subjects and sessions is challenging and necessitates the presence of a trained therapist. This is in contrast with the general shift from hospital care to home-based care that has been observed recently [258, 259], which would be desirable to reduce healthcare costs and burden of care for subjects with disabilities and caregivers because functional activities could be practiced in the actual home environment, without the necessity to go to hospitals [287].

In this scenario, textile-based electrodes are emerging as a valid alternative for long-time and domestic use of FES. These electrodes increase the user's comfort [288], better adapting to the body shape [289], and reduce the risk of skin irritations, due to their good ventilation and flexibility [123]. Furthermore, they could be easily integrated into clothes, improving the overall efficacy of wearable FES systems [290]. In fact, this reduces the donning time, eases the cleaning processes [123] and allows to target

predefined location of the body without expert knowledge [286], which consequently increases the user's independence.

3.1.1. Electrodes characteristics

Various conductive textile materials were investigated and compared for manufacturing textile stimulation electrodes [289].
This process was boosted by the increasing interest in developing wearable electrochemical devices, mainly realized with the screen printing technology where a printing ink is inserted in a mesh with an appropriately designed pattern and pressed onto the final substrate. Considering the intended wearable use, these inks should be stretchable and flexible in order to maintain their structural integrity and conductive properties under conditions commonly experienced by the human body, such as repeated deformations and stretches. Indeed, these capabilities facilitate seamless integration with the biological tissue, minimizing potential irritations [291]. A rich variety of ink formulations has been developed, comprising different materials such as carbon nanotubes, graphene, and noble metal-based nanoparticles, intended to improve the system stretchability and minimize concentrated stress locations that may lead to crack formations. Furthermore, there is a focus on tailoring the device's design so that it can accommodate additional stress. Promising results were also reported from literature studies that developed textile electrodes for delivering Neuromuscular Electrical Stimulation, by integrating conductive textiles into fabric strips [123] or clothes [285, 289].
In general, the mainly employed materials for producing electrodes to be integrated into garments are inorganic metal conductors [122]. Silver, in particular, is generally used as ink or as particles/flakes in coating or printing pastes.
Considering the dimension, textile electrodes follow the same guidelines typically used for hydrogel ones: smaller pad when a high stimulation complexity or selectivity is desired (to avoid activation of motoneurons which in turn co-activates non-synergistic muscles); larger pads to avoid localized electrical field, thus reducing pain and improving user comfort [122, 292].
Regarding the shape, usually round and rectangular-shaped electrodes are preferred because the former avoid sharp corners and elongated shapes that may cause needle-like stinging sensations, while the latter better cover the skin surface and reduce the risk of insufficient selectivity for motor points [122]. However, in the majority of studies, a water layer at the skin-electrode interface was needed to increase moisture and conductivity of the skin and guarantee a comfortable stimulation. This also applies to commercial systems [293, 294] but precise guidelines on the moisturizing process are lacking. According to the review published by Euler et al. [122], the majority of studies regarding textile electrodes use them in wet conditions with either water, saline solutions or gel, while only two studies [295, 296] employed dry textile electrodes.
Although these latter studies successfully developed dry textile electrodes that did not exceed users' pain thresholds, wet electrodes have shown increased reliability and reduced pain. Zhou et al [123] observed significantly improved stimulation comfort and motor threshold with wet electrodes. Similarly, Euler et al. [122] found a significantly lower skin-electrode impedance for the same textile electrode construction when it was wetted with tap water. An intermediate solution was presented in the work of Dolker et al. [295] where the skin was moistened with a wet towel before placing the electrodes, making them a between-state among dry or wet electrodes.

3.1.2. Production Methods

Taking into account the production methods of textile electrodes and their integration into garments, Guo et al. [292] have distinguished four different levels of possible integration:

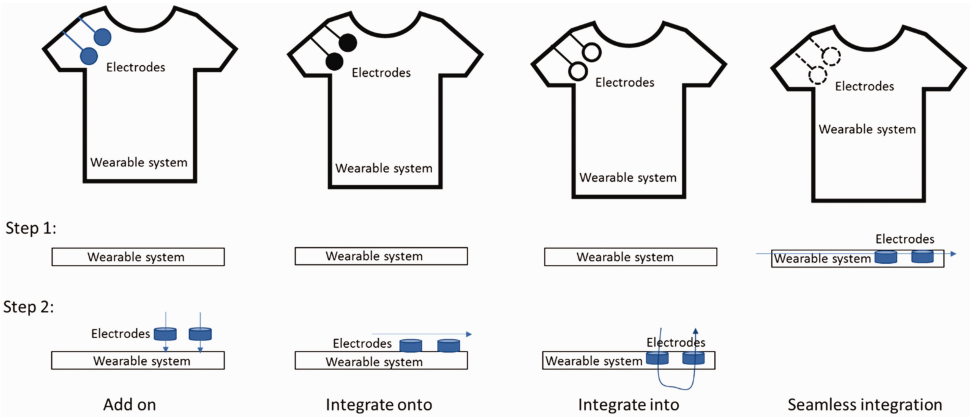

Figure 3.1: Integration levels for textile electrodes in wearable systems. Image taken from [292].

- in *level 1 (add on)* electrodes are made by weaving, knitting or nonwoven conductive fabrics [122], whilst textiles only act as a substrate to position them [292]. The integration of conductive fabrics into garments is realized using embroidery, glue, or detachable fixtures, such as snap buttons or hook-and-loop fasteners [122].
- in *level 2 (integrate onto)* electrodes are applied to the textile substrate by coating or printing. Differently from the *add on* class, here the electrode shape and size are defined during the integration process.
- in *level 3 (integrate into)* conductive yarns are integrated into the garment by sewing or embroidery, which guarantees a more robust fixation.
- in *level 4 (seamless integration)* conductive yarns are seamlessly integrated into the textile non-conductive substrate by Intarsia or Jacquard knitting as a "pattern". The core characteristic of this level is that both electrodes and the wearable system are simultaneously created, without requiring pre or post-processing.

3.1.3. Evaluation Methods

Various quantitative and qualitative methods have been developed to evaluate and compare the electrical properties and the stimulation comfort associated with different types of electrodes.

Electrical properties: The evaluation of the electrical properties of electrodes considers their general conductivity, related to the concepts of resistance and impedance, and the current distribution through their surface. In general, the desired characteristics for electrodes intended for stimulation are a low resistance or impedance and a homogeneous current distribution, essential to avoid hot spots that may cause discomfort and pain.
Some methods developed for acquiring these measures are hereby listed, together with the main results obtained from the literature studies applying them.

In [286], the electrode resistance was evaluated by applying two identical periodic pulses with a voltage of 20 V, frequencies of 15 Hz, 30 Hz, 60 Hz and 120 Hz, and fixed pulsewidth directly to the electrode. The output waveforms were acquired by an oscilloscope, and those obtained from hydrogel and textile samples demonstrated a similar behavior.
Differently, in [296] the electrical resistance was measured by placing the electrode between two conductive plates and using a multimeter, subtracting the resistance of the plates in the calculation. Then, the electrical resistivity was extracted using the formula:

$$\rho = \frac{R \times S}{L} \tag{3.1}$$

where R is the resistance, S is the area of the cross-section and L is the thickness of the electrode.
By comparing this measure in the case of a different pressure applied on the electrode, they notice a decrease in resistivity with an increase in pressure. This proves that textile electrodes should be placed tightly on the skin to ensure better conductivity.
In the same study, they also measured the current distribution in nine points on the electrode by applying current to the conductive yarn layer under the electrode, which then flew via nine conductive pins on top of it. Then, a heatmap was used to represent the current distribution. Many conductive yarn patterns with different grid sizes were evaluated and the outcomes showed an influence of the grid size on the current distribution.
An alternative method to measure the surface resistance of electrodes was employed in [297], applying the triple method from 16 different points using a multimeter. It also allowed us to retrieve the distribution of the resistance values, which is related to the concept of the current distribution. Moreover, Signal-to-Noise Ratio (SNR) values of electrodes were calculated using a signal generator to create square waveforms at 10 V and 60 Hz and employing a digital oscilloscope to collect the signals. Results reported a higher resistance for conventional hydrogel Ag/AgCl electrodes than almost all tested textile ones, while comparable SNR outcomes were obtained for the two electrode types.
In the study by Zhou et al [123], the electrode-skin impedance was measured by a potentiostat with a 10-mV (RMS) AC sinusoidal signal in a frequency range from 0.1 Hz to 100 kHz. A two-electrode cell configuration was applied, by placing a pair of electrodes over the skin with a proximal inter-electrode distance of 4 cm. Tests were carried out for hydrogel electrodes and both dry and wet textile ones. Results showed that hydrogel electrodes had a significantly higher resistance than both textiles. With respect to the impedance, hydrogel electrodes demonstrated an intermediate behavior between wet and dry textiles.

Intensity thresholds: The definition of subject-specific stimulation amplitude thresholds is a fundamental prerequisite when delivering current to humans in order to get the desired effect without causing any discomfort.
Moineau et al. [285] compared these thresholds for gel and fabric electrodes for NMES. To this aim, they delivered asymmetric, biphasic and balanced pulses with a frequency of 30 Hz, a pulsewidth of 300 μs and an increasing amplitude, continuously growing with 1 mA steps. During this ramp, the following thresholds were identified: the sensory threshold as the one eliciting a consistent buzzing sensation under the electrodes, the movement threshold as the one inducing a limb movement (not against gravity), the full range-of-motion threshold as the one fully mobilizing the limb against gravity, the maximal threshold as the maximum value that the subject could tolerate. Every time one of these thresholds was identified,

the stimulation was turned off and then on again to repeat the test for confirmation. Overall, the measurement was performed four times to evaluate the consistency of the found values.
A similar analysis was performed by Zhou et al. [123] who delivered monophasic and rectangular stimulation pulses with a frequency of 30 Hz, a pulsewidth of 200 μs and an increasing amplitude, continuously growing with 1 mA steps starting from 1 mA. In this case, the sensory, movement (referred to as motor in this case) and pain thresholds were estimated. Similarly to before, thresholds were acquired four times, with the first two sessions intended to accustom the subject to the stimulation sensation and the other two used to extract the thresholds' mean values.

Stimulation comfort: Usually the assessment of stimulation thresholds was combined with qualitative pain evaluation methods, which can be categorized into both unidimensional and multidimensional questionnaires. The former assess pain as an overall feeling, while the latter consider pain divided into perception categories. The most common examples of unidimensional questionnaires are the Visual Analog Scale (VAS) and the Numeric Rating Scale (NRS). The VAS method assesses pain on a 10 cm line where one end represents "no pain" and the other "worst pain". The subject is asked to place a mark on the position that best represents the perceived pain and the score is calculated as the distance of this mark from the "no pain" ending. Differently, the NRS method uses a segmented numeric scale from "no pain" to "worst pain".
Examples of multidimensional questionnaires are the Fhort-Form McGill Pain Questionnaire (SF-MPQ) and the Transcutaneous Electrostimulation Comfort Questionnaire (TESCQ). The SF-MPQ is a shortened version of the McGill Pain Questionnaire that, similarly to its original form, considers 3 classes of descriptors (sensory, affective and evaluative) but fewer descriptors for the sensory and affective dimensions (15 instead of 78). Each descriptor is ranked on a scale comprising 0=none, 1=mild, 2=moderate and 3=severe. The TESCQ, instead, is a modified form of the SF-MPQ that, compared to the original SFMPQ, discards the affective descriptors and adds keywords of pricking, pulling, tingling and stinging taken from the full version Mc Gill Pain Questionnaire [122, 298].
The main advantage of unidimensional questionnaires is their easy and fast implementation; on the other hand, multidimensional ones allow a more detailed and multifaceted characterization.

3.1.4. Examples

The study by Moineau et al. [285] describes a pilot study on able-bodied subjects of shirts and pants containing custom-size electrodes knitted with a conductive yarn for FES delivery. The FES-shirt was used to perform repetitive drink-like motions by stimulating the anterior deltoid, posterior deltoid, biceps and triceps, with a stimulation sequence lasting 6s followed by 6s of rest with no stimulation. The FES-pants, instead, were used to execute repetitive mobilizations of knee and ankle muscles on both legs simultaneously, with the subject seated on a chair. In this case, the FES sequence lasted 18 s, followed by 18 s of rest with no stimulation. Results showed that both stimulation comfort and induced muscle contractions were comparable to that of standard self-adhesive gel electrodes. Further advantages were the high level of customization that they enabled and their simplicity of use which allowed a significant saving of time and subject independence in donning/doffing phases. The main limitations highlighted by the authors were the compressing action, the need to apply water on the outside of the electrode before stimulation which is time-consuming, the limited selectivity due to the large size of electrodes and the

simple open-loop FES protocol implemented.
In another study [286], garments were developed for delivering Transcutaneous Electrical Nerve Stimulation (TENS) for pain relief. These were based on the intarsia knitting technique with silver conductive yarn knitted into a knitwear. The experimental setup aimed to compare the TENS knitwear with the hydrogel electrode, focusing on washability and conductivity. The former was investigated through 10 washing cycles which did not affect the overall resistance of textile electrodes. The latter, instead, was explored by applying two identical periodic pulses to both electrodes and comparing the output signals, acquired by a cathode ray oscilloscope. Also in this case, similar results were obtained, demonstrating comparable electrical properties and stimulation efficacy for textile and hydrogel electrodes.
However, in all cases, an electrolytic layer at the skin-electrode interface was needed to increase moisture and deliver a comfortable stimulation. In fact, compared to dry electrodes, wet ones reduce the skin-electrode impedance and thus the induced pain [299]. This also applies to commercial systems [293, 294] but precise guidelines on the moisturizing process are lacking.

3.2. Objective of the study

Although the theoretical feasibility of textile electrodes was proved by various literature studies, some aspects still require a deeper investigation. Examples are the impedance of such electrodes and the need of a conductive layer to assure an adequate conveying of electric signals at the electrode/skin interface, related to the resulting stimulation comfort and performance [101].
These aspects are explored in this proof-of-concept study which aims to compare a novel set of ink-based printed textile electrodes with respect to self-adhesive hydrogel ones, focusing on the following aspects:

- impedance characteristics;
- performance of stimulation-induced contractions during both dynamic and isometric tests;
- perceived stimulation comfort.

The first aspect was fundamental for exploring differences between the two electrodes in terms of current delivery. Its trend over time was investigated for new and used electrodes and, for textile samples, it was also studied after washing them. The second one aimed at comparing their efficacy either in providing an effective functional movement or in inducing muscle fatigue. Additionally, the EMG of the stimulated muscle was acquired to compare its activity with and without stimulation for the two electrode types and rule out the presence of voluntary contractions.

The third one allowed the subjective evaluation of their usability and acceptability.
Differently from other works with a limited sample size, only involving one non-disabled individual [285, 288] or a few spinal-injured individuals [300], here an extensive testing procedure was conducted involving 14 subjects without disability. Results obtained from the overall study were used to conclude about possible applications of textile electrodes in rehabilitation, promoting their further employment for home-based therapies.

3.3. Materials and Methods

3.3.1. Ink-based printed textile electrodes

Textile electrodes were realized by integrating screen-printed electrodes (commercial ElastaTrode™ by Conductive Transfers UK Ltd) into cotton strips by thermal adhesivation (Figure 3.2). The electrodes were attached to the textile using a thermopress at 180° for 20 seconds and with a pressure of 2 atm; this allows for a permanent and lasting connection that ensures stability of the electrodes both during washing and sterilization.

The electrodes were built with ink added with conductive powder while the tracks were built with a conductive and elastic paste. The tracks were covered with thermoadhesive tape to preserve washability and durability and allow for attaching the electrodes to the textile. The electrode/cable interface was realized by integrating a metallic button into each electrode terminal to be connected to the button-like extremities of the stimulator cable. Velcro straps were added to each strip to anchor it to the subject's leg.

Screen-printed electrodes (SPEs) are made by thick film deposition onto plastic substrates, where different types of conductive ink are printed to create the electrode pattern. The ElastaTrode ink-based electrodes are mainly composed of silver, which ensures good electrical conductivity and reliable signal transmission while providing an abacterial and washable solution. Despite this, the proprietary nature of the electrodes

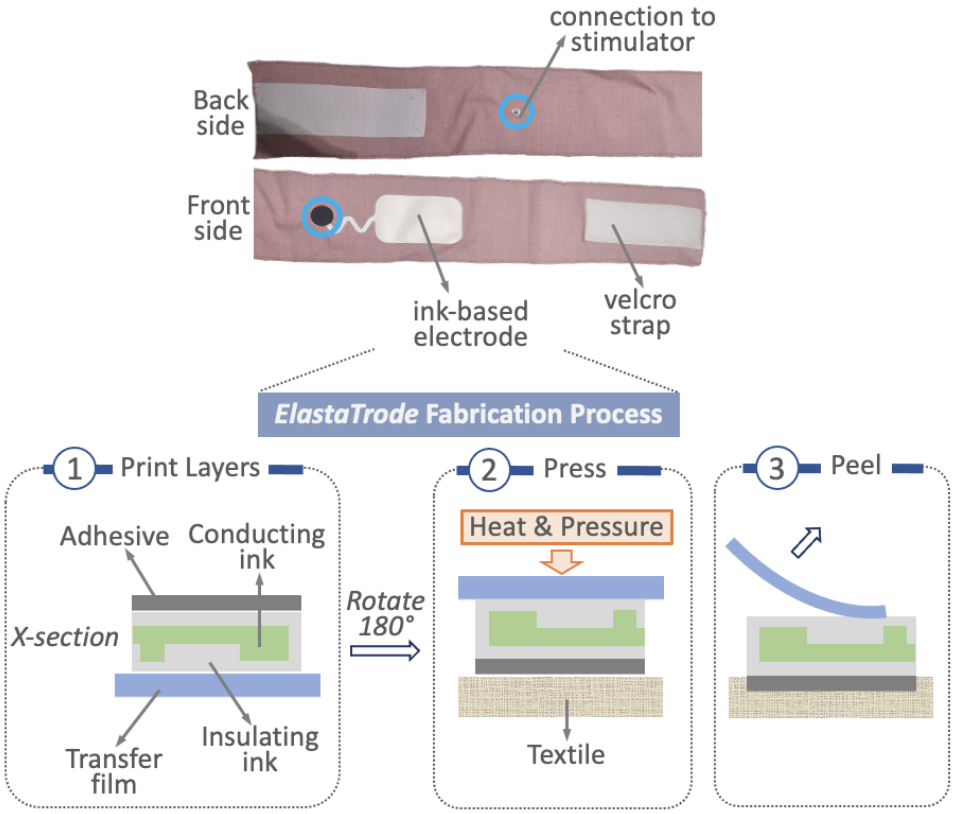

Figure 3.2: Back and front side of the used textile electrodes (ElastaTrode™) and zoom on their composition and the process followed to realize them.

prevents disclosure of the composition of the conductive material.
The used ink is biocompatible, guaranteeing its safety for prolonged use on the skin, and offers flexibility and stretchability. This allows the electrodes to conform to body's movements without causing any discomfort [123] or compromising conductivity, unlike classical systems based on conductive ink, elastic conductive wire, or graphene. All these aspects make them ideal for wearable healthcare applications.

3.3.2. Self-adhesive hydrogel electrodes

In the present work, we used self-adhesive disposable Ag/AgCl electrodes (PALS®, Axelgaard Manufacturing Co Ltd). These are pre-gelled electrodes as they already incorporate the Axelgaard patented multi-layer MultiStick® hydrogel. They have a stainless-steel knit fabric design which allows good flexibility and, together with the hydrogel layer, guarantees a comfortable stimulation by evenly dispersing current and eliminating stinging, edge biting, and hot spots [301]. For the sake of simplicity, these electrodes will be referred to as "hydrogel" in the text.

3.3.3. Skin-electrode impedance

An estimate of the skin-electrode impedance was carried out with an LCR meter (GW INSTEK LCR-6000 Series), measuring the impedance over a wide range of frequencies ([10 Hz; 300 kHz]). The device (Figure 3.3b) has a power cable receptacle used for the power supply and an RS-232 Interface for the PC connection, enabling the utilization of the corresponding LCR- 6000 PC software for further applications. The device can be connected to the Device Under Test (DUT) by using a four-terminal measurement configuration that simultaneously measures four components of complex impedance (parameters) in a measurement cycle. These include a primary parameter, a secondary parameter and two monitor param-

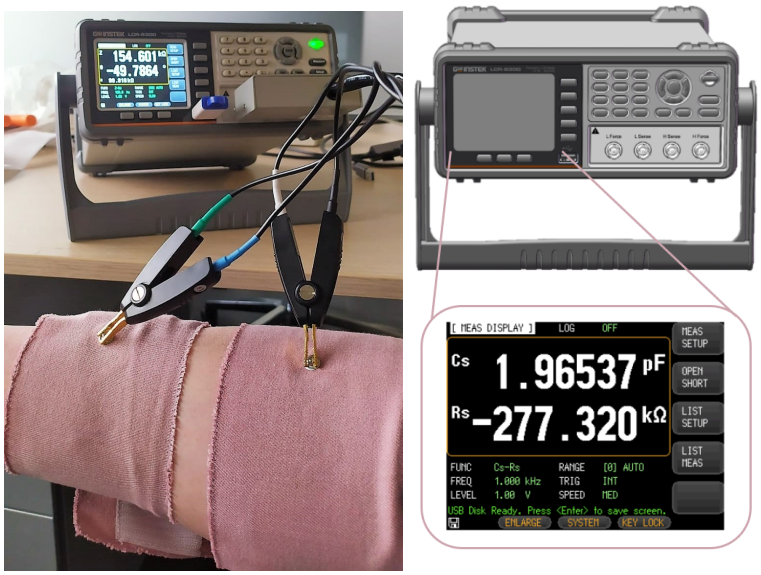

(a) (b)

Figure 3.3: LCR measurement system: measurement setup with the LCR meter terminals connected to a pair of electrodes placed on the subject leg (a) and LCR meter device (b), with a zoom on its display.

eters, which can be set on the *SETUP* page. On the same page, also the test frequency can be set over a wide range of possible values. The internal buffer allows the LCR-6000 to store up to 10000 measurement readings that can be saved to an external USB drive in a *.csv* file format.
One subject (female, 24 years old) was involved in this measurement. She was seated on a chair and was required to keep the tested leg in a horizontal position. A pair of electrodes was placed over the tibialis anterior muscle with a proximal inter-electrode distance of 6 cm [123], as shown in Figure 3.3a. The electrodes were connected to the LCR meter using two of the four available terminals. Z (absolute impedance) was set as the primary outcome measure, evaluated with a 1V AC sinusoidal signal at different frequencies between 10 Hz and 100 Hz, as this represents the frequency range commonly used in FES applications. 10 points were obtained for each frequency value and their average was considered. The test was replicated for textile and hydrogel electrodes and, in both cases, for a set of new and worn-out electrodes to evaluate their impedance change over time. The term worn-out electrodes indicates samples used for 15 hours of non-continuous stimulation for textile ones, or for 5 hours of non-continuous stimulation for hydrogel ones, before the drying of the conductive gel. For textile electrodes, the test was carried out both with and without the application of a moisturizing cream on the skin.
Additionally, we tested the impedance of textile electrodes after 10 washing cycles. The washing procedure was performed with a standard washing machine, using a delicate detergent and a program with these parameters: 30°, 400 rpm and 45 minutes. This test aimed to evaluate the durability of textile electrodes, related to the possibility of cleaning and re-using them.

3.3.4. Tests on non-disabled subjects

Experimental Setup

The experimental setup used for the acquisitions (Figure 3.4) included three main components: a single-joint test bench, a neuromuscular electrical stimulator and an EMG amplifier.

Test bench The single-joint test bench comprised a Sensojoint 5012 torque-controlled complete drive (Sensodrive GmbH) working at 1 kHz and enabling knee flexion-extension movements. It includes a BLDC motor with a 48 V DC voltage supply, a motor controller, a gearbox (Harmonic Drive) plus an encoder and a completely integrated torque sensor, for the real-time acquisition of the knee angle and the leg-structure interaction torque, respectively. The leg of the subject was anchored to the structure mounted on the actuator using two velcro straps at the ankle and the calf. This structure was composed of an adjustable aluminum bar coupled with the user's shank and a pedal to hold the foot.
The test bench movements were managed by a general-purpose computer (Linux-based OS) through EtherCAT-based communication. The computer was sending time-by-time packages to the motor in a master-slave configuration using the Power Of Ethernet (POE) protocol.

Stimulator The test bench was integrated with the stimulation block which consisted of a current-controlled stimulator (MotiMove-8, 3F - FIT FABRICANDO FABER, Serbia). It generates asymmetric biphasic pulses with exponential discharge and allows to vary the stimulation parameters in the following ranges: frequency from 1 to 500 Hz, pulsewidth from 50 to 1000 μs and amplitude from 1 to 170 mA, with steps of 1mA. It has a rechargeable Li-Ion battery, Bluetooth communication with a PC or a Tablet, a remote controller with a safety switch to stop the stimulation and I2C buses for communication with external sensors and actuators. An RS485 communication link (Baud 115200, Data 8bit, Stop 1bit, No

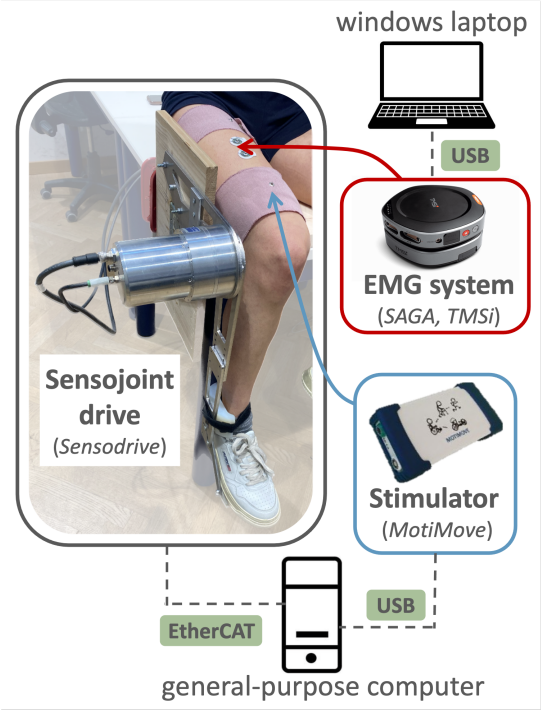

Figure 3.4: Schematic representation of the experimental setup: single-joint test bench, electrical stimulator connected to a pair of electrodes (textile in this case) and EMG system recording the Rectus Femoris muscle activity. Dotted lines indicate the connections between components.

parity) allows the research mode use, in which the stimulator acts as a slave device, which is the modality used in the present work. The stimulator is then connected to the electrodes through monopolar stimulation cables and stimulation is delivered in the *pulse-by-pulse* modality where each command generates one pulse for each channel (8 channels available), allowing a better control of the stimulation delivery.
The stimulator was connected via USB (RS485) to the general-purpose computer (Linux-based OS), the same one used for the test bench control. It was sending time-by-time packages to the stimulator in a master-slave configuration to modulate the stimulation parameters at a frequency of 40 Hz.
For the purpose of this work, only one channel was connected to a pair of stimulation electrodes since only one muscle (the Rectus Femoris of the right leg) was stimulated.
Two electrode types were alternatively placed over the muscle belly: either self-adhesive disposable Ag/AgCl electrodes (PALS®, Axelgaard Manufacturing Co Ltd) or ink-based printed textile electrodes described in the previous paragraph and shown in Figure 3.2. Electrodes were matched in terms of size, which was equal to 5x9 cm.

EMG system The EMG system was a SAGA 64+ Device (TMS International), which is a DC-coupled electro-physiological amplifier characterized by low input noise (<1 μV), high input impedance ($>$ 1 GΩ), high common mode rejection ratio (equal to 100 dB at 50/60 Hz) and high resolution (24 bits). The system has a maximum sampling rate of 4 kHz, an input range from -150 mV to +150 mV and allows for both common and average reference amplification. It uses active signal shielding to minimize the electrode cable capacitance and thereby minimize cable movement artifacts and sensitivity to main

interferences (50/60 Hz). The SAGA device consisted of a Data Recorder and a Docking Station. The former was intended to capture and digitize electrophysiological signals and/or sensor data; the latter acted as a data receiver, transmitting data to the acquisition PC. The Docking Station was connected to a second general-purpose PC (HP Pavilion laptop) via a USB cable. This connection was used to transfer data to the PC, where they were stored for further processing, and to control the device by sending commands from the application software to the SAGA system.
The main application software is the TMSi Polybench, the framework on which another software (SAGA Quick Recording Application) was built. This latter contains an interface to manage the recordings with the SAGA system and configure the SAGA Data Recorder.
We employed bipolar input connectors (BIP 1-2 and BIP 3-4) characterized by a pair of cables, for the positive and the negative input signal, the difference of which is recorded. The reference is represented by a separate lead connected to the GND input.
In the present work, the SAGA device was used to acquire the EMG signals of the Rectus Femoris of the right leg at a sample frequency of 4 kHz. EMG signals were recorded by connecting a bipolar cable to disposable snap-on electrodes; in particular, silver chloride circular (recording diameter of 24 mm) surface Ag/AgCl pre-gelled self-adhesive electrodes (Kendall H124SG) were used, placed according to SENIAM [302] with an inter-electrode distance of about 2 cm.

Experimental Protocol

The acquisition protocol aiming at comparing textile and hydrogel electrodes adheres to the Helsinki Declaration and the Ethical Committee of Politecnico di Milano (Nr 13/2021) approved it. The following inclusion criteria were defined:

- good health status;
- age $>$ 18 years old;
- intact skin;
- good tolerance to electrical stimulation.

All subjects voluntarily agreed to participate and provided their written informed consent before starting the acquisition. They had minimal or no prior experience with FES.
The experimental protocol (described in Figure 3.5) consisted of 4 different tests (thresholds identification, dynamic test, isometric test and comfort evaluation) and was repeated for both electrode types (labeled type A and B). At the beginning of the test, a randomization procedure was applied to assign each subject either to group 1 (type A electrodes: hydrogel, type B electrodes: textile) or group 2 (type A electrodes: textile, type B electrodes: hydrogel). In this way, any bias due to the accommodation to the stimulation sensation was removed from the results. To ensure the same electrodes' placement among tests, the position of the first pair of electrodes was marked on the subject's leg.
Each acquisition started with the threshold identification for type A electrodes, followed by a 3-minute pause to let the muscle cool down, and then thresholds were identified for type B electrodes. Subsequently, dynamic and static tests were performed, first with type B electrodes and then with type A ones. A pause of 10 minutes was inserted before repeating these tests for the second type of electrodes because the static test could have induced muscular fatigue. Finally, the last step was filling out the post-training questionnaire to evaluate the stimulation comfort with both electrodes.

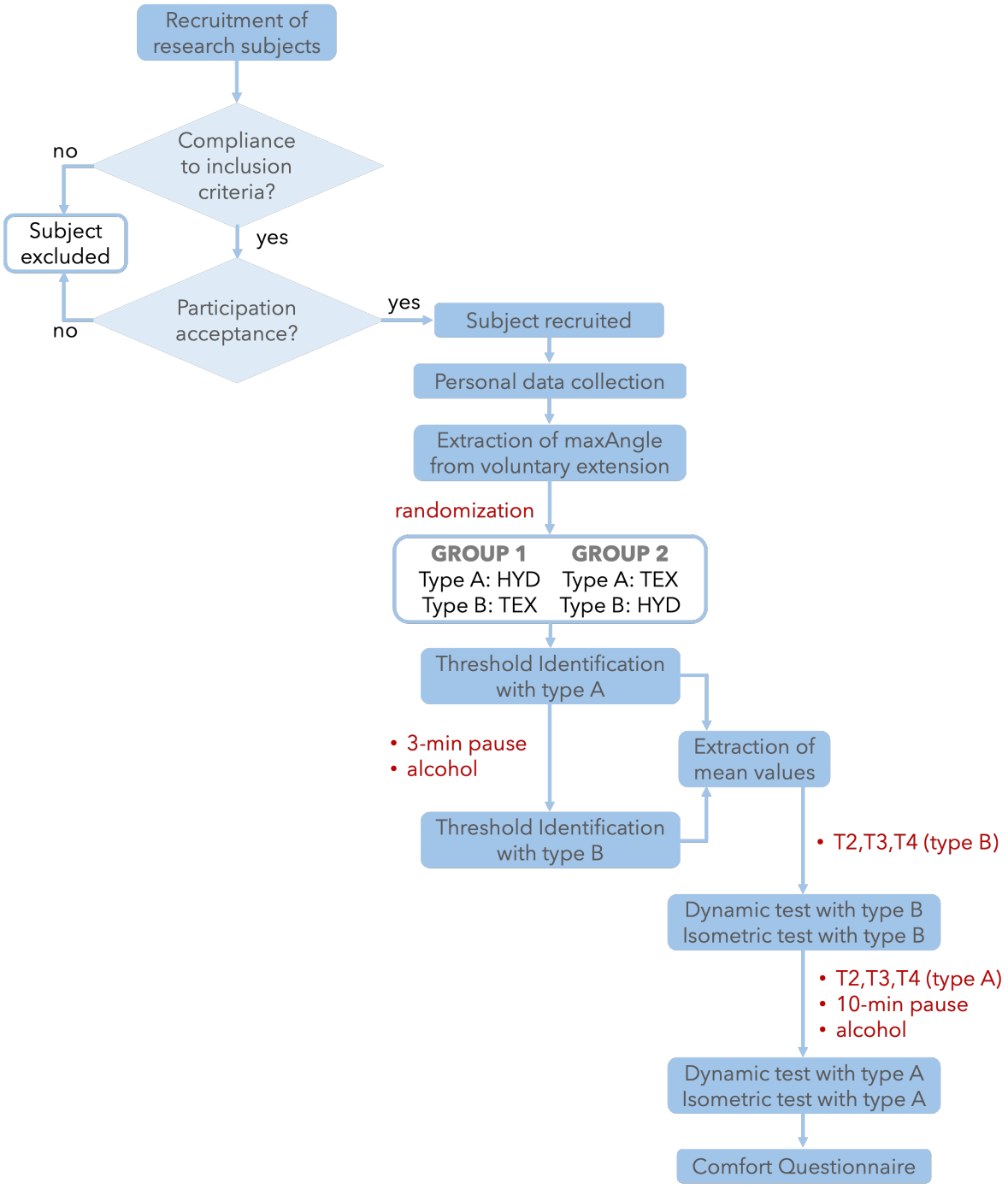

Figure 3.5: Flow chart of the acquisition protocol.

At first, the test bench size was adjusted to the length of the right leg of the subject (four different levels were available) and then the leg was anchored to the structure by using two velcro straps. Before starting with acquisitions, each subject was required to perform three consecutive voluntary extensions and the mean value of the reached angle was saved as the specific maximum extension angle for the subject, and used for further normalization. During this phase the motor was in transparent mode, meaning that it compensates for its inertia, gravity and friction in order not to interfere with the movement.

For all tests, the stimulation pulsewidth and frequency were fixed at 400 μs and 40 Hz, respectively. During the overall protocol, subjects were asked to stay as passive as possible in order not to interfere with the task. To quantify the eventual voluntary participation of subjects in the movement, the surface EMG of the right leg Rectus Femoris (RF) muscle was recorded by using a single acquisition channel. To reduce the electrode-skin impedance, the skin area over the muscle was adequately prepared by shaving and cleaning it with alcohol before placing snap-on EMG electrodes. When textile electrodes were used, also a thin layer of moisturizing cream was spread over the skin under the electrodes and then removed with alcohol before placing hydrogel samples to avoid any performance perturbation.
All protocol steps are hereby detailed:

- *Thresholds Identification.* To provide safe currents to subjects and customize the stimulation delivery according to each one's tolerance level, individual stimulation thresholds were identified. During this phase, the motor was in transparent mode, allowing the leg to freely swing. An increasing current, from 0 mA with 1 $\frac{mA}{s}$ steps, was delivered to the subject's Rectus Femoris and sensory (*T1*), movement (*T3*), maximum (*T4*) and pain (*T5*) thresholds were identified.
  T1 was defined as the current value at which the stimulation started to be felt by the subject, while *T5* as the one over which FES was not tolerated anymore; both levels were verbally reported by participants. *T3* and *T4*, instead, were the current values inducing a first leg movement and the full knee extension, respectively; both values were automatically identified through the encoder angle: *T3* as the value inducing a knee angle change of 2° from the initial position, *T4* as the one inducing a knee extension over 80% of the subject-specific maximum extension angle. An additional threshold, defined as motor threshold ($\hat{T2}$), was defined as the stimulation intensity for which motor fibers were activated and was only estimated during the protocol execution as *T3* minus 2 mA. The accuracy of this estimate was then assessed by comparing $\hat{T2}$ with the real motor threshold value *T2*, retrieved through the offline analysis of the EMG signal.
  The overall procedure was repeated four times for each type of electrode: the first one was intended as a familiarization of the subject with the sensation of the surface stimulation, while the other three (experimental trials) were used to compute the mean and standard deviation of each threshold value, to account for intra-subject variability.

- *Dynamic Test.* In this phase the motor was in transparent mode, allowing free swings of the leg while recording its angular position. A rising current was delivered in the form of a 5-steps ramp (Figure 3.6), from $\hat{T2}$ to a level in the [$\hat{T2}$; *T4*] subject- and electrode-specific range. Each step of the ramp was tested 3 times for a total of 15 movements and the step-wise increase (δ) between them was computed as:

$$\delta = \frac{(T4 - \hat{T2})}{NumberOfLevels} \tag{3.2}$$

  The FES wave was shaped to induce the knee extension and support its flexion, supposed to occur passively under gravity. Each single movement (zoomed in Figure 3.6) lasted 4 seconds. The first 2 seconds were intended to induce knee extension: they included 1 second of increasing current from $\hat{T2}$ to the maximum, shaped as a beta-function, followed by 1 second of constant current. Then, as flexion was supposed to occur passively under gravity, the current was linearly decreased to $\hat{T2}$ in 0.5 seconds and then maintained constant to zero for 1.5 seconds. At the beginning of the test, 2 seconds before starting the stimulation, a single biphasic pulse at 10 mA (pulsewidth

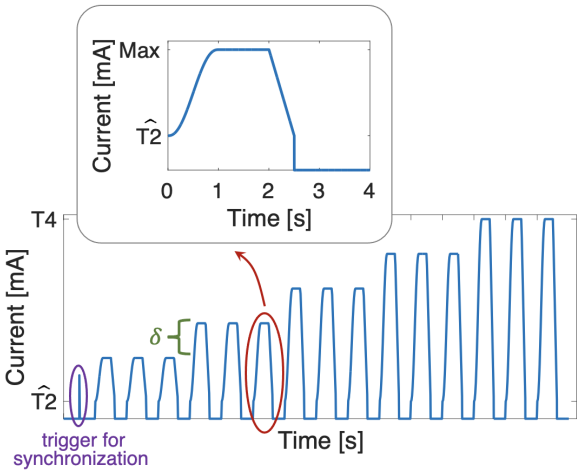

Figure 3.6: Shape of the current wave used for the dynamic test. It includes the EMG trigger followed by 15 flexion/extension repetitions, 3 repetitions for each of the 5 tested levels, with an amplitude difference of δ. A zoom on the shape of the single generic extension is added.

of 400 μs) was delivered and was then used as a trigger to synchronize the EMG signal with angle and torque signals acquired by the test bench.

- *Isometric Test.* In this phase the motor was locked, keeping the knee flexed at 90° without allowing any movement. The current level was increased from $\hat{T2}$ to $T4$ with a 2-second ramp and then kept constant (Figure 3.7). The test was stopped when the mean torque, computed from the loadcell value with a moving average over a 500 ms window, went below 50% of its maximum value. As in the previous test, 2 seconds before switching on the stimulation, a single 10 mA biphasic pulse was delivered to synchronize the EMG signal acquisition.

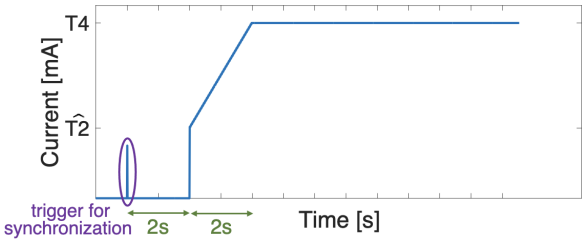

Figure 3.7: Shape of the current wave used for the isometric test. It includes the EMG trigger followed by 2 seconds of pause, 2 seconds of increasing ramp from $\hat{T2}$ to $T4$. Then current is maintained constant until the end of the test.

- *Comfort Questionnaire.* At the end, each participant was required to fill the Transcutaneous Electrical Stimulation Comfort Questionnaire (TESCQ), a modified form of the short-term McGill questionnaire [298] (Figure 3.8), to judge the stimulation comfort for both electrodes.

Data Analysis and Statistics

EMG analysis The EMG signal was filtered with an 8-th order high-pass Butterworth filter with a cutoff frequency of 20 Hz. Stimulation artifacts were identified with a thresholding analysis on the differential

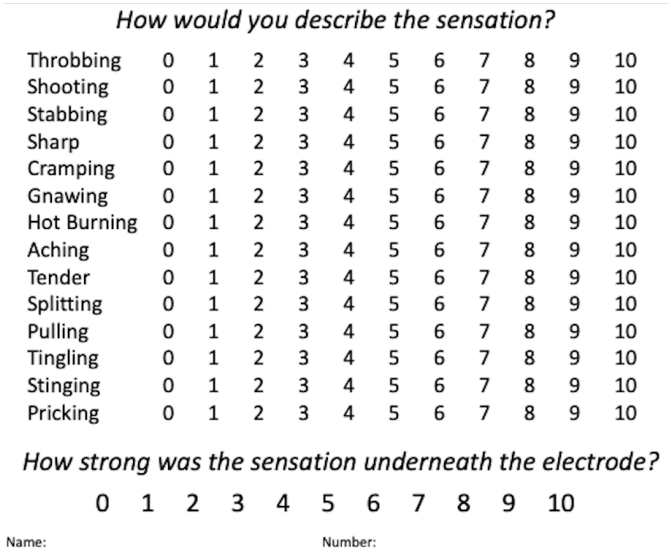

How would you describe the sensation?

Throbbing	0	1	2	3	4	5	6	7	8	9	10
Shooting	0	1	2	3	4	5	6	7	8	9	10
Stabbing	0	1	2	3	4	5	6	7	8	9	10
Sharp	0	1	2	3	4	5	6	7	8	9	10
Cramping	0	1	2	3	4	5	6	7	8	9	10
Gnawing	0	1	2	3	4	5	6	7	8	9	10
Hot Burning	0	1	2	3	4	5	6	7	8	9	10
Aching	0	1	2	3	4	5	6	7	8	9	10
Tender	0	1	2	3	4	5	6	7	8	9	10
Splitting	0	1	2	3	4	5	6	7	8	9	10
Pulling	0	1	2	3	4	5	6	7	8	9	10
Tingling	0	1	2	3	4	5	6	7	8	9	10
Stinging	0	1	2	3	4	5	6	7	8	9	10
Pricking	0	1	2	3	4	5	6	7	8	9	10

How strong was the sensation underneath the electrode?

0 1 2 3 4 5 6 7 8 9 10

Name: Number:

Figure 3.8: Transcutaneous Electrical Stimulation Comfort Questionnaire (TESCQ) filled by subjects after completing the protocol, both for textile and hydrogel electrodes.

EMG (when the difference in EMG amplitude among consecutive samples was $>$ 100 mV). For each stimulation window lasting 25 ms (equal to the stimulation period), the first 3.7 ms were blanked as corresponding to the stimulation artifact in our data. The following 20 ms were considered as signal regions where the muscle activity could be observed. The EMG signal was used to extract:

- *Motor threshold (T2).* This was obtained through the analysis of the evoked M-wave in the EMG signal acquired during the threshold identification test. Specifically, in the 20 ms windows considered, a signal deviation from baseline exceeding 5 mV was categorized as an M-wave [303]. *T2* was set as the average across the three repetitions of the minimum current levels at which the typical M-wave shape first appeared.
- *Voluntary participation during FES-induced muscle contractions.* This was quantified by analyzing the 20 ms windows of the EMG signal acquired during static and dynamic tests. The power of the volitional EMG was computed during phases without stimulation (REST) and with stimulation (STIM-ON). The REST phase consisted of the 2 seconds between the time point at which the synchronization trigger was sent and the start of the stimulation ramp.
  For each window, the mean was removed and an adaptive filter was applied, following the procedure described in [304]. The present stimulation period was predicted from a linear combination of M foregoing stimulation periods. The output of the filter was computed as:

$$eEMG_{\mathrm{v}}(n) = EMG_{\mathrm{f}}(n) - \sum_{j=1}^{M} b_j EMG_{\mathrm{f}}(n - jN) \tag{3.3}$$

  where $\mathrm{eEMG_v}$ is the voluntary EMG estimated by the filter, $\mathrm{EMG_f}$ is the measured EMG after windowing and high-pass filtering, M is the number of previous stimulation periods used for prediction (M=9 in our case), and N is the number of samples of each stimulation period. The optimal filter coefficients ($\mathrm{b_j}$) were updated after each stimulation period by solving a least square algorithm based on the minimization of the output energy of the current stimulation period with

respect to the filter coefficients (Cholesky decomposition). After extracting the power of $eEMG_v$ for both REST and STIM-ON phases, the respective mean values were computed.

Based on the analysis of position and torque sensor data, as well as of the stimulation parameters used during the trials, the following outcome measures were computed for both electrode types.

Thresholds Identification

- *Mean and Standard Deviation of thresholds.* For each threshold and each subject, the mean and the Standard Deviation (SD) was computed across the three repetitions.

Dynamic Test

- *Mean Range of Motion for each stimulation level.* For each subject, the knee angular trajectory was normalized with respect to his/her specific maximum extension angle. A moving average filter (400 ms window) was applied to the normalized signal and the Range Of Motion (ROM) achieved for each of the 15 movements was registered. Then, the mean value among the three ROM values obtained for each stimulation level was computed.

Isometric Test

- *Peak Torque.* A moving average filter (500 ms window) was applied to the torque signal and the maximum value of the filtered interaction torque since the onset of the stimulation plateau was computed.
- *Time-To-Fatigue (TTF).* The time interval between the Peak Torque and the 50% drop in the torque level with respect to the Peak Torque. This condition was hypothesized to coincide with the appearance of muscle fatigue.
- *Total Duration.* The time interval from the onset of the stimulation plateau to the end of the test.
- *Torque Integral.* The area below the torque by time graph, considering Total Duration as theime interval.

Comfort Questionnaire The items of the TESCQ questionnaire were grouped into cutaneous, deep and general categories. The cutaneous category included stinging, hot burning, sharp, stabbing and pricking; the deep one included pulling, aching, gnawing, and cramping; the general one included splitting, tender, tingling, shooting and throbbing.
For each item, the following quantities were computed:

- *Total Score.* The sum of scores among all subjects.
- *Median and Inter-Quartile Range (IQR).* The median and IQR considering all subjects' scores.

The statistical analysis was conducted to compare the outcome measures obtained with hydrogel and textile electrodes.
Once proved that data followed a non-normal distribution (using the Kolmogorov-Smirnov test), the non-parametric Wilcoxon matched pairs test was applied for all outcomes except questionnaire reports. In that case, in fact, subjects were asked to rate 14 items and thus a Generalized Linear Mixed Model

(GLMM) was applied considering ratings of all subjects across all items and using Electrode type, Item and their interaction as main factors. The Bonferroni method was used to correct for multiple comparisons.
All data elaboration and statistical analysis were performed in MatLab 2021b (MathWorks), except for the GLMM that was performed in SPSS Statistics (IBM).

3.4. Results and Discussion

3.4.1. Skin-electrode impedance

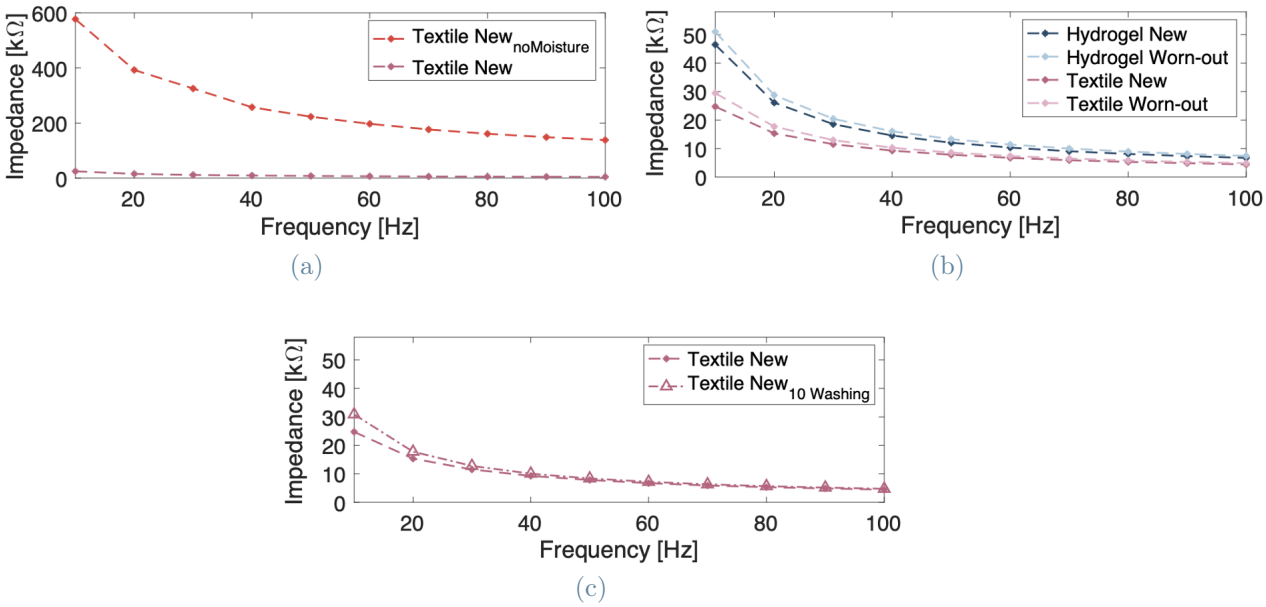

Figure 3.9: Impedance [kΩ] as a function of frequency [Hz]. Panel a is relative to new textile electrodes without cream (no moisture) and with cream. Panel b is relative to new and worn-out samples for both hydrogel (blue lines) and textile (pink lines) electrodes (always moisturized). Panel c is relative to new textile samples both pre (circle marker) and after (triangle marker) 10 washing cycles. Markers correspond to discrete values recorded with the LCR meter.

This first test was intended to evaluate the electrical properties of the studied electrodes. Indeed, given their influence on the resulting stimulation effectiveness and perception, it represents a crucial step to be carried out before performing stimulation tests on human subjects.
Figure 3.9a reports the impedance value recorded for new textile electrodes both with and without the application of moisturizing cream on the skin. The graph was obtained by interpolating the impedance data measured through the LCR meter and by displaying them as a function of frequency. It is evident that the moisturizing layer significantly decreases the electrodes' impedance. This observation is in agreement with other literature studies [122] and proves the necessity of applying a moisturizing layer on the skin before delivering FES through textile electrodes in order not to provoke painful sensations [299]. We can suppose that the presence of this conductive layer reduces the impedance of such electrodes and makes them comparable to hydrogel ones. In this work, the cream was used as moisture and was

preferred to water as it avoids the wetness feeling on the skin [122]. Figure 3.9b, instead, reports the impedance for new and worn-out samples of both hydrogel and textile electrodes. For the latter ones, we only consider the case in which they were applied together with the moisturizing cream because it allows us to have comparable impedance values for the two electrode types.
For all samples, the impedance decreases as the frequency increases.
Comparing hydrogel and textile samples, a higher impedance is observed for the former ones, both in the new and worn-out case. This could be attributed to a different amount of conductive material (gel for the former and moisturizing cream for the latter) at the electrode-skin interface. In fact, it was not possible to precisely control the amount of applied moisturizing cream. At the stimulation frequency (40 Hz), the impedance of new and worn-out samples is equal to 14.6 kΩ and 16.1 kΩ for hydrogel electrodes and to 9.3 kΩ and 10.3 kΩ for textile ones.
Focusing on the electrodes' behaviour over time, instead, it can be noticed that both types of electrodes display a slightly higher impedance in the worn-out case compared to the new samples, probably due to the gradual drying of the conductive layer over time.
Lastly, Figure 3.9c evaluates the washability of textile electrodes. In particular, we performed 10 washing cycles and evaluated the impedance of new textile electrodes before and after the washing cycles. The impedance shows a slight increase after 10 washing cycles, reaching values comparable to those observed for worn-out textiles (panel b), with a value of 10.1 kΩ at 40 Hz. Given that the washing procedure does not significantly impact the impedance value, we can conclude that our textile electrodes can be washed and reused for some time.

3.4.2. Tests on non-disabled subjects

After establishing comparable electrical properties between hydrogel and moisturized textile electrodes, their effectiveness and usability as FES-delivering electrodes were assessed through tests on non-disabled participants.
Sixteen non-disabled subjects were recruited, but then only fourteen of them (8 females and 6 males, mean age of 24.9±1.9 years old) took part in the experimental protocol. For each subject, the current amplitudes used during the experimental procedure were adjusted to the personal feeling of stimulation by registering the stimulation thresholds, defined as the current levels at which a different movement or sensation was generated by FES.
Figure 3.10a reports the boxplots of all stimulation thresholds. For all thresholds, no significant differences were found in the values recorded for textile and hydrogel electrodes (Wilcoxon test, p-value>0.05).
Additionally, for the motor threshold, its real value *T2* was extracted from the M-wave analysis and compared to its estimated value $\hat{T}2$. EMG data were available for 13 out of 14 subjects, due to acquisition problems. Figure 3.10b reports this comparison for both hydrogel and textile electrodes. In both cases, no significant differences were found (Wilcoxon test, p-value>0.05).
Thus, we can conclude that these levels were comparable for the two electrode types. This result assumes particular relevance for the motor threshold (T2) as it strictly relates to the muscle response. In fact, its value was computed by analyzing the M-wave induced in the EMG signal. This was done for 13 out of 14 subjects because for one subject EMG data were not available due to acquisition problems. Then, a pairwise comparison was carried out between T2 and its estimated value $\hat{T}2$ and, both for hydrogel and textile electrodes, no significant differences were found (Wilcoxon test, p-value>0.05).

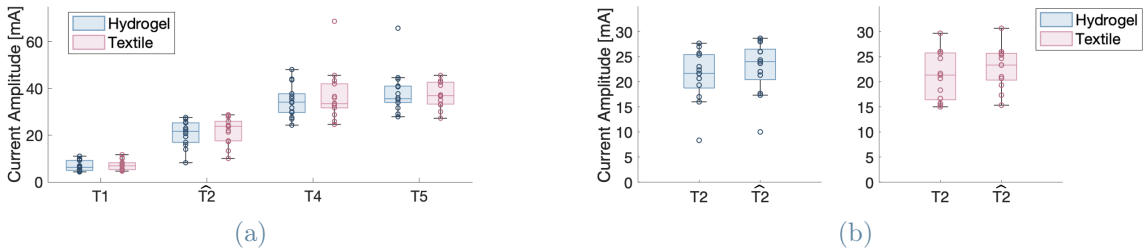

Figure 3.10: Boxplots of stimulation thresholds recorded during the test (a). For the motor threshold T2, also the boxplots comparing its estimated value (T2) and its real value $\hat{T2}$, as retrieved from EMG recordings, are displayed (b). This latter graph only considers data from 13 subjects out of 14.

Regarding the dynamic test, boxplots of the normalized ROMs are displayed for each stimulation level and both types of electrodes in Figure 3.11. No significant differences (Wilcoxon test, p-value>0.05) were registered between the two electrode types for all levels, except L1, in which a slightly higher ROM was found for the textile electrodes. However, considering that L1 is the level with the lowest current amplitude, not much relevance was given to this result.

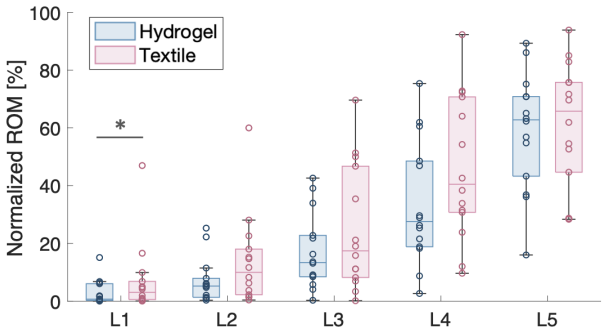

Figure 3.11: Boxplot of the normalized ROMs performed during dynamic tests for the 5 stimulation amplitudes (L1-L5). For each subject, the normalization is computed with respect to the maximum extension angle achieved by each subject during the initial voluntary contraction.

Regarding the isometric test (Figure 3.12), no statistically significant differences emerged between the two electrode types (Wilcoxon test, p-value>0.05) for any metrics. Only a trend towards a higher variability can be observed for Time to Fatigue and Torque Integral for textile electrodes.

The similar outcomes observed in dynamic and isometric tests demonstrated that the two electrodes behave similarly in terms of movement and generated torque. In all tests we observed a higher variability for textile electrodes which could be caused by the non-repeatable moisturizing procedure. The results' variability may have also been influenced by the less stable positioning of textile electrodes that are not stuck to the skin.

Following the signal processing described in Section 3.3.4, the estimated volitional EMG ($eEMG_v$) was extracted from EMG signals recorded when stimulation was on (STIM phase) and off (REST phase) during the Dynamic and Static Tests. In particular, for the former one, the analysis was performed on signals coming from 12 of the 14 subjects (ID10 and ID13 excluded); while for the latter one, the analysis was performed on signals coming from 11 of the 14 subjects (ID4, ID6 and ID10 excluded). Data were

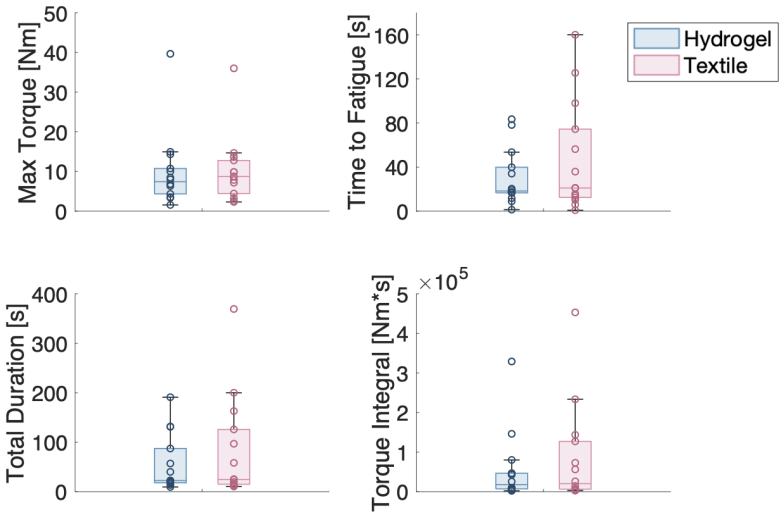

Figure 3.12: Boxplots for the metrics recorded during the isometric test: Max Torque, Time To Fatigue (TTF), Total Duration and Torque Integral.

discarded due to a failed connection of the EMG system.
The estimated volitional EMG was estimated both in the presence of stimulation artifacts and M-waves (STIM phase) and without stimulation (REST phase). Considering that subjects without disability were involved in the tests, this step was necessary to verify if any volitional contribution was present during the experimental procedure.
Figure 3.13 shows the estimated volitional EMG (eEMGv) during the dynamic and the isometric test for both REST and STIM-ON phases. For both electrode types and tests, no significant differences were found between the two phases. Only a trend towards a higher variability was observed when stimulation was ON, as expected, but it was not statistically significant.
As subjects were asked not to voluntarily participate during trials, this result was expected and desired. Anyhow, this verification allows us to rule out that the volitional participation of subjects might have altered the test results.

The similarity between the two electrodes was also confirmed by questionnaire reports about comfort evaluation. Table 3.1 reports the TESCQ scores summed across subjects for each item. The direction of the arrow next to each item indicates a higher comfort; for all items, but tender (which is a "positive" sensation), the lower the score, the higher the comfort.
Cutaneous sensations displayed similar values for the two electrode types, while deep and general categories showed higher values in the hydrogel case for all items, except for tender, overall suggesting a better acceptability and comfort perceived in the case of textile electrodes. Across subjects, the sensation with the highest rating for both electrode types was tingling.
Figure 3.14 reports the median value of the TESCQ scores for all items. Similar results were achieved for both types of electrodes, except for prinking, cramping, splitting and throbbing for which the hydrogel electrodes resulted to be less tolerated, and tingling for which the opposite occurred. However, for all items, no statistically significant differences were recorded between the two electrode types (p-value=0.39). Furthermore, the Item x Electrode interaction was not significant (p-value=0.79).

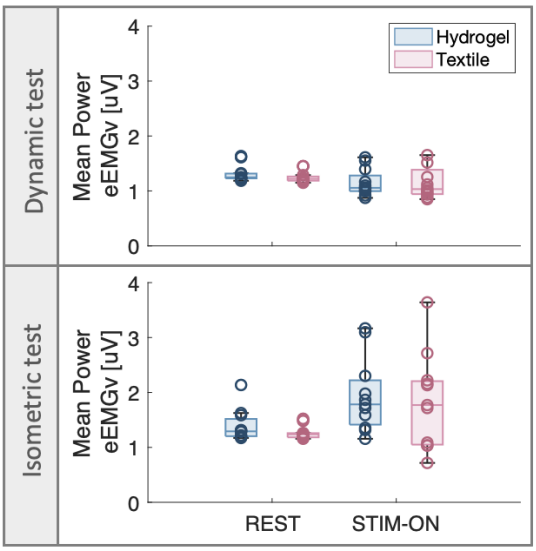

Figure 3.13: Mean power of eEMGv. Data from 12 subjects are considered in the Dynamic test, while data from 11 subjects are considered in the Isometric test.

		Hydrogel	Textile
Cutaneous category	Stabbing ↓	8	8
	Pricking ↓	22	21
	Sharp ↓	18	13
	Stinging ↓	15	15
	Hot burning ↓	15	16
Deep category	Pulling ↓	14	12
	Aching ↓	17	11
	Gnawing ↓	5	3
	Cramping ↓	22	19
General category	Splitting ↓	10	6
	Tender ↑	4	7
	Tingling ↓	33	31
	Shooting ↓	14	9
	Throbbing ↓	25	18

Table 3.1: Sum across subjects of all TESCQ items scores for the two types of electrodes. The direction of the arrow indicates greater comfort.

Overall, the experimental procedure did not show significant differences between the two types of electrodes in terms of stimulation thresholds, induced muscle contractions under dynamic and isometric conditions and perceived comfort, for all fourteen tested subjects.

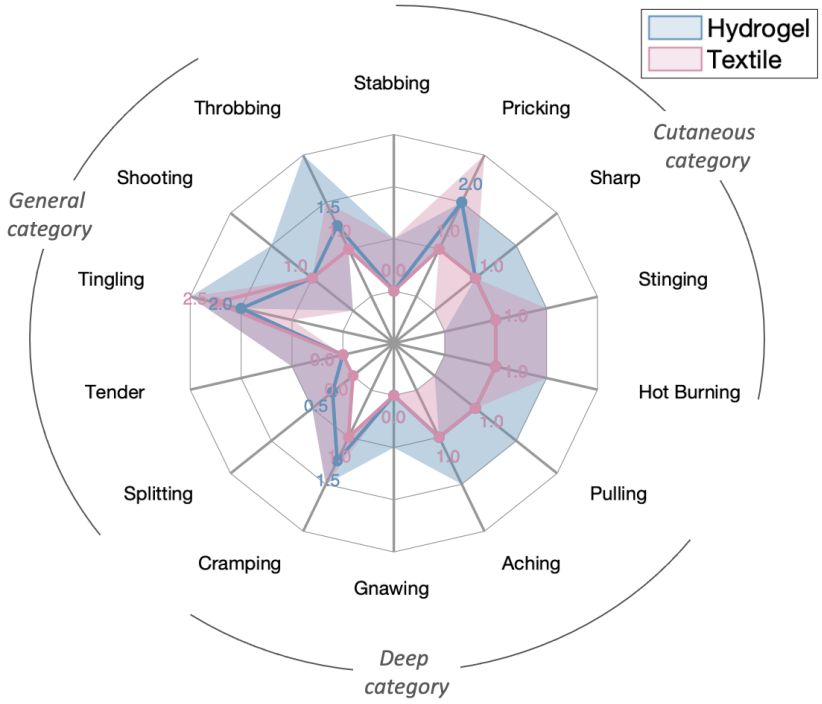

Figure 3.14: Spider plot of the scores of all TESCQ items. Solid lines connect the median values of items across subjects while the shaded area represents their IQR.

3.4.3. Limitations

The collected results represent a promising finding and serve as a starting point toward replacing hydrogel electrodes with textile alternatives. Nevertheless, further investigations are needed as this study is associated with some limitations.

Among them, the main limitation is the necessity for a moisturizing procedure when using textile electrodes. It is beneficial in terms of comfort but makes the effect of the textile-delivered stimulation less repeatable, as it is not possible to exactly quantify the amount of used cream. Additionally, we proved that our textile electrodes can resist some washing procedures, but further studies should be conducted to test their durability in sterilization and stretching processes. Another drawback of our study is the fact that we could not evaluate the electrodes' stability during movements, considering the static nature of our tests. Thus, it would be relevant in the future to explore whether these electrodes stay in place or move while performing daily life activities, such as walking. A further intrinsic limitation of textile electrodes is their high cost. However, this primarily pertains to the fabrication of the initial sample, whereas the production of duplicates is cheaper. Thus, a cost analysis is suggested to understand whether the expenses for both electrodes become comparable when considering large-scale production.

3.5. Conclusions

In the last decades, textile electrodes have been investigated as an alternative to conventional hydrogel ones for surface Functional Electrical Stimulation (FES) applications. Their main advantages are the flexibility, washability and ease of integration into clothes.

This proof-of-concept study developed a new set of ink-based printed textile electrodes for FES and tested their efficacy in comparison with state-of-the-art self-adhesive hydrogel electrodes on human subjects. The focus was on exploring electrodes' properties in terms of current conductivity, stimulation performance and usability for guiding further use of textiles in rehabilitation practices.

The overall results showed no significant differences between textile and hydrogel samples, both in terms of movement performances and painful sensations. Thus, despite the mentioned limitations, the proposed textile electrodes are a valid and innovative alternative to hydrogel ones. In particular, they represent a starting point in the attempt to realize garments for the FES delivery and integrate electrodes into clothes to ease donning and doffing procedures. Smart textiles would enable the domestic and long-term use of electrostimulation, which is particularly relevant considering the current shift towards home-based care for individuals recovering from SCI and stroke, as opposed to traditional hospital care [258, 259].

In the future, it might be interesting to explore the potential integration of EMG electrodes in the same smart garments to have the possibility to simultaneously measure and stimulate the muscles so as to develop EMG-controlled neuroprostheses which have been shown to enhance neural plasticity [152] and motor recovery [305].

4 | Neurorehabilitation effects of transcutaneous Spinal Cord Stimulation

Chapter Highlights

This chapter offers an overview of transcutaneous SCS, focusing on its working principles and potential applications. In particular, Section 4.1 details the state of the art about tSCS, its parameters setting and its usage as a rehabilitation tool in spinal injuries. Then, Section 4.2 presents the aim of the two preliminary studies hereby described, one on non-disabled individuals and one on subjects with SCI. The *Materials and Methods* of both studies are reported in Section 4.3 while their *Experimental setup*, *Data analysis* and *Results and Discussion* are divided into two sections, Section 4.4 for the one on individuals without disability and Section 4.5 for the one on people with SCI. Lastly, the *Conclusions* (Section 4.6) contain the main *take-home messages* of the study, together with some considerations about possible future works.

Chapter Contents

4.1 State of the Art . . . 114
4.1.1 tSCS parameters and setting . . . 115
4.1.2 tSCS applications for spinal injury recovery . . . 119
4.2 Objective of the study . . . 120
4.3 Materials and Methods . . . 121
4.3.1 Experimental Setup . . . 121
4.4 Testing on non-disabled subjects . . . 123
4.4.1 Experimental Protocol . . . 123
4.4.2 Data Analysis . . . 124
4.4.3 Results and Discussion . . . 124
4.5 Testing on subjects with SCI . . . 126
4.5.1 Experimental Protocol . . . 126
4.5.2 Data Analysis . . . 128
4.5.3 Results and Discussion . . . 129
4.6 Conclusions . . . 134

4.1. State of the Art

At the spinal cord level, the afferent terminals triggered by tSCS make synaptic contacts with many homonymous and heteronymous spinal moto-neurons and interneurons. These latter integrate supraspinal information with the one from these synapses to generate the final motor output. Thus, rather than inducing a motor output by itself, tSCS can be intended as a technique to increase the excitability state of spinal circuits. Indeed, it could strengthen residual supraspinal inputs reaching the spinal cord and make them capable of inducing an Action Potential (AP).
Therefore, motor fibers are activated through a reflex activity, referred to as Posterior Root Muscle Reflex (PRM reflex), which can be observed in the EMG recordings of the main leg muscles as the motor response to single pulses of current. Its characteristics and a complete comparison with the H-reflex were introduced in Section 1.4.3.
Given its potential benefits on the motor system, in the past decades, spinal stimulation has been proposed as an effective rehabilitation tool in neurologically impaired individuals, in particular in the SCI scenario. Originally, SCS was developed as a chronic pain treatment in the 60s with the epidural (invasive) approach. It was based on Melzack and Wall's (1965) gate control theory for peripheral neuromodulation of pain perception. Later, around the 70s, the motor effects of epidural spinal stimulation were investigated, opening a new research line and highlighting the potential rehabilitation role of the technology. The first decades of research and development focused on epidural stimulation; then, in the late 90s, transcutaneous SCS (tSCS) was introduced. This research was triggered by the discovery of low-threshold sites in the posterior structure of the human lumbosacral cord that could be accessed from the surface, causing muscle twitches [306]. Indeed, in the following decade, the motor reflexes elicited by non-invasive stimulation were studied and fully characterized [214], showing that posterior root afferents could be accessed by tSCS.
Alongside the discussion about the rehabilitative effects of SCS, multiple studies investigated the neuroplasticity effects of both epidural and transcutaneous SCS [212], highlighting its potential benefits and influences on the CNS structures. In the past decade, both the invasive and non-invasive approaches reported significant results, with both clinical and technical improvements. Focusing on tSCS, it reported significant results in motor recovery and neurorehabilitation, improving stepping [218] and walking [231] performances, and effectively reduced spasticity [225, 226] in neurologically impaired individuals. Furthermore, tSCS was suggested as a neuroprosthesis to promote locomotor-related physiological changes within the SC circuitry [224]. Particularly when combined with functional motor therapy, this stimulation was proved to induce neuroplasticity after SCI [307]. Indeed, the combination of SCS with the execution of movements, involving efferent motor commands (residual voluntary activations) and afferent proprioceptive information, is crucial for beneficial neuroplastic changes because both endogenous and exogenous (FES-induced) signals increase the firing probability of anterior horn cells, following the Hebbian-type learning effect [87, 211]. These benefits allowed this technology to become a competitive alternative to the invasive epidural solution. Indeed, complications related to the invasive approach have been highlighted in the past years [217], contributing to increased attention towards tSCS, especially in the motor rehabilitation setting, where temporary and less invasive solutions are preferred. A complete comparison of the invasive and non-invasive approaches for SCS was discussed in Section 1.4.3. Among the main advantages of the transcutaneous approach, we have its non-invasiveness, easy accessibility and cost-effectiveness. The main disadvantage, instead, lies in its low selectivity. The following paragraphs discuss the technical aspects of transcutaneous stimulation and their relevance within rehabilitative scenarios.

4.1.1. tSCS parameters and setting

In literature, a variety of protocols, pulse sequences and electrode placements have been employed for tSCS, allowing a standard framework for the application of tSCS.
Malik et al. [308] proposed a scheme (shown in Figure 4.1) defining the minimum set of parameters required to report SCS in spinal cord injury research. As depicted in the figure, the proposed framework identifies three parameters' categories: (1) SCS characteristics, which describes the pulse sequences imposed, (2) SCS intervention, which details the followed intervention protocol, and (3) SCS hardware, which specifies the stimulator and electrodes hardware.

Considering tSCS applications reported by literature studies, their main characteristics are hereby listed:

- **Frequency**: pulse trains were delivered with frequency bursts from 5 to 30 Hz and a carrier frequency from 2.5 to 10 kHz [234, 309, 310]. Concerning the carrier frequency, studies yielded valid results regardless of its application. Currently, there is little solid justification for its use, except for its ability to decrease the sensitivity of noci-receptors, consequently reducing discomfort and pain induced by the stimulation. The issue of High-Frequency (HF) carriers was settled by Dalrymple et al. [311], who discouraged their use. In fact, by comparing the two delivery methods, they concluded that no benefits come from employing HF carriers as these are comparable to the conventional approach for stimulation comfort and less efficient in terms of Motor Evoked Potential.
  Other therapeutic experiments selected either biphasic or monophasic rectangular waves with frequencies in the [1–90 Hz] range, with [20–30 Hz] being the most common one in motor-oriented protocols [224, 312–315].
- **Amplitude**: current amplitudes span from 10-20 mA to 100-200 mA, and it is often chosen as the maximum bearable amplitude for the subject. Defining threshold the amplitude at which a visible PRM reflex is observed, an over-threshold current level is used for PRM reflex identification and analysis, while continuous stimulation is usually delivered at a threshold or under-threshold level (around 80% of the threshold).
- **Pulsewidth**: the square waves' pulsewidth (PW) is often around 0.5-2 ms, and inter-pulse width depends on the stimulation frequency.
- **Wave shape**: usually rectangular waves are used, both biphasic and monophasic. Inanici et al. [316] compared the two modalities during cervical tSCS and reported that monophasic stimulation improved strength, whereas biphasic stimulation promoted fine motor skills. For sustained pulse trains lasting several seconds, the biphasic configuration is preferred because being charge-balanced it does not induce net polarization, avoiding skin irritation and potential skin damage.
- **Electrode configuration**: the bipolar electrode configuration was observed to generate a more localized electric field, affecting spinal segments more selectively [317].
- **Electrode placement**: in most studies, the cathode was positioned dorsally and consisted of one electrode over the longitudinal axis of the spine or a couple of electrodes placed laterally to the median of the spine (one on the left and one on the right). The vertebral level most commonly stimulated to target the lower limbs was T11-T12, which appears to be the most favorable location for activating the Central Pattern Generator (CPG) [317]. Exceptions are two studies [318, 319] that placed the cathode in T10 and a second electrode on the coccygeal bone [219, 234] and

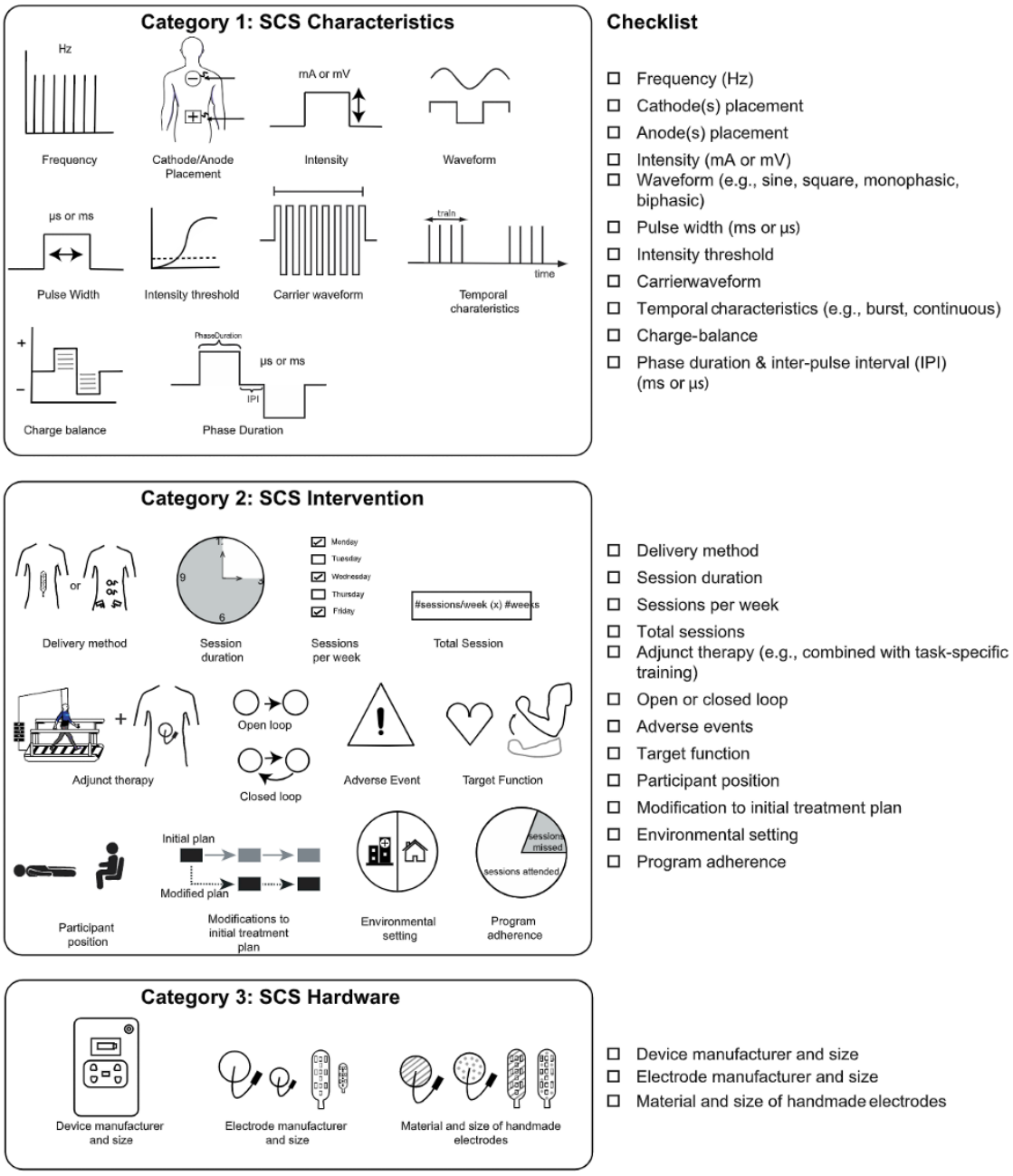

Figure 4.1: Minimum parameters framework to report SCS. Figure from Malik et al. [308].

three studies that targeted the L1-L2 lumbar area [310, 320, 321]. For targeting the upper limbs, instead, the cathode site varied between C3-C4, C5-C6 or C6-C7 [309, 314, 315, 322]. On the other hand, the anode position varied between the anterosuperior iliac spine (ASIS) and the iliac or para-umbilical ridges on the anterior abdomen, with two studies [318, 319] recording the use of both positions depending on the user comfort.

- **Body position**: Most therapeutic interventions targeting lower limb responses were conducted in the upright and/or supine position. Sitting position was evaluated for trunk control and balance [310] and also described in one study for lower limb control [231]. Danner et al. [323] investigated

the influence of the body position on the neural structures' recruitment during lumbosacral tSCS. They reported that supine and standing positions were ideal for the selective stimulation of sensory fibers. In fact, when stimulating non-disabled subjects in the prone position, a concomitant stimulation of motor fibers was observed.

- **Dose**: when part of a clinical or rehabilitation protocol, multiple sessions are performed, with durations spanning from 5 to 45 minutes, and often paired with rehabilitation therapy [231].
- **Hardware**: standard stimulators from Medtronic® and Digitimer® are commonly used with adhesive superficial electrodes, rectangular or square, in sizes from 5 to 10 cm. Some studies develop their own multi-electrode arrays [218], mainly with the aim of improving selectivity.

Study	*Electrodes* (number, dimensions, position)		*Parameters*			
Author	**Cathode**	**Anode**	**Shape**	**PW**	**Frequency**	**Amplitude**
Hofstoetter [226]	2(5x5 cm), T11-T12	2(8x13 cm), lower abdomen	Biphasic rect.	1 ms	50 Hz	20 V
Meyer [324]	1(5x9 cm), T11-T12	2(8x13 cm), lower abdomen	Biphasic rect.	1 ms	50 Hz	13-65 mA
Shapkova [313]	1(3x4 cm), T12	1(3x4 cm), abdomen	Monophasic sq.	0.5 ms	/	1.4 x Mot_{th}
Krenn [325]	1(5x5 cm), T11-T12	2(8x13 cm), abdomen	Monophasic	1 ms	35 ms	max 100 mA
Danner [323]	3(1 cm), T11-T12	2(8x13 cm), lower abdomen	Biphasic	1 ms	30 ms	max 125 mA
Gad [219]	1(2.5 cm), T11-T12 or Co1	2(5x10.2 cm), iliac crests	/	/	30/5 Hz	Max tolerance
Rath [310]	2(3.2 cm), T11-L1	2(7.5x13 cm), iliac crests	Monophasic rect.	1 ms	30/15 Hz	10-150 mA
Gerasimenko [234]	1(2.5 cm), T11-T12 or Co1	2(5x10 cm), iliac crests	Monophasic rect.	1 ms	15/30 Hz	80-180 mA
Inanici [309]	2(2.5 cm), C3-C4/C6-C7	2(5x10 cm), iliac crests	Biphasic rect	1 ms	30 Hz	80-120 mA
Bedi [320]	2(4.5x9 cm), T10-L1	/	/	/	20 Hz	Sensory
Benadives [322]	1(3.2 cm), C5-C6	1(7.5x12 cm), iliac crests	Biphasic	0.2 ms x 5	30 Hz	67-91.4 mA
Freyvert [314]	more than 1, C5	Monophasic rect.	/	/	5-30 Hz	20-100 mA
Roberts [321]	1(5 cm), L1-L2	2(5x10 cm), abdomen	Biphasic rect.	0.5 ms	30 Hz	15-50 mA
Mayr [99]	1(20 cm^2)	1(300 cm^2), abdomen	/	/	/	/
Hofstoetter [225]	2(5x5 cm), T11-T12	2(8x13 cm), abdomen	Biphasic rect.	1 ms	30 Hz	15-90 mA
Skiadopoulos [319]	2(5.1x10.2 cm), T10	2, abdomen/iliac crest	Biphasic	1 ms	30 Hz	/
Minassian [214]	2(5 cm), T11-T12	2(8x13 cm), abdomen	Biphasic rect.	2 ms	50 ms	max 50 V
Islam [318]	1(5.1x10.2 cm), T10	2(5.1x10.2 cm), abdomen/iliac crests	/	/	/	max TEP
Zhang [315]	2, C3-C4/C7-T1	2(8x13 cm), iliac crests	Monophasic rect.	1 ms	30 Hz	15 and 50 mA

Table 4.1: Summary of the electrodes parameters.

4.1.2. tSCS applications for spinal injury recovery

The main application and research focus of tSCS is SCI rehabilitation. tSCS applied alone or in combination with activity-based rehabilitation programs to improve motor function for individuals with chronic SCI has been studied in the last decade receiving considerable scientific, clinical, and media attention. tSCS has been proposed as a viable option for increasing voluntary motor response of the upper and lower limbs, trunk stability, and improvement of function and quality of life of SCI subjects [220]. As previously anticipated, the underlying mechanism is the fact that the delivery of electrical stimulation at the spinal level targets sensory afferents that increase spinal excitability [211]. Consequently, it modulates the functional status of the spinal network below the injury level, improving its interaction with the motor drive from the cortex.
Even if the advantages of both cervical and lumbo-sacral tSCS were investigated, in this thesis work we will focus on the lumbo-sacral tSCS and its effect on lower limbs rehabilitation.

tSCS demonstrated significant results for lower limbs rehabilitation, from improving stepping performance [218] to restoring walking and regaining voluntary control in previously paralyzed muscles [231]. The combination of voluntary drive and stimulation has shown better results in multiple cases, underlining the significant neuromodulatory effects of spinal stimulation [211, 224]. When dealing with lower limbs rehabilitation, usually the targeted spinal circuits are those dedicated to cyclic movements, namely those relative to the Central Pattern Generator (CPG). Indeed, both walking and cycling are cyclic movements relying on CPGs interactions, which are often below the injury and thus not affected by it, resulting in viable targets for the stimulation. The use of spinal neurostimulation during cyclic movements has shown increased activation of CPG circuits, inducing rhythmic motor patterns in complete SCI subjects [312] and causing motor facilitation both in walking [218, 231] and cycling [232]. Minassian and colleagues [206] showed that locomotor-like EMG activity and leg flexion-extension movements were induced by SCS at 22-50 Hz in individuals with chronic, motor-complete SCI lying supine. Cycling-based rehabilitation represents a valid alternative to walking since it eliminates the risk of falling and avoids the weight-bearing issues that characterize walking-based therapy [211]. Due to the decreased risks and high engagement of spinal circuits, it might act as an early stage in SCS-based rehabilitation protocols. In general, multiple studies have proposed rehabilitation protocols that combine SCS with movement-based therapy [231, 326, 327], and proved that SCS is most effective when paired with physical activity and volitional intent, in particular in the direction of regaining voluntary movements [234].

tSCS was also investigated as a valid technique for spasticity treatment.
Spasticity is characterized by abnormal muscle tightness due to prolonged muscle contraction and it is one of the most prevalent impairments following SCI [328]. In fact, this pathology affects descending fibers with a neuromodulator role, causing the decrease of inhibitory effects and augmenting muscular contraction. Spasticity increases the motor impairment of users and complicates the rehabilitation process. Common treatments range from oral medication and physical interventions to motor nerve block injections and drug delivery [226]; nevertheless, the control of spasticity is still an issue in neurologically impaired subjects.
The benefits of SCS on spasticity were investigated for the first time by Dimitrijevic in 1986 [329], who reported that epidural SCS was significantly effective in reducing spasticity in more than half of the SCI participants in his study. In the 90s, Pinter's and colleagues [330] showed a significant suppression of

severe lower limb spasticity when placing epidural electrodes over the lumbar posterior roots. They suggested that the underlying mechanism was the modification of the excitability of spinal lumbar circuits through continuous activation of the posterior roots.
In the last decade, also transcutaneous techniques were considered. In 2014, Hofstetter and colleagues [226], showed a successful reduction of lower limbs spasticity in incomplete SCI subjects through a 30-minute protocol of lumbar continuous tSCS at 50 Hz. The reduction in spasticity led to benefits in coactivation patterns and walking speed, improving the residual volitional motor control. Alashram and colleagues [328] reviewed the current state of the art on SCS for spasticity control in SCI in 2023 and suggested that the observed reduction in spasticity is caused by the SCS recruitment of inhibitory spinal circuits through the continuous stimulation of afferent fibers.

Concerning secondary and non-motor benefits of SCS, researchers found improved bladder function both in rats [331] and in 110 of 169 SCI subjects treated with cervical stimulation [228]. This represents a crucial aspect as it has been shown that, in addition to the recovery of motor functions, a priority for SCI individuals is the improvement of their bladder control [332].

4.2. Objective of the study

As previously explained, tSCS has shown a positive influence on the functional recovery of movements and the reduction of spasticity in SCI subjects. However, there is still no absolute consensus on the optimal electrode placement and stimulation parameters to be used. This is mainly due to the fact that there is not a standardized procedure for tSCS but, depending on the specific application case, an ad-hoc protocol is defined.
The work hereby presented aims to understand the working principles underlying Transcutaneous Spinal Cord Stimulation (tSCS), replicating and verifying what was found in the literature. Particular attention was paid to exploring its efficacy and the possible advantages coming from its integration into the rehabilitation of neurally impaired individuals. In collaboration with Villa Beretta Rehabilitation Center, we developed a protocol for the definition of the optimal parameters for the tSCS to be then applied continuously during functional movements such as walking or cycling. Relevant tSCS parameters were taken into account, such as electrodes' positioning, configuration, current amplitude, pulsewidth and frequency, to understand their influence on the final effects induced by the stimulation.
At first, we carried out a study on non-disabled subjects in which we tested and compared different electrical configurations to induce the PRM reflex and better understand the influence of each parameter. The aim was to define a valid procedure for identifying the PRM threshold current, namely the lowest current amplitude able to induce a visible reflex, which represents a crucial preliminary step in most tSCS studies. The procedure was repeated for two body positions, *Standing* and *Supine*, as these are the most relevant ones for further tSCS application during functional movements, such as walking or cycling.
Then we conducted a second study to investigate the effects of lumbosacral tSCS on the motor facilitation during cycling in individuals with complete SCI. Specifically, we applied tSCS during motor-assisted cycling and collected data about muscle activations and the force on pedals to assess the stimulation effects on lower limb motor outcomes. We also evaluated the combination of tSCS and volitional effort to determine the potential contribution of residual volitional signals during motor training, as suggested by the literature [326].

4.3. Materials and Methods

4.3.1. Experimental Setup

This section presents the experimental setup used to deliver tSCS and to collect lower-limb EMG, both in the study with non-disabled and in the one with SCI subjects. Additionally, this latter included a motor-assisted trike to evaluate the possible motor facilitation effects of the stimulation during cycling.

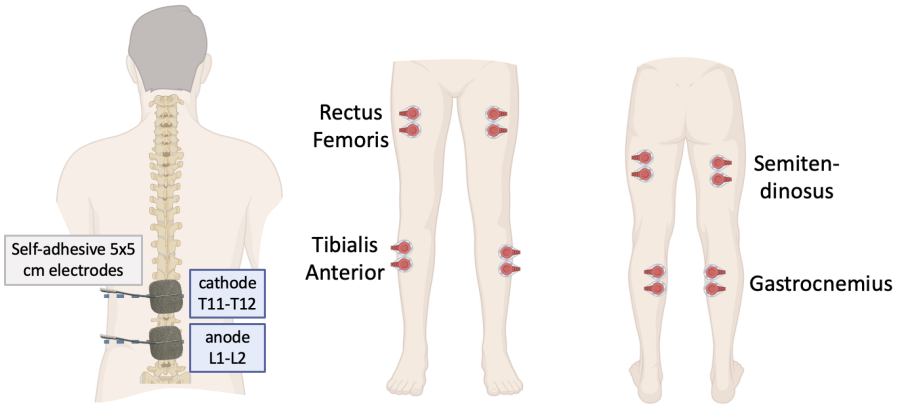

Figure 4.2: Detailed positioning for stimulation electrodes on the lower back (a) and EMG electrodes on the main four leg muscles (figures composed on `BioRender.com`).

Stimulator. The RehaMove3 (Hasomed GmbH, Germany) commercial electrical stimulator was used for both studies, the same one employed in the work presented in Chapter 2 (Section 2.3.1). It was selected because of its flexibility in the setting of parameters and pulse shape. Specifically, charge-balanced, biphasic square pulses were delivered in a bipolar configuration, with 1 ms pulsewidth and amplitude and frequency adapted to the specific subject and test. One of the four stimulator's channels was connected to a pair of surface self-adhesive electrodes (Pals®from Axelgaard Manufacturing Co. Ltd., Fallbrook, USA) with a rectangular shape of 5x5 cm. They were placed centrally along the spine, the anode over L1-L2 spinous processes and the cathode over T11-T12 spinous processes, as shown in Figure 4.2a. The anode cable (identified with an oscilloscope) was positioned on the L1-L2 region since in the biphasic configuration the "stimulating" electrode is the anode [214] and thus an anodic stimulation is more effective in this case [126].
The stimulator was programmed and controlled with a C++ Qt-based custom interface developed in QtCreator (version 4.5.2, 2018, based on Qt 5.9.5). The code runs on a Dell laptop (operative system Ubuntu 18.04.5 LTS) connected to the stimulator via USB cable. The interface offers two different stimulation settings, the *Single Stimuli* and the *Continuous Stimulation*, with different stimulation parameters. The *Single Stimuli* modality applies blocks of ten single stimuli at a chosen time distance, with a one-minute pause in between blocks and the current increased by a predefined value. The *Continuous Stimulation* modality, instead, applies a continuous stimulation at a chosen frequency and current amplitude. The defined current amplitude is reached with a gradual ramp of a few seconds to reduce any discomfort caused by an abrupt start of the stimulation.

Electromiography. For both studies, an electromyograph was used to record the surface electromyog-

raphy (EMG) of eight lower limb muscles (*Rectus Femoris*, *Semitendinosus*, *Gastrocnemius* and *Tibialis Anterior* of both legs). For the study on non-disabled subjects, eight bipolar channels of the Porti TMSi's system were employed with a sampling frequency of 1024 Hz. The active shielding of cables ensures that disturbances such as cable movement artifacts and main interferences (50 Hz) are reduced to a minimum. It was managed through a General Purpose Dell PC with Linux operating system using a dedicated Simulink file. For the study on SCI subjects, instead, the new TMSi system was adopted, namely the TMSi SAGA 32+/64+ REV 2 (Twente Medical Systems International B.V., Netherlands). EMG signals were acquired with 16 monopolar channels and a sampling frequency of 2000 Hz. The system was managed through its proprietary software SAGA, running on a Windows 11 (version 23H2) laptop. In both studies, self-adhesive hydrogel electrodes (Cardinal Health, Waukegan, USA) were placed with a 1 cm inter-electrode distance, as shown in Figure 4.2b. For the study involving the pedaling movement, an extra bipolar channel was connected to the trike's trigger, which gave an impulse at the start of each pedaling revolution, to align the trike data with the EMG activations later in the post-processing.

Trike. A trike model 700 (Catrike, US) with a cycling-assist motor was used for the second study involving cycling. It includes a pair of sensorized pedals (X-Power, SRM GmbH, Germany), a motor controlled by a Raspberry central unit, which communicates with a custom Android app on a tablet, and an encoder for the crank angle acquisition. This app controls the motor state and cadence and allows real-time monitoring of the power produced by the subject. Orthesis are mounted on the pedals to keep the subject's legs in the correct position. The following data are provided: mean-cycle motor power, instantaneous motor power, instantaneous force on each pedal and the respective crankarm angle. This trike setup was developed within the NearLab (PoliMi) in the scope of other projects.

Figure 4.3: Experimental Setup. The RehaMove Pro stimulator provides tSCS and is controlled from a laptop via the custom-developed GUI. EMG data are acquired with eight channels on the TMSI device and visualized in real-time on a laptop running the proprietary SAGA interface. The motor is controlled by a Raspberry, which is programmed via Visual Studio from a laptop (figure composed on `BioRender.com`).

The setup for the study on SCI subjects is shown in Figure 4.3, where the subject is sitting on the trike and three laptops control the cycling-assist motor, the stimulation and the EMG acquisition. A similar setup was employed in the first study, with the exception that it does not include the trike component.

4.4. Testing on non-disabled subjects

4.4.1. Experimental Protocol

The experimental procedure adheres to the Helsinki Declaration and the Ethical Committee of the Politecnico di Milano approved it with protocol number *Nr 13/2021*. This work was intended as a feasibility study and thus the protocol was carried out only on non-disabled subjects. Generally, all participants responded positively to the spinal stimulation.
The following inclusion criteria were taken into account for the protocol:

- No disability
- No implanted electronic devices
- Age > 18
- Good response to stimulation

At the beginning, for each subject, the satisfaction of all inclusion criteria was verified and then he/she was required to sign the informed consent and accept to take part in experiments.
The first step was the collection of some personal parameters, such as age, sex, height, and weight. Then, the subject was prepared for the test. Before placing EMG electrodes, the skin was cleaned with alcohol to remove dead cells that might introduce artifacts in the recorded EMG signal, worsening its overall quality. Next, EMG electrodes were placed over the four target muscles in a bipolar configuration, meaning that, for each muscle, a pair of electrodes was positioned along the longitudinal axis of the muscle as shown in Figure 4.2b. Additionally, a common ground electrode was positioned over the fibula heads, as a reference for all measured voltage potentials. Next, stimulation electrodes were placed as previously explained and shown in Figure 4.2a).
During the protocol definition, different configurations were tested, with one electrode on the back and one on the abdomen, as reported by some studies (Table 4.1). Nevertheless, many subjects reported feelings of pain and cramping in the abdomen and two of them also fainted, probably because of the current crossing through soft tissues, including the *Solar Plexus*. Thus, we discarded this electrode configuration. Different settings for the stimulation parameters (frequency, pulsewidth, amplitude and shape of current pulses) were also attempted to better understand their effect in terms of induced muscular responses and make a point about the variety of information found in the literature.
After replicating the various configurations found in the literature, the stimulation waveform was defined as rectangular biphasic because, being charge-balanced, it does not induce a net polarization. The pulses' pulsewidth was set to 1 ms, while the amplitude was adjusted for each subject depending on its specific responses and tolerance. This procedure for identifying the *PRMs Threshold* was carried out by sending single electrical pulses, as these were proved able to induce such reflex [220]. Specifically, the *Single Stimuli* modality was employed (previously explained in Section 4.3.1), with an inter-pulse distance of 5 s and the current amplitude that, starting from 30 mA, was block-by-block increased by 5 mA. The overall procedure was stopped when reaching the pain tolerance of the subject, which was verbally reported to the experimenter. The overall procedure was repeated for two body positions, *Standing* and *Supine*, to study their influence on the PRM threshold amplitude.

4.4.2. Data Analysis

EMG data analysis was performed using MATLAB (R2021b version). Data from the EMG channels of interest were extracted and filtered with a 10-250 Hz band-pass filter. The cut frequency of the low-pass component was limited by the low sampling frequency (1024 Hz). Stimulation artifacts, superimposed on the recorded physiological EMG activities, were identified with the *findpeaks* MATLAB function. These artifacts are easier to identify in proximal muscles because they have a higher amplitude due to their closer position to the stimulation site, while they are significantly smaller in distal muscles. Thus, the artifacts detection primarily focused on the *Rectus Femoris* by examining the entire signal. Then, for all other muscles, artifacts were sought within narrow time frames surrounding the instants at which artifacts were detected in the *Rectus Femoris*. Afterward, the 50 ms-windows of signal following each stimulation peak were extracted as this represents the time interval in which the reflex is expected to occur (when present). In this way, for each electrical pulse, it was possible to study whether the reflex response was induced in muscles and eventually analyze its characteristics. In particular, we were interested in its peak-to-peak amplitude (i.e., the difference between the maximum and minimum wave peaks) and its latency (i.e., the period between the stimulation artifact and the beginning of the reflex wave). The onset of the reflex wave was defined as the first deflection from baseline larger than 5% of the reflex peak-to-peak amplitude [214]. For each subject and amplitude, the baseline was computed by considering the EMG signal in the windows from 1s to 1.5 s after each pulse and by averaging them over the ten delivered pulses. Based on the literature [333], both for the supine and standing position, the PRM current threshold was identified as the current amplitude evoking a reflex response with a peak-to-peak amplitude greater than $50uV$ in at least half of the ten pulses.
Finally, Generalized Linear Mixed Models (GLMM) were defined in SPSS Statistics (IBM) to compare the two different positions. Specifically, the mean latency and peak-to-peak amplitude over the ten pulses and the PRM threshold for each subject were considered as the target for each model following a gamma regression distribution with a log link to the linear model.

4.4.3. Results and Discussion

The study included 11 non-disabled subjects (6 men and 5 women, age: 25 years ± 12.5, height: 172 cm ± 11.5, weight: 65 kg ± 21).
Results are reported only for the Rectus Femoris and Semitendinosus because of the low quality of EMG signals in the distal muscles. In one subject out of 11 (ID2), the threshold of the PRM reflexes could not be identified for both muscles, sides and positions because the subject felt pain before reaching the stimulation amplitude that would have triggered the reflex activation. For all other subjects, instead, there were only some specific cases in which the threshold could not be registered. Those subjects on which the PRM reflex could be observed were defined as "responders". The percentage of stimulation responders divided by positions, muscles and sides over the eleven tested individuals is reported in Table 4.2. Figure 4.4 reports, for both positions and muscles, the median PRM threshold (a) and the median latency (b) and peak-to-peak amplitude (c) for the reflexes recorded at the same amplitude of the PRM threshold. These medians are computed by joining the left and right sides and by considering only the responders for each combination (muscle and position). For the latency and peak-to-peak amplitude, the mean value over the ten delivered pulses is taken into account for each subject. Considering the PRM threshold, no significant differences were found between the two conditions for both muscles, with median

	RectusFemoris		*Semitendinosus*	
	Right	**Left**	**Right**	**Left**
Standing	64%	64%	73%	82%
Supine	64%	64%	73%	73%

Table 4.2: Percentage of stimulation responders divided by positions, muscles and sides over the eleven tested individuals. The term "responders" refers to those subjects on which the PRM reflex could be observed.

± IQR (Inter-Quartile Range) values in the *Standing* and *Supine* conditions of 55±20 mA and 57.5±30 mA for the *Rectus Femoris* and 50±10 mA and 55±20 mA for the *Semitendinosus*.
Similarly, for the latency parameter no significant differences were found among the two conditions, with median ± IQR values for the *Standing* and *Supine* conditions of 9.86±0.29 ms and 9.77±0.39 ms for the *Rectus Femoris*, and 10.2±0.81 ms and 9.92±0.78 ms for the *Semitendinosus*. Concerning the peak-to-peak amplitudes, even if slightly higher values were registered in the *Supine* condition with respect to the *Standing* one, no significant differences were noticed also in this case.

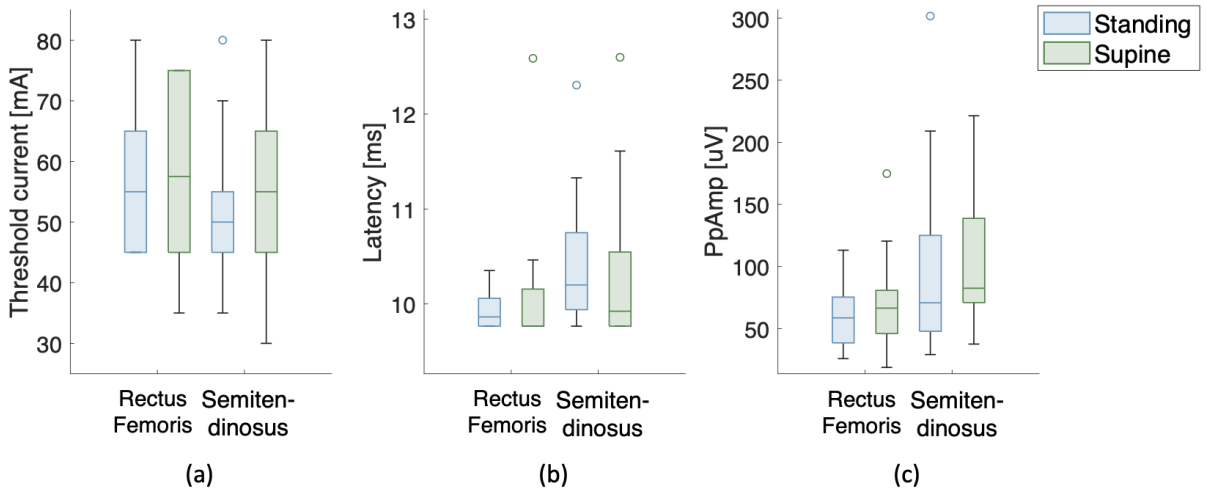

Figure 4.4: Boxplots of data computed for the two muscles and positions, across all responder subjects and sides. Reported medians are relative to the PRM threshold current (a) and the average latency (b) and peak-to-peak amplitude (c) calculated over the reflexes induced by the ten delivered pulses at the same amplitude of the PRM threshold. Differences among the two positions were considered statistically significant when p-value$<$0.05.

The gathered results allowed us to verify what was found in the literature and define a valid procedure for identifying the threshold amplitude able to induce the PRM reflex. This represents a crucial step for tSCS studies because in the majority of cases the spinal stimulation is applied at the threshold level. As previously explained, several configurations and stimulation parameters were tried before defining the used ones. In particular, we decided to place both electrodes on the back instead of one on the back and one on the abdomen (as seen in various studies) because it equally demonstrated the possibility of evoking reflex responses [325] and it represented a safer setup, without current flowing through the body. Indeed, by placing both electrodes on the back, soft tissues are not affected and sensations of pain

and abdominal contraction are reduced. In particular, electrodes were placed at the L1-L2 and T11-T12 levels. In general, the electrodes' position must be accurately determined as it is known to influence the arousal threshold and the amount of induced motor response [220]. Although the spinal stimulation elicits a multi-segment response, the absence of a valid reflex in most of the distal muscles may be explained by the fact that electrodes were mainly targeting spinal circuits directed to proximal muscles.
The PRM threshold values that we obtained across all muscles (54.35±11.2 mA for standing, 56.67±13.7 mA for supine) are in line with the ones reported by Danner and colleagues [323] for the *Supine* position (56.4±3.5 mA) but not for the standing one (44.7±2.8 mA). Indeed, they reported significantly lower values in the *Standing* condition, while in our study the body position did not have a significant effect. On the other hand, we reported a significantly higher variability for both positions. Taking into account the latency parameter, by averaging data across body positions while maintaining the distinction between muscles, the following average latencies were obtained: 10.02±0.5 ms for the *Rectus Femoris* and 10.40±0.7 ms for the *Semitendinosus*. These results align with those reported in other literature studies [214, 221]. Nevertheless, as the adopted configurations vary widely among studies, the comparison of the results is not straightforward.
To conclude, the main *take home message* of this study is the definition of a suitable protocol for delivering tSCS as it proved able to induce a valid PRM reflex in the majority of cases. The absence of a visible reflex noticed for some EMG recordings across subjects and for all recordings of one subject (ID 2), might be attributed to the necessity of higher current levels for eliciting the reflex, which were however impractical as dealing with non-disabled subjects. On the other hand, the absence of the reflex in most distal muscles is probably due to electrodes' positioning that was favoring spinal circuits innervating proximal muscles rather than those directed to distal ones. For future studies, a real-time verification of the EMG signal of all muscles is suggested together with the adjustment of the electrodes' position (if necessary).

4.5. Testing on subjects with SCI

4.5.1. Experimental Protocol

Once defined a proper configuration for delivering tSCS and validated a suitable procedure for detecting the PRM threshold, a second experimental protocol was proposed to determine a possible tSCS-induced motor facilitation in people with SCI during leg cycling. In particular, EMG activations of lower-limb muscles were analyzed to observe whether there was any cycling-related modulation.

The experimental protocol conforms to the Helsinki Declaration and the Ethical Committee of the Politecnico di Milano approved it with protocol number *Nr 50/2023* on 12/12/2023.

Subjects with complete SCI (classified as ASIA A and B) were recruited. They had no prior experience with spinal stimulation and their medications were not changed during the study. The inclusion and exclusion criteria are summed up in Table 4.3.

For safety reasons, each subject's clinical history was reviewed by Franco Molteni, MD, the study's clinical supervisor, who confirmed the absence of contraindications to spinal stimulation. In the beginning, subjects were required to sign the informed consent to accept to take part in the experiment. Then,

Inclusion Criteria	Exclusion Criteria
• Age: 18-75 years • Complete spinal cord lesion (ASIA A or B) • Autonomous trunk motor control to allow independent sitting • Good response to spinal stimulation	• chronically denervated muscles • neurogenic paraosteoartropatia • cardiovascular diseases • fractures in the lower limbs in the last 12 months • absence of response to spinal cord stimulation • allergy to the stimulation electrodes • implanted pacemaker or other electrical devices • metal implants • inability to independently consent to the participation

Table 4.3: Inclusion and exclusion criteria for the experimental protocol

anamnestic data were collected and double-checked by an on-site clinician to confirm the absence of metal implants in the subjects and their health status at the time of the stimulation session was verified by acquiring the following basal data: Heart Rate (HR), Arterial blood Pressure (AP), and blood oxygen saturation (SatO2 %), and by controlling them against physiological ranges.
After that, the proper experimental session could start and lasted nearly 90 minutes. The EMG and stimulation electrodes are placed on the legs and lower back, respectively, with the same setup used for non-disabled subjects (Section 4.4.1). Then, the subject is asked to sit on the trike and his legs are fastened to the pedals' orthoses.
Each session can be subdivided into three phases:

1. **Calibration**: the subject is seated on the trike in the standard position (right pedal up), with the legs resting and the motor off. The PRM reflex threshold current amplitude is identified following the same procedure previously validated on non-disabled subjects (Section 4.4.1) by looking at the real-time EMG signal.

2. **Passive cycling**: this phase consists of three minutes of passive cycling, where the movement is completely generated by the trike's motor at a constant cadence while the stimulation is off. This represents the baseline condition to which the following stimulation conditions will be compared.

3. **tSCS cycling**: this step comprises six minutes of cycling with both the motor on at a constant cadence and the continuous tSCS on. The stimulation amplitude was set to the PRM reflex threshold if the subject could stand it, or to the maximum tolerated amplitude otherwise. During the first three minutes, the subject is required to do nothing, while during the following three minutes, he is asked to think about moving his legs voluntarily.
   This step is repeated for three frequencies (20 Hz, 50 Hz and 80 Hz) in random order and tSCS is switched off for 1 minute after each 6-minute block. During this pause participants are asked to fill out a questionnaire rating the pain, burning, cramping and pressure sensations on a 0-10 scale and investigating any perceptible motor facilitation effect.
   The rationale for testing different frequencies originates from the fact that this parameter was

varied in the literature, usually in the [1-90 Hz] range [317], observing different outcomes. Usually, lower frequencies were employed in motor-oriented SCS studies [317] while higher ones ([50-80 Hz]) demonstrated to suppress severe lower limb spasticity [330].

The overall protocol is summed up in Figure 4.5, detailing the state of stimulation, motor and voluntary effort during each step.
Participants were also asked to report any other relevant sensation they felt during the test and feedback calls were conducted about 24/48 hours after the session to take note of any stimulation-induced change they may have noticed.

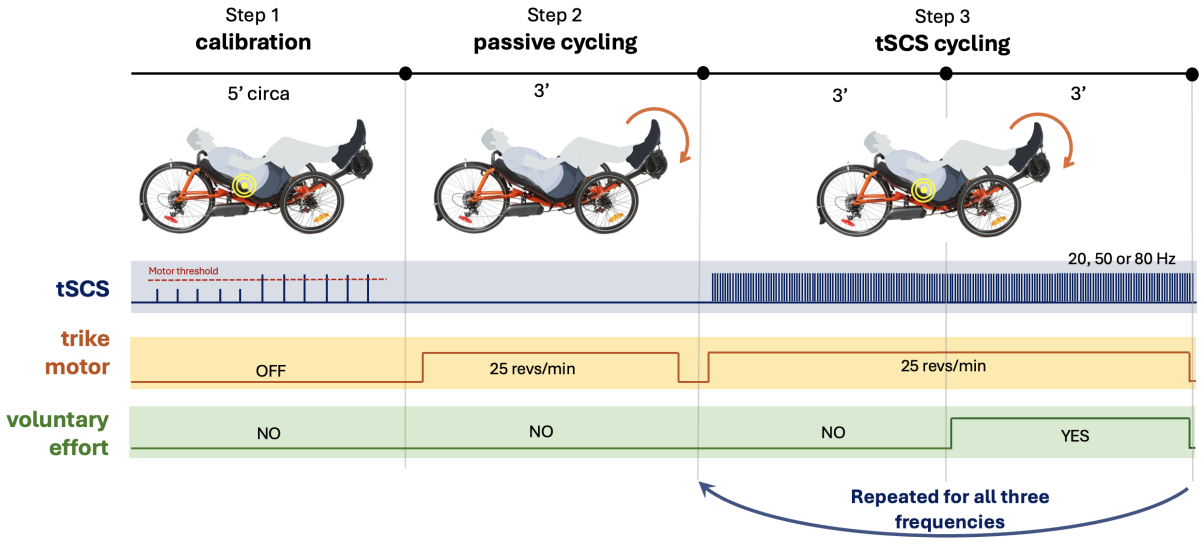

Figure 4.5: Experimental protocol with three steps: *calibration*, *passive cycling* and *tSCS cycling*. The diagram shows the combination of stimulation, motor, and subject's voluntary effort in the three stages.

4.5.2. Data Analysis

The data analysis was performed using MATLAB (R2021b version).
EMG data were filtered with a 10-500 Hz band-pass filter and a 50 Hz notch filter to remove static noise from the trigger channel and stimulation artifacts were identified. For the EMG acquired during the *Calibration* step, the analysis focused on identifying the PRM reflex by considering the 50 ms-windows following each stimulation pulse, similarly to the previous study (Section 4.4.2). The aim was to verify the PRM reflex threshold extracted in real-time during the test. The EMG signal of the other two steps, instead, was used to extract and compare muscle activations. In particular, 2-5 ms blanking intervals were applied around the identified stimulation artifacts to remove them and substitute them with the signal offset. Then, offset subtraction and rectification were performed on the whole signal, and its envelope was extracted using a 5th-order low-pass Butterworth filter with a 10 Hz cutoff frequency. Cycling revolutions were then segmented based on the trigger EMG channel and averaged to obtain a sample cycling revolution for each muscle and cycling condition. These average cycling revolutions were then rescaled to the subject's baseline, computed as the average amplitude of the EMG acquired for a few seconds before calibration, with the legs of the subject still in the standard position and both motor and stimulation off.

4.5.3. Results and Discussion

The study included four male participants aged from 25 to 40 years old, whose main characteristics are reported in Table 4.4, together with the PRM reflex thresholds identified during the *Calibration* phase and the current amplitude of the continuous tSCS delivered during the *tSCS cycling* phase.

Sub.	Lesion type	Lesion level	Time since lesion	Metal implants	BMI (kg/m^2)	Medication	PRM threshold	cont. tSCS amp.
01	A	D4	52 months	D1-D7	19.11	baclofen, movicol, resolor	60 mA	60 mA
02	A	D3	23 months	D3-D9	21.97	ossibutinine, urimesk	55 mA	55 mA
03	B	D12	29 months	none	21.92	baclofen, lyrica	70 mA	50 mA
04	B	D2	$\approx$ 12 months	none	25.18	ossibutinine, urivesch	65 mA	65 mA

Table 4.4: Included subjects' characteristics

All subjects, but subject 04, were used to FES-cycling as they had been consistently trained with a FES-bike in the past years but had never undergone spinal stimulation. Subjects 03 and 04 had lower limb muscle rigidity and hypertonia and presented some involuntary contractions and clonuses. Subject 04 scored 1 on the spasticity Ashworth scale six months before the study. He also presented a clonus on the right leg, triggered by the ankle joint at 90°, and thus the trike's orthosis was adapted during his trial to avoid reaching this angle. Medication data show that subjects 01 and 03 were undergoing anti-spasticity treatments and that all participants took medication to control urination and intestine functionality. All participants but subject 03, who has preserved sensibility in the entire lower back region, tolerated the PRM threshold amplitude for the continuous tSCS. Subjects 01, 02 and 03 underwent two stimulation sessions a week apart, while subject 04 underwent a single session.

EMG and force results

EMG and forces data were analyzed individually for each participant rather than as a population, given the participants' unique clinical histories and the low number of performed trials. These data are summed up in Figures 4.6 and 4.7, where each row is relative to a different tested frequency, and data are reported over an average cycling revolution starting at a null right crank angle (standard position). Panel (a) reports the EMG data for the right *Rectus Femoris* and *Semitendinosus* normalized to the subject's baseline (left) and the mean RMS values and Standard Deviations (SD) of EMG amplitudes of the same trial (right). Hip and knee flexion and extension ranges for the specific experimental setup were evaluated by measuring the crank angle (through the encoder) corresponding to the different joints' phases. These were then superimposed with grey and black lines on the top of the plots. Panels (b) and (c) report force data for the right pedal, with panel (b) showing the absolute force of the considered tSCS test together with the passive one (left) and the active force, computed as the difference between the force during tSCS and the passive one (right). A positive active force indicates a functional participation of the subject in

the movement. Panel (c), instead, reports the mean active force with its SD for all performed tests.
EMG and forces data acquired during passive cycling were compared to those relative to tSCS sessions to evaluate the modulation of muscle activations induced by the stimulation and study eventual motor-facilitating effects. The results for the left side are not reported here since they show an analog behaviour. Those relative to the *Gastrocnemius* and *Tibialis Anterior*, instead, are not displayed because of their low quality probably caused by the pedals' orthoses touching the EMG electrodes.
Interestingly, subjects 01 and 02 showed similar behaviours for EMG activations and pedals' forces, which were distinct from those common to subjects 03 and 04 during both passive and tSCS cycling. These differences are probably due to the fact that subjects 01 and 02 have a higher level of spinal injury, while subjects 03 and 04 have a lower one together with hypertonia and clonuses. Thus, we decided to discuss the two trends separately in *Case Studies* 01 and 02.

Case Study 01
EMG and force results for subject 02 in the first session are reported in Figure 4.6, as representative of both sessions of subjects 01 and 02 included in this group.
Focusing on panel (a) and considering the right *Rectus Femoris* we notice that the EMG amplitude is moderately over the baseline during the passive trial while it is slightly amplified and reduced by the 20 Hz and 80 Hz stimulation frequencies, respectively. Differently, the 50 Hz stimulation amplifies the activation up to three times the baseline. On the other hand, the *Semitendinosus* activation is at its highest during the passive condition, reaching approximately 2.2 times the baseline, while it is reduced by all stimulation frequencies. The 50 Hz stimulation is the only one introducing a cyclic trend on both muscles and, interestingly, an opposite cycling pattern is induced by the 50 Hz and the combined 50 Hz plus voluntary intent conditions. Despite none of them resembled a proper voluntary activation, the one introduced by the case without the voluntary intent was closer to the expected behaviour.
Both participants showed small oscillations in amplitude with respect to the passive cycling force, as depicted for subject 02 in panel (b). A minimum of cycling cooperation during *tSCS cycling* condition with respect to the passive one can be observed around 200-300°, during the pulling phase of the pedal's revolution. On the other hand, the negative active force around 0-50° indicates a resistance introduced by tSCS at the beginning of the cycle in the majority of the sessions. The overall mean active forces (panel c) show an average increase for all tSCS conditions compared to passive cycling, underlining that the positive phase during pulling overcomes the negative one at the push. Similar mean values are reported for all frequencies and for the tSCS-only and tSCS+voluntary conditions.
While EMG data for subjects 01 and 02 do not suggest noticeable motor facilitation during the stimulation, mean force data show a promising preliminary result.

Case Study 02
EMG and force results for subject 03 in the second session are reported in Figure 4.7, as representative of sessions of subjects 03 and 04 included in this group.
Focusing on panel (a) and considering the right *Rectus Femoris* we notice that the EMG amplitude is around the baseline during the passive trial, it is slightly reduced and amplified by the 80 and 20 Hz stimulations respectively and it is significantly amplified by the 50 Hz stimulation, with a clear cyclic component. While this behaviour resembles the one of the first *Case Study*, that on the *Semitendinosus* reveals the critical difference between the two groups. Indeed, here the *Semitendinosus* shows a significant cyclic activation with amplitude up to 8 times the baseline, both during passive- and the stimulation-cycling, with the stimulation not affecting the cyclic pattern and sometimes reducing and sometimes

amplifying its amplitude. For subject 04 these cyclic activations were particularly increased in the right leg, which is more affected by hypertonia. However, comparing these cyclic activations with the physiological knee and hip extension and flexion ranges, it can be noticed that they were not in phase. Thus, we supposed that, given the muscle hypertonia of the two subjects, the observed cyclic contractions were not functional to the movement but rather caused by the stretch reflex during hip extension. The spinal stimulation did not seem to affect such activations in terms of temporal characteristics but only in terms of amplitude.
Differently from the *Case Study 1*, force values (panel b) show significant oscillations around the mean passive force over the cycle, suggesting alternated phases of cooperation and resistance to the movement. The oscillations observed during tSCS-only trials are similar to those of subject 02 (Figure 4.6, panel b), with cooperation during the final pulling phase for all frequencies. On the other hand, the oscillations are particularly relevant when the stimulation is combined with the voluntary intent of movement, where collaboration around 50° (pushing phase) is suggested by an increase in the active force (Figure 4.7, panel b). This underlines spinal stimulation's potential of amplifying residual volitional signals and lays out promising perspectives. However, this increase of active force is followed by a resistance (negative active force) at the end of the pushing phase (100-200°). As for the positive phase, for all stimulation frequencies, this behaviour is augmented by the voluntary intent addition compared to the stimulation alone, suggesting that residual volitional signals may not be functional to the movement during the entire cycle, at least not during these preliminary trials.
Considering subject 04, given his minimum residual motor ability on the right leg, we decided to perform passive trials also with the addition of the voluntary effort and to repeat them twice, before and after the *tSCS cycling* blocks. Both trials reported a negative mean active force meaning that the addition of the voluntary intent caused resistance to the pedalling. However, the post-tSCS trial scored slightly better than the initial one, suggesting some tSCS-related improvements. Similarly to subject 03, forces during stimulation cycling blocks were significantly higher than the passive one for all frequencies, but without consistent differences between the tSCS-only sessions and those with combined tSCS and voluntary intent. These results suggest a tSCS-related amplification of the residual motor ability of the subject, together with a benefit in decreasing hypertonia, suggested by the reduced EMG amplitude during tSCS cycling compared to the passive case, where it was causing resistance to movement.

Overall, EMG data among subjects show that the stimulation does not consistently increase muscle activations compared to passive cycling, but it rather modulates them, both amplifying and reducing depending on the muscle and the session, with no particular scheme. Contrary to expectations, EMG during passive cycling was neither null nor inactive in multiple muscles and subjects. Although we could not identify a stimulation frequency consistently increasing muscle activations over the passive level, the 80 Hz tSCS showed reduced EMG amplitude in all participants and muscles, suggesting that it may be a viable option for spasticity reduction. The 50 and 20 Hz stimulations, instead, showed values sometimes slightly below the passive range but in most of the cases over it, with the 50 Hz scoring as the most amplifying frequency on average.
Although higher EMG activations did not consistently lead to cycling force improvements, these results align with the literature, where a 30-50 Hz frequency is usually employed in motor-oriented SCS studies [317]. The lack of motor outcomes in our study is probably due to the low number of trials and not to the stimulation frequency; indeed, studies reporting improved motor outcomes do so after months-long stimulation protocols.

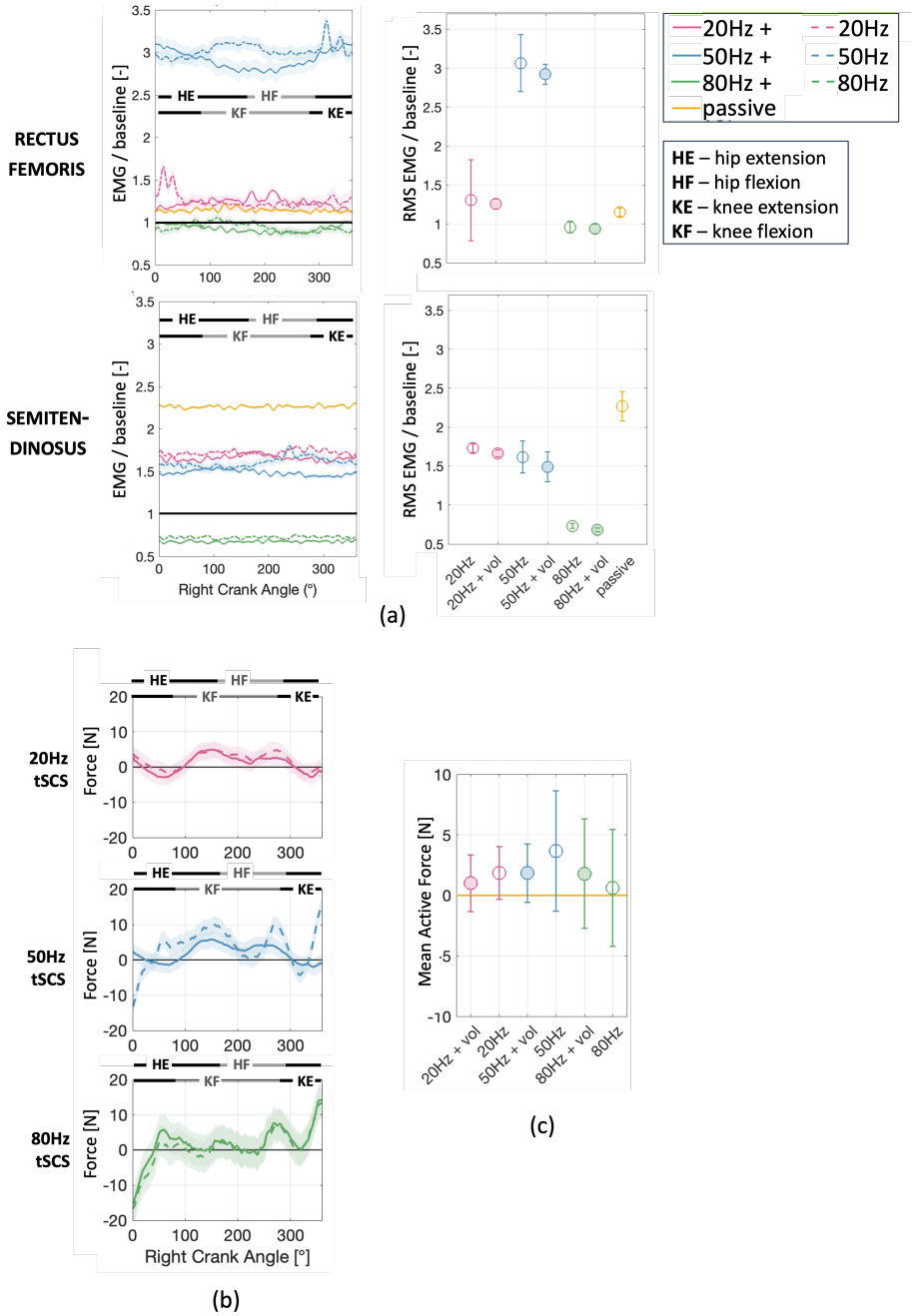

Figure 4.6: Data from the first trial of subject 02, representing the *Case Study 01*. (a) Right Rectus Femoris and Semitendinosus EMG during an average cycling revolution (left), reported as mean ± SD (Standard Deviation), and mean RMS values of the EMG amplitudes (right). Data are normalized to the subject's baseline and reported with respect to the right crank angle, which is null when the right pedal is at 90° upright. Knee and hip flexion and extension intervals are superimposed with black (extension) and grey (flexion) bars on the graphs. (b) Average cycles of the active force computed as the difference between the one during tSCS trials and the one during the passive trial. Each row is relative to a different tested frequency. (c) Mean and SD of the active force for all tSCS cycling conditions.

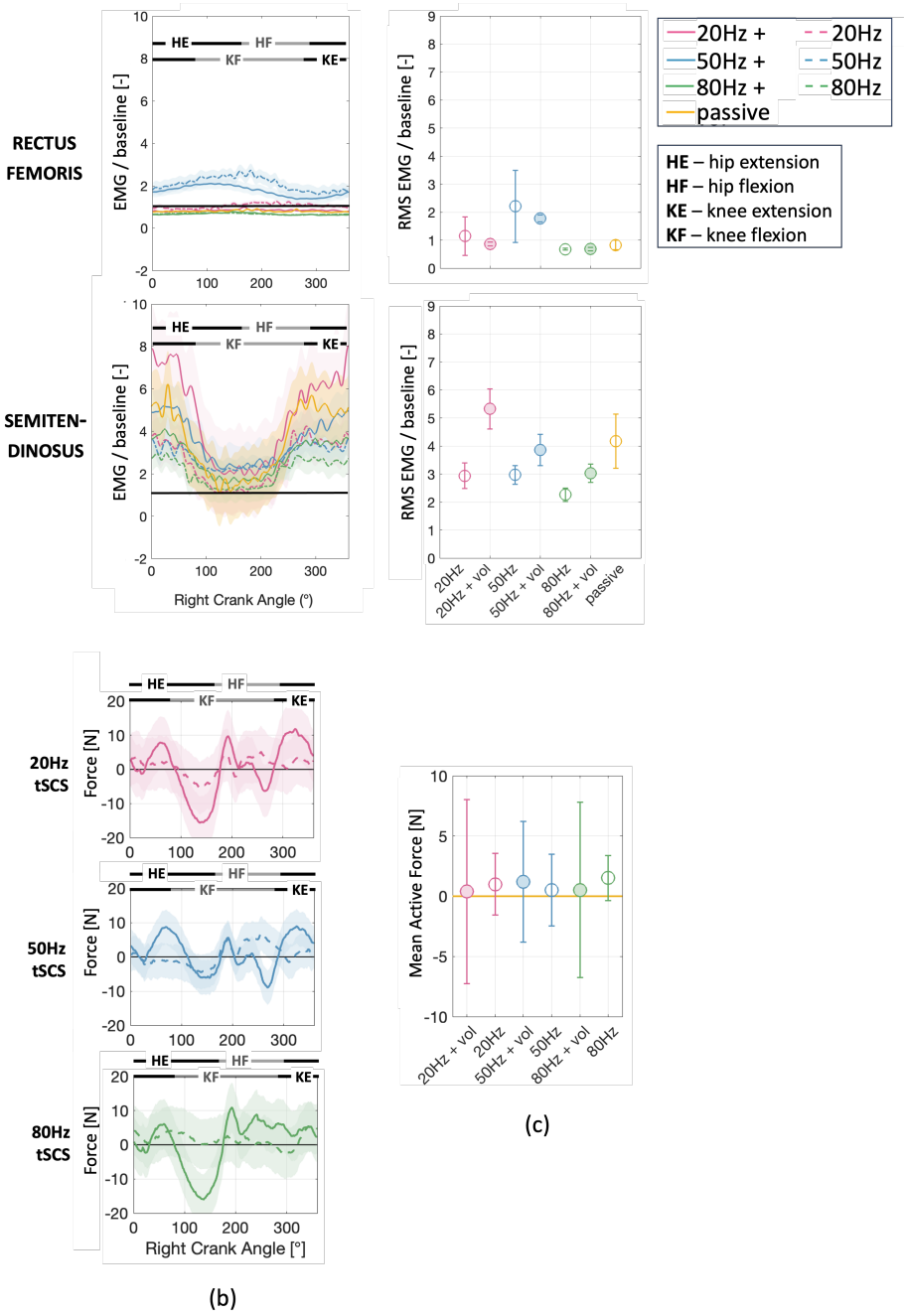

Figure 4.7: Data from second trial of subject 03, representing the *Case Study 02*. (a) Right rectus femoris and Semitendinosus EMG during an average cycling revolution (left), reported as mean $\pm SD$ (Standard Deviation), and mean RMS values of the EMG amplitudes (right). Data are normalized to the subject's baseline and reported with respect to the right crank angle, which is null when the right pedal is at 90° upright. Knee and hip flexion and extension intervals are superimposed with black (extension) and grey (flexion) bars on the graphs. (b) Average cycles of the active force computed as the difference between the one during tSCS trials and the one during the passive trial. Each row is relative to a different tested frequency. (c) Mean and SD of the active force for all tSCS cycling conditions.

tSCS induced sensations

For each stimulation frequency, participants were asked to rate feelings of pain, burning, cramping, tingling and pressure on a scale from 0 to 10, with eventual additional comments. Subject 01 scored 0 in all categories, indicating no stimulation perception. The other participants reported feeling the stimulation as an intense tingling both in the lower back and proximal legs, and, in some cases, as a heating or painful sensation. The single pulses delivered during the calibration phase were described as a "push" on the lower back, while the continuous tSCS caused higher discomfort. However, it decreased over the three-minute session, indicating an adaptation phenomenon. Supporting this latter hypothesis, subjects 02 and 03 scored lower in all categories in the second session compared to the first one. Those who tried FES-cycling before argued that the tSCS sensation was similar to the one induced by FES, when stimulation is directly applied to lower-limb muscles.
As expected, reported scores were proportionate to the lesions' levels, with subject 03 communicating the most discomfort (lesion D12). Subject 02 declared increased discomfort with increasing frequencies. For subject 01, instead, the highest discomfort was experienced during the 50 Hz tSCS. Subject 03 reported a significant increase in pain when adding the volitional effort to the 20 Hz stimulation. Nevertheless, no clear consensus was found among subjects regarding the stimulation type perceived as the most uncomfortable.

Secondary effects of tSCS

Participants were asked for feedback 24/48 hours after the stimulation session. No one reported any discomfort or negative feelings following the stimulation. On the other hand, non-motor effects were observed, which are worth mentioning, even if not strictly related to the motor facilitation aim of the study. On one hand, bladder- and bowel-related benefits were reported. Specifically, subject 01 communicated reduced bowel evacuation time while subject 02 regained bladder sensibility for 5-7 days after the stimulation and also bowel sensibility after the second stimulation session. On the other hand, a reduced lower-limb muscles' rigidity, with less spasticity and clonuses, was reported by subjects 02, 03 and 04 for 48 hours after the spinal stimulation session. This result is in line with literature reports [225, 226, 328], with Hofstoetter et al. [225] demonstrating improved spasticity for 2h after a 30-minute tSCS session and a carry-over effect up to 7 days after the session. These secondary tSCS-induced effects offer promising perspectives for further research, suggesting that SCS could have a substantial influence on the daily activities of SCI individuals.

4.6. Conclusions

Spinal Cord Stimulation (SCS) is a promising non-invasive motor rehabilitation technique in individuals with Spinal Cord Injury (SCI), showing reinstatement of volitional motor control in previously completely paralyzed subjects in its epidural, invasive version. Transcutaneous SCS (tSCS) is the non-invasive, accessible and cost-effective alternative to the epidural approach that, despite a significant lack of selectivity, has shown promising neurorehabilitation results.
Given these benefits, we decided to start investigating tSCS. As this was the first approach for our laboratory, initially we carried out an exploratory study that tested different configurations and parameters on non-disabled subjects to define a suitable setup for inducing visible effects. As the literature lacks a clear consensus on the best protocol to be used, this work was also intended as a verification of the stud-

ied literature. It represented a necessary preliminary work that allowed us to define a valid stimulation protocol, capable of inducing a visible muscle reflex, to be then applied to users with neuromotor deficits. As follows, we delivered a cycling-based protocol to four SCI individuals to evaluate the stimulation's motor-facilitating effects during pedaling. We also assessed a combination of tSCS and volitional effort to determine the potential contribution of volitional signals to the movement.

Our trials demonstrated the feasibility of the proposed protocol, without any discomfort experienced by subjects during cycling with tSCS. Our results are preliminary and do not reflect the significant motor improvements reported in the literature but they have to be contextualized to the low number of trials performed. Indeed, motor benefits described by the literature were observed after weeks of SCS sessions. Nevertheless, we proved the tSCS ability to modulate muscle activations but with no correlation between higher muscle activations and improved forces during cycling.

Interestingly, one subject improved his pedaling force when stimulation was combined with the volitional effort compared to the sole stimulation, highlighting SCS's potential amplification of residual volitional signals. For participants with hypertonia, EMG data showed the stretch reflex, often reduced in amplitude by the stimulation, underlining the spasticity-related benefits of SCS. This aligns with the reduced lower-limbs rigidity communicated by participants in the days following the stimulation. Additionally, they observed reduced bowel evacuation time and regained bladder sensitivity, which represent interesting side benefits of a motor-oriented protocol, with positive impacts on the subjects' quality of life.

Overall, tSCS combined with cycling was proved as a feasible approach for SCI motor rehabilitation, with different effects depending on the frequency and the specific subject. This suggests that the tSCS therapy should be intended as a subject-specific treatment. Moreover, further physiological benefits were observed, demonstrating the multi-modal effects of this technique. Its main limitations are related to the small number of participants recruited and trials conducted and the absence of long-term evaluations. Future work should evaluate the motor-facilitating effects of this protocol for longer periods, both during and after stimulation.

5 | Comparison of the neuromodulatory effects of peripheral and central electrical stimulation

Chapter Highlights

This chapter considers those stimulations targeting the sensory fibers, namely Sensory-Afferent Electrical Stimulation (SAES) and Spinal Cord Stimulation (SCS), and compares their neuromodulatory effects. In particular, Section 5.1 details the state of the art about SAES and its usage in the rehabilitation of neuromuscular injuries. A detailed description of the SCS strategy was instead offered at the beginning of the previous chapter (Section 4.1). Then, Section 5.2 presents the aim of a preliminary study conducted on non-disabled individuals where the two stimulations are compared. This research was conducted during the 6 months I spent at the Medical University of Vienna in collaboration with Professor Winfried Mayr. Then, Section 5.3 details the *Experimental Setup*, *Experimental Protocol* and *Data Analysis* used during the study, while its main results are presented and discussed in Sections 5.4 and 5.5. Lastly, Section 5.6 presents the main findings of the study and suggests the path that future research should take to drive stronger conclusions in the clinical field.

Chapter Contents

5.1 State of the Art . . . 138
5.2 Objective of the study . . . 139
5.3 Materials and Methods . . . 140
5.3.1 Experimental Setup . . . 140
5.3.2 Experimental Protocol . . . 141
5.3.3 Data Analysis . . . 143
5.4 Results . . . 144
5.4.1 Representative Subject . . . 144
5.4.2 All Subjects . . . 147
5.5 Discussion . . . 150
5.6 Conclusion . . . 152

5.1. State of the Art

SAES is a form of Neuro-Muscular Electrical Stimulation (NMES) delivered to peripheral mixed nerves and targeting sensory (afferent) fibers with low amplitudes, usually around the sensory threshold. Its primary goal is to elicit changes in sensorimotor functions [97] but it has also been used for active and task-oriented therapies, with the aim of improving motor abilities and drive cortical plasticity [98]. Indeed, even if targeting sensory nerves, this stimulation also determines the trans-synaptic activation of motor nerves. In particular, it elicits a reflex response in motor fibers, referred to as H-reflex, which can be observed in peripheral muscles' electromyographic (EMG) activity when stimulating their nerves at low amplitudes. Then, when increasing the amplitude, also the M-wave appears, resulting from the direct motor fibers stimulation [334].
At the central level, this technique induces neuromodulatory effects in the area of short-term, long-term and structural neuroplasticity, with the sprouting of new synapses and the formation of new anatomical connections (wiring) [194]. In an fMRI study [195], it was proved to increase the excitability of the sensorimotor cortex through the transformation of pre-existing silent synapses into functional ones. A typical consequence of such plastic changes in the motor cortex is the increase in the amplitude of Motor Evoked Potential (MEP) of the stimulated muscle and thus an improvement of its functionality. These benefits would be particularly relevant in treating muscles weakened by neuromuscular diseases, as demonstrated by Ridding and colleagues [155]. Further advantages were reported from studies combining SAES with motor therapy, reporting higher functional benefits and better motor and somatosensory performance compared to the sole motor therapy [199, 201, 202].
On the other hand, SCS targets spinal circuits by placing electrodes over the posterior region of the Spinal Cord (SC). Similarly to SAES, it targets sensory nerve fibers (those contained in the dorsal roots in this case) and then, through the synapses, it triggers motor nerve fibers (those contained in the ventral roots) [99]. Consequently, also this stimulation induces a reflex response in motor fibers, referred to as Posterior Root Muscle Reflex (PRM reflex) and observed in the EMG recordings of the main lower-limb muscles.
Its main characteristics and usages were already detailed in the previous Chapter (Section 4.1). There, it was highlighted that this technique proved capable of inducing neuroplastic changes by modulating the excitability of spinal circuits. Given these beneficial effects, it was used to treat decreased motor abilities typical of neuromuscular diseases, demonstrating positive results for the functional recovery of movements [99, 211, 215, 220, 224], the reduction of spasticity [220, 225–227] and the improvement of bladder functions [228].
Previous studies proved a similar working principle for these two types of stimulation. Indeed, the PRM reflex and the H-reflex are essentially elicited by the same sensory fibers stimulated at different locations in the afferent reflex arc, either in the posterior roots of the SC or in the mixed peripheral nerves [214]. This was demonstrated in literature for the Triceps Surae muscle [215].
Furthermore, in both cases, the Post-activation Depression (PaD) phenomenon is observed, typical of reflex-mediated responses. It is defined as a reduction in the Monosynaptic Excitatory Postsynaptic Potential (EPSP) which refers to the reduction of the potential induced in a postsynaptic motor fiber, trans-synaptically stimulated by a sensory fiber, due to the previous activation of the same fiber [216]. Therefore, when two SCS stimuli are delivered close in time (Inter-Stimulus-Interval around 50 ms), the EMG response to the second stimulus is much smaller in amplitude compared to that of the first stimulus [206, 214].

Even if the PRM reflex and the H-reflex are very similar, they differ in some aspects, as investigated by Minassian and colleagues [213]:

- The PRM reflex has shorter latencies than the H-reflex because the latter depolarizes afferent fibers more distally than the former. Thus, APs elicited by peripheral nerve stimulation need a longer time to travel to the spinal cord. Mean latencies reported from literature recordings of the gastrocnemius muscle are around 31 ms for the H-reflex evoked by the tibial nerve stimulation and 20 ms for the PRM reflex [214].
- In the PRM reflex generation, SCS selectively activates only afferent sensory fibers. Differently, in the peripheral nerve stimulation, mixed nerves are excited and thus both motor and sensory fibers. This limits the possible current amplitudes employed by SAES because higher amplitudes would determine an increase in the direct recruitment of motor fibers. This would cause both an orthodromic short-latency M-wave and an antidromic volley that collides with the H-reflex induced in the same motor axon (caused by the orthodromic activation of sensory fibers and monosynaptic activation of motor ones). Consequently, the maximal attainable proportion of the motoneuron pool is larger in the PRM reflex than in the H-reflex, limiting the maximum size of the H-reflex.
- Related to the previous point, the recovery cycles of the two reflexes, studied by Hofstoetter and colleagues [335], showed that the PRM reflex has a stronger depression than the H-reflex and that this depression is greater in subjects without disability. This may depend on the different targets stimulated to evoke the reflexes (i.e., the spinal cord and the peripheral nerves), with a larger pool of neurons being excited in the PRM reflex.

The collision of ascending and descending signals on motor fibers is a phenomenon known as *Collision Block* which represents one of the main limitations of the SAES technique, affecting the resulting H-reflex. Future research should focus on more precise guidelines about the optimal electrode location to maximize the stimulation of sensory nerve fibers. SCS also exhibits a similar phenomenon, resulting from the collision between the antidromic signal on sensory fibers (efferent) and the one transmitting the proprioceptive information (afferent). This prevents the propagation of the proprioceptive information towards the SC and the brain, which is instead fundamental for locomotion [235], but does not affect the PRM reflex.
Further limitations of the tSCS application are: i) the impossibility of using this technique on individuals with a metal implant on their spine, which is common in SCI cases; ii) the difficulty for subjects to autonomously position electrodes on their back; iii) the higher risks associated with the delivery of greater current amplitudes usually involved with SCS.

5.2. Objective of the study

Both for SAES and SCS, there is no clear consensus in the literature about the induced benefits, in particular when considering recovery in terms of neuroplasticity. Additionally, the ideal parameters to be used are not exactly known [197], but frequency and intensity seem to have the greatest influence on neuromodulation.
This study aims to compare the two stimulation techniques, focusing on the induced reflex signals, particularly on their shape, latency and current levels needed to generate them. To do this, single

stimulation pulses are applied at the spinal level (for SCS) and on three different peripheral nerves (for SAES). Contemporarily, the EMG activity of the four main lower-limb muscles (Rectus Femoris, Biceps Femoris, Gastrocnemius and Tibialis Anterior) of one leg is recorded to acquire the generated PRM reflex and H-reflex, respectively.
For the sake of simplicity, the two stimulation techniques will be sometimes referred to as *Central* and *Peripheral* stimulation.
An extensive testing procedure has been carried out on twelve non-disabled subjects to evaluate the two reflexes in terms of shape, amplitude and latency.
The final objective was to understand whether a similar neuromodulatory effect could be hypothesized for the two techniques. By demonstrating this, SAES could substitute SCS in all those situations where the latter is not applicable. Additionally, benefits would be obtained in terms of subject independence and reduction of involved currents.

5.3. Materials and Methods

5.3.1. Experimental Setup

Both the central and the peripheral stimulation were delivered with the STIMISOLA stimulator (BIOPAC Systems, Inc.). It is a 1-channel Linear Isolated Stimulator (shown in Figure 5.1a) delivering customizable electrical pulses; in particular, it allows to select the shape of the pulse (monophasic or biphasic), the pulsewidth (i.e., the duration of each phase of the pulse), the amplitude and the frequency. The stimulator is connected to a two-fold cable which terminals are then coupled to stimulation electrodes attached to the skin of the subject. Standard transcutaneous commercial electrodes (Comepa Industries) were used in both cases but with different sizes: 2 identical square electrodes (5x5 cm) were selected for the back stimulation; a round anode electrode (Ø 30 mm) and a rectangular cathode electrode (5x10 cm) were used for the peripheral stimulation. The stimulator was connected to a Windows PC via the USB interface and was controlled through an own-made application realized with the LabVIEW software.
For the EMG acquisition, the Powerlab system (ADInstruments) was used (shown in Figure 5.1b), in particular the 16/35 model, which is a data acquisition and analysis system for use in research. It has a 16-bit resolution, a maximum recording speed of 400 kHz and incorporates 16 input channels. In this work only 2 channels were used, connected to 2 Biological Amplifiers FE231 (ADInstruments), suitable for the acquisition of biological signals. The interface with the subject was realized via a cable with 3 terminals at both endings: on one side it was connected to the 3 inputs of the amplifier (Ref, + and -), while on the other side to the 3 electrodes on the subject's skin. Specifically, the Blue Sensor N, ECG Electrodes (Ambu) were used. For each EMG signal to be acquired, 3 electrodes were necessary: a pair of recording electrodes placed over the target muscle and a reference electrode placed close to a bone, as far as possible from other interfering muscle activities. We selected the area of the fibula heads as it is considered a suitable location for the reference electrode.

The software acquisition of the EMG signal was made with the official ADInstruments application LabChart which communicates with the front-end via an appropriate front-end driver. This application runs on a Windows PC (different from the one used for the stimulation), connected to the PowerLab via a high-speed USB (2.0). Through this application, we could set a sampling frequency of 40 kHz and

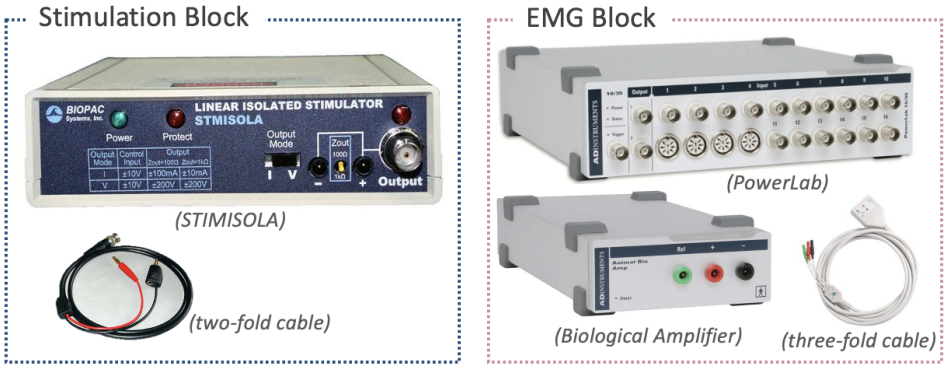

(a) (b)

Figure 5.1: Experimental setup for the stimulation component (a) with the STIMISOLA stimulator and its cable for electrodes connection, and for the EMG component (b) with the PowerLab acquisition system, the biological amplifier and its three-fold cable for electrodes connection.

add a hardware band-pass filter between 10 Hz and 500 Hz.

5.3.2. Experimental Protocol

The study conforms to the Helsinki Declaration and the Ethical Committee of the Medical University of Wien approved the study. Twelve non-disabled participants (9 males, 3 females, mean age of 27.75±5.1 years old) took part in the trials after providing their written informed consent. Before starting, participants were informed about the content and details of the study by the attending physician who also verified that they were meeting all the inclusion criteria.
In the case of female subjects, they were also required to take a pregnancy test to prove they were not pregnant at the time of the test.

Central Stimulation Protocol

For the central stimulation, 2 square electrodes were positioned on the back of the subject, the anode at the level of the iliac crests (L1-L2) and the cathode at the level of the last rib (T11-T12), with the same setup already used in our previous study (displayed in Figure 4.2a). During the acquisition, the subject was comfortably lying on his back while receiving a ramp of electrical pulses with increasing intensity. Specifically, the ramp started at 10 mA and stopped between 70 mA and 100 mA (maximum stimulator amplitude), depending on the subject sensitivity. In fact, all tested individuals were required to inform whenever the stimulation was becoming uncomfortable or painful. The amplitude step between pulses was set to 2 mA, the inter-pulse-interval was 5 s, leading to a frequency of 0.2 Hz, and the pulsewidth was 1 ms. The low frequency value indicates that we were not delivering a continuous stimulation pattern but a single-pulse one to be able to see the reflex responses, which would be otherwise impossible because of the refractory period of nerve fibers. Lastly, the biphasic pulse shape was selected as it is charge-balanced and offers a more efficient recruitment.
After this primary stimulation, the Post Activation Depression (PaD) was tested out by sending two close pulses with a time distance of 50 ms. The amplitude of the pulses was different for each individual and

it was selected as the amplitude able to induce a strong and visible reflex response but lower than the maximum in order not to induce discomfort in the subject. This step aimed to verify the presence of the PaD phenomenon and thus prove that the observed EMG signal indeed represented a reflex response, meaning that the muscle activity was not due to a direct motor fibers stimulation but to a trans-synaptic one, caused by the stimulation of sensory fibers.
To study the PRM reflex induced by the stimulation, the EMG activity was recorded for the 4 main leg muscles: Rectus Femoris (RF), Biceps Femoris (BF), Tibialis Anterior (TA) and Gastrocnemius (G). The position of the 4 pairs of EMG electrodes is the same already used in our previous study (displayed in Figure 4.2b). Before placing the electrodes the skin was cleaned and exfoliated using the Nuprep skin preparation gel (Weaver and Company) to improve the signal quality. Considering that we only had two Biological Amplifiers (i.e., we could record only 2 muscles at a time), in order not to prolong the test duration we decided to acquire the EMG activity only from one leg (left side), repeating the same current ramp two times, once while recording the RF and BF muscles and the other while recording the TA and G muscles.

Peripheral Stimulation Protocol

In this case, three different tests were carried out, each one stimulating a different leg nerve and thus changing the electrodes' location. In particular, 3 nerves were tested: the femoral nerve passing through the femoral triangle, the sciatic nerve located below the gluteal fold and the tibial nerve on the popliteal fossa. In all cases, a large rectangular reference electrode (cathode) was placed on the patella while a

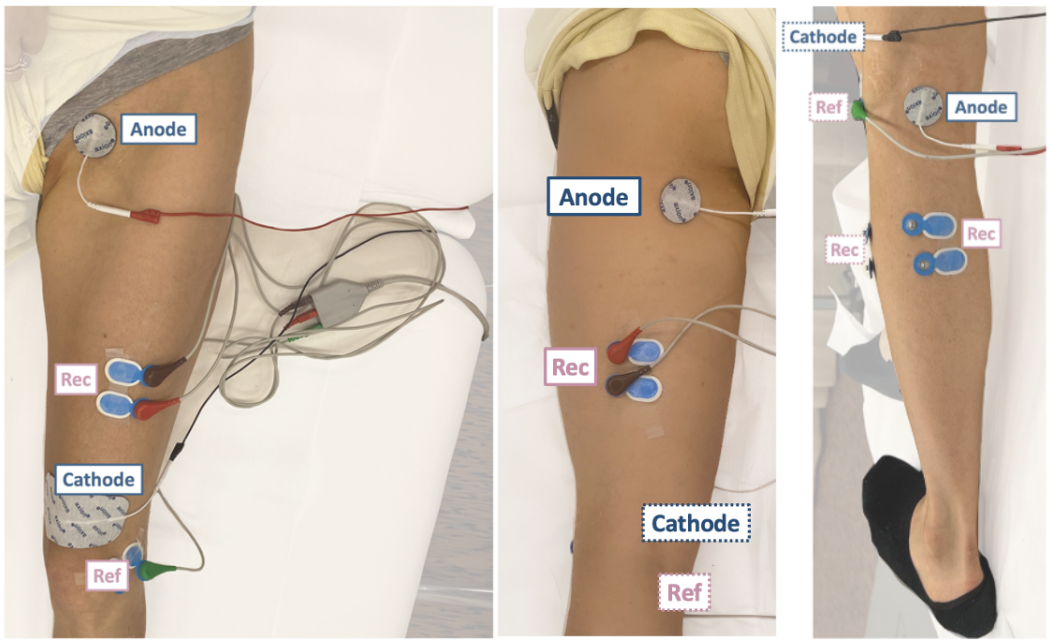

(a) (b) (c)

Figure 5.2: Position of stimulation electrodes (anode and cathode) and EMG ones (one reference and two recording) in the 3 peripheral tests: stimulation of femoral nerve (a), sciatic nerve (b) and tibial nerve (c). Blue labels mark the position of stimulation electrodes, pink labels the one of EMG electrodes. Labels with a dotted line indicate that the electrode is on the other side of the leg and thus covered.

small round stimulation electrode (anode) was used to target the nerve and thus it had a different position in the three tests. The aim of using a small electrode was to increase the selectivity of the stimulation as we were interested in stimulating only sensory nerve fibers and not motor ones to optimize the induction of the H-reflex.
However, the identification of the right electrode location is complicated by the fact that the peripheral nervous system has mixed nerves and thus sensory and motor fibers are in the same location. To optimize the positioning of the stimulation electrode, a preliminary exploratory phase was carried out by moving a metal electrode around the area where the sensory nerve fibers were expected to be located. During this phase, the EMG signal on the LabChart software was monitored to find an electrode position suitable for inducing a visible H-reflex and, at the same time, a small M-wave or no M-wave at all.
Similarly to before, the stimulation was delivered in the form of a ramp but with different parameters. Here the starting current level was determined as the first amplitude able to produce a visible activity on the EMG signal (seen from the LabChart application) while the stimulation was stopped when the H-reflex wave was no longer visible. The amplitude step between pulses was set to 1 mA and the inter-pulse-interval was 2 s, leading to a frequency of 0.5 Hz. The pulsewidth was 1 ms and the pulse shape was biphasic. Here, differently from before, 10 pulses were repeated for each amplitude because of the higher variability of the muscles' response to the peripheral nerve stimulation.
For the EMG acquisition, not all the 4 leg muscles were acquired during all tests but, depending on the specific stimulated nerve, we acquired only the one or ones where an H-reflex was expected to be induced.

Specifically, 3 different test configurations were tried out:

1. Stimulating electrode on the femoral nerve and EMG acquisition of the Rectus Femoris muscle (Figure 5.2a);
2. Stimulating electrode on the sciatic nerve and EMG acquisition of the Biceps Femoris muscle (Figure 5.2b);
3. Stimulating electrode on the tibial nerve and EMG acquisition of the Tibialis Anterior and Gastrocnemius muscles (Figure 5.2c).

Following the same protocol explained for the central case, also in the three peripheral conditions the occurrence of the PaD phenomenon was tested out.

5.3.3. Data Analysis

For the central stimulation, the EMG signal recorded for each stimulation amplitude was extracted. Then, for each stimulation amplitude, the following indexes were extracted:

- Stimulation index: sample time at which the stimulation pulse is observed on the EMG signal;
- Start wave index: sample time at which the reflex wave starts, computed as the instant at which the EMG signal displays a deflection from baseline higher than the 5% of its maximum peak-to-peak amplitude [214];
- Latency: time delay between the instant in which the stimulation pulse was sent and the one in which the reflex response was recorded;

- Peak-to-Peak amplitude: the absolute difference between the maximum and minimum voltages of the EMG signal.

For the central stimulation, as 10 pulses were sent for each amplitude, the average EMG signal of the 10 pulses was considered and then the following indexes were extracted:

- Stimulation index
- Start wave index
- Latency: both for H-reflex and M-wave;
- Peak-to-Peak amplitude: both for H-reflex and M-wave.

Lastly, the following average indexes were extracted for each muscle under both stimulations:

- Reflex threshold current: the current amplitude at which the first reflex response is visible;
- M-wave threshold current: the current amplitude at which the first M-wave is visible (only for peripheral stimulation cases);
- Average and Standard Deviation (SD) of the latencies across all tested current amplitudes;
- Amplitude ratio between the 1st and 2nd reflex responses obtained when sending two pulses close in time (i.e., when testing the PaD phenomenon).

Data were analyzed using MATLAB 2021b (Mathworks).
Finally, a non-parametric test for correlated samples was defined in SPSS Statistics (IBM) to compare the four muscles among them both in the Central and Peripheral case. Then also for pairwise comparisons of the 2 types of stimulation (Peripheral and Central) in the four muscle alternatives.

5.4. Results

The results are hereby presented, distinguishing between those of a representative subject and of all subjects.

5.4.1. Representative Subject

Here the single EMG waves recorded on one exemplary subject (ID5) are reported to offer an idea of the shape of these waves and their characteristics. The subject was selected because his results are in line with literature reports and thus represent the standard behaviour that we would expect when stimulating the posterior spinal roots and the peripheral nerves.
Figure 5.3 reports the PRM Reflex waves recorded on the four tested muscles under central stimulation for the selected user. For all muscles, the same current amplitude range was tested, from 10 mA to 70 mA with steps of 2 mA. To ease the visualization, not all tested amplitudes are displayed but, for each muscle, waves are shown for the reflex threshold current and then for increasing current amplitudes from 30 mA to 70 mA with steps of 10 mA.
Looking at the graphs it can be noticed that the reflex threshold current is different for each muscle as well as the voltage amplitudes spanned by the waves, with higher amplitudes for posterior muscles

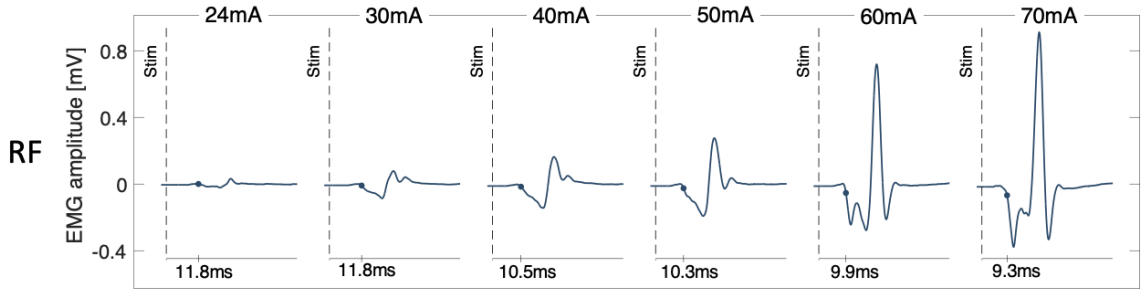

(a)

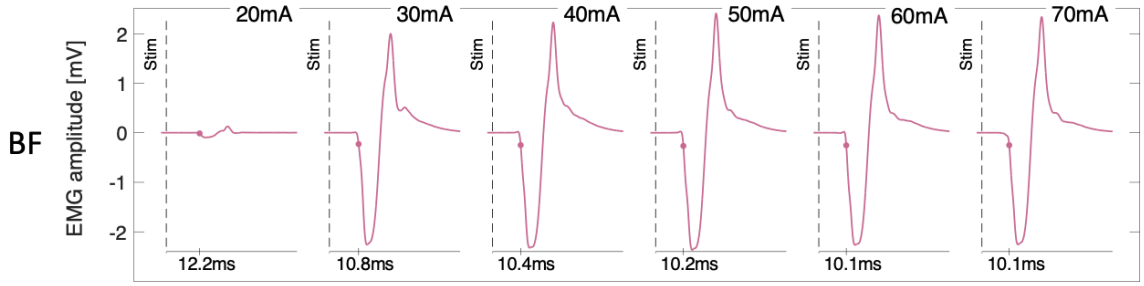

(b)

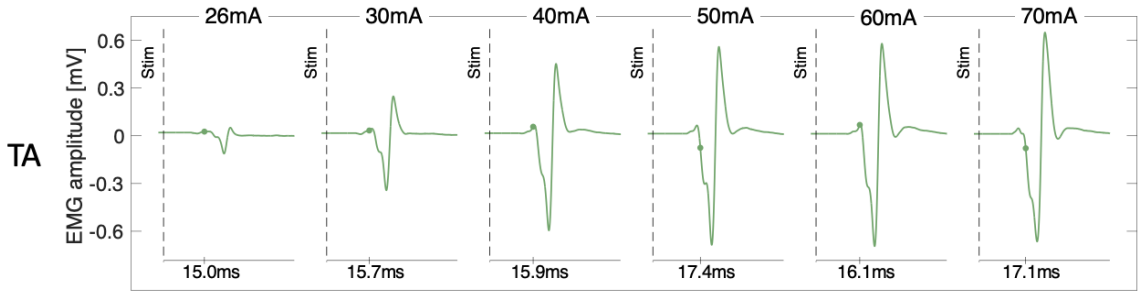

(c)

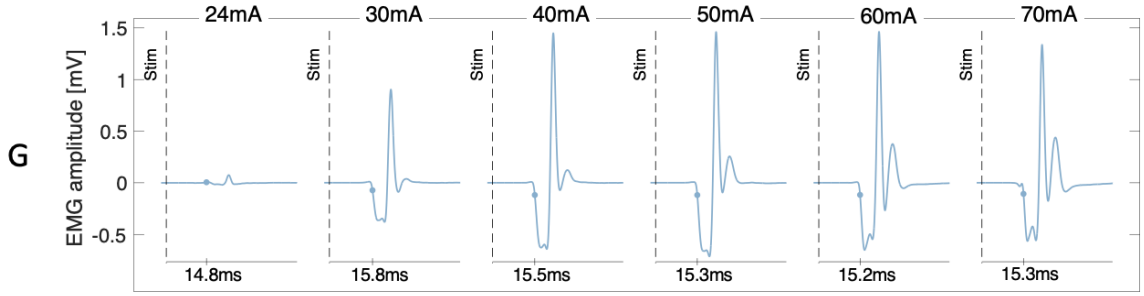

(d)

Figure 5.3: PRM reflex waves in mV for a single subject on the 4 tested muscles: RF (a), BF (b), TA (c) and G (d), displayed one per row. The used current amplitude is reported on the top of each panel. Dots on the graphs indicate the starting point of the reflex and its latency with respect to the stimulation instant (vertical dotted line) is reported in ms on the x-axis.

(BF and G) and lower for anterior ones (RF and TA). Focusing on the shape of the reflex waves, this

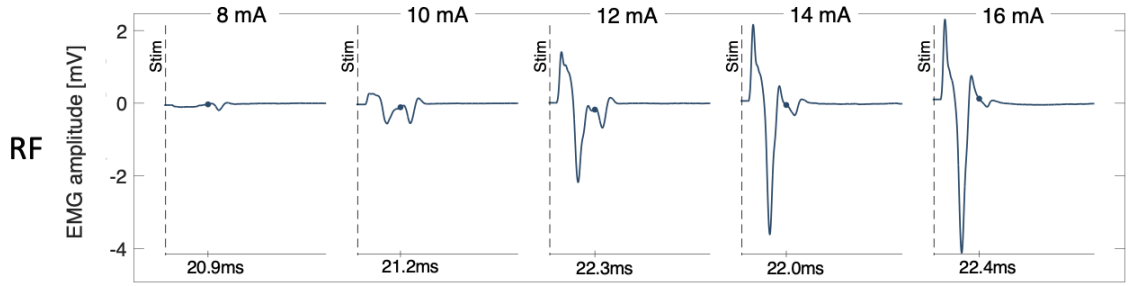

(a)

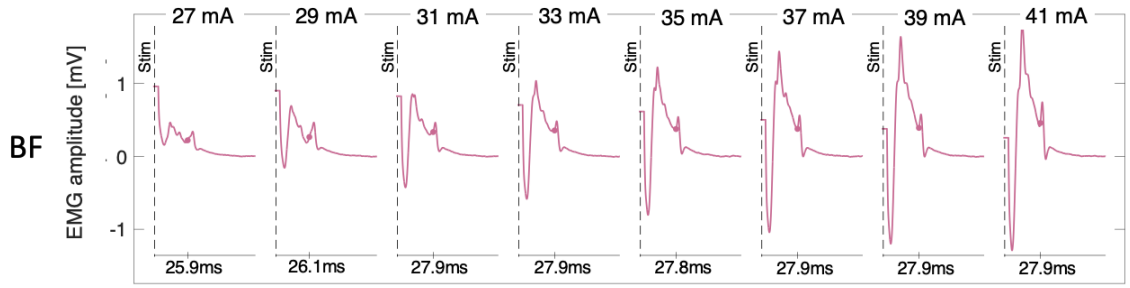

(b)

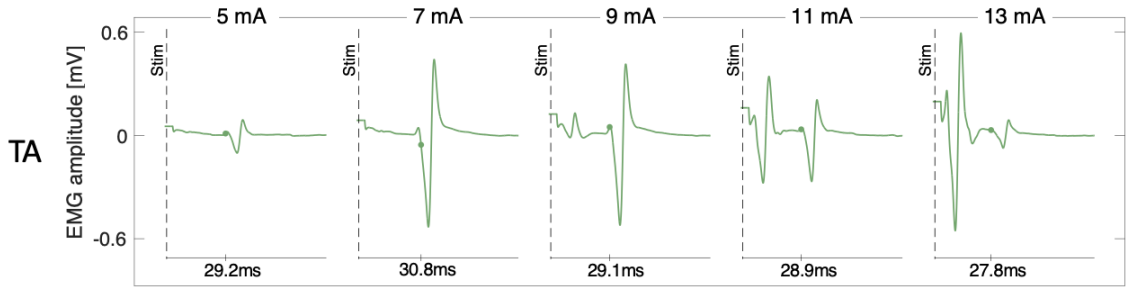

(c)

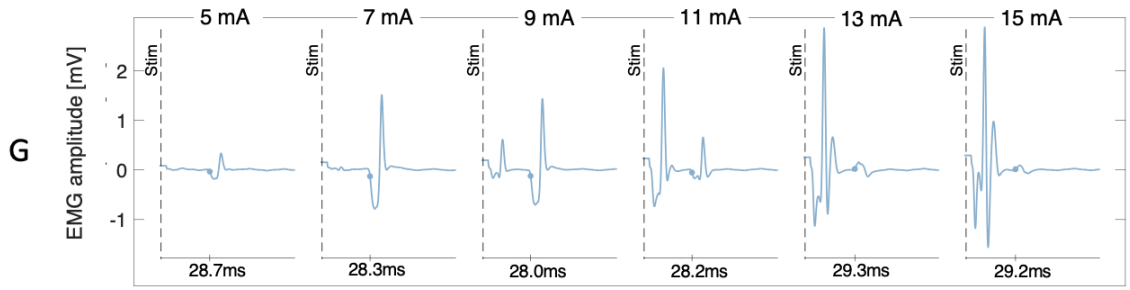

(d)

Figure 5.4: H-reflex and M-waves in mV for a single subject on the 4 tested muscles: RF (a), BF (b), TA (c) and G (d), displayed one per row. The used current amplitude is reported on the top of each panel. Dots on the graphs indicate the starting point of the H-reflex and its latency with respect to the stimulation instant (vertical dotted line) is reported in ms on the x-axis.

is consistent for the reflex waves recorded on the same muscle at different amplitudes but changes when considering different muscles. Nevertheless, some similar patterns can be spotted, such as the presence of a maximum and a minimum peak.
Figure 5.4, instead, reports the peripheral waves recorded on the same subject on the four tested muscles. In this case, as we started from the lowest current amplitude able to elicit a visible H-reflex (reflex threshold) and stopped when the reflex was not visible anymore, a different amplitude range was tested on the various muscles. In the figure, we reported some of the tested amplitudes with a distance of 2 mA; as a consequence, similarly to before, a different number of current levels (with a different value) are shown for each muscle.
Here, two different EMG waves appear after the stimulation artifact: the first one is the M-wave, induced by the direct stimulation of motor fibers, and the second one is the H-reflex, induced by the trans-synaptic stimulation of motor fibers.
For the RF, TA and G muscles, we observe the standard behaviour of the M-waves and H-reflexes, which we would have expected from the literature. In particular, some of the expected features are:

- Clear separation in time between the two waves;
- Lower H-reflex threshold than M-wave threshold (i.e., H-reflex waves appear before M-waves);
- Decrease of the H-reflex amplitude and opposite increase of the M-wave amplitude when increasing the current level.

For the BF muscle, instead, these features are less visible because the high magnitude of the M-wave covers in part the H-reflex; in fact, we suppose the H-reflex is the second wave that appears over the first one, but it is difficult to clearly define its starting and ending points. The big amplitude of the M-wave, in this case, is caused by the fact that we are using higher current levels for this muscle with respect to other ones, as we could not see this double wave phenomenon at lower current amplitudes.

Figure 5.5 represents the Post Activation Depression (PaD) phenomenon on the same representative subject (ID5). Only one muscle was reported (the BF muscle under central stimulation) as this phenomenon displayed a similar behaviour in all the other cases. The graph displays two stimulation pulses (inter-pulse distance of 50 ms) together with the induced reflex waves. The numerical value of the peak-to-peak amplitude for the two waves is reported in the graph and it can be noticed that, as expected from the literature, the amplitude of the 1st reflex (ppAmp=4.6 mV) is significantly higher than the one of the 2nd reflex (ppAmp=0.935 mV).

5.4.2. All Subjects

This subsection shows cumulative results that take into account all subjects' data, reported for each muscle and stimulation type in terms of median and Inter-Quartile Range (IQR).
It has to be remarked that not all reflexes could be recorded for all subjects; the percentage of responders (i.e., those subjects on which the specific reflex could be registered) for each reflex on each muscle is reported in Table 5.1.

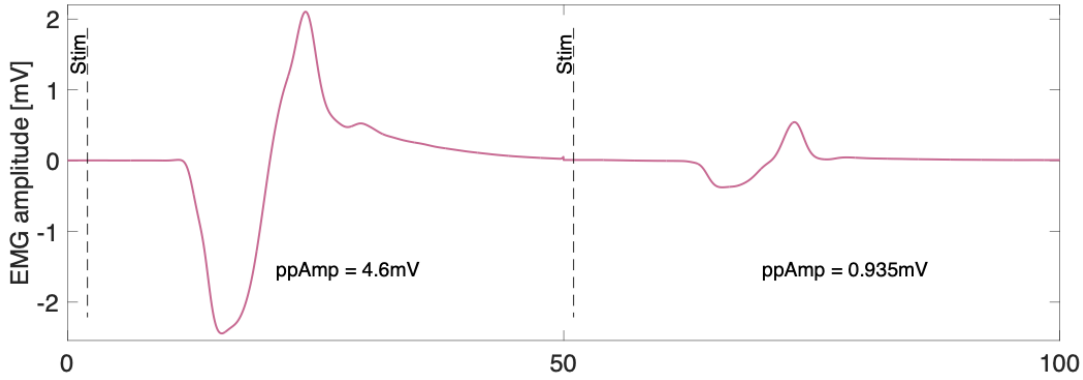

Figure 5.5: PaD phenomenon for the BF muscle during the central stimulation protocol on the representative subject (ID5).

CentralStimulation				*PeripheralStimulation*			
RF	**BF**	**TA**	**G**	**RF**	**BF**	**TA**	**G**
100%	100%	100%	100%	83%	25%	100%	92%

Table 5.1: Percentage of stimulation responders for the two stimulation types and different muscles over the twelve tested individuals. The term "responders" refers to those subjects on which the PRM reflex could be observed.

Figure 5.6 compares the following metrics for the central and peripheral stimulation over the four muscles: reflex thresholds (a), reflex latencies (b) and amplitude ratios between the 1st and 2nd reflex responses during PaD (c).

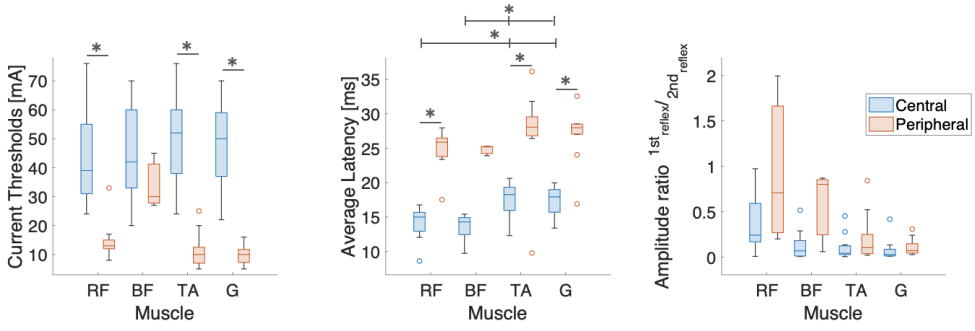

Figure 5.6: Boxplots comparing the reflexes induced by the two stimulation types across all subjects in terms of reflex threshold (a), reflex latency (b) and amplitude ratio between the 2nd and 1st reflex response when testing PaD (c).

The reflex threshold (Figure 5.6a) refers to the lowest current level at which the reflex was observed. By comparing its value for the central and peripheral stimulation, we can see that for all muscles the threshold is significantly lower in the latter case ($p<0.05$), except for BF. If focusing on a single type of stimulation and analyzing the similarities and dissimilarities among muscles, we can notice that for the

central reflexes, comparable threshold values were reported by the two distal muscles (TA and G) and by the two proximal ones (RF and BF), with higher median values in the distal condition but without significant differences. For the peripheral reflexes, instead, similarly to before, we have comparable values for the distal muscles, lower than those for the proximal ones. These latter, instead, display different values, with a much higher current level for the BF but not reaching the level of significance.
Considering the average reflex time latency (Figure 5.6b), a remarkable difference can be noticed between the central and peripheral conditions, with significantly higher latencies for the peripherally-induced reflexes of all muscles ($p<0.05$), except BF. Focusing, instead, on a single type of stimulation, we observe a pattern similar to the one already discussed for the current thresholds. Both for the peripheral and for the central case, in fact, the two distal muscles and the two proximal ones can be grouped as they display similar median latencies, higher in the former case with respect to the latter one. For the central case, RF and BF were significantly different from TA and G; for the peripheral case, instead, no significant differences were retrieved.
Lastly, when comparing the amplitude of the reflex responses induced by two close pulses (Figure 5.6c), no significant differences between the central and peripheral cases were reported by all muscles. The central stimulation displays small ratios for all muscles except the RF, which reports a higher median and a wider variability among data points with respect to other muscles but without significant differences. The peripheral stimulation, instead, presents small ratios for the distal muscles (comparable to those of the central one), while the medians of the proximal muscles are much higher as well as their data variability. Nevertheless, in all eight cases, the median amplitude ratio is lower than 1, meaning that the amplitude of the 2nd reflex response is always smaller than the one of the 1st response, aligning with the expected behaviour outlined in the literature.

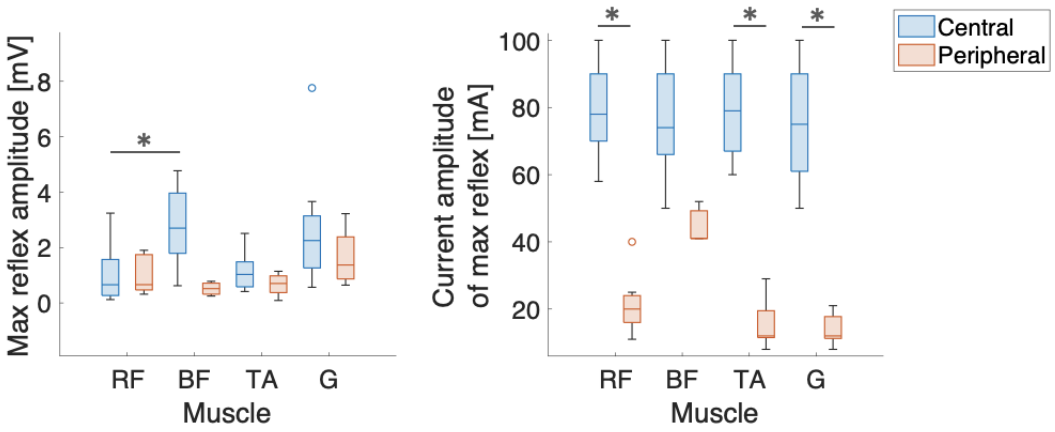

Figure 5.7: Boxplots of the max amplitudes of the PRM reflex (central) and H-reflex (peripheral) across all subjects (a), together with the current amplitudes at which this maximum reflex was registered (b).

Figure 5.7a displays the maximum amplitude recorded for both reflexes on the four muscles across all subjects. It can be noticed that for all muscles, except the BF, results are comparable both in terms of median and IQR, with slightly lower values for the peripheral reflex compared to the central one but without significant differences. The higher value of the BF may be due to the fact that its H-reflex could be registered only on three subjects out of twelve while the PRM one was recorded for all the twelve

individuals (as reported in Table 5.1). The absence of significant differences is interesting considering that for all muscles (except BF) the current amplitude at which the maximum reflex was registered was instead significantly different ($p<0.05$). This was around the lowest tested currents for the peripheral H-reflex, and around the highest ones for the central PRM reflex (5.7b).
Taking into account, instead, pairwise comparisons among muscles, we notice that the only significant difference is for the maximum reflex amplitude at the central level between RF and BF (0.009). Differently, the current amplitude of the maximum reflex reported no significant pairwise differences both at the central level and at the peripheral level.

5.5. Discussion

In this study Central and Peripheral Stimulations were investigated as possible neuromodulation techniques, analyzing their similarities and differences. In particular, the main interest was to give guidelines on how to apply them and understand whether the known advantages given by the Central stimulation could also be replicated with the Peripheral approach. Indeed, particularly for the peripheral stimulation, the literature lacks clear guidelines about the electrodes' position and parameters to be used to better address the sensory fibers. Indeed, considering that the SCS stimulates the sensory fibers in the posterior roots of the spinal cord, in an attempt to replicate the same neural processes induced by this stimulation, also the peripheral technique should mainly target these fibers. To this aim, both stimulations were delivered to twelve non-disabled subjects while contemporarily recording the EMG signal of four lower-limb muscles.
The main difference between central and peripheral stimulation lies in the fact that the former only triggers sensory nerve fibers while the latter, targeting mixed nerves, elicits both sensory and motor fibers. Indeed, when considering single-subject recordings (Figures 5.3 and 5.4), a single EMG response (PRM reflex) is displayed in the former case, while two waves appear in the latter case, both the direct motor response (M-wave) and the reflex one (H-wave). The fact of stimulating mixed nerves is also associated with a higher difficulty in identifying the electrode's position, which should be the optimal one for triggering sensory fibers. Despite this difference, the two reflexes are similar in terms of shape, with the presence of a minimum and maximum peak, across all considered muscles. However, it must be underlined that this standard behaviour reported for one subject is not representative of all tested subjects. Particularly for the peripheral stimulation, there were some cases in which the reflex activity could not be recorded. In fact, as previously said, the results of the peripheral stimulation on the BF are only available for 3 out of 12 subjects and those on the RF for 10 out of 12 subjects. This was due to the fact that the current level required to obtain a visible reflex in such cases was higher than the maximum current level that the tested person could tolerate. It happened with nerves innervating proximal muscles (RF and BF) and not distal ones (TA and G) because these nerves are more difficult to localize and stimulate as they are deeper [336] and covered by a bigger amount of fat mass that, increasing the tissue impedance, elevates the current level needed to get the same potential difference.
This inspection is in line with the fact that considering data across all subjects, the H-reflex threshold amplitude displays a higher median for proximal muscles compared to distal ones. The opposite behaviour was instead observed for the central stimulation, with higher currents needed to induce a reflex in distal muscles compared to proximal ones. In this case, it is not explained by anatomical considerations but rather by the location of the stimulation electrodes: the threshold for distal muscles can be decreased by moving the lower electrode caudal, while the opposite occurs when moving it more apical. This is

coherent with the observation that threshold values are similar for the two distal muscles and for the two proximal ones, confirming the link between them.
Considering both reflexes, generally, the current threshold amplitude is always higher for the PRM reflex compared to the H-reflex because of the deeper location of nerve roots in the spinal posterior horns, which require a higher current than peripheral nerves to get a similar depolarization level. Related to this, when considering maximum reflex amplitudes, we observed similar values for the central and peripheral case across all muscles (except the BF) but induced by significantly higher currents in the former case compared to the latter. The BF is an exception because of the difficulty of observing the H-reflex in this muscle. Nevertheless, for all other muscles, this represents a relevant result, supporting the theory that the two stimulations may induce similar neuromodulatory effects, with the advantage that the peripheral one involves significantly lower current amplitudes. Of course, a deeper investigation in this direction is needed, but this result reinforces the rationale behind our research. If similar neuromodulatory effects were demonstrated, subjects could use the peripheral stimulation in place of the central one, gaining the same benefits while being injected with significantly lower charges. Moreover, this would enable an autonomous application of the treatment, strengthening the independence of subjects and the shift of rehabilitation from hospital-based settings to home-based ones, strongly promoted in recent years [258, 259].
Significantly higher latencies were registered for the peripheral reflexes due to the larger distance that the signal has to travel: from the stimulation site on the leg, it goes up to the spinal cord through sensory fibers and then back again to the recording site on the leg through motor fibers. For the central case, instead, the stimulation site is already at the spinal cord level and thus only the descending path has to be travelled. Related to this, both reflexes reported lower latencies in proximal muscles than distal ones, because the former are closer to the spinal cord.
Given that this study was based on the comparison of two reflex responses, the Post Activation Depression phenomenon was verified for both cases to guarantee that the observed waves on the EMG signal were actual reflex responses. This test was carried out on all subjects by sending two close pulses (inter-pulse interval of 50 ms) and by noticing that the median amplitude ratio between the 2nd and 1st reflex responses was always lower than 1, meaning that the 2nd one was always attenuated. However, computed ratios varied across muscles, with lower values for distal muscles than proximal ones, especially in the peripheral case. A possible explanation may be the fact that the electrical signal travels a lower distance in proximal nerves, reducing their refractory period and thus making these fibers ready to spike again before those innervating distal muscles.
Overall, the present work collected some interesting observations, supporting further investigations in this field. Nevertheless, this study also faced some limitations. The main one is given by the fact that only subjects without disability were tested and consequently, moderate current levels could be delivered. This mainly limited the central stimulation setup because, as previously discussed, the SCS requires higher current levels which are not always tolerated by non-disabled subjects. Furthermore, it also prevented the application of a continuous stimulation pattern as it would have resulted in higher pain. However, testing this protocol on neurologically impaired subjects would represent a crucial step for this research, enabling to prove the therapeutic benefits of SCS, like the reduction of spasticity-induced side effects [226, 330]. Thus, future studies should apply both approaches to neurologically impaired subjects and compare them in terms of induced therapeutical effects.
Secondly, a precise mapping for electrode positioning was not performed but they were rather placed where the nerve was expected to be located. Then, by looking at the real-time EMG signals, some

trial-and-error adjustments were made to find the nearby location in which the strongest EMG signal was induced. As a consequence, we cannot state whether the optimal location was identified or not, and this may be the reason why we also observed some unexpected results, not in line with literature reports. For example, sometimes it was difficult to get a clean H-wave and a later appearance of the M-wave but rather the contemporary presence of the two signals was observed. Future studies should optimize the electrodes' positioning step by mapping mixed nerves and spotting ideal locations for the preferential triggering of sensory fibers.

5.6. Conclusion

This study proposes the comparison of two stimulation approaches targeting sensory nerve fibers, Spinal Cord Stimulation (SCS) and Sensory Afferent Electrical Stimulation (SAES). The comparison focused on the reflex responses induced by the two techniques, in the attempt to understand whether these could induce similar neuromodulatory effects. Indeed, while there has been growing attention on exploring the benefits of SCS for individuals with neuromuscular diseases in recent years, the SAES investigation has received less attention. The peripheral approach is usually adopted for the direct stimulation of motor fibers and the induction of artificial contractions, while its effect on the afferent sensory nerves has been rarely attempted. Only in recent years, some interest was observed towards the development of full-body or half-body suits, already integrating electrodes, intended to deliver a sensory stimulation or haptic feedback. Some examples include the TeslaSuit [294], the Exopulse Mollii Suit [293] (by Ottobock) and the Neural Sleeve [337] (by Cionic).
The rationale of this study lies in the fact that demonstrating similar effects for SCS and SAES would enable to substitute the former with the latter and thus overcome some inherent SCS disadvantages. Among them, are its inapplicability in individuals with spinal metal implants and the difficulty for subjects to place back electrodes independently. The gathered results proved similar characteristics for the two reflex waves in terms of shape and amplitude, proving that similar excitation levels could be obtained for sensory fibers by using significantly different current amplitudes, lower for the peripheral condition. Tests were only conducted on non-disabled subjects delivered with single electrical pulses but a study on neurologically impaired users is strongly suggested, together with the application of a continuous stimulation. Nevertheless, the collected evidence represents a promising starting point that paves the way for future studies on possible uses of SAES in place of SCS, encouraging higher subject independence and enabling the shift of rehabilitation treatments from hospital-based settings to home-based ones.

6 | Conclusion and future perspectives

Chapter Highlights

The research work outlined in the present thesis is hereby summarized, enhancing its main findings and the key insights derived from it. Then, a perspective of the potential future research direction is offered, along with insights into interesting points that warrant further exploration.

Chapter Contents

6.1 Key take-home messages of the thesis, limitations and future perspectives 153

6.1. Key take-home messages of the thesis, limitations and future perspectives

My Ph.D. research deals with the use of different neuromodulation approaches for optimizing the rehabilitation process of people affected by neuromuscular disorders. In particular, I concentrated on non-invasive Electrical Stimulation(ES)-based technologies, which have received growing attention in recent years and could be employed in routine clinical practices to address conditions such as Spinal Cord Injury (SCI) or Stroke. Their main objective is to restore subjects' motor-sensory functions but also to improve their quality of life by inducing secondary physiological benefits and enhancing their social participation. The diffusion of these strategies was supported by the rapid evolution of engineering technologies, that continuously propose advanced solutions, increasingly accepted by users and tailored to their specific needs. During my Ph.D., I investigated the different existing electrical stimulation techniques, particularly focusing on their working principles and on their induced effects at the central and peripheral neurological levels. Starting from this, novel therapeutic approaches were hereby proposed where, depending on the sought effect, the optimal stimulation strategy was applied, within an innovative setup that has been rarely or never tested in the literature.

The primary objective is to offer technological advancements that could lead potential enhancements in the rehabilitation of neuromuscular diseases. Indeed, conducted studies gathered promising, albeit

sometimes preliminary, results when applying such approaches to both disabled and non-disabled subjects. Therefore, this thesis serves as a starting point, stimulating future applications of such innovative therapeutic strategies to draw stronger conclusions about their effects and benefits.

This conclusive chapter aims to provide an overview of the different studied techniques, with their advantages and disadvantages, and with insights about their potential usage in the future. The idea is to support the reader in understanding which is the most suitable stimulation to be set up depending on the specific conditions he/she is dealing with. These conclusive remarks result from an initial theoretical study, mainly retrieved from literature research, then supported by more practical procedures that I conducted during my Ph.D., comprising experiments in which the electrical stimulation was applied at different levels along the nervous system tree. Some tests have been carried out in the form of preliminary feasibility studies, only involving non-disabled participants; others instead were more extensive, reaching the clinical environment and thus individuals affected by neurological diseases, which represent the final target of my study.
The main take-home messages that I collected throughout my research are hereby presented.

- The combination of FES with an active robotic device within a hybrid structure enables the reduction of the power demanded to motors and thus the realization of lighter and less cumbersome systems (i.e., integrating smaller motors and batteries). Indeed, by delivering pulses above the motor threshold, FES induces functional muscular contraction and thus provides torque inputs positively participating in the movement execution.
  However, such advantages are gained if defining a cooperative FES-motor control strategy, where the two components are integrated within the same control loop rather than being merely summed together but operating independently. Indeed, only with a connection among them, the two components are aware of each other's state and can react to eventual variations of their performances over time. On one hand, the FES control can continuously adapt the stimulation parameters to compensate for motor torque reductions; on the other hand, the motor intervenes in case of stimulation inefficiencies, such as in cases of muscle fatigue.
  Additionally, being applied at the peripheral level and thus triggering mixed (both sensory and motor) nerve fibers, FES also induces benefits at the central level. Indeed, the afferent fibers stimulation provides excitatory inputs back to the brain which promotes neural plasticity and motor relearning [152, 153]. This phenomenon is emphasized when FES is coordinated with residual volitional activations [154] because the intention of the action is combined with the perception of effectively completing it, allowing subjects to perceive movements as self-generated [158].
  Both these aspects support a general improvement of the usability of *hybrid* devices when compared to standard robots. On one side, users are more willing to use these technologies if presenting a less cumbersome structure; on the other side, the perception of the active participation of their muscles in the movement execution determines psychological benefits, besides the FES-related physiological ones (previously listed in Section 1.4.1).
  A further alternative to enhance the usability of these devices, in particular considering the donning and doffing processes, is the usage of textile-based electrodes that can be directly integrated into the system's structure. In this way, the electrode positioning process is avoided. This represents a strong advantage because it is time-consuming and often requires the presence of an expert to identify the optimal skin locations for their placement.

This was demonstrated in Chapter 2 of this thesis, which reports the development and testing of the TwinFES hybrid system, characterized by a novel cooperative controller.

The second research question investigates alternative non-invasive ES solutions acting on afferent neural circuits with the aim of maximizing the neuromodulation effects.

- When the stimulation only aims at inducing a neuromodulatory effect, instead, other two alternative non-invasive ES solutions are possible, besides the FES. These are SCS and SAES which trigger afferent fibers at the central and peripheral levels respectively. They aim to send upward signals directed toward the center to increase the overall excitability of the nervous system and ease the processing of incoming inputs. Indeed, rather than directly inducing contractions, these strategies are intended to facilitate the performance of movement. They are particularly useful in the case of residual volitional efforts that reach the spinal cord but are too weak to trigger fiber depolarization. By providing additional input, these strategies increase the central state of excitability and allow these signals to overcome the firing threshold.
  SCS received increasing attention in recent years, in particular for its demonstrated ability to reduce spasticity [226] thanks to the inhibition of the hyperactivity of antagonist muscles. Additionally, it is known that the combination of electrical stimulation with descending motor commands is beneficial for neuroplastic changes, resulting in a Hebbian-type learning effect [211]. However, the definition of therapeutic protocols applying this stimulation, potentially in combination with the execution of functional movements, is still scarce in the present literature. As a consequence, no clear consensus has been found so far about the real effects of this stimulation, in particular when considering long-term applications.
  With regards to SAES, instead, it was rarely investigated in the literature and thus its potential advantages in terms of neuromodulation and brain plasticity are still unknown. Nevertheless, it was proved that SAES and SCS are initiated in the same type of sensory axons, even if at different locations along them [214]. Therefore, it is reasonable to imagine that the two stimulations could also induce similar therapeutic effects.

  In Chapter 5 of this thesis, we demonstrated similar characteristics for their induced reflexes but further study should test their eventual similarity in terms of therapeutic effects on users.

Concerning the first point, we could draw such conclusions by addressing the first research question of this thesis. In particular, the first aim was to integrate FES within a motorized robotic lower-limb exoskeleton (*Twin*, Italian Institute of Technology [77, 271]), with a particular focus on the developed control strategy.
Indeed, as already discussed in this thesis (refer to Section 1.4.1 for more details), the possibility of integrating FES within active robotic devices has gained increasing interest in recent years. Nevertheless, many times they were managed with autonomous controls, with one component acting regardless of what the other was doing. This was due to the difficulty of managing the actuation redundancy due to the presence of two power sources. Such systems take advantage of the FES-related physiological benefits but do not enable a motor torque reduction because, even if FES-induced movements effectively go in the direction of the intended activity, the motor assistance, acting independently, is not decreased.
Differently, our research was prompted by the possibility of reducing motors' power enabled by the FES integration. The novel component of our system is the definition of a cooperative control strategy in

which the motor power is decreased and the FES component is continuously adapted to compensate for this reduction. In particular, the target trajectory tracking error was used as the common control signal. In this scenario, FES primarily contributes to the movement generation by modulating the current amplitude, while the motors' assistance is intended as a corrective component that guarantees the correct task execution. This strategy was defined for controlling one joint during walking movements, namely the knee during the swing phase, in combination with the stimulation of Quadriceps and Hamstirngs.
An extensive testing procedure was carried out both on non-disabled and neurologically-impaired individuals, proving the validity of our hypothesis. In particular, thanks to the presence of FES-induced muscle torques, we could get significant motor torque reductions without observing relevant worsening in the trajectory tracking performance. In particular, the motor torque was reduced by 51.5% across non-disabled subjects and 48% across target users, with a median RMSE $<7^\circ$ for non-disabled subjects and $<8^\circ$ for target users.
This demonstration paves the way for the future realization of robotic systems that, by integrating FES, experience reduced power output demands and thus can incorporate smaller and lighter motors and batteries.
Furthermore, questionnaire reports from target users proved that the FES addition increased the overall device usability. This is justified by the fact that the active muscles' participation in the movement positively impacts the overall sensorimotor experience of users.
However, despite being higher for the case with FES, the overall usability scored low ratings. To this aim, the potential realization of less cumbersome devices could enhance also this aspect, making users more willing to employ them. A further step forward in this direction would be the development of cable-based soft exoskeletons that could render these systems effectively usable as assistive devices during everyday activities.
In the direction of enhancing the device's usability, a further alternative is represented by the usage of textile-based electrodes. Their main advantage is the possibility of being integrated into clothes or fabric components that would improve the overall system wearability, easing donning and doffing processes. This aspect constitutes the second aim of this research question and was addressed by developing a textile-based solution for delivering stimulation by integrating screen-printed electrodes (Conductive Transfers UK Ltd) into cotton strips. These were then compared to standard hydrogel electrodes in terms of electrical properties and stimulation comfort and performance over fourteen non-disabled individuals. Collected results revealed no significant differences between the two types of electrodes. Even if they were not tested on disabled subjects, this result already represents a strong confirmation of the possibility of using textile electrodes, eventually integrated into robotic systems, in place of self-adhesive hydrogel ones. In recent years we assisted to the development of various suits integrating electrodes for the delivery of different types of stimulation, such as the TeslaSuit [294], the Exopulse Mollii Suit [293] (Ottobock) and the Neural Sleeve [337] (Cionic).
Furthermore, this would support the rehabilitation shift from a clinical-based setting to a home-based one, which was noticed as a growing trend in recent years because it simplifies the handling of the therapy for patients, not requiring them to reach the clinic or the hospital to get it.
Besides the low usability, another limitation of the *TwinFES* study resides in the fact that the cooperative control was only defined at a single joint level. This was done because Quadriceps and Hamstrings are bi-articular muscles with an opposite effect on the hip and knee joints which prevents the induction of contemporary knee and hip flexion and extension during the early and late swing phases, respectively. In particular, for both muscles, the effect on the knee joint would overcome the one on the hip joint, because

hip-actuating muscles are more difficult to stimulate given their depth and the higher torques required in this case.
From these considerations, we concluded that the possibility of stimulating hip-actuating muscles does not represent a viable option also for future studies. Rather, it would be helpful to integrate locking systems, such as brakes, to support the hip extension in the stance phase. Indeed, from the tests on target users, we noticed that a non-negligible motor current and thus power was required from the motor, which was not instead observed during trials on non-disabled subjects. This is probably due to the fact that a greater effort is needed to sustain them during stance, considering their partial or complete inability to maintain standing posture.
A further future advancement could be the increase in the number of muscles integrated into the cooperative control and thus actively participating in the movement. Distal muscles (Gastrocnemius and Tibialis Anterior), here only integrated into the synchronous control and thus stimulated at amplitudes below the motor threshold, could induce plantar flexion and extension by being combined with an actuated ankle joint.

With regard to the second theme, we investigated it through the second research question of this thesis. First, we reviewed the present state of the art about SCS, its working principle and its main advantages. Despite demonstrating interesting benefits at the neuromuscular level, this stimulation still pertains to the research field. In response to it, the first aim of this research question is to propose a possible therapeutic application integrating tSCS within a rehabilitative activity. The rationale of this study originates from the consideration that, given the proven potentiality of this technology to augment volitional signals [210, 234], tSCS could provide significant advantages when combined with functional movements, particularly in the case of subjects with residual volitional abilities.
In our study we developed a cycling-based tSCS protocol by combining this stimulation with the assisted pedaling activity on a motorized trike. Four complete SCI individuals were tested and their leg EMG was acquired to verify whether any activity was induced in their muscles during the protocol execution. We noticed some interesting EMG modulation, also directed towards the reduction of spasticity in the case of users with hypertonic muscles. Moreover, some advantages and sensation recovery were reported for bowel and bladder control, which is even more significant for subjects' quality of life than a recovery of motor abilities [338]. Overall, our results tendency confirmed some literature observations even if we could not observe direct motor effects such as movement facilitation, probably because of the limited number of performed SCS sessions.
Future research should consider this (or similar) therapeutic technological platform and test its effects and benefits in the long-term scenario.
Among the main tSCS limitations, we find the impossibility of applying it on subjects with spinal metal implants, the high current amplitudes required by this stimulation and the difficulty of autonomous electrode positioning on the back. These considerations boosted the second aim within our research on afferent stimulation, which is the investigation of its peripheral approach, referred to as SAES. Very little evidence was found in the literature about its neuromodulatory effect [195] and possible applications. Nevertheless, given that it was demonstrated to affect the same spinal circuits as SCS [214], we hereby wanted to compare the two stimulation types in terms of induced reflex waves. This was done by applying both stimulation on twelve non-disabled participants: SCS at the spinal level and SAES on three peripheral nerves (femoral, sciatic and tibial). The reflex waves induced in the two cases, PRM reflex and H-wave respectively, were then compared in terms of shape, current threshold and latency. The shape

of the two reflexes were similar, while observed differences in the current threshold and latency were in line with the hypothesis that the two stimulation types are directed to different levels of the nervous system tree. This result confirms literature observations and makes it reasonable to suppose that the two strategies might provoke a similar neuromodulatory impact as well.
However, our analysis was more of a preliminary experimental verification and thus further investigations testing the therapeutic effects of this stimulation are needed. If comparable benefits of SCS and SAES are confirmed, then one could decide to use one approach or the other depending on the specific case he is dealing with and considering their specific disadvantages. With respect to SAES, the main challenge is given by the difficulty of specifically targeting sensory fibers, given that this stimulation is directed to mixed nerves in the periphery.
Future research should also move towards the combination of robotic devices with afferent stimulations. At present, little research in this field is encountered in the literature [313] but this represents an interesting point to be further explored, given the beneficial motor-facilitating effects previously discussed.
In this thesis, we attempted to combine the *Twin* robotic system with a stimulation below the motor threshold when in the synchronous approach we delivered a proprioceptive stimulation. The aim here was not to generate a movement but rather to combining the walking activity with an afferent sensory input synchronized with it. Nevertheless, we only proved its feasibility but did not test whether some central effects were specifically triggered by this stimulation. Indeed, even if the TwinFES system reported higher usability with respect to the sole exoskeleton, we cannot draw any conclusion on whether also this stimulation (in addition to FES) contributed to this result. Future studies should test it, for example by verifying whether an increase in the system usability would be registered also in the case of using the exoskeleton with the sole proprioceptive stimulation, without FES.
Besides the peripheral one, also the central afferent stimulation (SCS) could be integrated into such devices. Indeed, targeting the Central Pattern Generator [230], this stimulation may influence the generation of rhythmic movements, involved in cyclic activities such as walking or cycling. Stunning results were already reported by literature studies [339] applying the epidural SCS for walking restoration in SCI individuals. All this collected evidence makes us optimistic about the potential benefits that could be obtained when combining tSCS with robotic devices for walking or cycling. Even if not directly inducing a movement as in the epidural case (notably more selective and effective), we can expect it to facilitate the performance of functional tasks.
A further step forward would be the possibility of combining SCS and FES. In fact, such integration was not found in the literature but we think that the understanding of how these stimulations would interact in the nervous system is of particular relevance.

Bibliography

[1] World Health Organization. *Neurological disorders: public health challenges*. World Health Organization, 2006.

[2] Susan Charlifue and Kenneth Gerhart. Community integration in spinal cord injury of long duration. *NeuroRehabilitation*, 19(2):91–101, 2004.

[3] P Kennedy, P Lude, and N Taylor. Quality of life, social participation, appraisals and coping post spinal cord injury: a review of four community samples. *Spinal cord*, 44(2):95–105, 2006.

[4] Zhengrun Gao, Zhen Pang, Yiming Chen, Gaowei Lei, Shuai Zhu, Guotao Li, Yundong Shen, and Wendong Xu. Restoring after central nervous system injuries: neural mechanisms and translational applications of motor recovery. *Neuroscience Bulletin*, 38(12):1569–1587, 2022.

[5] National Institutes of Health (NIH).

[6] Frederick M Maynard, Michael B Bracken, Graham Creasey, William H Donovan, Thomas B Ducker, Susan L Garber, Ralph J Marino, Samuel L Stover, Charles H Tator, Robert L Waters, et al. International standards for neurological and functional classification of spinal cord injury. *Spinal cord*, 35(5):266–274, 1997.

[7] World Health Organization and International Spinal Cord Society. *International perspectives on spinal cord injury*. World Health Organization, 2013.

[8] James R McCammon and Karen Ethans. Spinal cord injury in manitoba: a provincial epidemiological study. *The journal of spinal cord medicine*, 34(1):6–10, 2011.

[9] Michel Wyndaele and Jean-Jacques Wyndaele. Incidence, prevalence and epidemiology of spinal cord injury: what learns a worldwide literature survey? *Spinal cord*, 44(9):523–529, 2006.

[10] American Spinal Cord Association (ASIA).

[11] RL Waters, RH Adkins, and JS Yakura. Definition of complete spinal cord injury. *Spinal Cord*, 29(9):573–581, 1991.

[12] Yuying Chen, Ying Tang, Lawrence Vogel, and Michael DeVivo. Causes of spinal cord injury. *Topics in spinal cord injury rehabilitation*, 19(1):1–8, 2013.

[13] Susan B O'Sullivan, Thomas J Schmitz, and George Fulk. *Physical rehabilitation*. FA Davis, 2019.

[14] Anthony S Burns, David A Rivas, and John F Ditunno. The management of neurogenic bladder and sexual dysfunction after spinal cord injury. *Spine*, 26(24S):S129–S136, 2001.

[15] William O McKinley, Amie B Jackson, Diana D Cardenas, and J Michael. Long-term medical complications after traumatic spinal cord injury: a regional model systems analysis. *Archives of physical medicine and rehabilitation*, 80(11):1402–1410, 1999.

[16] Melanie M Adams and Audrey L Hicks. Spasticity after spinal cord injury. *Spinal cord*, 43(10):577–586, 2005.

[17] Jonathan Myers, Matthew Lee, and Jenny Kiratli. Cardiovascular disease in spinal cord injury: an overview of prevalence, risk, evaluation, and management. *American journal of physical medicine & rehabilitation*, 86(2):142–152, 2007.

[18] Robert Brown, Anthony F DiMarco, Jeannette D Hoit, and Eric Garshick. Respiratory dysfunction and management in spinal cord injury. *Respiratory care*, 51(8):853–870, 2006.

[19] Ricardo A Battaglino, Antonio A Lazzari, Eric Garshick, and Leslie R Morse. Spinal cord injury-induced osteoporosis: pathogenesis and emerging therapies. *Current osteoporosis reports*, 10:278–285, 2012.

[20] Andreas Ludwig Reiter, Andreas Volk, Jens Vollmar, Bernd Fromm, and Hans Juergen Gerner. Changes of basic bone turnover parameters in short-term and long-term patients with spinal cord injury. *European Spine Journal*, 16:771–776, 2007.

[21] Mahdi Safdarian, Eugen Trinka, Vafa Rahimi-Movaghar, Aljoscha Thomschewski, Amirali Aali, Gdiom Gebreheat Abady, Semagn Mekonnen Abate, Foad Abd-Allah, Aidin Abedi, Denberu Eshetie Adane, et al. Global, regional, and national burden of spinal cord injury, 1990–2019: a systematic analysis for the global burden of disease study 2019. *The Lancet Neurology*, 22(11):1026–1047, 2023.

[22] Michael DeVivo, Yuying Chen, Stephen Mennemeyer, and Anne Deutsch. Costs of care following spinal cord injury. *Topics in spinal cord injury rehabilitation*, 16(4):1–9, 2011.

[23] Kim D Anderson. Targeting recovery: priorities of the spinal cord-injured population. *Journal of neurotrauma*, 21(10):1371–1383, 2004.

[24] PL Ditunno, M Patrick, M Stineman, and JF Ditunno. Who wants to walk? preferences for recovery after sci: a longitudinal and cross-sectional study. *Spinal cord*, 46(7):500–506, 2008.

[25] Catherine Donnelly, Janice J Eng, Jill Hall, Lindsay Alford, Rob Giachino, Kathy Norton, and Debbie Scott Kerr. Client-centred assessment and the identification of meaningful treatment goals for individuals with a spinal cord injury. *Spinal Cord*, 42(5):302–307, 2004.

[26] National Institutes of Health (NIH).

[27] Steven C Cramer, Gereon Nelles, Randall R Benson, Jill D Kaplan, Robert A Parker, Ken K Kwong, David N Kennedy, Seth P Finklestein, and Bruce R Rosen. A functional mri study of subjects recovered from hemiparetic stroke. *Stroke*, 28(12):2518–2527, 1997.

[28] Samar M Hatem, Geoffroy Saussez, Margaux Della Faille, Vincent Prist, Xue Zhang, Delphine Dispa, and Yannick Bleyenheuft. Rehabilitation of motor function after stroke: a multiple systematic review focused on techniques to stimulate upper extremity recovery. *Frontiers in human neuroscience*, 10:442, 2016.

[29] Valery L Feigin, Benjamin A Stark, Catherine Owens Johnson, Gregory A Roth, Catherine Bisignano, Gdiom Gebreheat Abady, Mitra Abbasifard, Mohsen Abbasi-Kangevari, Foad Abd-Allah, Vida Abedi, et al. Global, regional, and national burden of stroke and its risk factors, 1990–2019: a systematic analysis for the global burden of disease study 2019. *The Lancet Neurology*, 20(10):795–820, 2021.

[30] Catherine A Scott, Linxin Li, and Peter M Rothwell. Diverging temporal trends in stroke incidence in younger vs older people: a systematic review and meta-analysis. *JAMA neurology*, 2022.

[31] Yannick Béjot, Henri Bailly, Mathilde Graber, Lucie Garnier, Annabel Laville, Lucile Dubourget, Nathalie Mielle, Corinne Chevalier, Jérôme Durier, and Maurice Giroud. Impact of the ageing population on the burden of stroke: the dijon stroke registry. *Neuroepidemiology*, 52(1-2):78–85, 2019.

[32] Valery L Feigin, Mayowa O Owolabi, Foad Abd-Allah, Rufus O Akinyemi, Natalia V Bhattacharjee, Michael Brainin, Jackie Cao, Valeria Caso, Bronte Dalton, Alan Davis, et al. Pragmatic solutions to reduce the global burden of stroke: a world stroke organization–lancet neurology commission. *The Lancet Neurology*, 2023.

[33] Dorcas BC Gandhi, Albert Sterba, Himani Khatter, and Jeyaraj D Pandian. Mirror therapy in stroke rehabilitation: current perspectives. *Therapeutics and clinical risk management*, pages 75–85, 2020.

[34] Stefano Masiero, Patrizia Poli, Giulio Rosati, Damiano Zanotto, Marco Iosa, Sefano Paolucci, and Giovanni Morone. The value of robotic systems in stroke rehabilitation. *Expert review of medical devices*, 11(2):187–198, 2014.

[35] VM Parker, DT Wade, and R Langton Hewer. Loss of arm function after stroke: measurement, frequency, and recovery. *International rehabilitation medicine*, 8(2):69–73, 1986.

[36] Susan E Lord, Kathryn McPherson, Harry K McNaughton, Lynn Rochester, and Mark Weatherall. Community ambulation after stroke: how important and obtainable is it and what measures appear predictive? *Archives of physical medicine and rehabilitation*, 85(2):234–239, 2004.

[37] Cesar Marquez-Chin and Milos R Popovic. Functional electrical stimulation therapy for restoration of motor function after spinal cord injury and stroke: a review. *Biomedical engineering online*, 19(1):1–25, 2020.

[38] Braden Te Ao, Paul Brown, Martin Tobias, Shanthi Ameratunga, Suzanne Barker-Collo, Alice Theadom, Kathryn McPherson, Nicola Starkey, Anthony Dowell, Kelly Jones, et al. Cost of traumatic brain injury in new zealand: evidence from a population-based study. *Neurology*, 83(18):1645–1652, 2014.

[39] Keith Andrews, JC Brocklehurst, Bernard Richards, and PJ Laycock. The rate of recovery from stroke-and its measurement. *International rehabilitation medicine*, 3(3):155–161, 1981.

[40] Clive E Skilbeck, Derick T Wade, R Langton Hewer, and Victorine A Wood. Recovery after stroke. *Journal of Neurology, Neurosurgery & Psychiatry*, 46(1):5–8, 1983.

[41] Markus Butz, Florentin Wörgötter, and Arjen van Ooyen. Activity-dependent structural plasticity. *Brain research reviews*, 60(2):287–305, 2009.

[42] Nick S Ward. Neural plasticity and recovery of function. *Progress in brain research*, 150:527–535, 2005.

[43] Naohiko Okabe, Naoyuki Himi, Emi Maruyama-Nakamura, Norito Hayashi, Kazuhiko Narita, and Osamu Miyamoto. Rehabilitative skilled forelimb training enhances axonal remodeling in the corticospinal pathway but not the brainstem-spinal pathways after photothrombotic stroke in the primary motor cortex. *PLoS One*, 12(11):e0187413, 2017.

[44] Eran Dayan and Leonardo G Cohen. Neuroplasticity subserving motor skill learning. *Neuron*, 72(3):443–454, 2011.

[45] PCE De Groot, N Hjeltnes, AC Heijboer, W Stal, and K Birkeland. Effect of training intensity on physical capacity, lipid profile and insulin sensitivity in early rehabilitation of spinal cord injured individuals. *Spinal cord*, 41(12):673–679, 2003.

[46] Jocelyn E Harris, Janice J Eng, William C Miller, and Andrew S Dawson. A self-administered graded repetitive arm supplementary program (grasp) improves arm function during inpatient stroke rehabilitation: a multi-site randomized controlled trial. *Stroke*, 40(6):2123–2128, 2009.

[47] T George Hornby, Donald S Straube, Catherine R Kinnaird, Carey L Holleran, Anthony J Echauz, Kelly S Rodriguez, Eric J Wagner, and Elizabeth A Narducci. Importance of specificity, amount, and intensity of locomotor training to improve ambulatory function in patients poststroke. *Topics in stroke rehabilitation*, 18(4):293–307, 2011.

[48] Gert Kwakkel, Robert C Wagenaar, Jos WR Twisk, Gustaaf J Lankhorst, and Johan C Koetsier. Intensity of leg and arm training after primary middle-cerebral-artery stroke: a randomised trial. *The Lancet*, 354(9174):191–196, 1999.

[49] Pamela Duncan, Stephanie Studenski, Lorie Richards, Steven Gollub, Sue Min Lai, Dean Reker, Subashan Perera, Joni Yates, Victoria Koch, Sally Rigler, et al. Randomized clinical trial of therapeutic exercise in subacute stroke. *Stroke*, 34(9):2173–2180, 2003.

[50] John W Krakauer. Motor learning: its relevance to stroke recovery and neurorehabilitation. *Current opinion in neurology*, 19(1):84–90, 2006.

[51] John Whyte, Marcel P Dijkers, Tessa Hart, Jarrad H Van Stan, Andrew Packel, Lyn S Turkstra, Jeanne M Zanca, Christine Chen, and Mary Ferraro. The importance of voluntary behavior in rehabilitation treatment and outcomes. *Archives of physical medicine and rehabilitation*, 100(1):156–163, 2019.

[52] Roberto Colombo, Fabrizio Pisano, Alessandra Mazzone, Carmen Delconte, Silvestro Micera, M Chiara Carrozza, Paolo Dario, and Giuseppe Minuco. Design strategies to improve patient motivation during robot-aided rehabilitation. *Journal of neuroengineering and rehabilitation*, 4:1–12, 2007.

[53] Naoyuki Takeuchi, Shin-Ichi Izumi, et al. Maladaptive plasticity for motor recovery after stroke: mechanisms and approaches. *Neural plasticity*, 2012, 2012.

[54] Edward Taub, Neal E Miller, Thomas A Novack, Edwin W Cook, William C Fleming, Cecil S Nepomuceno, Jane S Connell, JE Crago, et al. Technique to improve chronic motor deficit after stroke. *Archives of physical medicine and rehabilitation*, 74(4):347–354, 1993.

[55] Claudia Alia, Cristina Spalletti, Stefano Lai, Alessandro Panarese, Giuseppe Lamola, Federica Bertolucci, Fabio Vallone, Angelo Di Garbo, Carmelo Chisari, Silvestro Micera, et al. Neuroplastic changes following brain ischemia and their contribution to stroke recovery: novel approaches in neurorehabilitation. *Frontiers in cellular neuroscience*, 11:76, 2017.

[56] Nicolas Schweighofer, Younggeun Choi, Carolee Winstein, and James Gordon. Task-oriented rehabilitation robotics. *American Journal of Physical Medicine & Rehabilitation*, 91(11):S270–S279, 2012.

[57] Lucille Cazenave, Martin Einenkel, Aaron Yurkewich, Satoshi Endo, Sandra Hirche, and Etienne Burdet. Hybrid robotic and electrical stimulation assistance can enhance performance and reduce mental demand. *IEEE Transactions on Neural Systems and Rehabilitation Engineering*, 2023.

[58] Peter S Lum, Charles G Burgar, Peggy C Shor, Matra Majmundar, and Machiel Van der Loos. Robot-assisted movement training compared with conventional therapy techniques for the rehabilitation of upper-limb motor function after stroke. *Archives of physical medicine and rehabilitation*, 83(7):952–959, 2002.

[59] Roger Gassert and Volker Dietz. Rehabilitation robots for the treatment of sensorimotor deficits: a neurophysiological perspective. *Journal of neuroengineering and rehabilitation*, 15(1):1–15, 2018.

[60] Stefan Hesse, Dietmar Uhlenbrock, et al. A mechanized gait trainer for restoration of gait. *Journal of rehabilitation research and development*, 37(6):701–708, 2000.

[61] Gery Colombo, Matthias Joerg, Reinhard Schreier, Volker Dietz, et al. Treadmill training of paraplegic patients using a robotic orthosis. *Journal of rehabilitation research and development*, 37(6):693–700, 2000.

[62] Tommaso Proietti, Vincent Crocher, Agnes Roby-Brami, and Nathanael Jarrasse. Upper-limb robotic exoskeletons for neurorehabilitation: a review on control strategies. *IEEE reviews in biomedical engineering*, 9:4–14, 2016.

[63] Antonio J Del-Ama, Aikaterini D Koutsou, Juan C Moreno, Ana De-Los-Reyes, Ángel Gil-Agudo, and José L Pons. Review of hybrid exoskeletons to restore gait following spinal cord injury. *Journal of Rehabilitation Research & Development*, 49(4), 2012.

[64] Francisco Anaya, Pavithra Thangavel, and Haoyong Yu. Hybrid fes–robotic gait rehabilitation technologies: a review on mechanical design, actuation, and control strategies. *International journal of intelligent robotics and applications*, 2:1–28, 2018.

[65] Carolee J Winstein and Dorsa Beroukhim Kay. Translating the science into practice: shaping rehabilitation practice to enhance recovery after brain damage. *Progress in brain research*, 218:331–360, 2015.

[66] Giorgio Carpino, Alessandra Pezzola, Michele Urbano, and Eugenio Guglielmelli. Assessing effectiveness and costs in robot-mediated lower limbs rehabilitation: a meta-analysis and state of the art. *Journal of healthcare engineering*, 2018, 2018.

[67] Kenneth Lo, Matthew Stephenson, and Craig Lockwood. The economic cost of robotic rehabilitation for adult stroke patients: a systematic review. *JBI Evidence Synthesis*, 17(4):520–547, 2019.

[68] Andreas Mayr, Ellen Quirbach, Alessandro Picelli, Markus Kofler, Nicola Smania, and Leopold Saltuari. Early robot-assisted gait retraining in non-ambulatory patients with stroke: a single blind randomized controlled trial. *European journal of physical and rehabilitation medicine*, 54(6):819–826, 2018.

[69] Joseph Hidler, Diane Nichols, Marlena Pelliccio, Kathy Brady, Donielle D Campbell, Jennifer H Kahn, and T George Hornby. Multicenter randomized clinical trial evaluating the effectiveness of the lokomat in subacute stroke. *Neurorehabilitation and neural repair*, 23(1):5–13, 2009.

[70] Gert Kwakkel, Boudewijn J Kollen, and Hermano I Krebs. Effects of robot-assisted therapy on upper limb recovery after stroke: a systematic review. *Neurorehabilitation and neural repair*, 22(2):111–121, 2008.

[71] Mohd Khairul Anwar Kamdi, Mohd Nazri Shafei, Kamarul Imran Musa, Muhammad Hafiz Hanafi, Mohd Azmi Suliman, and Mohd Azmi Bin Suliman. Comparison of the modified barthel index (mbi) score trends among workers with stroke receiving robotic and conventional rehabilitation therapy. *Cureus*, 15(1), 2023.

[72] Laura Marchal-Crespo and David J Reinkensmeyer. Review of control strategies for robotic movement training after neurologic injury. *Journal of neuroengineering and rehabilitation*, 6(1):1–15, 2009.

[73] Luciano Bissolotti, Federico Nicoli, and Mario Picozzi. Domestic use of the exoskeleton for gait training in patients with spinal cord injuries: Ethical dilemmas in clinical practice. *Frontiers in neuroscience*, 12:78, 2018.

[74] Wandercraft. Atalante x - hands-free walk exoskeleton. Last accessed 20 January 2024.

[75] eksoBionics. eksobionics - the leader in exoskeleton technology. Last accessed 20 January 2024.

[76] Cyberdyne. Cyberdyne - pioneering the future with cybernics. Last accessed 20 January 2024.

[77] Christian Vassallo, Samuele De Giuseppe, Chiara Piezzo, Stefano Maludrottu, Giulio Cerruti, Maria Laura D'Angelo, Emanuele Gruppioni, Claudia Marchese, Simona Castellano, Eleonora Guanziroli, et al. Gait patterns generation based on basis functions interpolation for the twin lower-limb exoskeleton. In *2020 IEEE International Conference on Robotics and Automation (ICRA)*, pages 1778–1784. IEEE, 2020.

[78] Parker. Indego exoskeleton by parker. Last accessed 20 January 2024.

[79] ReWalk. Rewalk - more than walking. Last accessed 20 January 2024.

[80] Rex Bionics. Rex bionics - reimagining rehabilitation. Last accessed 20 January 2024.

[81] ExoAtlet. Exoatlet - wearable medical and industrial exoskeleton. Last accessed 20 January 2024.

[82] Fourier Intelligence. Fourier intelligence - empowering you. Last accessed 20 January 2024.

[83] FREE Bionics. Free bionics. Last accessed 20 January 2024.

[84] Roki Robotics. Roki robotics. Last accessed 20 January 2024.

[85] Nancy E Mayo, Sharon Wood-Dauphinee, Robert Côté, Liam Durcan, and Joseph Carlton. Activity, participation, and quality of life 6 months poststroke. *Archives of physical medicine and rehabilitation*, 83(8):1035–1042, 2002.

[86] Peter J Grahn, Igor A Lavrov, Dimitry G Sayenko, Meegan G Van Straaten, Megan L Gill, Jeffrey A Strommen, Jonathan S Calvert, Dina I Drubach, Lisa A Beck, Margaux B Linde, et al. Enabling task-specific volitional motor functions via spinal cord neuromodulation in a human with paraplegia. In *Mayo Clinic Proceedings*, volume 92, pages 544–554. Elsevier, 2017.

[87] David N Rushton. Functional electrical stimulation and rehabilitation—an hypothesis. *Medical engineering & physics*, 25(1):75–78, 2003.

[88] Brian A Karamian, Nicholas Siegel, Blake Nourie, Mijail D Serruya, Robert F Heary, James S Harrop, and Alexander R Vaccaro. The role of electrical stimulation for rehabilitation and regeneration after spinal cord injury. *Journal of Orthopaedics and Traumatology*, 23(1):2, 2022.

[89] Lynne R Sheffler and John Chae. Neuromuscular electrical stimulation in neurorehabilitation. *Muscle & Nerve: Official Journal of the American Association of Electrodiagnostic Medicine*, 35(5):562–590, 2007.

[90] Thomas Schick. Introduction and history of functional electrical stimulation history of functional electrical stimulation. In *Functional Electrical Stimulation in Neurorehabilitation: Synergy Effects of Technology and Therapy*, pages 1–8. Springer, 2022.

[91] Barbara M Doucet, Amy Lam, and Lisa Griffin. Neuromuscular electrical stimulation for skeletal muscle function. *The Yale journal of biology and medicine*, 85(2):201, 2012.

[92] MOE JH. Functional electrical stimulation for ambulation in hemiplegia. *The Journal-lancet*, 82:285–288, 1962.

[93] Milos R Popovic, Kei Masani, and Silvestro Micera. Functional electrical stimulation therapy: recovery of function following spinal cord injury and stroke. *Neurorehabilitation Technology*, pages 513–532, 2016.

[94] T Adam Thrasher and Milos R Popovic. Functional electrical stimulation of walking: function, exercise and rehabilitation. In *Annales de réadaptation et de médecine physique*, volume 51, pages 452–460. Elsevier, 2008.

[95] Trisha M Kesar, Ramu Perumal, Angela Jancosko, Darcy S Reisman, Katherine S Rudolph, Jill S Higginson, and Stuart A Binder-Macleod. Novel patterns of functional electrical stimulation have an immediate effect on dorsiflexor muscle function during gait for people poststroke. *Physical therapy*, 90(1):55–66, 2010.

[96] Liberson Wt. Functional electrotherapy: stimulation of the peroneal nerve synchronized with the swing phase of the gait of hemiplegic patients. *Arch Phys Med Rehabil*, 42:101, 1961.

[97] S Golaszewski and V Frey. Neuromodulation in der neurorehabilitation nach schlaganfall. *Jatros Neurol Psychiartrie*, 3:12–8, 2019.

[98] Monica Christova, Dietmar Rafolt, Stefan Golaszewski, Raffaele Nardone, and Eugen Gallasch. Electrical stimulation during skill training with a therapeutic glove enhances the induction of

cortical plasticity and has a positive effect on motor memory. *Behavioural brain research*, 270:171–178, 2014.

[99] Winfried Mayr, Matthias Krenn, and Milan R Dimitrijevic. Epidural and transcutaneous spinal electrical stimulation for restoration of movement after incomplete and complete spinal cord injury. *Current opinion in neurology*, 29(6):721–726, 2016.

[100] P Hunter Peckham and Jayme S Knutson. Functional electrical stimulation for neuromuscular applications. *Annu. Rev. Biomed. Eng.*, 7:327–360, 2005.

[101] Giorgio Sandrini, Volker Homberg, Leopold Saltuari, Nicola Smania, Alessandra Pedrocchi, et al. *Advanced technologies for the rehabilitation of gait and balance disorders*, volume 19. Springer, 2018.

[102] J Mortimer. Handbook of physiology-the nervous system ii eds jm brookshart & vb mountcastle. *American Physiology Society*, 1981.

[103] Joachim H Nagel. The biomedical engineering handbook, 2000.

[104] Yocheved Laufer, Julie Deanne Ries, Peter M Leininger, and Gad Alon. Quadriceps femoris muscle torques and fatigue generated by neuromuscular electrical stimulation with three different waveforms. *Physical therapy*, 81(7):1307–1316, 2001.

[105] F Brunetti, A Garay, JC Moreno, and Jose L Pons. Enhancing functional electrical stimulation for emerging rehabilitation robotics in the framework of hyper project. In *2011 IEEE International Conference on Rehabilitation Robotics*, pages 1–6. IEEE, 2011.

[106] LUCINDA L BAKER, BRUCE R BOWMAN, and DONALD R MCNEAL. Effects of waveform on comfort during neuromuscular electrical stimulation. *Clinical Orthopaedics and Related Research (1976-2007)*, 233:75–85, 1988.

[107] Joke R de Kroon, Maarten J IJzerman, John Chae, Gustaaf J Lankhorst, and Gerrit Zilvold. Relation between stimulation characteristics and clinical outcome in studies using electrical stimulation to improve motor control of the upper extremity in stroke. *Journal of Rehabilitation Medicine*, 37(2):65–74, 2005.

[108] Kathleen A Sluka and Deirdre Walsh. Transcutaneous electrical nerve stimulation: basic science mechanisms and clinical effectiveness. *The Journal of pain*, 4(3):109–121, 2003.

[109] Elwood Henneman. Relation between size of neurons and their susceptibility to discharge. *Science*, 126(3287):1345–1347, 1957.

[110] Elisabetta Peri, Eleonora Guanziroli, Simona Ferrante, Alessandra Pedrocchi, and Franco Molteni. Functional electrical stimulation and its use during cycling for the rehabilitation of individuals with stroke. *Advanced Technologies for the Rehabilitation of Gait and Balance Disorders*, pages 293–306, 2018.

[111] Warren M Grill and J Thomas Mortimer. Stimulus waveforms for selective neural stimulation. *IEEE Engineering in Medicine and Biology Magazine*, 14(4):375–385, 1995.

[112] John L Parker, Nastaran H Shariati, and Dean M Karantonis. Electrically evoked compound action potential recording in peripheral nerves. *Bioelectronics in medicine*, 1(1):71–83, 2018.

[113] Cheryl L Lynch and Milos R Popovic. Functional electrical stimulation. *IEEE control systems magazine*, 28(2):40–50, 2008.

[114] GREGORY R Adams, ROBERT T Harris, Daniel Woodard, and GARY A Dudley. Mapping of electrical muscle stimulation using mri. *Journal of applied physiology*, 74(2):532–537, 1993.

[115] Ashraf S Gorgey, Christopher D Black, Christopher P Elder, and Gary A Dudley. Effects of electrical stimulation parameters on fatigue in skeletal muscle. *journal of orthopaedic & sports physical therapy*, 39(9):684–692, 2009.

[116] Stuart A Binder-Macleod and Lynn Snyder-Mackler. Muscle fatigue: clinical implications for fatigue assessment and neuromuscular electrical stimulation. *Physical therapy*, 73(12):902–910, 1993.

[117] C Scott Bickel, Chris M Gregory, and Jesse C Dean. Motor unit recruitment during neuromuscular electrical stimulation: a critical appraisal. *European journal of applied physiology*, 111:2399–2407, 2011.

[118] Dario Farina, Andrea Blanchietti, Marco Pozzo, and Roberto Merletti. M-wave properties during progressive motor unit activation by transcutaneous stimulation. *Journal of Applied Physiology*, 97(2):545–555, 2004.

[119] Marco Knaflitz, Roberto Merletti, and CARLO J De Luca. Inference of motor unit recruitment order in voluntary and electrically elicited contractions. *Journal of Applied Physiology*, 68(4):1657–1667, 1990.

[120] CW Caldwell and JB Reswick. A percutaneous wire electrode for chronic research use. *IEEE Transactions on Biomedical Engineering*, (5):429–432, 1975.

[121] Aikaterini D Koutsou, Juan C Moreno, Antonio J Del Ama, Eduardo Rocon, and José L Pons. Advances in selective activation of muscles for non-invasive motor neuroprostheses. *Journal of neuroengineering and rehabilitation*, 13(1):1–12, 2016.

[122] Luisa Euler, Li Guo, and Nils-Krister Persson. A review of textile-based electrodes developed for electrostimulation. *Textile Research Journal*, 92(7-8):1300–1320, 2022.

[123] Hui Zhou, Yi Lu, Wanzhen Chen, Zhen Wu, Haiqing Zou, Ludovic Krundel, and Guanglin Li. Stimulating the comfort of textile electrodes in wearable neuromuscular electrical stimulation. *Sensors*, 15(7):17241–17257, 2015.

[124] Antonela Curteza, Viorica Cretu, Laura Macovei, and Marian Poboroniuc. The manufacturing of textile products with incorporated electrodes. *Autex Research Journal*, 16(1):13–18, 2016.

[125] Alberto Botter, Gianmosè Oprandi, Fabio Lanfranco, Stefano Allasia, Nicola A Maffiuletti, and Marco Alessandro Minetto. Atlas of the muscle motor points for the lower limb: implications for electrical stimulation procedures and electrode positioning. *European journal of applied physiology*, 111:2461–2471, 2011.

[126] Winfried Mayr. Role of electrical parameters electrical parameters in functional electrical stimulation. In *Functional Electrical Stimulation in Neurorehabilitation: Synergy Effects of Technology and Therapy*, pages 29–41. Springer, 2022.

[127] Ines Bersch. Upper and lower motoneuron lesions in tetraplegia-diagnostic and therapeutic implications of electrical stimulation. 2019.

[128] Jan Faust and Carsten Kroker. Functional electrical stimulation in dysphagia treatment. In *Functional Electrical Stimulation in Neurorehabilitation: Synergy Effects of Technology and Therapy*, pages 167–182. Springer, 2022.

[129] Jaakko Malmivuo and Robert Plonsey. *Bioelectromagnetism: principles and applications of bioelectric and biomagnetic fields*. Oxford University Press, USA, 1995.

[130] AJ Bergquist, JM Clair, O Lagerquist, CS Mang, Y Okuma, and DF Collins. Neuromuscular electrical stimulation: implications of the electrically evoked sensory volley. *European journal of applied physiology*, 111:2409–2426, 2011.

[131] Olle Lagerquist and David F Collins. Influence of stimulus pulse width on m-waves, h-reflexes, and torque during tetanic low-intensity neuromuscular stimulation. *Muscle & nerve*, 42(6):886–893, 2010.

[132] Satoru Kai and Koji Nakabayashi. Evoked emg makes measurement of muscle tone possible by analysis of the h/m ratio. *Electrodiagnosis in New Frontiers of Clinical Research*, 2013:195–212, 2013.

[133] Gerald L Gottlieb and Gyan C Agarwal. Extinction of the hoffman reflex by antidromic conduction. *Electroencephalography and Clinical Neurophysiology*, 41(1):19–24, 1976.

[134] Emmanuel Pierrot-Deseilligny and Dominique Mazevet. The monosynaptic reflex: a tool to investigate motor control in humans. interest and limits. *Neurophysiologie Clinique/Clinical Neurophysiology*, 30(2):67–80, 2000.

[135] Warren M Grill and J Thomas Mortimer. The effect of stimulus pulse duration on selectivity of neural stimulation. *IEEE Transactions on Biomedical Engineering*, 43(2):161–166, 1996.

[136] Matthew C Kiernan, Ilona Mogyoros, and David Burke. Differences in the recovery of excitability in sensory and motor axons of human median nerve. *Brain*, 119(4):1099–1105, 1996.

[137] Ilona Mogyoros, Matthew C Kiernan, and David Burke. Strength-duration properties of human peripheral nerve. *Brain*, 119(2):439–447, 1996.

[138] Marcela Panizza, Jan Nilsson, Bradley J Roth, Peter J Basser, and Mark Hallett. Relevance of stimulus duration for activation of motor and sensory fibers: implications for the study of h-reflexes and magnetic stimulation. *Electroencephalography and Clinical Neurophysiology/Evoked Potentials Section*, 85(1):22–29, 1992.

[139] Hans Hultborn, M Illert, J Nielsen, A Paul, M Ballegaard, and H Wiese. On the mechanism of the post-activation depression of the h-reflex in human subjects. *Experimental brain research*, 108:450–462, 1996.

[140] Armin Blickenstorfer, Raimund Kleiser, Thierry Keller, Birgit Keisker, Martin Meyer, Robert Riener, and Spyros Kollias. Cortical and subcortical correlates of functional electrical stimulation of wrist extensor and flexor muscles revealed by fmri. *Human brain mapping*, 30(3):963–975, 2009.

[141] Elliot S Krames, P Hunter Peckham, Ali Rezai, and Farag Aboelsaad. What is neuromodulation? In *Neuromodulation*, pages 3–8. Elsevier, 2009.

[142] Jennifer A Iddings, Anastasia Zarkou, and Edelle C Field-Fote. Non-invasive neuromodulation and rehabilitation to promote functional restoration in persons with spinal cord injury. *Current opinion in neurology*, 34(6):812, 2021.

[143] D Hebb. The organization of behavior, 1949.

[144] Shiyu Luo, Haonan Xu, Yi Zuo, Xiaogang Liu, and Angelo H All. A review of functional electrical stimulation treatment in spinal cord injury. *Neuromolecular medicine*, 22:447–463, 2020.

[145] Samar Hamid and Ray Hayek. Role of electrical stimulation for rehabilitation and regeneration after spinal cord injury: an overview. *European Spine Journal*, 17:1256–1269, 2008.

[146] Mary K Nagai, Cesar Marquez-Chin, and Milos R Popovic. Why is functional electrical stimulation therapy capable of restoring motor function following severe injury to the central nervous system? *Translational neuroscience: fundamental approaches for neurological disorders*, pages 479–498, 2016.

[147] Dries M Hettinga and Brian J Andrews. Oxygen consumption during functional electrical stimulation-assisted exercise in persons with spinal cord injury: implications for fitness and health. *Sports medicine*, 38:825–838, 2008.

[148] Glen M Davis, Nur A Hamzaid, and Ché Fornusek. Cardiorespiratory, metabolic, and biomechanical responses during functional electrical stimulation leg exercise: health and fitness benefits. *Artificial organs*, 32(8):625–629, 2008.

[149] Pamela E Houghton, Karen E Campbell, Christine H Fraser, Connie Harris, David H Keast, Patrick J Potter, Keith C Hayes, and M Gail Woodbury. Electrical stimulation therapy increases rate of healing of pressure ulcers in community-dwelling people with spinal cord injury. *Archives of physical medicine and rehabilitation*, 91(5):669–678, 2010.

[150] Graham H Creasey and Michael D Craggs. Functional electrical stimulation for bladder, bowel, and sexual function. *Handbook of clinical neurology*, 109:247–257, 2012.

[151] Bruce H Dobkin and Andrew Dorsch. New evidence for therapies in stroke rehabilitation. *Current atherosclerosis reports*, 15:1–9, 2013.

[152] Marta Gandolla, Lorenzo Niero, Franco Molteni, Elenora Guanziroli, Nick S Ward, and Alessandra Pedrocchi. Brain plasticity mechanisms underlying motor control reorganization: pilot longitudinal study on post-stroke subjects. *Brain Sciences*, 11(3):329, 2021.

[153] Gergely I Barsi, Dejan B Popovic, Ina M Tarkka, Thomas Sinkjær, and Michael J Grey. Cortical excitability changes following grasping exercise augmented with electrical stimulation. *Experimental brain research*, 191:57–66, 2008.

[154] Simona Denisia Iftime-Nielsen, Mark Schram Christensen, Rune Jersin Vingborg, Thomas Sinkjær, Andreas Roepstorff, and Michael James Grey. Interaction of electrical stimulation and voluntary hand movement in sii and the cerebellum during simulated therapeutic functional electrical stimulation in healthy adults. *Human Brain Mapping*, 33(1):40–49, 2012.

[155] MC Ridding, B Brouwer, TS Miles, JB Pitcher, and PD Thompson. Changes in muscle responses to stimulation of the motor cortex induced by peripheral nerve stimulation in human subjects. *Experimental brain research*, 131:135–143, 2000.

[156] Patricia Meier. Plasticity plasticity and motor learning motor learning. In *Functional Electrical Stimulation in Neurorehabilitation: Synergy Effects of Technology and Therapy*, pages 9–18. Springer, 2022.

[157] Michael E Knash, Aiko Kido, Monica Gorassini, K Ming Chan, and Richard B Stein. Electrical stimulation of the human common peroneal nerve elicits lasting facilitation of cortical motor-evoked potentials. *Experimental brain research*, 153:366–377, 2003.

[158] Marta Gandolla, Simona Ferrante, Franco Molteni, Eleonora Guanziroli, Tiziano Frattini, Alberto Martegani, Giancarlo Ferrigno, Karl Friston, Alessandra Pedrocchi, and Nick S Ward. Re-thinking the role of motor cortex: context-sensitive motor outputs? *Neuroimage*, 91:366–374, 2014.

[159] TJ Sejnowski and GJ Tesauro. The hebb rule for synaptic plasticity: implementations and applications. *Neural Models of Plasticity*, pages 94–103, 1989.

[160] Marta Gandolla, Nick S Ward, Franco Molteni, Eleonora Guanziroli, Giancarlo Ferrigno, Alessandra Pedrocchi, et al. The neural correlates of long-term carryover following functional electrical stimulation for stroke. *Neural Plasticity*, 2016, 2016.

[161] Clarissa L Martin, Beverley A Phillips, TJ Kilpatrick, Helmut Butzkueven, Niall Tubridy, Elizabeth McDonald, and MP Galea. Gait and balance impairment in early multiple sclerosis in the absence of clinical disability. *Multiple Sclerosis Journal*, 12(5):620–628, 2006.

[162] Jayme S Knutson, Nathaniel S Makowski, Kevin L Kilgore, and John Chae. Neuromuscular electrical stimulation applications. In *Atlas of Orthoses and Assistive Devices*, pages 432–439. Elsevier, 2019.

[163] Tamsyn Street, Ian D Swain, and Paul Taylor. Training and orthotic effects related to functional electrical stimulation of the peroneal nerve in stroke. *Journal of Rehabilitation Medicine*, 49(2):113–119, 2017.

[164] Dirk G Everaert, Aiko K Thompson, Su Ling Chong, and Richard B Stein. Does functional electrical stimulation for foot drop strengthen corticospinal connections? *Neurorehabilitation and neural repair*, 24(2):168–177, 2010.

[165] Yocheved Laufer, Haim Ring, Elliot Sprecher, and Jeffrey M Hausdorff. Gait in individuals with chronic hemiparesis: one-year follow-up of the effects of a neuroprosthesis that ameliorates foot drop. *Journal of Neurologic Physical Therapy*, 33(2):104–110, 2009.

[166] Kevin L Kilgore, Robert F Kirsch, and P Hunter Peckham. Skeletal motor neuroprostheses. In *Neuroprosthetics: Theory and Practice*, pages 491–536. World Scientific, 2017.

[167] Richard B Stein, P Hunter Peckham, and Dejan Popović. Neural prostheses: replacing motor function after disease or disability. *(No Title)*, 1992.

[168] Maarten Joost IJzerman, TS Stoffers, FACG In'T Groen, MAP Klatte, GJ Snoek, JHC Vorsteveld, RH Nathan, and HJ Hermens. The ness handmaster orthosis: restoration of hand function in c5 and

stroke patients by means of electrical stimulation. *Journal of rehabilitation sciences*, 9(3):86–89, 1996.

[169] Arthur Prochazka, Michel Gauthier, Marguerite Wieler, and Zoltan Kenwell. The bionic glove: an electrical stimulator garment that provides controlled grasp and hand opening in quadriplegia. *Archives of physical medicine and rehabilitation*, 78(6):608–614, 1997.

[170] Brian Smith, Zhengnian Tang, Mark W Johnson, Soheyl Pourmehdi, Martha M Gazdik, James R Buckett, and P Hunter Peckham. An externally powered, multichannel, implantable stimulator-telemeter for control of paralyzed muscle. *IEEE Transactions on Biomedical Engineering*, 45(4):463–475, 1998.

[171] Milos R Popovic and Thierry Keller. Modular transcutaneous functional electrical stimulation system. *Medical engineering & physics*, 27(1):81–92, 2005.

[172] Deborah A Hebert, James M Bowen, Cindy Ho, Irene Antunes, Daria J O'Reilly, and Mark Bayley. Examining a new functional electrical stimulation therapy with people with severe upper extremity hemiparesis and chronic stroke: a feasibility study. *British journal of occupational therapy*, 80(11):651–659, 2017.

[173] Ronald J Triolo, Carol Bieri, James Uhlir, Rudi Kobetic, Avram Scheiner, and E Byron Marsolais. Implanted functional neuromuscular stimulation systems for individuals with cervical spinal cord injuries: clinical case reports. *Archives of physical medicine and rehabilitation*, 77(11):1119–1128, 1996.

[174] Paul N Taylor, Jane H Burridge, Anna L Dunkerley, Duncan E Wood, Jonathan A Norton, Christine Singleton, and Ian D Swain. Clinical use of the odstock dropped foot stimulator: its effect on the speed and effort of walking. *Archives of physical medicine and rehabilitation*, 80(12):1577–1583, 1999.

[175] Thor Petersen and Benny Klemar. Electrical stimulation as a treatment of lower limb spasticity. *Journal of Neurologic Rehabilitation*, 2(3):103–108, 1988.

[176] Laurence Kenney, Gerrit Bultstra, Rik Buschman, Paul Taylor, Geraldine Mann, Hermie Hermens, Jan Holsheimer, Anand Nene, Martin Tenniglo, Hans Van der Aa, et al. An implantable two channel drop foot stimulator: initial clinical results. *Artificial organs*, 26(3):267–270, 2002.

[177] Jane Burridge, Morten Haugland, Birgit Tine Larsen, Ruth M Pickering, Niels Svaneborg, Helle K Iversen, P Brøgger Christensen, Jens Haase, Jannick Brennum, and Thomas Sinkjaer. Phase ii trial to evaluate the actigait implanted drop-foot stimulator in established hemiplegia. *Journal of rehabilitation medicine*, 39(3):212–218, 2007.

[178] TA Thrasher, HM Flett, and MR Popovic. Gait training regimen for incomplete spinal cord injury using functional electrical stimulation. *Spinal Cord*, 44(6):357–361, 2006.

[179] Daniel Graupe and Kate H Kohn. Functional neuromuscular stimulator for short-distance ambulation by certain thoracic-level spinal-cord-injured paraplegics. *Surgical Neurology*, 50(3):202–207, 1998.

[180] BJ Andrews, RH Baxendale, R Barnett, GF Phillips, T Yamazaki, JP Paul, and PA Freeman.

Hybrid fes orthosis incorporating closed loop control and sensory feedback. *Journal of biomedical engineering*, 10(2):189–195, 1988.

[181] Kurage. Kurage - brings back mobility to those who lost it. Last accessed 20 February 2024.

[182] Dejan Popovic, Rajko Tomovic, and Laszlo Schwirtlich. Hybrid assistive system-the motor neuroprosthesis. *IEEE Transactions on Biomedical Engineering*, 36(7):729–737, 1989.

[183] L Vodovnik, A Kralj, U Stank, R Acimovic, and N Gros. Recent applications of functional electrical stimulation to stroke patients in ljubljana. *Clinical Orthopaedics and Related Research®*, (131):64–70, 1978.

[184] R Merletti, F Zelaschi, D Latella, M Galli, S_ Angeli, and M Bellucci Sessa. A control study of muscle force recovery in hemiparetic patients during treatment with functional electrical stimulation. *Scandinavian journal of rehabilitation medicine*, 10(3):147–154, 1978.

[185] Tadej Bajd, Alojz Kralj, Martin Štefančič, and Nada Lavrač. Use of functional electrical stimulation in the lower extremities of incomplete spinal cord injured patients. *Artificial Organs*, 23(5):403–409, 1999.

[186] Dejan Popović, Aleksandar Stojanović, Andjelka Pjanović, Slobodanka Radosavljević, Mirjana Popović, Stevan Jović, and Dragan Vulović. Clinical evaluation of the bionic glove. *Archives of physical medicine and rehabilitation*, 80(3):299–304, 1999.

[187] Milos R Popovic, Naaz Kapadia, Vera Zivanovic, Julio C Furlan, B Cathy Craven, and Colleen McGillivray. Functional electrical stimulation therapy of voluntary grasping versus only conventional rehabilitation for patients with subacute incomplete tetraplegia: a randomized clinical trial. *Neurorehabilitation and neural repair*, 25(5):433–442, 2011.

[188] Naaz Kapadia, Vera Zivanovic, and Milos Popovic. Restoring voluntary grasping function in individuals with incomplete chronic spinal cord injury: pilot study. *Topics in spinal cord injury rehabilitation*, 19(4):279–287, 2013.

[189] Naji Alibeji, Nicholas Kirsch, and Nitin Sharma. An adaptive low-dimensional control to compensate for actuator redundancy and fes-induced muscle fatigue in a hybrid neuroprosthesis. *Control Engineering Practice*, 59:204–219, 2017.

[190] HJ Chizek, Rudi Kobetic, EB Marsolais, James J Abbas, Irah H Donner, and EASE Simon. Control of functional neuromuscular stimulation systems for standing and locomotion in paraplegics. *Proceedings of the IEEE*, 76(9):1155–1165, 1988.

[191] Patrick E Crago, P Hunter Peckham, and Geoffrey B Thrope. Modulation of muscle force by recruitment during intramuscular stimulation. *IEEE Transactions on Biomedical Engineering*, (12):679–684, 1980.

[192] Joanne Riess and James J Abbas. Adaptive control of cyclic movements as muscles fatigue using functional neuromuscular stimulation. *IEEE Transactions on neural systems and rehabilitation engineering*, 9(3):326–330, 2001.

[193] Nathan Dunkelberger, Jeffrey Berning, Eric M Schearer, and Marcia K O'Malley. Hybrid fes-

exoskeleton control: Using mpc to distribute actuation for elbow and wrist movements. *Frontiers in Neurorobotics*, 17:1127783, 2023.

[194] Kerstin Schwenker and Stefan M Golaszewski. Sensory afferent stimulation. In *Functional Electrical Stimulation in Neurorehabilitation: Synergy Effects of Technology and Therapy*, pages 139–150. Springer, 2022.

[195] SM Golaszewski, CM Siedentopf, F Koppelstaetter, P Rhomberg, GM Guendisch, A Schlager, E Gallasch, W Eisner, SR Felber, and FM Mottaghy. Modulatory effects on human sensorimotor cortex by whole-hand afferent electrical stimulation. *Neurology*, 62(12):2262–2269, 2004.

[196] Stefan M Golaszewski, Jürgen Bergmann, Monica Christova, Raffaele Nardone, Martin Kronbichler, Dietmar Rafolt, Eugen Gallasch, Wolfgang Staffen, Gunther Ladurner, and Roland Beisteiner. Increased motor cortical excitability after whole-hand electrical stimulation: a tms study. *Clinical Neurophysiology*, 121(2):248–254, 2010.

[197] Lucinda S Chipchase, Siobhan M Schabrun, and Paul W Hodges. Peripheral electrical stimulation to induce cortical plasticity: a systematic review of stimulus parameters. *Clinical Neurophysiology*, 122(3):456–463, 2011.

[198] C Shona Charlton, Michael C Ridding, Philip D Thompson, and Timothy S Miles. Prolonged peripheral nerve stimulation induces persistent changes in excitability of human motor cortex. *Journal of the neurological sciences*, 208(1-2):79–85, 2003.

[199] SH Peurala, K Pitkänen, J Sivenius, and IM Tarkka. Cutaneous electrical stimulation may enhance sensorimotor recovery in chronic stroke. *Clinical rehabilitation*, 16(7):709–716, 2002.

[200] Sharareh Sharififar, Jonathan J Shuster, and Mark D Bishop. Adding electrical stimulation during standard rehabilitation after stroke to improve motor function. a systematic review and meta-analysis. *Annals of physical and rehabilitation medicine*, 61(5):339–344, 2018.

[201] Aija Marie Ladda, Joerg Peter Pfannmoeller, Tobias Kalisch, Sybille Roschka, Thomas Platz, Hubert R Dinse, and Martin Lotze. Effects of combining 2 weeks of passive sensory stimulation with active hand motor training in healthy adults. *PloS one*, 9(1):e84402, 2014.

[202] Adriana Bastos Conforto, Karina Nocelo Ferreiro, Camilla Tomasi, Renata Laurenti dos Santos, Viviane Loureiro Moreira, Suely Kazue Nagahashi Marie, Silvia Cristina Baltieri, Milberto Scaff, and Leonardo G Cohen. Effects of somatosensory stimulation on motor function after subacute stroke. *Neurorehabilitation and neural repair*, 24(3):263–272, 2010.

[203] Meta M Dimitrijevic, Dobrivoje S Stokié, Artur W Wawro, and Chuan-Chuan C Wun. Modification of motor control of wrist extension by mesh-glove electrical afferent stimulation in stroke patients. *Archives of physical medicine and rehabilitation*, 77(3):252–258, 1996.

[204] Georg Kerkhoff. Modulation and rehabilitation of spatial neglect by sensory stimulation. *Progress in brain research*, 142:257–271, 2003.

[205] Volker Dietz and Karim Fouad. Restoration of sensorimotor functions after spinal cord injury. *Brain*, 137(3):654–667, 2014.

[206] Karen Minassian, W Barry McKay, Heinrich Binder, and Ursula S Hofstoetter. Targeting lumbar

spinal neural circuitry by epidural stimulation to restore motor function after spinal cord injury. *Neurotherapeutics*, 13:284–294, 2016.

[207] MR Dimitrijević. Residual motor functions in spinal cord injury. *Advances in neurology*, 47:138–155, 1988.

[208] BA Kakulas. The applied neuropathology of human spinal cord injury. *Spinal cord*, 37(2):79–88, 1999.

[209] Marc P Powell, Nikhil Verma, Erynn Sorensen, Erick Carranza, Amy Boos, Daryl P Fields, Souvik Roy, Scott Ensel, Beatrice Barra, Jeffrey Balzer, et al. Epidural stimulation of the cervical spinal cord for post-stroke upper-limb paresis. *Nature medicine*, 29(3):689–699, 2023.

[210] Claudia A Angeli, V Reggie Edgerton, Yury P Gerasimenko, and Susan J Harkema. Altering spinal cord excitability enables voluntary movements after chronic complete paralysis in humans. *Brain*, 137(5):1394–1409, 2014.

[211] Lynsey D Duffell and Nicholas de Neufvillle Donaldson. A comparison of fes and scs for neuroplastic recovery after sci: Historical perspectives and future directions. *Frontiers in neurology*, 11:607, 2020.

[212] Fabien B Wagner, Jean-Baptiste Mignardot, Camille G Le Goff-Mignardot, Robin Demesmaeker, Salif Komi, Marco Capogrosso, Andreas Rowald, Ismael Seáñez, Miroslav Caban, Elvira Pirondini, et al. Targeted neurotechnology restores walking in humans with spinal cord injury. *Nature*, 563(7729):65–71, 2018.

[213] Karen Minassian, Brigitta Freundl, and Ursula S Hofstoetter. The posterior root-muscle reflex. In *Neurophysiology in Neurosurgery*, pages 239–253. Elsevier, 2020.

[214] Karen Minassian, Ilse Persy, Frank Rattay, Milan R Dimitrijevic, Christian Hofer, and Helmut Kern. Posterior root–muscle reflexes elicited by transcutaneous stimulation of the human lumbosacral cord. *Muscle & Nerve: Official Journal of the American Association of Electrodiagnostic Medicine*, 35(3):327–336, 2007.

[215] Ursula S Hofstoetter, Karen Minassian, Christian Hofer, Winfried Mayr, Frank Rattay, and Milan R Dimitrijevic. Modification of reflex responses to lumbar posterior root stimulation by motor tasks in healthy subjects. *Artificial Organs*, 32(8):644–648, 2008.

[216] Karen Minassian, Bernhard Jilge, Frank Rattay, MM Pinter, H Binder, Franz Gerstenbrand, and Milan R Dimitrijevic. Stepping-like movements in humans with complete spinal cord injury induced by epidural stimulation of the lumbar cord: electromyographic study of compound muscle action potentials. *Spinal cord*, 42(7):401–416, 2004.

[217] Giuliano Taccola, Sean Barber, Phillip J Horner, Humberto A Cerrel Bazo, and Dimitry Sayenko. Complications of epidural spinal stimulation: lessons from the past and alternatives for the future. *Spinal Cord*, 58(10):1049–1059, 2020.

[218] Yury Gerasimenko, Ruslan Gorodnichev, Tatiana Moshonkina, Dimitry Sayenko, Parag Gad, and V Reggie Edgerton. Transcutaneous electrical spinal-cord stimulation in humans. *Annals of physical and rehabilitation medicine*, 58(4):225–231, 2015.

[219] Parag Gad, Yury Gerasimenko, Sharon Zdunowski, Amanda Turner, Dimitry Sayenko, Daniel C

Lu, and V Reggie Edgerton. Weight bearing over-ground stepping in an exoskeleton with non-invasive spinal cord neuromodulation after motor complete paraplegia. *Frontiers in neuroscience*, 11:333, 2017.

[220] Alvaro Megía García, Diego Serrano-Muñoz, Julian Taylor, Juan Avendaño-Coy, and Julio Gómez-Soriano. Transcutaneous spinal cord stimulation and motor rehabilitation in spinal cord injury: a systematic review. *Neurorehabilitation and neural repair*, 34(1):3–12, 2020.

[221] Ursula S Hofstoetter, Brigitta Freundl, Heinrich Binder, and Karen Minassian. Common neural structures activated by epidural and transcutaneous lumbar spinal cord stimulation: Elicitation of posterior root-muscle reflexes. *PloS one*, 13(1):e0192013, 2018.

[222] C Norman Shealy, J Thomas Mortimer, and James B Reswick. Electrical inhibition of pain by stimulation of the dorsal columns: preliminary clinical report. *Anesthesia & Analgesia*, 46(4):489–491, 1967.

[223] Philip L Gildenberg. History of electrical neuromodulation for chronic pain, 2006.

[224] Ursula S Hofstoetter, Matthias Krenn, Simon M Danner, Christian Hofer, Helmut Kern, William B McKay, Winfried Mayr, and Karen Minassian. Augmentation of voluntary locomotor activity by transcutaneous spinal cord stimulation in motor-incomplete spinal cord-injured individuals. *Artificial organs*, 39(10):E176–E186, 2015.

[225] Ursula S Hofstoetter, Brigitta Freundl, Simon M Danner, Matthias J Krenn, Winfried Mayr, Heinrich Binder, and Karen Minassian. Transcutaneous spinal cord stimulation induces temporary attenuation of spasticity in individuals with spinal cord injury. *Journal of neurotrauma*, 37(3):481–493, 2020.

[226] Ursula S Hofstoetter, William B McKay, Keith E Tansey, Winfried Mayr, Helmut Kern, and Karen Minassian. Modification of spasticity by transcutaneous spinal cord stimulation in individuals with incomplete spinal cord injury. *The journal of spinal cord medicine*, 37(2):202–211, 2014.

[227] Sean J Nagel, Saul Wilson, Michael D Johnson, Andre Machado, Leonardo Frizon, Matthieu K Chardon, Chandan G Reddy, George T Gillies, and Matthew A Howard III. Spinal cord stimulation for spasticity: historical approaches, current status, and future directions. *Neuromodulation: Technology at the Neural Interface*, 20(4):307–321, 2017.

[228] JOSEPH M WALTZ, WAYNE H ANDREESEN, and DAVID P HUNT. Spinal cord stimulation and motor disorders. *Pacing and Clinical Electrophysiology*, 10(1):180–204, 1987.

[229] E Paul Zehr, Trevor S Barss, Katie Dragert, Alain Frigon, Erin V Vasudevan, Carlos Haridas, Sandra Hundza, Chelsea Kaupp, Taryn Klarner, Marc Klimstra, et al. Neuromechanical interactions between the limbs during human locomotion: an evolutionary perspective with translation to rehabilitation. *Experimental brain research*, 234:3059–3081, 2016.

[230] Milan R Dimitrijevic, Yuri Gerasimenko, and Michaela M Pinter. Evidence for a spinal central pattern generator in humans a. *Annals of the New York Academy of Sciences*, 860(1):360–376, 1998.

[231] Liza V McHugh, Ashley A Miller, Kristan A Leech, Cynthia Salorio, and Rebecca H Martin. Fea-

sibility and utility of transcutaneous spinal cord stimulation combined with walking-based therapy for people with motor incomplete spinal cord injury. *Spinal Cord Series and Cases*, 6(1):104, 2020.

[232] Trevor S Barss, Behdad Parhizi, Jane Porter, and Vivian K Mushahwar. Neural substrates of transcutaneous spinal cord stimulation: Neuromodulation across multiple segments of the spinal cord. *Journal of Clinical Medicine*, 11(3):639, 2022.

[233] Michael R Carhart, Jiping He, Richard Herman, S D'luzansky, and Wayne T Willis. Epidural spinal-cord stimulation facilitates recovery of functional walking following incomplete spinal-cord injury. *IEEE Transactions on neural systems and rehabilitation engineering*, 12(1):32–42, 2004.

[234] Yury P Gerasimenko, Daniel C Lu, Morteza Modaber, Sharon Zdunowski, Parag Gad, Dimitry G Sayenko, Erika Morikawa, Piia Haakana, Adam R Ferguson, Roland R Roy, et al. Noninvasive reactivation of motor descending control after paralysis. *Journal of neurotrauma*, 32(24):1968–1980, 2015.

[235] Emanuele Formento, Karen Minassian, Fabien Wagner, Jean Baptiste Mignardot, Camille G Le Goff-Mignardot, Andreas Rowald, Jocelyne Bloch, Silvestro Micera, Marco Capogrosso, and Gregoire Courtine. Electrical spinal cord stimulation must preserve proprioception to enable locomotion in humans with spinal cord injury. *Nature neuroscience*, 21(12):1728–1741, 2018.

[236] Rachele Bertani, Corrado Melegari, Maria C De Cola, Alessia Bramanti, Placido Bramanti, and Rocco Salvatore Calabrò. Effects of robot-assisted upper limb rehabilitation in stroke patients: a systematic review with meta-analysis. *Neurological Sciences*, 38:1561–1569, 2017.

[237] Janne M Veerbeek, Anneli C Langbroek-Amersfoort, Erwin EH Van Wegen, Carel GM Meskers, and Gert Kwakkel. Effects of robot-assisted therapy for the upper limb after stroke: a systematic review and meta-analysis. *Neurorehabilitation and neural repair*, 31(2):107–121, 2017.

[238] Dingguo Zhang, Yong Ren, Kai Gui, Jie Jia, and Wendong Xu. Cooperative control for a hybrid rehabilitation system combining functional electrical stimulation and robotic exoskeleton. *Frontiers in neuroscience*, 11:725, 2017.

[239] Kevin H Ha, Spencer A Murray, and Michael Goldfarb. An approach for the cooperative control of fes with a powered exoskeleton during level walking for persons with paraplegia. *IEEE Transactions on Neural Systems and Rehabilitation Engineering*, 24(4):455–466, 2015.

[240] Antonio J Del-Ama, Ángel Gil-Agudo, José L Pons, and Juan C Moreno. Hybrid fes-robot cooperative control of ambulatory gait rehabilitation exoskeleton. *Journal of neuroengineering and rehabilitation*, 11(1):1–15, 2014.

[241] Andrea Calanca, Riccardo Muradore, and Paolo Fiorini. A review of algorithms for compliant control of stiff and fixed-compliance robots. *IEEE/ASME transactions on mechatronics*, 21(2):613–624, 2015.

[242] Stefano Dalla Gasperina, Loris Roveda, Alessandra Pedrocchi, Francesco Braghin, and Marta Gandolla. Review on patient-cooperative control strategies for upper-limb rehabilitation exoskeletons. *Frontiers in Robotics and AI*, 8:745018, 2021.

[243] Goro Obinata, Shunro Fukada, Toshiki Matsunaga, Takehiro Iwami, Yoichi Shimada, Kazuto Miyawaki, Kazunori Hase, and Atsushi Nakayama. Hybrid control of powered orthosis and func-

tional neuromuscular stimulation for restoring gait. In *2007 29th Annual International Conference of the IEEE Engineering in Medicine and Biology Society*, pages 4879–4882. IEEE, 2007.

[244] Spencer A Murray, Ryan J Farris, Michael Golfarb, Clare Hartigan, Casey Kandilakis, and Don Truex. Fes coupled with a powered exoskeleton for cooperative muscle contribution in persons with paraplegia. In *2018 40th Annual International Conference of the IEEE Engineering in Medicine and Biology Society (EMBC)*, pages 2788–2792. IEEE, 2018.

[245] Mohamed Amine Alouane, Hala Rifai, Yacine Amirat, and Samer Mohammed. Cooperative control for knee joint flexion-extension movement restoration. In *2018 IEEE/RSJ International Conference on Intelligent Robots and Systems (IROS)*, pages 5175–5180. IEEE, 2018.

[246] Mark Nandor, Rudi Kobetic, Musa Audu, Ron Triolo, and Roger Quinn. A muscle-first, electromechanical hybrid gait restoration system in people with spinal cord injury. *Frontiers in Robotics and AI*, 8:645588, 2021.

[247] Rudi Kobetic, Curtis S To, John R Schnellenberger, Musa L Audu, Thomas C Bulea, Richard Gaudio, Gilles Pinault, Scott Tashman, and Ronald J Triolo. Development of hybrid orthosis for standing, walking, and stair climbing after spinal cord injury. *J Rehabil Res Dev*, 46(3):447–62, 2009.

[248] Yves Stauffer, Yves Allemand, Mohamed Bouri, Jacques Fournier, Reymond Clavel, Patrick Métrailler, Roland Brodard, and Fabienne Reynard. The walktrainer—a new generation of walking reeducation device combining orthoses and muscle stimulation. *IEEE Transactions on neural systems and rehabilitation engineering*, 17(1):38–45, 2008.

[249] Vahidreza Molazadeh, Qiang Zhang, Xuefeng Bao, and Nitin Sharma. An iterative learning controller for a switched cooperative allocation strategy during sit-to-stand tasks with a hybrid exoskeleton. *IEEE Transactions on Control Systems Technology*, 30(3):1021–1036, 2021.

[250] N Sharma, PM Patre, CM Gregory, and WE Dixon. Nonlinear control of nmes: Incorporating fatigue and calcium dynamics. In *Dynamic Systems and Control Conference*, volume 48920, pages 705–712, 2009.

[251] Nicholas Kirsch, Naji Alibeji, Lee Fisher, Chris Gregory, and Nitin Sharma. A semi-active hybrid neuroprosthesis for restoring lower limb function in paraplegics. In *2014 36th Annual International Conference of the IEEE Engineering in Medicine and Biology Society*, pages 2557–2560. IEEE, 2014.

[252] Francisco Resquín, Alicia Cuesta Gómez, Jose Gonzalez-Vargas, Fernando Brunetti, Diego Torricelli, Francisco Molina Rueda, Roberto Cano de la Cuerda, Juan Carlos Miangolarra, and José Luis Pons. Hybrid robotic systems for upper limb rehabilitation after stroke: A review. *Medical engineering & physics*, 38(11):1279–1288, 2016.

[253] Emilia Ambrosini, Giulio Gasperini, Johannes Zajc, Nancy Immick, Andreas Augsten, Mauro Rossini, Roberto Ballarati, Micheal Russold, Simona Ferrante, Giancarlo Ferrigno, et al. A robotic system with emg-triggered functional eletrical stimulation for restoring arm functions in stroke survivors. *Neurorehabilitation and Neural Repair*, 35(4):334–345, 2021.

[254] Christian Klauer, Thomas Schauer, Werner Reichenfelser, Jakob Karner, Sven Zwicker, Marta

Gandolla, Emilia Ambrosini, Simona Ferrante, Marco Hack, Andreas Jedlitschka, et al. Feedback control of arm movements using neuro-muscular electrical stimulation (nmes) combined with a lockable, passive exoskeleton for gravity compensation. *Frontiers in Neuroscience*, 8:262, 2014.

[255] Abidemi Bolu Ajiboye, Francis R Willett, Daniel R Young, William D Memberg, Brian A Murphy, Jonathan P Miller, Benjamin L Walter, Jennifer A Sweet, Harry A Hoyen, Michael W Keith, et al. Restoration of reaching and grasping in a person with tetraplegia through brain-controlled muscle stimulation: a proof-of-concept demonstration. *Lancet (London, England)*, 389(10081):1821, 2017.

[256] Derek Wolf, Nathan Dunkelberger, Craig G McDonald, Kyra Rudy, Christopher Beck, Marcia K O'Malley, and Eric Schearer. Combining functional electrical stimulation and a powered exoskeleton to control elbow flexion. In *2017 International Symposium on Wearable Robotics and Rehabilitation (WeRob)*, pages 1–2. IEEE, 2017.

[257] Naji A Alibeji, Vahidreza Molazadeh, Brad E Dicianno, and Nitin Sharma. A control scheme that uses dynamic postural synergies to coordinate a hybrid walking neuroprosthesis: Theory and experiments. *Frontiers in neuroscience*, 12:159, 2018.

[258] Caryn Langstaff, Cally Martin, Gwen Brown, Don McGuinness, Jo Mather, Jennifer Loshaw, Nancy Jones, Kim Fletcher, and John Paterson. Enhancing community-based rehabilitation for stroke survivors: creating a discharge link. *Topics in stroke rehabilitation*, 21(6):510–519, 2014.

[259] Linda L Madaris, Mirian Onyebueke, Janet Liebman, and Allyson Martin. Sci hospital in home program: bringing hospital care home for veterans with spinal cord injury. *Nursing Administration Quarterly*, 40(2):109–114, 2016.

[260] Robert Riener and Thomas Edrich. Identification of passive elastic joint moments in the lower extremities. *Journal of biomechanics*, 32(5):539–544, 1999.

[261] Robert Nguyen, Andres M Gonzalez, Silvestro Micera, and Manfred Morari. Increasing muscular participation in robot-assisted gait training using fes. In *16th Annual International FES Society Conference*. International Functional Electrical Stimulation Society (IFESS), 2011.

[262] Philipp Müller, Antonio J Del Ama, Juan C Moreno, and Thomas Schauer. Adaptive multichannel fes neuroprosthesis with learning control and automatic gait assessment. *Journal of neuroengineering and rehabilitation*, 17(1):1–20, 2020.

[263] S Dalla Gasperina, F Ferrari, M Gandolla, A Pedrocchi, and E Ambrosini. Hybrid cooperative control of functional electrical stimulation and robot assistance for upper extremity rehabilitation. *IEEE Transactions on Biomedical Engineering*, 2024.

[264] Xuefeng Bao, Zhiyu Sheng, Brad E Dicianno, and Nitin Sharma. A tube-based model predictive control method to regulate a knee joint with functional electrical stimulation and electric motor assist. *IEEE Transactions on Control Systems Technology*, 29(5):2180–2191, 2020.

[265] Nicholas A Kirsch, Xuefeng Bao, Naji A Alibeji, Brad E Dicianno, and Nitin Sharma. Model-based dynamic control allocation in a hybrid neuroprosthesis. *IEEE Transactions on Neural Systems and Rehabilitation Engineering*, 26(1):224–232, 2017.

[266] Chen-Hao Chang, Jonathan Casas, Steven W Brose, and Victor H Duenas. Closed-loop torque and

kinematic control of a hybrid lower-limb exoskeleton for treadmill walking. *Frontiers in Robotics and AI*, 8:702860, 2022.

[267] Davide Burchielli, Nicola Lotti, Francesco Missiroli, Casimir Bokranz, Alessandra Pedrocchi, Emilia Ambrosini, and Lorenzo Masia. Adaptive hybrid fes-force controller for arm exosuit. In *2022 International Conference on Rehabilitation Robotics (ICORR)*, pages 1–6. IEEE, 2022.

[268] Ashley Stewart, Christopher Pretty, and Xiaoqi Chen. A portable assist-as-need upper-extremity hybrid exoskeleton for fes-induced muscle fatigue reduction in stroke rehabilitation. *BMC Biomedical Engineering*, 1:1–17, 2019.

[269] Nathan Dunkelberger, Skye A Carlson, Jeffrey Berning, Eric M Schearer, and Marcia K O'Malley. Multi degree of freedom hybrid fes and robotic control of the upper limb. *IEEE Transactions on Neural Systems and Rehabilitation Engineering*, 2024.

[270] Federica Ferrari, Eva Zimei, Marta Gandolla, Alessandra Pedrocchi, and Emilia Ambrosini. An emg-triggered cooperative controller for a hybrid fes-robotic system. In *2023 IEEE International Conference on Metrology for eXtended Reality, Artificial Intelligence and Neural Engineering (MetroXRAINE)*, pages 852–857. IEEE, 2023.

[271] Matteo Laffranchi, Stefano D'Angella, Christian Vassallo, Chiara Piezzo, Michele Canepa, Samuele De Giuseppe, Mirco Di Salvo, Antonio Succi, Samuele Cappa, Giulio Cerruti, et al. User-centered design and development of the modular twin lower limb exoskeleton. *Frontiers in neurorobotics*, 15:709731, 2021.

[272] André Heck and Caroline van Dongen. Gait analysis by high school students. *Physics Education*, 43(3):284, 2008.

[273] David A Winter. *Biomechanics and motor control of human movement*. John wiley & sons, 2009.

[274] Elena Bardi, Stefano Dalla Gasperina, Alessandra Pedrocchi, and Emilia Ambrosini. Adaptive cooperative control for hybrid fes-robotic upper limb devices: a simulation study. In *2021 43rd Annual International Conference of the IEEE Engineering in Medicine & Biology Society (EMBC)*, pages 6398–6401. IEEE, 2021.

[275] Douglas A Bristow, Marina Tharayil, and Andrew G Alleyne. A survey of iterative learning control. *IEEE control systems magazine*, 26(3):96–114, 2006.

[276] Bruno P Chumpitazi, Mariella M Self, Danita I Czyzewski, Sydney Cejka, Paul R Swank, and Robert J Shulman. Bristol stool form scale reliability and agreement decreases when determining rome iii stool form designations. *Neurogastroenterology & Motility*, 28(3):443–448, 2016.

[277] D Erdem, D Hava, P Keskinoğlu, ÇİĞDEM Bircan, Ö Peker, K Krogh, and S Gülbahar. Reliability, validity and sensitivity to change of neurogenic bowel dysfunction score in patients with spinal cord injury. *Spinal Cord*, 55(12):1084–1087, 2017.

[278] Richard W Bohannon and Melissa B Smith. Interrater reliability of a modified ashworth scale of muscle spasticity. *Physical therapy*, 67(2):206–207, 1987.

[279] Mark P Jensen, Paul Karoly, and Sanford Braver. The measurement of clinical pain intensity: a comparison of six methods. *Pain*, 27(1):117–126, 1986.

[280] E Grossi, P Mosconi, N Groth, M Niero, and G Apolone. Il questionario psychological general well-being. *Versione Italiana. Milano: Edizioni "Mario Negri*, 2002.

[281] John Brooke et al. Sus-a quick and dirty usability scale. *Usability evaluation in industry*, 189(194):4–7, 1996.

[282] Viswanath Venkatesh and Hillol Bala. Technology acceptance model 3 and a research agenda on interventions. *Decision sciences*, 39(2):273–315, 2008.

[283] Bettina Laugwitz, Theo Held, and Martin Schrepp. Construction and evaluation of a user experience questionnaire. In *HCI and Usability for Education and Work: 4th Symposium of the Workgroup Human-Computer Interaction and Usability Engineering of the Austrian Computer Society, USAB 2008, Graz, Austria, November 20-21, 2008. Proceedings 4*, pages 63–76. Springer, 2008.

[284] Thierry Keller and Andreas Kuhn. Electrodes for transcutaneous (surface) electrical stimulation. *Journal of automatic control*, 18(2):35–45, 2008.

[285] Bastien Moineau, Cesar Marquez-Chin, Milad Alizadeh-Meghrazi, and Milos R Popovic. Garments for functional electrical stimulation: Design and proofs of concept. *Journal of Rehabilitation and Assistive Technologies Engineering*, 6:2055668319854340, 2019.

[286] Li Li, Wai Man Au, Yi Li, Kam Man Wan, Sai Ho Wan, and Kwok Shing Wong. Design of intelligent garment with transcutaneous electrical nerve stimulation function based on the intarsia knitting technique. *Textile Research Journal*, 80(3):279–286, 2010.

[287] Yu-Chung Chen, Willy Chou, Rong-Bin Hong, Jen-Ho Lee, and Jer-Hao Chang. Home-based rehabilitation versus hospital-based rehabilitation for stroke patients in post-acute care stage: Comparison on the quality of life. *Journal of the Formosan Medical Association*, 2023.

[288] Emanuel Gunnarsson, Kristian Rödby, and Fernando Seoane. Seamlessly integrated textile electrodes and conductive routing in a garment for electrostimulation: design, manufacturing and evaluation. *Scientific Reports*, 13(1):17408, 2023.

[289] Krzysztof Gniotek, Michał Frydrysiak, Janusz Zięba, Magdalena Tokarska, and Zbigniew Stempień. Innovative textile electrodes for muscles electrostimulation. In *2011 IEEE International Symposium on Medical Measurements and Applications*, pages 305–310. IEEE, 2011.

[290] Xueliang Xiao, Ke Dong, Chenhao Li, Guanzheng Wu, Hongtao Zhou, and Yanjia Gu. A comfortability and signal quality study of conductive weave electrodes in long-term collection of human electrocardiographs. *Textile Research Journal*, 89(11):2098–2112, 2019.

[291] Jayoung Kim, Rajan Kumar, Amay J Bandodkar, and Joseph Wang. Advanced materials for printed wearable electrochemical devices: A review. *Advanced Electronic Materials*, 3(1):1600260, 2017.

[292] Li Guo, Leif Sandsjö, Max Ortiz-Catalan, and Mikael Skrifvars. Systematic review of textile-based electrodes for long-term and continuous surface electromyography recording. *Textile Research Journal*, 90(2):227–244, 2020.

[293] Exopulse Mollii Suit. Exopulse mollii suit - reduce spasticity, activate muscles. Last accessed 17 January 2024.

[294] Teslasuit. Teslasuit - meet our haptic vr suit and glove with force feedback. Last accessed 17 January 2024.

[295] Eva-Maria Dölker, Alkisah binti Mubin, Eko Supriyanto, Elke Haase, Sybille Krzywinski, and Jens Haueisen. Sensation thresholds in electrocutaneous stimulation. *Current Directions in Biomedical Engineering*, 6(3):372–375, 2020.

[296] Meijing Liu, Tyler Ward, Dan Young, Helga Matos, Yang Wei, Jo Adams, and Kai Yang. Electronic textiles based wearable electrotherapy for pain relief. *Sensors and Actuators A: Physical*, 303:111701, 2020.

[297] Gozde Goncu Berk. Design of a wearable pain management system with embroidered tens electrodes. *International Journal of Clothing Science and Technology*, 30(1):38–48, 2018.

[298] Melissa Lawrence. *Transcutaneous electrode technology for neuroprostheses*. Lulu. com, 2015.

[299] Luisa Euler, Li Guo, and Nils-Krister Persson. Influence of the electrolyte concentration and amount on the performance of textile electrodes in electrostimulation: a systematic study. *Sensors and Actuators A: Physical*, 366:115010, 2024.

[300] Ana Popović-Bijelić, Goran Bijelić, Nikola Jorgovanović, Dubravka Bojanić, Mirjana B Popović, and Dejan B Popović. Multi-field surface electrode for selective electrical stimulation. *Artificial organs*, 29(6):448–452, 2005.

[301] Axelgaard. Pals electrodes. Last accessed 18 June 2024.

[302] Hermie J Hermens, Bart Freriks, Catherine Disselhorst-Klug, and Günter Rau. Development of recommendations for semg sensors and sensor placement procedures. *Journal of electromyography and Kinesiology*, 10(5):361–374, 2000.

[303] Anne E Hines, Patrick E Crago, Gregg J Chapman, and Carl Billian. Stimulus artifact removal in emg from muscles adjacent to stimulated muscles. *Journal of neuroscience methods*, 64(1):55–62, 1996.

[304] Emilia Ambrosini, Simona Ferrante, Thomas Schauer, Christian Klauer, Marina Gaffuri, Giancarlo Ferrigno, and Alessandra Pedrocchi. A myocontrolled neuroprosthesis integrated with a passive exoskeleton to support upper limb activities. *Journal of Electromyography and Kinesiology*, 24(2):307–317, 2014.

[305] Emilia Ambrosini, Simona Ferrante, Johannes Zajc, Maria Bulgheroni, Walter Baccinelli, Enrico d'Amico, Thomas Schauer, Constantin Wiesener, M Russold, Margit Gfoehler, et al. The combined action of a passive exoskeleton and an emg-controlled neuroprosthesis for upper limb stroke rehabilitation: First results of the retrainer project. In *2017 International Conference on Rehabilitation Robotics (ICORR)*, pages 56–61. IEEE, 2017.

[306] M Murg, H Binder, and MR Dimitrijevic. Epidural electric stimulation of posterior structures of the human lumbar spinal cord: 1. muscle twitches–a functional method to define the site of stimulation. *Spinal cord*, 38(7):394–402, 2000.

[307] KE Tansey, B Farrell, WB McKay, and J Bruce. Motor control changes in incomplete sci generated

by adding tonic transcutaneous spinal cord stimulation to robotic locomotor training: a test of concept study. In *Neuroscience Meeting Planner*. Society for Neuroscience San Diego, CA, 2013.

[308] Raza N Malik, Soshi Samejima, Claire Shackleton, Tiev Miller, Alessandra Laura Giulia Pedrocchi, Alexander G Rabchevsky, Chet T Moritz, David Darrow, Edelle C Field-Fote, Eleonora Guanziroli, et al. Report-scs: minimum reporting standards for spinal cord stimulation studies in spinal cord injury. *Journal of Neural Engineering*, 21(1):016019, 2024.

[309] Fatma Inanici, Soshi Samejima, Parag Gad, V Reggie Edgerton, Christoph P Hofstetter, and Chet T Moritz. Transcutaneous electrical spinal stimulation promotes long-term recovery of upper extremity function in chronic tetraplegia. *IEEE Transactions on Neural Systems and Rehabilitation Engineering*, 26(6):1272–1278, 2018.

[310] Mrinal Rath, Albert H Vette, Shyamsundar Ramasubramaniam, Kun Li, Joel Burdick, Victor R Edgerton, Yury P Gerasimenko, and Dimitry G Sayenko. Trunk stability enabled by noninvasive spinal electrical stimulation after spinal cord injury. *Journal of neurotrauma*, 35(21):2540–2553, 2018.

[311] Ashley N Dalrymple, Charli Ann Hooper, Minna G Kuriakose, Marco Capogrosso, and Douglas J Weber. Using a high-frequency carrier does not improve comfort of transcutaneous spinal cord stimulation. *Journal of Neural Engineering*, 20(1):016016, 2023.

[312] Karen Minassian, Ursula S Hofstoetter, Simon M Danner, Winfried Mayr, Joy A Bruce, W Barry McKay, and Keith E Tansey. Spinal rhythm generation by step-induced feedback and transcutaneous posterior root stimulation in complete spinal cord–injured individuals. *Neurorehabilitation and neural repair*, 30(3):233–243, 2016.

[313] Elena Y Shapkova, Elena V Pismennaya, Dmitriy V Emelyannikov, and Yury Ivanenko. Exoskeleton walk training in paralyzed individuals benefits from transcutaneous lumbar cord tonic electrical stimulation. *Frontiers in Neuroscience*, 14:496796, 2020.

[314] Yevgeniy Freyvert, Nicholas Au Yong, Erika Morikawa, Sharon Zdunowski, Melanie E Sarino, Yury Gerasimenko, V Reggie Edgerton, and Daniel C Lu. Engaging cervical spinal circuitry with non-invasive spinal stimulation and buspirone to restore hand function in chronic motor complete patients. *Scientific reports*, 8(1):15546, 2018.

[315] Fan Zhang, Kamyar Momeni, Arvind Ramanujam, Manikandan Ravi, Janelle Carnahan, Steven Kirshblum, and Gail F Forrest. Cervical spinal cord transcutaneous stimulation improves upper extremity and hand function in people with complete tetraplegia: a case study. *IEEE Transactions on Neural Systems and Rehabilitation Engineering*, 28(12):3167–3174, 2020.

[316] Fatma Inanici, Lorie N Brighton, Soshi Samejima, Christoph P Hofstetter, and Chet T Moritz. Transcutaneous spinal cord stimulation restores hand and arm function after spinal cord injury. *IEEE Transactions on Neural Systems and Rehabilitation Engineering*, 29:310–319, 2021.

[317] Clare Taylor, Conor McHugh, David Mockler, Conor Minogue, Richard B Reilly, and Neil Fleming. Transcutaneous spinal cord stimulation and motor responses in individuals with spinal cord injury: A methodological review. *PloS one*, 16(11):e0260166, 2021.

[318] Md Anamul Islam, Timothy S Pulverenti, and Maria Knikou. Neuronal actions of transspinal

stimulation on locomotor networks and reflex excitability during walking in humans with and without spinal cord injury. *Frontiers in Human Neuroscience*, 15:620414, 2021.

[319] Andreas Skiadopoulos, Grace O Famodimu, Shammah K Solomon, Parul Agarwal, Noam Y Harel, and Maria Knikou. Priming locomotor training with transspinal stimulation in people with spinal cord injury: study protocol of a randomized clinical trial. *Trials*, 24(1):145, 2023.

[320] Parneet Kaur Bedi and Narkeesh Arumugam. Activity based therapy and surface spinal stimulation for recovery of walking in individual with traumatic incomplete spinal cord injury: a case report. *Int J Recent Sci Res*, 6:5581–3, 2015.

[321] Brad WR Roberts, Darryn A Atkinson, Gerome A Manson, Rachel Markley, Teresa Kaldis, Gavin W Britz, Philip J Horner, Albert H Vette, and Dimitry G Sayenko. Transcutaneous spinal cord stimulation improves postural stability in individuals with multiple sclerosis. *Multiple sclerosis and related disorders*, 52:103009, 2021.

[322] Francisco D Benavides, Hang Jin Jo, Henrik Lundell, V Reggie Edgerton, Yuri Gerasimenko, and Monica A Perez. Cortical and subcortical effects of transcutaneous spinal cord stimulation in humans with tetraplegia. *Journal of Neuroscience*, 40(13):2633–2643, 2020.

[323] Simon M Danner, Matthias Krenn, Ursula S Hofstoetter, Andrea Toth, Winfried Mayr, and Karen Minassian. Body position influences which neural structures are recruited by lumbar transcutaneous spinal cord stimulation. *PloS one*, 11(1):e0147479, 2016.

[324] Christian Meyer, Ursula S Hofstoetter, Michèle Hubli, Roushanak H Hassani, Carmen Rinaldo, Armin Curt, and Marc Bolliger. Immediate effects of transcutaneous spinal cord stimulation on motor function in chronic, sensorimotor incomplete spinal cord injury. *Journal of clinical medicine*, 9(11):3541, 2020.

[325] Matthias J Krenn, Jose L Vargas Luna, Winfried Mayr, and Dobrivoje S Stokic. Bipolar transcutaneous spinal stimulation evokes short-latency reflex responses in human lower limbs alike standard unipolar electrode configuration. *Journal of Neurophysiology*, 124(4):1072–1082, 2020.

[326] Caleb Hoover, Willis Schuerger, David Balser, Patricia McCracken, Thomas A Murray, Leslie Morse, Ann Parr, Uzma Samadani, Theoden I Netoff, and David P Darrow. Neuromodulation through spinal cord stimulation restores ability to voluntarily cycle after motor complete paraplegia. *Journal of Neurotrauma*, 2023.

[327] Ursula S Hofstoetter, Ivan Perret, Aymeric Bayart, Peter Lackner, Heinrich Binder, Brigitta Freundl, and Karen Minassian. Spinal motor mapping by epidural stimulation of lumbosacral posterior roots in humans. *Iscience*, 24(1), 2021.

[328] Anas R Alashram, Elvira Padua, Manikandan Raju, Cristian Romagnoli, and Giuseppe Annino. Transcutaneous spinal cord stimulation effects on spasticity in patients with spinal cord injury: A systematic review. *The Journal of Spinal Cord Medicine*, 46(4):582–589, 2023.

[329] MM Dimitrijevic, MR Dimitrijevic, LS Illis, K Nakajima, PC Sharkey, and AM Sherwood. Spinal cord stimulation for the control of spasticity in patients with chronic spinal cord injury: I. clinical observations. *Central nervous system trauma*, 3(2):129–143, 1986.

[330] MM Pinter, F Gerstenbrand, and MR Dimitrijevic. Epidural electrical stimulation of posterior structures of the human lumbosacral cord: 3. control of spasticity. *Spinal cord*, 38(9):524–531, 2000.

[331] Maya Horst, Janine Heutschi, Rubia Van Den Brand, Karl-Erik Andersson, Rita Gobet, Tullio Sulser, Grégoire Courtine, and Daniel Eberli. Multisystem neuroprosthetic training improves bladder function after severe spinal cord injury. *The Journal of urology*, 189(2):747–753, 2013.

[332] Lisa A Simpson, Janice J Eng, Jane TC Hsieh, Wolfe, and Dalton L the Spinal Cord Injury Rehabilitation Evidence (SCIRE) Research Team. The health and life priorities of individuals with spinal cord injury: a systematic review. *Journal of neurotrauma*, 29(8):1548–1555, 2012.

[333] Yazi Al'joboori, Ricci Hannah, Francesca Lenham, Pia Borgas, Charlotte JP Kremers, Karen L Bunday, John Rothwell, and Lynsey D Duffell. The immediate and short-term effects of transcutaneous spinal cord stimulation and peripheral nerve stimulation on corticospinal excitability. *Frontiers in Neuroscience*, 15:749042, 2021.

[334] H Taborikova and DS Sax. Motoneurone pool and the h-reflex. *Journal of neurology, neurosurgery, and psychiatry*, 31(4):354, 1968.

[335] Ursula S Hofstoetter, Brigitta Freundl, Heinrich Binder, and Karen Minassian. Recovery cycles of posterior root-muscle reflexes evoked by transcutaneous spinal cord stimulation and of the h reflex in individuals with intact and injured spinal cord. *PLoS One*, 14(12):e0227057, 2019.

[336] Vincent WS Chan, Hugo Nova, Sherif Abbas, Colin JL McCartney, Anahi Perlas, and Da Quan Xu. Ultrasound examination and localization of the sciatic nerve: a volunteer study. *The Journal of the American Society of Anesthesiologists*, 104(2):309–314, 2006.

[337] Cionic. Cionic neural sleeve - the most advanced mobility solution to improve walking and strength. Last accessed 12 April 2024.

[338] Dennis Bourbeau, Abby Bolon, Graham Creasey, Wei Dai, Bill Fertig, Jennifer French, Tara Jeji, Anita Kaiser, Roman Kouznetsov, Alexander Rabchevsky, et al. Needs, priorities, and attitudes of individuals with spinal cord injury toward nerve stimulation devices for bladder and bowel function: a survey. *Spinal Cord*, 58(11):1216–1226, 2020.

[339] Henri Lorach, Andrea Galvez, Valeria Spagnolo, Felix Martel, Serpil Karakas, Nadine Intering, Molywan Vat, Olivier Faivre, Cathal Harte, Salif Komi, et al. Walking naturally after spinal cord injury using a brain–spine interface. *Nature*, 618(7963):126–133, 2023.

A | List of relevant scientific publications

A.1. International peer-reviewed journals

1. G. Preatoni*, **F. Dell'Eva***, G.Valle, A. Pedrocchi, S. Raspopovic. "Reshaping the full body illusion through visuo-electro-tactile sensations", *PLOS One*, 2023.
2. **F. Dell'Eva**, V. Oliveri, R. Sironi, P. Perego, G. Andreoni, S. Ferrante, A. Pedrocchi, E. Ambrosini. "Ink-based textile electrodes for wearable Functional Electrical Stimulation: a proof-of-concept study to evaluate their comfort and efficacy", *Artificial Organs*, 2024.
3. **F. Dell'Eva**, E. Ambrosini. "Design of a cooperative control for a hybrid FES-motorized exoskeleton to support locomotion: a validation study on healthy subjects". Under Preparation for Nature Machine Intelligence.

*** These authors equally contributed to the work.**

A.2. Contributions at international conferences

1. T. Del Grossi, **F. Dell'Eva**, V. Camerini, M. Gandolla, A. Pedrocchi, E. Ambrosini. "Cooperative control solutions for FES-motorized robotic systems: a narrative review", submitted for *CASE conference*. 2024.
2. **F. Dell'Eva**, S. Dalla Gasperina, M. Gandolla, L. De Micheli, A. Pedrocchi, E. Ambrosini. "A hybrid FES-motor cooperative control over a knee joint movement: a feasibility study", *IFESS conference, RehabWeek*. 2022.
3. F. Ferrari, N. Sanna, **F. Dell'Eva**, P. Brambilla, M. Tarabini, S. Ferrante, A. Pedrocchi, E. Ambrosini. "A mobile FES-cycling system with pedal force measurement to optimize training performance" *IFESS conference, RehabWeek*. 2021.
4. I. Ceroni, S. Ferrante, F. Conti, S. Javadzadeh, S. Dalla Gasperina, **F. Dell'Eva**, A. Pedrocchi, M. Tarabini, E. Ambrosini. "Comparing Fatigue Reducing Stimulation Strategies During Cycling Induced by Functional Electrical Stimulation: a Case Study with one Spinal Cord Injured Subject", *43rd Annual International Conference of the IEEE EMBC*. 2021.

List of Figures

1.1 Schematic representation of the different types of rehabilitation robots. Adapted from [59]. 7
1.2 Existent commercial Lower-limbs powered exoskeletons. 10
1.3 Neurophysiological working principle of the electrical stimulation. Considering the zoom over the single fiber, we notice a localized electric field generated by the movement of ions from the anode toward the cathode. This induces a hyperpolarization below the anode and a depolarization beneath the cathode, triggering the Action Potential wave. 14
1.4 Parameters of the typical stimulation square wave: amplitude (A) in mA, frequency (f) in Hz and pulsewidth (PW) in μs. 16
1.5 ES applications with their main usages. Different strategies are used for Upper and Lower Motoneuron Lesions [127]. 19
1.6 Localization of Upper Motoneuron (UMN) between brain and spinal cord and Lower Motoneuron (LMN) between spinal cord and peripheral muscles. Image adapted from [127]. . 19
1.7 (a) Stimulation square waves with shorter or longer pulsewidth for nerve and muscle stimulation, respectively. (b) Intensity-duration curves for pulses of nerve and muscle stimulation. Image taken from [129]. 20
1.8 Schematic representation of the signal traveling along motor (panel a) and sensory (panel b) fibers after the stimulation and correspondent induced waves in the EMG signal. Panel c illustrates the *Collision Block* phenomenon occurring when opposite signals collide. Image adapted from [132] and drawn on *BioRender.com*. 22
1.9 M-waves and H-waves induced on the Tibialis Anterior muscle during its stimulation at different amplitudes. Image realized by Matthias Krenn and used with his permission. . . 23
1.10 SCS-provided excitatory input moves the central state of excitability closer to the threshold and enables an otherwise ineffective supraspinal input to generate a motor output. Figure from Minassian et al., 2016 [206]. 31
1.11 PRM reflex: the electrical stimulation causes an action potential in the sensory afferent fibers, which elicit the motor fibers through trans-synaptic activation, resulting in a short-latency muscular contraction (figure drawn on *BioRender.com*). 32
1.12 Post activation depression in the soleus muscle with PRM reflex elicited from transcutaneous SCS. Black triangles indicate the stimuli while waves represent the EMG response recorded on the soleus muscle. It is easily observed that the second stimulus does not generate a muscle response at all in the case of 60 ms interval, or a very low amplitude response in the case of 100 ms and 150 ms intervals. Figure from Minassian et al., 2007 [214]. 33

2.1 Graphical representation of the work: the rationale and the objective of realizing a hybrid system, together with the main results. 58

2.2 (a) Hardware components of the TwinFES hybrid device: the Twin exoskeleton and the two RehaMove3 stimulators with their cables. (b) A scheme of the connections between components. 59

2.3 (a) Overall FES and motor control strategies for locomotion. Depending on the gait phase, joint motors are controlled either in position or impedance, while muscles are controlled either with biomimetic or ILC strategy. (b) Biomimetic stimulation profiles derived from literature EMG recordings [272, 273] and used for the synchronized control. (c) Cooperative control scheme. θ_t, $\dot{\theta}_t$, $\ddot{\theta}_t$ and θ_a, $\dot{\theta}_a$, $\ddot{\theta}_a$ are target and actual position, velocity and acceleration. τ_{FF}, τ_{FB} and τ_{TOT} are the feedforward, feedback and total torque components computed. τ_{TOT} is transferred to the motor and τ_{MOT} is the real exerted motor torque. α is the percentage of the subject's shank weight compensated by the motor. I is the FES current computed by the ILC block and delivered to muscles, generating the muscle torque τ_{MUSC}. 63

2.4 Panel (a) reports single-joint experiments of one representative subject (ID 1) for the three tested conditions: $MOT_{0\%}+FES$, $MOT_{100\%}$ and $MOT_{0\%}$. Reported variables are angular position (θ_{real} in [°]), motor current (I_{MOT} in [A]), total motor torque (τ_{TOT} in [Nm]) and Quadriceps stimulation current (I_{FES} in [mA]). Data of all extensions were averaged and are here displayed in terms of mean±SD (Standard Deviation) as a function of time (with 2s being the extension duration), except for the stimulation current, presented for the sole condition with FES in terms of median±IQR (Inter-Quartile Range). The dotted grey line in the first graph represents the target trajectory θ_{target}, those in the third graph the feedforward torque in $\alpha = 100\%$ and $\alpha = 0\%$ cases and those in the fourth graph I_{L1} and I_{L2} subject-specific calibration values. Panel (b) displays the boxplots of the single-joint metrics over the 6 subjects for the same conditions. Position RMSE (RMSE in [°]), motor current integral ($I_{MOT}Integral$ in [A]) and motor torque integral ($\tau_{MOT}Integral$ in [Nm]) are reported. The green background indicates that the cooperative control modality was applied in this case. Differences were considered statistically significant when p-value$<$0.05. 69

2.5 Data from one subject (ID 4) over a complete gait cycle, averaged across all performed cycles. Panel a reports the mean±SD of the target trajectory (θ_{target}, dotted grey line) juxtaposed to the actual one (θ_{real}) under two cases: $MOT_{100\%}$ (solid blue line) and $MOT_{0\%} + FES$ (solid pink line) for the knee and hip joint (upper/lower panel). Panel b illustrates the median±IQR of the current levels (I_{FES}) administered to Quadriceps and Hamstrings (upper/lower panel) in $MOT_{0\%} + FES$. 71

2.6 Results of the knee joint during selected swing movements of walking experiments on one representative subject (ID4) for the two tested conditions: $MOT_{0\%} + FES$ and $MOT_{100\%}$. Reported variables are the angular position (θ_{real} in [°]) in (a), the total motor torque in (τ_{TOT} in [Nm]) in (b) and the Quadriceps and Hamstrings stimulation current (I_{FES} in [mA]) in (c) for the sole condition with FES. Data are displayed for 6 swings, those from 3 to 5 and those from 17 to 19. The dotted grey line in (a) represents the target trajectory θ_{target}; the orange and purple ones in (c), the I_{L1} and I_{L2} subject-specific threshold values defined during calibration for the Quadriceps and Hamstrings respectively. 71

2.7 Results of the walking experiments under the two conditions ($MOT_{100\%}$ and $MOT_{0\%} + FES$) considering all tested subjects and strides of both sides. Boxplots report position RMSE ($RMSE$ in [°]) and integral of the motor current ($I_{MOT}Integral$ in [A]) for the hip joint during the stance (a) and swing (b) phase and for the knee motor during the stance phase (c). The yellow background indicates that these joints are under synchronous control. Panel (d) displays, in addition to the position RMSE and motor current integral, the motor torque integral ($\tau_{MOT}Integral$ in [Nm]) and Quadriceps and Hamstrings FES current integral ($I_{FES}Integral$ in [mA]) for the knee motor during swing. The same metrics are reported in panel (e) but averaging data into blocks of 5 consecutive steps for each subject and then mediating them for all subjects and sides. The green background of panels (d) and (e) indicates that these joints are under cooperative control. Differences were considered statistically significant when p-value<0.05. 73
2.8 p-values for the 5-by-5 swings comparisons. Tables must be read row by column and the arrow indicates whether the row value was higher or lower than the column value. Differences were considered statistically significant when p-value<0.05. 74
2.9 Flowchart of the protocol used for tests on target users. 76
2.10 Results of the Psychological General Well-Being Index (PGWBI) for all individuals. Single-subject data are reported, with a different marker depending on the pathology as detailed by the legend. Scores are reported on a 0-100 scale, with a higher value indicating a better psychological condition, except for anxiety and depression ("negative" feelings) for which the opposite occurs. 80
2.11 Results of the walking experiments under the two conditions ($MOT_{100\%}$ and $MOT_{0\%} + FES$) considering all eleven tested subjects and strides of both sides. For both conditions, the steps of all sessions were considered together. Boxplots report position RMSE ($RMSE$ in [°]) and integral of the motor current ($I_{MOT}Integral$ in [A]) for the hip joint during the stance (a) and swing (b) phase and for the knee motor during the stance phase (c). The yellow background indicates that these joints are under synchronous control. Panel (d) displays, in addition to the position RMSE and motor current integral, the motor torque integral ($\tau_{MOT}Integral$ in [Nm]) and Quadriceps and Hamstrings FES current integral ($I_{FES}Integral$ in [mA]) for the knee motor during swing. The same metrics are reported in panel (e) with a focus on the knee joint where users are separated based on their pathology: complete SCI (cSCI), incomplete SCI (iSCI), stroke - More Impaired side (stroke MI) and stroke - Less Impaired side (stroke LI). The green background of panels (d) and (e) indicates that these joints are under cooperative control. Differences were considered statistically significant when p-value<0.05. 81
2.12 Focus on the swing knee joint during walking experiments of one representative subject (ID1 - cSCI) under the two tested conditions ($MOT_{100\%}$ and $MOT_{0\%} + FES$). Results are reported separately for each session. Boxplots report the position RMSE (a), the integral of the motor current (b), the integral of the total torque (c) and the the integral of the Quadriceps and Hamstrings current amplitude (only for those conditions including FES) (d). 82
2.13 Results of the System Usability Scale (score between 0 and 100) reported subject-by-subject as the difference between the value given to the TwinFES system (T2 evaluation) and the one to the Twin system (T1 evaluation), computed as $SUS_{T2} - SUS_{T1}$. 83

2.14 Results of the Technological Acceptance Measure 3 (score between 1 and 5) reported subject-by-subject as the difference between the value given to the TwinFES system (T2 evaluation) and the one to the Twin system (T1 evaluation), computed as $TAM_{T2} - TAM_{T1}$. Answers to the 46 questions are divided into 13 categories. For all categories, a higher score corresponds to a better device evaluation. Single-subject data are superimposed to the boxplots, using a different marker to indicate the pathology (reported in the legend). 84
2.15 Results of the User Experience Questionnaire (UEQ) reported subject-by-subject as the difference between the value given to the TwinFES system (T2 evaluation) and the one to the Twin system (T1 evaluation), computed as $UEQ_{T2} - UEQ_{T1}$. The questionnaire asks subjects to rate, on a 1-7 scale (then rescaled between -3 and 3), 26 device characteristics then grouped into six categories. Single-subject data are superimposed to the boxplots, using a different marker to indicate the pathology (reported in the legend). 84

3.1 Integration levels for textile electrodes in wearable systems. Image taken from [292]. . . . 92
3.2 Back and front side of the used textile electrodes (ElastaTrode™) and zoom on their composition and the process followed to realize them. 96
3.3 LCR measurement system: measurement setup with the LCR meter terminals connected to a pair of electrodes placed on the subject leg (a) and LCR meter device (b), with a zoom on its display. 97
3.4 Schematic representation of the experimental setup: single-joint test bench, electrical stimulator connected to a pair of electrodes (textile in this case) and EMG system recording the Rectus Femoris muscle activity. Dotted lines indicate the connections between components. 99
3.5 Flow chart of the acquisition protocol. 101
3.6 Shape of the current wave used for the dynamic test. It includes the EMG trigger followed by 15 flexion/extension repetitions, 3 repetitions for each of the 5 tested levels, with an amplitude difference of δ. A zoom on the shape of the single generic extension is added. . 103
3.7 Shape of the current wave used for the isometric test. It includes the EMG trigger followed by 2 seconds of pause, 2 seconds of increasing ramp from $\hat{T2}$ to $T4$. Then current is maintained constant until the end of the test. 103
3.8 Transcutaneous Electrical Stimulation Comfort Questionnaire (TESCQ) filled by subjects after completing the protocol, both for textile and hydrogel electrodes. 104
3.9 Impedance [kΩ] as a function of frequency [Hz]. Panel a is relative to new textile electrodes without cream (no moisture) and with cream. Panel b is relative to new and worn-out samples for both hydrogel (blue lines) and textile (pink lines) electrodes (always moisturized). Panel c is relative to new textile samples both pre (circle marker) and after (triangle marker) 10 washing cycles. Markers correspond to discrete values recorded with the LCR meter. 106
3.10 Boxplots of stimulation thresholds recorded during the test (a). For the motor threshold T2, also the boxplots comparing its estimated value (T2) and its real value $\hat{T2}$, as retrieved from EMG recordings, are displayed (b). This latter graph only considers data from 13 subjects out of 14. 108
3.11 Boxplot of the normalized ROMs performed during dynamic tests for the 5 stimulation amplitudes (L1-L5). For each subject, the normalization is computed with respect to the maximum extension angle achieved by each subject during the initial voluntary contraction. 108

3.12 Boxplots for the metrics recorded during the isometric test: Max Torque, Time To Fatigue (TTF), Total Duration and Torque Integral. 109
3.13 Mean power of eEMGv. Data from 12 subjects are considered in the Dynamic test, while data from 11 subjects are considered in the Isometric test. 110
3.14 Spider plot of the scores of all TESCQ items. Solid lines connect the median values of items across subjects while the shaded area represents their IQR. 111

4.1 Minimum parameters framework to report SCS. Figure from Malik et al. [308]. 116
4.2 Detailed positioning for stimulation electrodes on the lower back (a) and EMG electrodes on the main four leg muscles (figures composed on `BioRender.com`). 121
4.3 Experimental Setup. The RehaMove Pro stimulator provides tSCS and is controlled from a laptop via the custom-developed GUI. EMG data are acquired with eight channels on the TMSI device and visualized in real-time on a laptop running the proprietary SAGA interface. The motor is controlled by a Raspberry, which is programmed via Visual Studio from a laptop (figure composed on `BioRender.com`). 122
4.4 Boxplots of data computed for the two muscles and positions, across all responder subjects and sides. Reported medians are relative to the PRM threshold current (a) and the average latency (b) and peak-to-peak amplitude (c) calculated over the reflexes induced by the ten delivered pulses at the same amplitude of the PRM threshold. Differences among the two positions were considered statistically significant when p-value$<$0.05. 125
4.5 Experimental protocol with three steps: *calibration*, *passive cycling* and *tSCS cycling*. The diagram shows the combination of stimulation, motor, and subject's voluntary effort in the three stages. 128
4.6 Data from the first trial of subject 02, representing the *Case Study 01*. (a) Right Rectus Femoris and Semitendinosus EMG during an average cycling revolution (left), reported as mean ± SD (Standard Deviation), and mean RMS values of the EMG amplitudes (right). Data are normalized to the subject's baseline and reported with respect to the right crank angle, which is null when the right pedal is at 90° upright. Knee and hip flexion and extension intervals are superimposed with black (extension) and grey (flexion) bars on the graphs. (b) Average cycles of the active force computed as the difference between the one during tSCS trials and the one during the passive trial. Each row is relative to a different tested frequency. (c) Mean and SD of the active force for all tSCS cycling conditions. . . . 132
4.7 Data from second trial of subject 03, representing the *Case Study 02*. (a) Right rectus femoris and Semitendinosus EMG during an average cycling revolution (left), reported as mean $\pm SD$ (Standard Deviation), and mean RMS values of the EMG amplitudes (right). Data are normalized to the subject's baseline and reported with respect to the right crank angle, which is null when the right pedal is at 90° upright. Knee and hip flexion and extension intervals are superimposed with black (extension) and grey (flexion) bars on the graphs. (b) Average cycles of the active force computed as the difference between the one during tSCS trials and the one during the passive trial. Each row is relative to a different tested frequency. (c) Mean and SD of the active force for all tSCS cycling conditions. . . . 133

5.1 Experimental setup for the stimulation component (a) with the STIMISOLA stimulator and its cable for electrodes connection, and for the EMG component (b) with the PowerLab acquisition system, the biological amplifier and its three-fold cable for electrodes connection. 141

5.2 Position of stimulation electrodes (anode and cathode) and EMG ones (one reference and two recording) in the 3 peripheral tests: stimulation of femoral nerve (a), sciatic nerve (b) and tibial nerve (c). Blue labels mark the position of stimulation electrodes, pink labels the one of EMG electrodes. Labels with a dotted line indicate that the electrode is on the other side of the leg and thus covered. 142
5.3 PRM reflex waves in mV for a single subject on the 4 tested muscles: RF (a), BF (b), TA (c) and G (d), displayed one per row. The used current amplitude is reported on the top of each panel. Dots on the graphs indicate the starting point of the reflex and its latency with respect to the stimulation instant (vertical dotted line) is reported in ms on the x-axis. 145
5.4 H-reflex and M-waves in mV for a single subject on the 4 tested muscles: RF (a), BF (b), TA (c) and G (d), displayed one per row. The used current amplitude is reported on the top of each panel. Dots on the graphs indicate the starting point of the H-reflex and its latency with respect to the stimulation instant (vertical dotted line) is reported in ms on the x-axis. 146
5.5 PaD phenomenon for the BF muscle during the central stimulation protocol on the representative subject (ID5). 148
5.6 Boxplots comparing the reflexes induced by the two stimulation types across all subjects in terms of reflex threshold (a), reflex latency (b) and amplitude ratio between the 2nd and 1st reflex response when testing PaD (c). 148
5.7 Boxplots of the max amplitudes of the PRM reflex (central) and H-reflex (peripheral) across all subjects (a), together with the current amplitudes at which this maximum reflex was registered (b). 149

List of Tables

2.1 Schematic table of main cooperative controllers developed in the literature for the control of lower-limbs hybrid approaches. Each study's characteristics are reported in terms of materials, methods (control), carried-out testing and key results. 57
2.2 Inclusion and exclusion criteria for the experimental protocol 61
2.3 Data of the 6 subjects who took part in single-joint tests. General information (ID, Sex and Age) are reported together with the I_{L1} and I_{L2} calibration amplitudes for the Quadriceps of the right leg (only stimulated muscle group). 68
2.4 Data of the 12 subjects who took part in walking tests. General information (ID, Sex and Age) are reported together with the I_{L1} and I_{L2} calibration amplitudes for Quadriceps and Hamstrings of left and right leg. 68
2.5 Characteristics of SCI subjects. 78
2.6 Characteristics of stroke subjects. 79

3.1 Sum across subjects of all TESCQ items scores for the two types of electrodes. The direction of the arrow indicates greater comfort. 110

4.1 Summary of the electrodes parameters. 118
4.2 Percentage of stimulation responders divided by positions, muscles and sides over the eleven tested individuals. The term "responders" refers to those subjects on which the PRM reflex could be observed. 125
4.3 Inclusion and exclusion criteria for the experimental protocol 127
4.4 Included subjects' characteristics 129

5.1 Percentage of stimulation responders for the two stimulation types and different muscles over the twelve tested individuals. The term "responders" refers to those subjects on which the PRM reflex could be observed. 148